UC Riverside

UC Riverside Electronic Theses and Dissertations

Title

The Regulation of Aquaporin-4 (AQP4) and Glutamate Transporter-1 (GLT1) in an Epilepsy Model

Permalink

https://escholarship.org/uc/item/6608g5hx

Author

Hubbard, Jacqueline Ann

Publication Date

2016

Copyright Information

This work is made available under the terms of a Creative Commons Attribution License, availalbe at https://creativecommons.org/licenses/by/4.0/

Peer reviewed|Thesis/dissertation

eScholarship.org Powered by the California Digital Library
University of California

UNIVERSITY OF CALIFORNIA
RIVERSIDE

The Regulation of Aquaporin-4 (AQP4) and Glutamate Transporter-1 (GLT1) in an Epilepsy Model

A Dissertation submitted in partial satisfaction
of the requirements for the degree of

Doctor of Philosophy

in

Biochemistry and Molecular Biology

by

Jacqueline Ann Hubbard

August 2016

Dissertation Committee:
Dr. Devin K. Binder, Chairperson
Dr. Iryna M. Ethell
Dr. Todd A. Fiacco

Copyright by
Jacqueline Ann Hubbard
2016

The Dissertation of Jacqueline Ann Hubbard is approved:

Committee Chairperson

University of California, Riverside

Acknowledgements

I would like to extend my sincerest gratitude to my advisor Devin Binder. His patience, expertise, and guidance has made him an exceptional mentor. He has always inspired me. I thank him for his continual support on all of my research projects and ideas, for all the opportunities he has presented to me over the years, for raising my spirits when research became cumbersome, and for being a kind person and a great friend. Together we have produced some great work and I look forward to becoming colleagues.

Thank you to all of my committee members for their guidance. Iryna Ethell and Todd Fiacco have served as mentors since my first year of graduate school and have provided useful feedback. I have been lucky to have them on my guidance committee and appreciate all the time they have spent with me. Thank you to Emma Wilson and Katie DeFea for both serving on my Qualifying Exam Committee and offering me access to valuable resources.

A special thank you to Dawn Loyola for all of her help. I would also like to state my appreciation to Monica Carson and the rest of the Division of Biomedical Sciences for serving as excellent role models for a young scientist. I have also enjoyed being a member of the Center for Glial-Neuronal Interactions (CGNI) and am so grateful it was founded at UCR.

Thank you to Jenny Szu and Jennifer Yonan, the best lab mates a gal could ask for! They have been instrumental to my success. I thank them for many hours of hard work, their moral support, and the generally great atmosphere they maintained in the lab. Because of them, I enjoyed coming into work and looked forward to both discussing our projects and venting about life. I would also like to give a special thanks to Andrew Nakla, an undergraduate student who has worked with me over the last couple of years. He is a bright student who took on and completed his own research project. He was a pleasure to work with and I am very proud of what he was able to accomplish. Thank you to all co-authors for your contributions to the previously published work used in this dissertation.

A debt of gratitude is owed to the Wilson laboratory. Emma Wilson has offered me invaluable guidance and feedback and has made it a pleasure to collaborate with her lab. Thank you to Kathryn McGovern, Danielle Worth, Clément David, Tyler Landrith, and the undergraduate students. They have been extraordinary colleagues and I appreciate all of their assistance. Finally, thank you all for making me feel at home in your lab!

A huge thank you to my amazing family. I would never have made it to graduate school without them. To my grandmother who has always believed in me. To my parents who have always been supportive and loving. To all of my wonderful and supportive siblings; their success has always inspired me. I love you all!

I want to acknowledge all of the friends that I have made at UCR. Graduate school can be an isolating place but thanks to them, I never felt alone. A special thanks to the “Gym Squad” (Michael Beaumier and Alexander Anderson-Natale) for their unconditional comradery and for keeping me sane. Thank you to Vilma Sielawa Ferreira, an exceptional person and an amazing friend, for your support, guidance, and kindness throughout the years. Thank you to Kayleigh Anderson-Natale for career advice and many nights of TV and wine! Thank you to all members (residents and visitors) of the FZX House for all the adventures that made me love and appreciate you all! I’d also like to acknowledge my cohort in Biochemistry for late nights of studying and years of collaborations (especially Kathryn McGovern, Ryan Arvidson, and Stephanie Dingwall). Finally, a special thank you to Tim Ngo, an extraordinary person who passed away in February 2016. His fun-loving personality and cherished friendship will be missed.

Last, but not least, I express my deepest appreciation to Oleg Martynov. Without him, I would not have survived graduate school. He has offered me insurmountable emotional and professional support. Thank you for helping me prepare for presentations and expediting my analyses. Thank you for taking care of me when I was overwhelmed and for helping me take care of two adorable pets (Chloey and Babou, our helpful furballs). Thank you for your patience, for always making me laugh, for believing in me, and for convincing me that I am strong. I love you and I am forever grateful that you are in my life.

ABSTRACT OF THE DISSERTATION

The Regulation of Aquaporin-4 (AQP4) and Glutamate Transporter-1 (GLT1) in an Epilepsy Model

by

Jacqueline Ann Hubbard

Doctor of Philosophy, Graduate Program in Biochemistry and Molecular Biology
University of California, Riverside, August 2016
Dr. Devin K. Binder, Chairperson

Epilepsy is a group of chronic neurological disorders characterized by abnormally synchronized activity among neurons that presents as seizures. It is a major health problem that is estimated to affect 1 in 26 people during their lifetime. Many antiepileptic drugs (AEDs) currently exist, but approximately 30% of patients taking AEDs cannot control their seizures with drugs alone. In addition, adverse effects such as cognitive impairment are common. This may be because current AEDs act as central nervous system depressants and target neuronal channels to control tissue excitability. Therefore, new drugs based on non-neuronal targets may serve as novel therapeutic strategies with fewer deleterious effects. Astrocytes maintain glutamate and water homeostasis primarily through glutamate transporters and aquaporin-4 (AQP4), respectively. The two astrocyte-specific glutamate transporters are glutamate transporter-1 (GLT1) and glutamate aspartate transporter (GLAST), of which GLT1 is

responsible for the majority of glutamate uptake in the forebrain. Alterations in both glutamate and water homeostasis have powerful effects on excitability, but the regulation of GLT1, GLAST, and AQP4 in epilepsy is not well understood. Furthermore, the β-lactam antibiotic ceftriaxone has previously been shown to upregulate GLT1 expression, but its efficacy in a chronic epilepsy model has not been well studied. Here I describe AQP4, GLT1, and GLAST hippocampal expression changes in a model of epilepsy. I begin by characterizing the intrahippocampal kainic acid (IHKA) model of epilepsy, focusing on astrocyte reactivity during the development of epilepsy (epileptogenesis). I then describe the highly polarized AQP4 expression in the healthy brain and show reduced hippocampal levels during epileptogenesis. After that, I discuss alterations of GLT1 levels after IHKA-induced epileptogenesis. Next, I discuss the lack of effect of β-lactam drugs on regulating AQP4 and GLT1 expression, thereby eliminating it as a potential antiepileptic therapeutic. I then describe the co-localization patterns of AQP4 and GLT1; these two proteins do not co-immunoprecipitate, suggesting the lack of a strong interaction between them. In the penultimate chapter, I briefly describe the minimal changes in GLAST expression during epileptogenesis. I conclude with a summary of my findings and suggested future directions for this line of research.

Table of Contents

Chapter 1: Introduction 1
1.1 Epilepsy 1
1.1.1 Seizure classification 2
1.1.2 Epilepsy syndromes 4
1.1.3 Temporal lobe epilepsy with hippocampal sclerosis 6
1.1.4 Antiepileptic drugs (AEDs) 8
1.2 Animal models of epilepsy 10
1.2.1 Intrahippocampal kainic acid model of epilepsy 11
1.3 Astrocytes 12
1.3.1 Astrocyte functions 13
1.3.2 Tripartite synapse 14
1.3.3 Astrocytes in epilepsy 15
1.4 Glutamate 16
1.4.1 Glutamate transporters 19
1.4.2 Glial glutamate transporter expression 21
1.4.3 Neuronal glutamate transporter expression 22
1.5 Glial glutamate transporters in epilepsy 23
1.5.1 Glial glutamate transporters in animal models of epilepsy 24
1.5.2 Glial glutamate transporters in human epilepsy 26
1.6 Ceftriaxone 27
1.7 Aquaporins 31
1.7.1 Aquaporin-4 in epilepsy 32
1.8 Summary 34
1.9 References 36
Chapter 2: Characterization of the intrahippocampal kainic acid (IHKA) model of epilepsy 56
2.1 Abstract 56
2.2 Introduction 57
2.3 Methods 61
2.3.1 Animals 61

2.3.2 Intrahippocampal kainic acid surgery and EEG implants 62
2.3.3 Kainic acid-induced status epilepticus 65
2.3.4 Immunohistochemistry 68
2.3.5 Western blot 70
2.3.6 RT-PCR 71
2.3.7 Statistical analysis 72
2.4 Results 72
2.4.1 Histological confirmation and characterization of the sclerotic hippocampus 72
2.4.2 Histological characterization of the microglial marker, Iba1 74
2.4.3 Increased expression of the astrocyte marker, GFAP 78
2.5 Discussion 90
2.6 References 95
Chapter 3: Expression of aquaporin-4 in the mouse brain 102
3.1 Abstract 102
3.2 Introduction 103
3.3 Methods 106
3.3.1 Animals 106
3.3.2 Western blot 107
3.3.3 Immunohistochemistry 108
3.3.4 Confocal microscopy 109
3.4 Results 110
3.4.1 Differential expression of AQP4 in the mouse brain 110
3.4.2 AQP4 expression in the wild-type and knockout mouse brain 111
3.4.3 AQP4 expression in the mouse forebrain 112
3.4.4 AQP4 expression in the mouse brainstem 116
3.4.5 Cerebellar expression of AQP4 119
3.5 Discussion 121
3.6 References 131
Chapter 4: Regulation of aquaporin-4 (AQP4) expression in a model of epilepsy 140
4.1 Abstract 140
4.2 Introduction 141

4.3 Methods 144
4.3.1 Animals 144
4.3.2 Surgery 145
4.3.3 Immunohistochemistry 146
4.3.4 Western blot analysis 146
4.3.5 Real-time polymerase chain reaction (RT-PCR) analysis 147
4.3.6 Statistical analysis 149
4.4 Results 150
4.4.1 Decreased AQP4 immunoreactivity 150
4.4.2 Changes in aquaporin-4 (AQP4) expression 150
4.5 Discussion 154
4.6 References 158
Chapter 5: Regulation of glutamate transporter-1 (GLT1) expression in a model of epilepsy 165
5.1 Abstract 165
5.2 Introduction 166
5.3 Methods 169
5.3.1 Animals 169
5.3.2 Surgery 169
5.3.3 Immunohistochemistry 170
5.3.4 Western blot analysis 172
5.3.5 Real-time polymerase chain reaction (RT-PCR) analysis 174
5.3.6 Statistical analysis 175
5.4 Results 176
5.4.1 Alterations in glutamate transporter-1 (GLT1) immunoreactivity 176
5.4.2 Alterations in GLT1 protein expression 186
5.5 Discussion 190
5.6 References 194
Chapter 6: β-lactam antibiotics are an ineffective treatment option for restoration of aquaporin-4 (AQP4) and glutamate transporter-1 (GLT1) in an epilepsy model 198
6.1 Abstract 198
6.2 Introduction 199

6.3 Methods 202
6.3.1 Animals 202
6.3.2 Drug Treatment 203
6.3.3 Western blot 204
6.3.4 Intrahippocampal kainic acid injections 205
6.3.5 Immunohistochemistry 207
6.4 Results 208
6.4.1 β-lactam drugs do not alter GLT1 expression in wild-type mice 208
6.4.2 β-lactam drugs do not alter AQP4 expression in wild-type mice 211
6.4.3 Tazobactam does not ameliorate histological changes in the IHKA epilepsy model 214
6.4.4 Ceftriaxone fails to ameliorate histological changes in the IHKA model of epilepsy 226
6.5 Discussion 229
6.6 References 234
Chapter 7: Lack of a physical interaction between glutamate transporter-1 (GLT1) and aquaporin-4 (AQP4) 242
7.1 Abstract 242
7.2 Introduction 243
7.3 Methods 245
7.3.1 Animals 245
7.3.2 Tissue collection 246
7.3.3 Co-immunoprecipitation (co-IP) 247
7.3.4 Western blot 248
7.3.5 Immunohistochemistry 248
7.4 Results 249
7.4.1 AQP4 and GLT1 do not co-immunoprecipitate 249
7.4.2 GLT1 expression levels are not altered in AQP4 knockout mice 251
7.4.3 AQP4 and GLT1 co-localize in the brain 257
7.5 Discussion 260
7.6 References 265

Chapter 8: Characterization of glutamate aspartate transporter (GLAST) expression in an epilepsy model 270
8.1 Abstract 270
8.2 Introduction 271
8.3 Methods 274
8.3.1 Animals 274
8.3.2 Intrahippocampal injections 274
8.3.3 Immunohistochemistry 275
8.3.4 Western blot analysis 276
8.3.5 Real-time polymerase chain reaction (RT-PCR) analysis 277
8.3.6 Statistical analysis 278
8.4 Results 278
8.4.1 GLAST immunoreactivity in an epilepsy model 278
8.5 Discussion 282
8.6 References 286
Chapter 9: Conclusions and future directions 289
9.1 Intrahippocampal kainic acid model of epilepsy 289
9.2 Aquaporin-4 (AQP4) in epilepsy 290
9.3 Astrocytic glutamate transporters in epilepsy 293
9.4 Summary 298
9.5 References 299

List of Figures

Figure 1.1. Model for role of astrocyte swelling in neuronal excitability. 18
Figure 2.1. Intrahippocampal kainic acid (IHKA) injections and video-EEG recording in a mouse. 64
Figure 2.2. EEG recording of status epilepticus immediately after intrahippocampal kainic acid (IHKA) injections. 66
Figure 2.3. EEG recordings in intrahippocampal kainic acid model. 67
Figure 2.4. Method for analysis of hippocampal immunoreactivity. 70
Figure 2.5. Marked histological changes occur during epileptogenesis in the mouse hippocampus. 73
Figure 2.6. Iba1 immunoreactivity in the hippocampus of naïve, saline injected, and kainic acid injected mice. 75
Figure 2.7. Iba1 immunoreactivity in the cortex of naïve, saline injected, and kainic acid injected mice 77
Figure 2.8. Microglia (Iba1) immunoreactivity 1 day after intrahippocampal kainic acid-induced status epilepticus. 78
Figure 2.9. Astrocyte (GFAP) immunoreactivity in naïve mice and 1 day after intrahippocampal saline injections. 79
Figure 2.10. Astrocyte (GFAP) immunoreactivity after intrahippocampal saline injections. 80
Figure 2.11. Glial fibrillary acidic protein (GFAP) immunoreactivity in the ipsilateral hippocampus after kainic acid-induced status epilepticus (SE). 82
Figure 2.12. Glial fibrillary acidic protein (GFAP) immunoreactivity in the ipsilateral CA3 region of the hippocampus after kainic acid-induced status epilepticus (SE). 84
Figure 2.13. Glial fibrillary acidic protein (GFAP) immunoreactivity in the contralateral hippocampus after kainic acid-induced status epilepticus (SE). 86
Figure 2.14. Glial fibrillary acidic protein (GFAP) immunoreactivity in the contralateral CA3 region of the hippocampus after kainic acid-induced status epilepticus (SE). 88
Figure 2.15 Hippocampal protein and mRNA quantification of glial fibrillary acidic protein (GFAP) after kainic acid-induced status epilepticus (SE). 89
Figure 3.1. Western blot analysis of various brain regions. 111
Figure 3.2. AQP4 immunoreactivity in the wild-type and AQP4 knockout mouse whole brain. 113
Figure 3.3. AQP4 immunoreactivity within forebrain regions, 10x images. 115
Figure 3.4. AQP4 immunoreactivity within the brainstem, 10x images. 117
Figure 3.5. AQP4 and brevican immunoreactivity within the cerebellum. 120
Figure 4.1. Western blot analysis of aquaporin-4 (AQP4) antibodies using wild-type and AQP4 knockout mouse tissue. 148

Figure 4.2. Hippocampal aquaporin-4 (AQP4) immunoreactivity following intrahippocampal kainic acid (IHKA)-induced status epilepticus (SE)..... 151
Figure 4.3. Dorsal hippocampal aquaporin-4 (AQP4) protein and mRNA levels after kainic acid-induced status epilepticus (SE). 152
Figure 4.4. Aquaporin-4 (AQP4) protein and mRNA whole hippocampal levels after kainic acid-induced status epilepticus (SE). 153
Figure 5.1. Glutamate transporter-1 (GLT1) immunoreactivity in naïve mice and 1 day after intrahippocampal saline injections. 171
Figure 5.2. Glutamate transporter-1 (GLT1) immunoreactivity after intrahippocampal saline injections. 173
Figure 5.3. Glutamate transporter-1 (GLT1) immunoreactivity in the ipsilateral hippocampus after kainic acid-induced status epilepticus (SE). 178
Figure 5.4. Confocal images of glutamate transporter-1 (GLT1) and glial fibrillary acidic protein (GFAP) in the ipsilateral hippocampus after kainic acid-induced status epilepticus (SE). 180
Figure 5.5. Glutamate transporter-1 (GLT1) immunoreactivity in the ipsilateral CA3 region of the hippocampus after kainic acid-induced status epilepticus (SE). 182
Figure 5.6. Glutamate transporter-1 (GLT1) immunoreactivity in the contralateral hippocampus after kainic acid-induced status epilepticus (SE). 184
Figure 5.7. Glutamate transporter-1 (GLT1) immunoreactivity in the contralateral CA3 region of the hippocampus after kainic acid-induced status epilepticus (SE). 186
Figure 5.8: Confocal images of glutamate transporter-1 (GLT1) and glial fibrillary acidic protein (GFAP) in the contralateral hippocampus after kainic acid-induced status epilepticus (SE). 187
Figure 5.9. Dorsal hippocampal glutamate transporter-1 (GLT1) protein and mRNA levels after kainic acid-induced status epilepticus (SE). 188
Figure 5.10. Glutamate transporter-1 (GLT1) protein and mRNA whole hippocampal levels after kainic acid-induced status epilepticus (SE). 189
Figure 6.1. No change in wild-type glutamate transporter-1 (GLT1) cortical protein levels after treatment with β-lactam drugs. 208
Figure 6.2. No change in wild-type glutamate transporter-1 (GLT1) cortical immunoreactivity after treatment with β-lactam drugs. 209
Figure 6.3. No change in wild-type glutamate transporter-1 (GLT1) hippocampal protein levels after treatment with β-lactam drugs. 210
Figure 6.4. No change in wild-type glutamate transporter-1 (GLT1) hippocampal immunoreactivity after treatment with β-lactam drugs. 211
Figure 6.5. No change in wild-type aquaporin-4 (AQP4) cortical protein levels after treatment with β-lactam drugs. 212
Figure 6.6. No change in wild-type aquaporin-4 (AQP4) cortical immunoreactivity after treatment with β-lactam drugs. 213
Figure 6.7. No change in wild-type aquaporin-4 (AQP4) hippocampal protein levels after treatment with β-lactam drugs. 214

Figure 6.8. No change in wild-type aquaporin-4 (AQP4) cortical immunoreactivity after treatment with β-lactam drugs. 215
Figure 6.9. Tazobactam failed to ameliorate histological changes in the ipsilateral hippocampus in a severe intrahippocampal kainic acid (IHKA) model of epilepsy. 216
Figure 6.10. Tazobactam failed to ameliorate histological changes in the contralateral hippocampus in a severe intrahippocampal kainic acid (IHKA) model of epilepsy..... 217
Figure 6.11. Pre- and post-treatment with tazobactam failed to ameliorate histological changes in the ipsilateral hippocampus in the intrahippocampal kainic acid (IHKA) model of epilepsy. 220
Figure 6.12. Pre- and post-treatment with tazobactam failed to ameliorate histological changes in the contralateral hippocampus in the intrahippocampal kainic acid (IHKA) model of epilepsy. 223
Figure 6.13. Two weeks of tazobactam treatment failed to ameliorate histological changes in the ipsilateral hippocampus in the intrahippocampal kainic acid (IHKA) model of epilepsy. 224
Figure 6.14. Two weeks of tazobactam treatment failed to ameliorate histological changes in the contralateral hippocampus in the intrahippocampal kainic acid (IHKA) model of epilepsy. 225
Figure 6.15. Ceftriaxone failed to ameliorate histological changes in the ipsilateral hippocampus in the intrahippocampal kainic acid (IHKA) model of epilepsy. 227
Figure 6.16. Ceftriaxone failed to ameliorate histological changes in the contralateral hippocampus in the intrahippocampal kainic acid (IHKA) model of epilepsy. 228
Figure 7.1. Lack of co-immunoprecipitation between glutamate transporter-1 (GLT1) and aquaporin-4 (AQP4) in C57BL/6 mice. 250
Figure 7.2. Lack of co-immunoprecipitation between glutamate transporter-1 (GLT1) and aquaporin-4 (AQP4) in CD1 mice. 251
Figure 7.3. Glutamate transporter-1 (GLT1) protein expression in whole brain tissue from C57BL/6 and CD1 wild-type and aquaporin-4 (AQP4) knockout mice. 252
Figure 7.4. Glutamate transporter-1 (GLT1) protein expression in hippocampal and cortical tissue from C57BL/6 wild-type and aquaporin-4 knockout (AQP4) knockout mice..... 253
Figure 7.5. Glutamate transporter-1 (GLT1) immunoreactivity in C57BL/6 wild-type aquaporin-4 (AQP4) knockout mice. 254
Figure 7.6. Glutamate transporter-1 (GLT1) protein expression in hippocampal and cortical tissue from CD1 wild-type and aquaporin-4 (AQP4) knockout mice. 255
Figure 7.7. Glutamate transporter-1 (GLT1) immunoreactivity in CD1 wild-type and aquaporin-4 (AQP4) knockout mice. 256

Figure 7.8. Aquaporin-4 (AQP4) and glutamate transporter-1 (GLT1) immunoreactivity in C57BL/6 and CD1 wild-type mice. 257
Figure 7.9. Aquaporin-4 (AQP4) and glutamate transporter-1 (GLT1) immunoreactivity in the hippocampus of C57BL/6 and CD1 wild-type mice. 258
Figure 7.10. Aquaporin-4 (AQP4) and glutamate transporter-1 (GLT1) immunoreactivity in the cortex of C57BL/6 and CD1 wild-type mice..... 259
Figure 8.1. Glutamate aspartate transporter (GLAST) immunoreactivity in the ipsilateral hippocampus after kainic acid-induced status epilepticus (SE). 279
Figure 8.2. Glutamate aspartate transporter (GLAST) immunoreactivity in the contralateral hippocampus after kainic acid-induced status epilepticus (SE). .. 280
Figure 8.3. Glutamate aspartate transporter (GLAST) protein and mRNA levels in the ipsilateral hippocampus after kainic acid-induced status epilepticus (SE). 281
Figure 8.4. Glutamate aspartate transporter (GLAST) protein and mRNA levels after in the contralateral hippocampus after kainic acid-induced status epilepticus (SE). 282

List of Tables

Table 1.1. Overview of seizure types. 3
Table 2.1. The Racine scale modified for rodent seizures (Racine 1972). 68
Table 2.2. Antibodies used for immunohistochemistry. 69
Table 2.3. Primers used for RT-PCR experiments. 71
Table 4.1. Primers used for RT-PCR experiments. 149
Table 5.1. Primers used for RT-PCR experiments. 175
Table 6.1. β-lactam drug Information. 203
Table 6.2. Treatment paradigms. 206
Table 8.1. Primers used for RT-PCR experiments. 277

Abbreviations

Antiepileptic drugs (AEDs)

Aquaporins (AQPs)

Aquaporin-4 (AQP4)

Blood-brain barrier (BBB)

Bovine serum albumin (BSA)

Central nervous system (CNS)

Cerebrospinal fluid (CSF)

Cornu ammonis (CA)

Co-immunoprecipitation (Co-IP)

4',6-diamidino-2-phenylindole (DAPI)

Electroencephalogram (EEG)

Excitatory amino acid transporter (EAAT)

Extracellular space (ECS)

Focal cortical dysplasia (FCD)

Gamma-aminobutyric acid (GABA)

Glial fibrillary acidic protein (GFAP)

Glutamate aspartate transporter (GLAST)

Glutamate transporter-1 (GLT1)

Granule cell layer (GCL)

Hippocampal sclerosis (HS)

International League against Epilepsy (ILAE)

Intrahippocamal kainic acid (IHKA)

Intraperitoneal (i.p.)

Ionized calcium-binding adapter molecule-1 (Iba1)

Kilodalton (KDa)

N-methyl-D-aspartate (NMDA)

Neuronal specific nuclear protein (NeuN)

Nuclear factor κ-light-chain-enhancer of activated B cells (NF- κB)

Pentylenetetrazol (PTZ)

Phosphate buffered saline (PBS)

Radioimmunoprecipitation assay (RIPA)

Real-time polymerase chain reaction (RT-PCR)

Status epilepticus (SE)

Stratum lacunosum moleculare (SLM)

Temporal lobe epilepsy (TLE)

Chapter 1: Introduction

1.1 Epilepsy

The International League Against Epilepsy (ILAE) describes epilepsy as a class of diseases of the brain defined by (1) the occurrence of two or more unprovoked seizures within a 24 hour period; (2) one unprovoked seizure and a 60% or more probability of the recurrence of seizures after two unprovoked seizures within the next 10 years; or (3) diagnosis of an epilepsy syndrome (Fisher, Acevedo et al. 2014). It is the fourth most common neurological disorder and affects people of all ages. The risk of developing epilepsy is hard to measure, but it is currently estimated that 1 in 26 people will develop epilepsy in their lifetime (Hesdorffer, Logroscino et al. 2011) with the most common form being temporal lobe epilepsy (Wiebe 2000). People with epilepsy have a reduced quality of life. They often suffer from impaired cognition, increased risk of depression or anxiety disorders, reduced quality of sleep, increased risk for bruising and fracturing, reproductive health problems, and an increased risk of death (Devinsky, Vickrey et al. 1995; Crawford 2005; McCagh, Fisk et al. 2009; Jacoby, Snape et al. 2015). A number of antiepileptic drugs (AEDs) are available to patients today, but they come with several drawbacks including difficulties with memory and cognition (Aldenkamp, De Krom et al. 2003), increased risk of teratogenicity in women (Crawford 2005; Wlodarczyk, Palacios et al. 2012), mood alterations, suicidality, hepatotoxicity,

and weight management problems (Perucca and Gilliam 2012). In addition, up to 30% of patients may develop pharmacoresistant epilepsy (also called drug resistant epilepsy, refractory epilepsy, and intractable epilepsy), meaning they cannot gain control of seizures with AEDs alone (Cockerell, Johnson et al. 1995; Picot, Baldy-Moulinier et al. 2008; Berg 2009). Clearly there is an unmet need for better pharmacological intervention for the treatment of epilepsy.

1.1.1 Seizure classification

A seizure is the clinical manifestation of abnormal synchronized activity among neurons in the brain. Seizures are composed of four main phases: preictal (period before the seizure), ictal (period during the seizure), interictal (period in between seizures), and postictal (post-seizure period where the patient returns to the normal level of awareness and function) (Hubbard and Binder 2016). Several different types of seizures exist, but they can be divided into just two main sub-classes: focal (also called partial) or generalized seizures (Table 1.1, Raol and Brooks-Kayal 2012).

As the name suggests, focal seizures often originate at a “focal” point in the brain and are usually limited to one hemisphere (Berg, Berkovic et al. 2010). Focal seizures can be further divided into 2 main categories: simple partial, which do not involve loss of consciousness, and complex partial, which do (Hubbard and

Binder 2016). Otherwise, partial seizures are often characterized by the area of the brain from which they originate. For example, temporal lobe seizures originate within the mesial structures, such as the hippocampus.

Seizure Type	Brief Description
Focal	Seizure onset from one area of the brain and limited to one hemisphere
Neocortical	Seizure generation from the neocortex; manifestation depends on exact location of origin and pattern of spread
Temporal Lobe	Seizure generation within the mesial structures, such as the hippocampus; often consists of epigastric aura followed by automatisms, dystonia of contralateral hand, and post-ictal confusion
Multifactorial	Simultaneous seizure generation from two independent foci
Generalized	Seizure onset simultaneously from both hemispheres
Absence	Brief (≥ 1 minute) loss of consciousness, eye blinking and staring, and/or facial movements with no post-ictal confusion
Myoclonic	Quick, repetitive, arrhythmic muscle twitching involving one or both sides of the body; consciousness remains intact
Clonic	Seizures consist of rhythmic muscle jerks during impaired consciousness
Tonic	An increase in muscle tone causes flexion of head, trunk, and/or extremities for several seconds
Tonic-clonic	Tonic extension of muscles followed by clonic rhythmic movements and postictal confusion
Atonic	Brief loss of postural tone, which can result in falls and injuries

Table 1.1. Overview of seizure types.
Modified, with permission, from (Hubbard, Hsu et al. 2013).

Generalized seizures, on the other hand, do not have a focal point of seizure onset but, instead are conceptualized as rapidly engaging and disrupting networks bilaterally (Berg, Berkovic et al. 2010). The types of generalized seizures are absence (petit mal), myoclonic, clonic, tonic, tonic-clonic (grand

mal), and atonic seizures. Briefly, absence seizures are characterized by a short period of impaired awareness and staring spells. Myoclonic seizures are very brief seizures characterized by shock-like jerks of muscles. Clonic seizures are also characterized by these jerk-like motions but the repetition rate is slower. Tonic seizures involve rigid posturing or flexion of the head, torso, or limbs. Combined, tonic-clonic, or grand mal, seizures are composed of a tonic phase and a clonic phase. During the tonic phase, patients become rigid and may exhibit several additional symptoms including respiratory impairment, increased heart rate, and vocal outbursts. During the clonic phase, the seizure evolves into jerking movements of the extremities. Tonic-clonic seizures may evolve into status epilepticus (SE), a condition defined by the ILAE as continuous seizure activity that results from either the failure of the seizure termination mechanism or from the initiation of mechanisms which lead to abnormally prolonged seizures (Trinka, Cock et al. 2015). SE can have long-term consequences including neuronal injury or death and altered neuronal networks. Finally, atonic seizures comprise sudden loss of postural tone, which can produce head nods or jaw drops in mild cases but can result in falls in severe cases.

1.1.2 Epilepsy syndromes

The classification of epilepsies is complex and is limited by our understanding of each disease. The ILAE, however, has continuously revised the concepts,

terminology, and approaches for the classifications of seizures and forms of epilepsy (ILAE 1989; Engel 2001; Engel 2006; Engel 2006; Berg, Berkovic et al. 2010; Fisher, Acevedo et al. 2014). For example, the etiologic classification for epilepsy used to be genetic, structural/metabolic, or unknown (Berg, Berkovic et al. 2010). The ILAE now recommends 6 different categories for the etiology of epilepsy: genetic, structural, metabolic, immune, infections, and unknown (Scheffer, Berkovic et al. 2014). The diagnosis of epilepsy involves careful clinical evaluation, electroencephalogram (EEG) and magnetic resonance imaging (MRI) information. Together with age of onset, cognitive and developmental antecedents, motor and sensory examination, triggering factors, and patterns of seizure occurrence with respect to sleep are all required to characterize the type of epilepsy afflicting the patient (Berg, Berkovic et al. 2010; Scheffer, Berkovic et al. 2014).

There are easily over 50 epilepsy syndromes (Engel 2001) and they can be classified in a number of different ways. Recently, they have been categorized by age of onset (neonatal period, infancy, childhood, adolescence to adult, and those with a less specific age relationship) (Berg, Berkovic et al. 2010; Scheffer, Berkovic et al. 2014). For example, early myoclonic encephalopathy and benign familial neonatal epilepsy usually arise during infancy whereas juvenile absence epilepsy and juvenile myoclonic epilepsy have a typical age of onset during adolescence. In addition, epilepsy can be categorized by distinctive

constellations (e.g., mesial temporal lobe epilepsy with hippocampal sclerosis, Rasmussen syndrome, etc.), epilepsies with a structural-metabolic cause (e.g., cortical malformations, neurocutaneous syndromes, tumor, trauma, etc.), angiomas (e.g. perinatal insults, stroke, etc.), or unknown cause (Berg, Berkovic et al. 2010). Inclusive, yet still incomplete, lists of the epilepsies can be found in (Berg, Berkovic et al. 2010; Scheffer, Berkovic et al. 2014; Hubbard and Binder 2016).

1.1.3 Temporal lobe epilepsy with hippocampal sclerosis

Temporal lobe epilepsy (TLE) is a category of epilepsies defined by seizures originating in the temporal lobe. TLE is characterized by a combination of seizure phenotypes (often simple partial seizures with autonomic and sensory phenomena; complex partial seizures usually beginning with motor arrest and typically followed by oroalimentary automatism), memory deficits, hypometabolism, and distinct EEG patterns (temporal spikes, sharp and/or slow waves). Hippocampal seizures are the most common form seen in TLE (ILAE 1989). The estimated incidence of TLE is 50-60% of all epilepsies, although incidences of up to 66% have been reported (Wiebe 2000). This makes TLE the most common form of partial epilepsy. The exact prevalence of TLE, however, is hard to estimate due to the uncertainty of localization in population-based

studies, bias of TLE patients being good surgical candidates in specialty units, and variability in case definitions (Wiebe 2000).

The most common histopathological feature of TLE is hippocampal sclerosis (HS). Again, the incidence has been hard to estimate, but reports of HS in patients with TLE have been as high as 70% (Blümcke, Thom et al. 2013). The ILAE has listed segmental pyramidal cell loss and a severe pattern of astrogliosis (reactive astrocytes defined by immunostained glial fibrillary acidic protein, GFAP) as the hallmarks of HS (Blümcke, Thom et al. 2013). Other reproducible characteristics include broadening of the granule cell layer (granule cell dispersion), mossy fiber sprouting, atrophic behavior of microglia (similar to astrogliosis, but termed microgliosis), microvascular proliferation, and synaptic reorganization (Margerison and Corsellis 1966; Mathern, Pretorius et al. 1995; Blümcke, Beck et al. 1999; Clasadonte and Haydon 2012; de Lanerolle, Lee et al. 2012). Due to the lack of international consensus and the diversity of presentation, the ILAE has recently come up with a classification of HS based on a system of semiquantitative hippocampal cell loss patterns (Blümcke, Thom et al. 2013). HS type 1 is the most common (60-80% of all TLE-HS cases) and is defined as at least 80% cell loss in the CA1 region of the hippocampus accompanied by significant neuronal cell loss in other regions of the hippocampus (CA2-4). HS type 2 is described as having CA1 predominant cell loss with CA2-4 being minimally affected; HS type 2 is estimated to occur in 5-

10% of all surgical epilepsy cases. HS type 3 is characterized by a predominant neuronal loss in CA4 and the dentate gyrus with only a moderate cell loss in CA1-4. The prevalence of HS type 3 is about 4-7.4% of all TLE surgical cases. Finally, no hippocampal sclerosis (gliosis only) is found in about 20% of all TLE surgical cases. Although granule cell dispersion occurs in approximately 50% of epilepsy cases, it was excluded from the classification criteria because it has been variably reported in HS type 1, 2, and 3 (Blümcke, Thom et al. 2013).

1.1.4 Antiepileptic drugs (AEDs)

The management of seizures may involve treatment with AEDs, surgery, dietary restrictions, or lifestyle changes. AEDs are still the primary treatment for patients with epilepsy, but surgery may be necessary after pharmacoresistance has been established. The type of AED used depends on several factors, including the epilepsy syndrome, comorbidities, tolerability by the patient, and mode of action of the drug. Most current AEDs target neuronal glutamate receptors, or γ-aminobutyric acid (GABA) systems, voltage gated sodium channels and calcium channels (Rogawski and Löscher 2004). For example, phenytoin and carbamazepine block sodium channels whereas vigabatrin inhibits GABA transaminase. The mechanisms of several commonly prescribed AEDs, however, are not completely understood (Rogawski and Löscher 2004; Perucca 2005; Kwan, Schachter et al. 2011).

Current AEDs are accompanied by at least two major drawbacks. First, AEDs result in a number of adverse effects, with the most common complaint being impaired cognition or mental slowing (Aldenkamp, De Krom et al. 2003). Other side effects include lethargy, fatigue, insomnia, skin rash, decreased bone mineral density, poor weight management, alopecia, aseptic meningitis, anemia, and vertigo (Perucca and Gilliam 2012). In addition, AEDs can alter the effectiveness of hormonal forms of contraception and can lead to an increased risk of birth defects in pregnant women (Crawford 2005; Wlodarczyk, Palacios et al. 2012). Second, about 30% of patients have poor seizure control and become pharmacoresistant (Cockerell, Johnson et al. 1995; Picot, Baldy-Moulinier et al. 2008; Berg 2009). Interestingly, this estimate may change depending on the definition of pharmacoresistance. While some consider pharmacoresistant epilepsy to mean having more than 1 seizure per month after trying 3 different AEDs, other consider pharmacoresistant epilepsy to mean having any seizures at all after trying at least 2 different AEDs (Berg 2009). Therefore, this statistic is highly varied from study to study. Recently, the ILAE has come up with a consensus on defining pharmacoresistant epilepsy with hierarchical categories (Kwan, Arzimanoglou et al. 2010) which will hopefully aid in future studies on the prevalence of this disease. Nonetheless, it is clear that new pharmacological treatments with non-neuronal targets would aid in the design of new AEDs.

1.2 Animal models of epilepsy

Animal models of epilepsy are crucial to understanding the changes occurring in the healthy brain that converts it to an epileptic one, a process known as epileptogenesis. These models can also be used to test the efficacy and safety of current AEDs, identify new treatment paradigms (pharmacological agents, implants, etc.), and to determine the “disease modifying” effects (i.e., prevention of epileptogenesis), if any, of new treatments (Hubbard and Binder 2016). Due to the importance of all of these factors, it is critical to have reproducible animal models that recapitulate the pathology seen in human epilepsies.

Animal models can be divided into two main categories: acute (seizure) models and chronic (epilepsy) models (Kandratavicius, Balista et al. 2014). Compounds such as pentylenetetrazol (PTZ) and NDMA are widely used to induce acute seizures, but do not result in chronic epilepsy. Electrical stimulation can also be used to generate seizures. Chemical or electrical kindling, however, can result in a chronic model of epilepsy. Other chronic models include genetic and chemoconvulsant models (Sharma, Reams et al. 2007; Kandratavicius, Balista et al. 2014). Hyperthermic, hypoxic, acoustic, and posttraumatic epilepsy models are also frequently employed, although whether they are acute or chronic is debated and dependent on the exact model used (Kandratavicius, Balista et al. 2014).

The two most commonly used chemoconvulsants are kainic acid and pilocarpine, a kainate receptor and muscarinic acetylcholine receptor agonist, respectively. Both of these models involve a sustained period of SE before the development of spontaneous seizures (epilepsy). More importantly, both models are highly reproducible and mimic several histopathological features observed in TLE, including HS. Both chemoconvulsants can be given systemically or focally in the brain, however intraperitoneal injections are often costly, inordinately variable, result in widespread damage, and have a high mortality rate (Babb, Pereira-Leite et al. 1995). Therefore, focal treatment, such as intrahippocampal injections, is often preferred. Pilocarpine, however, can be more variable than kainic acid and can result in extrahippocampal areas being compromised whereas kainic acid has the advantage of causing habitually hippocampus-restricted injuries (Kandratavicius, Balista et al. 2014). Due to the variable pathological presentations of TLE, however, both models are considered valid.

1.2.1 Intrahippocampal kainic acid model of epilepsy

The intrahippocampal kainic acid (IHKA) model is a well-established model of temporal lobe epilepsy (Bouilleret, Ridoux et al. 1999; Riban, Bouilleret et al. 2002; Arabadzisz, Antal et al. 2005; Lee, Hsu et al. 2012; Hubbard, Szu et al. 2016). One major advantage of this model is that animals exhibit one sclerotic hippocampus and one non-sclerotic hippocampus. As discussed earlier, HS is

one of the most common features observed in TLE. Furthermore, non-HS still exhibits extreme gliosis in human TLE, which is also observed in the IHKA model (see Chapter 2). Therefore, the IHKA model of TLE is beneficial because it both mimics the human condition and allows for the comparison of the non-HS to the sclerotic hippocampus.

After IHKA injections are administered, mice wake up in a state of SE that lasts for several hours but subsides spontaneously. Importantly, mice experience a short "latency" period of roughly 7 days where they are not exhibiting behavioral seizures (although altered EEG characteristics have been noted (Lee, Hsu et al. 2012)). In this time, the brain is undergoing extensive morphological alterations and expression changes. After this short time period, mice start exhibiting spontaneous, recurrent seizures. Therefore, that latency period is considered the time when the brain is undergoing epileptogenesis. Increasing our understanding of this critical time period is essential to our understanding of the development of epilepsy.

1.3 Astrocytes

Glial cells found in the central nervous system (CNS) include macroglia (astrocytes, NG2 cells, and oligodendrocytes) and microglia. The most well studied glial cell type is astrocytes, a group of "star-shaped cells" that are

heterogeneous in structure and function. Astrocytes can be divided into protoplasmic and fibrous astrocytes. Protoplasmic astrocytes are found in the gray matter, are highly arborized, appose synapses (Ventura and Harris 1999), and occupy individual domains (Bushong, Martone et al. 2002; Oberheim, Wang et al. 2006; Wilhelmsson, Bushong et al. 2006). Fibrous astrocytes, on the other hand, are found in the white matter, are less arborized, and generally lack domain organization (Butt, Colquhoun et al. 1994). Interestingly, the ratio and morphology of astrocytes increases with the complexity of species (i.e., rodents to humans) (Oberheim, Wang et al. 2006).

1.3.1 Astrocyte functions

The classical view of glial cells was that they were primarily passive, serving as the “glue” to hold neurons together, whereas neurons were thought to be solely responsible for brain information processing (Perea, Sur et al. 2014). Glia were largely ignored in terms of brain function and synaptic transmission. This was likely due to the fundamental difference between neurons and astrocytes: neurons are electrically excitable (can produce “all-or-none” action potentials that propagate through neuronal networks) whereas astrocytes are not. Because of this, astrocytes were often thought of as “silent” partners in the brain. This view has been challenged, however, with the discovery of a number of astrocytic properties which led to the dismissal of the “passive” astrocyte theory; it was

replaced with our current understanding of the “active” astrocyte that plays a role in neurotransmission and neuronal physiology.

Astrocytes were believed to play a primarily supportive role in the brain by maintaining ion and water homeostasis, removing neurotransmitters from the extracellular space, and maintaining the integrity of the blood-brain barrier (Nedergaard 1994; Anderson and Swanson 2000; Simard and Nedergaard 2004; Volterra and Meldolesi 2005). More recently, additional roles for astrocytes have been discovered. These roles include, but are not limited to, the regulation of cerebral blood flow (Zonta, Angulo et al. 2003; Mulligan and MacVicar 2004; Takano, Tian et al. 2006), participation in the brain immune response (Farina, Aloisi et al. 2007), and even the release of neurotransmitters in a process known as gliotransmission (Parpura, Basarsky et al. 1994).

1.3.2 Tripartite synapse

The chemical synapse was traditionally thought to be composed of a pre-synaptic neuron and a post-synaptic neuron. The concept that a 3rd component (the astrocyte) was involved gained popularity in the 1990s, although evidence for a communication system between neurons and astrocytes involving chemical transmitters was hypothesized well before then (Martin 1992). This led to the term “tripartite synapse” to highlight the direct role of astrocytes in synaptic

function (Halassa, Fellin et al. 2007). Astrocytes are actively involved in synaptic transmission, both structurally and functionally, and can determine the strength of synaptic transmission by regulating the extent to which glutamate is rapidly cleared from the extracellular space (Murphy-Royal, Dupuis et al. 2015; Al Awabdh, Gupta-Agarwal et al. 2016).

1.3.3 Astrocytes in epilepsy

Epilepsy has traditionally viewed as a neuronal disease resulting from hypersyncrhonized activity within neuronal networks. It is becoming increasingly clear, however, that astrocytes also play a prominent role in disease progression and maintenance (Tian, Azmi et al. 2005; Binder and Steinhäuser 2006; Seifert, Schilling et al. 2006; Seifert, Carmignoto et al. 2010; Clasadonte and Haydon 2012; Devinsky, Vezzani et al. 2013; Hubbard, Hsu et al. 2013; Coulter and Steinhauser 2015; Wilcox, Gee et al. 2015; Ziebell, Adelson et al. 2015; Eyo, Murugan et al. 2016; Hubbard and Binder 2016). In the epileptic brain, astrocytes undergo morphological and molecular expression changes; they become hypertrophic and “reactive”, as measured by an increase in GFAP immunoreactivity, in the scar forming process of astrogliosis. The expression and function of several astrocytic channels and transporters also become altered resulting in the dysregulation of ion and water homeostasis, disruption of gliotransmission, increase in neuroinflammation, and swelling of astrocytes

(Heinemann, Jauch et al. 2000; Hinterkeuser, Schröder et al. 2000; Kivi, Lehmann et al. 2000; Steinhäuser and Seifert 2002; de Lanerolle and Lee 2005; Seifert, Schilling et al. 2006; Wetherington, Serrano et al. 2008; Seifert, Carmignoto et al. 2010; Binder, Nagelhus et al. 2012; Clasadonte and Haydon 2012; Hubbard, Hsu et al. 2013; Hubbard and Binder 2016; Hubbard, Szu et al. 2016). Just a subset of alterations occurring in epileptic tissue are depicted in Figure 1.1. Therefore, astrocytes play a critical role in epilepsy.

1.4 Glutamate

Glutamate is the main excitatory neurotransmitter in the CNS. It is an L-amino acid with a carboxylic acid side chain that exerts its signaling role by acting on glutamate receptors found on cell membranes. Extracellular glutamate levels determine the extent of receptor stimulation; consequently, it is important to maintain low levels of glutamate in the extracellular space to ensure a high signal-to-noise ratio. Extracellular glutamate concentrations have been estimated to be between 1-30 μM, with the majority of studies finding levels below 5 μM (Danbolt 2001; Moussawi, Riegel et al. 2011). Intracellular glutamate levels are several thousand-fold higher, with the highest concentrations of glutamate found within nerve terminals (Danbolt 2001). During synaptic transmission, extracellular glutamate within the synapse peak at levels

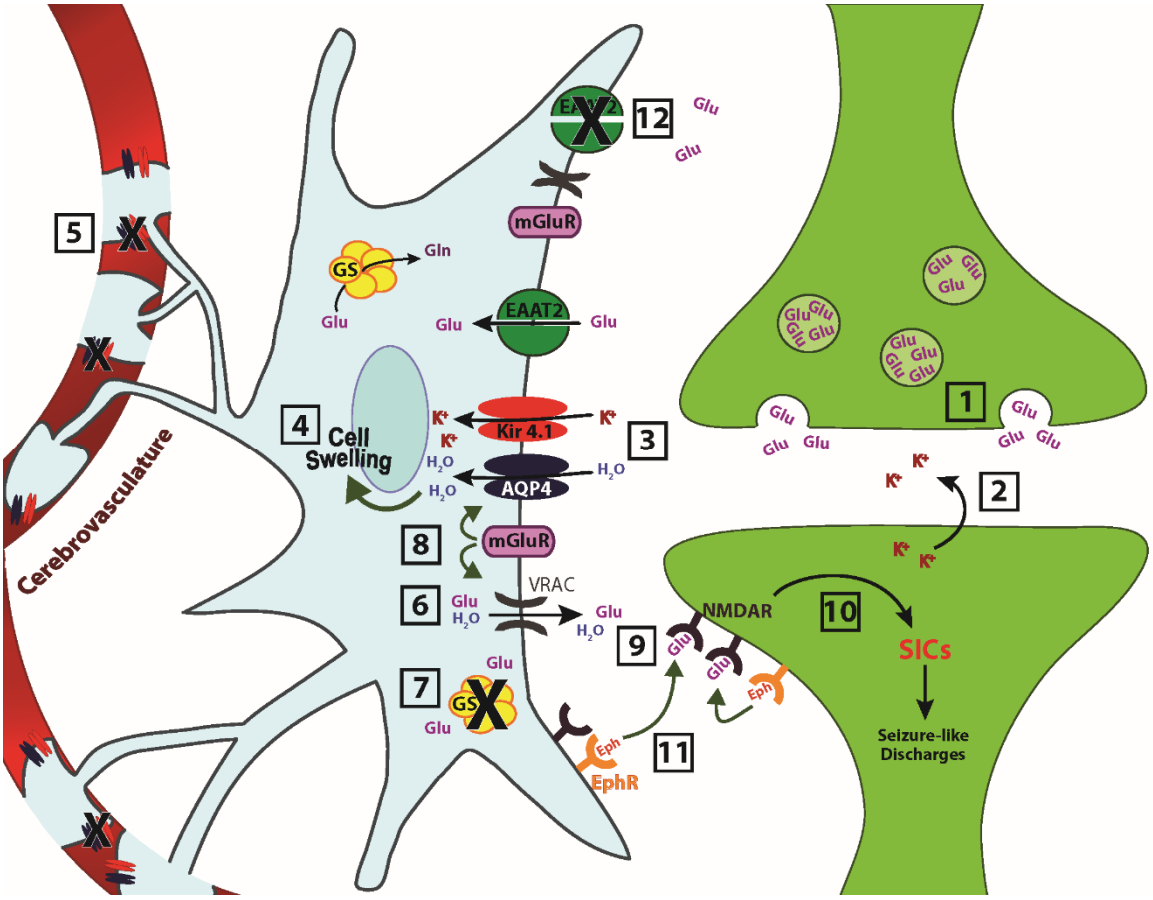

Cerebrovasculature
5
4
Cell Swelling
12
Glu
Glu
mGluR
GS
Gln
Glu
EAAT2
Glu
Glu
K+
K+
Kir 4.1
K+
3
H2O
H2O
AQP4
H2O
8
mGluR
6
Glu
H2O
VRAC
Glu
H2O
7
Glu
GS
Glu
Eph
EphR
11
9
Glu
Glu
Eph
NMDAR
10
SICs
Seizure-like Discharges
1
Glu
2
K+
K+
K+

Figure 1.1. Model for role of astrocyte swelling in neuronal excitability. At an excitatory synapse the neurotransmitter glutamate (Glu) is released from vesicles within the presynaptic terminal (1). Glu binds to receptors on the postsynaptic membrane and opens ion channels (not shown) allowing the movement of ions across the membrane, including the release of potassium ions (2). Elevated levels of K^+ are taken up by perisynaptic astrocytes along with water (H_2O) predominantly by $K_{ir}4.1$ potassium channels and aquaporin-4 (AQP4) channels, respectively (3). This leads to cell swelling and a reduction in extracellular space (4). Loss or redistribution of AQP4 and $K_{ir}4.1$ away from astrocytic endfeet (5) would exacerbate astrocyte swelling since water flux into astrocytes at synapses would be increased while efflux via endfeet into the cerebrovasculature would be decreased. Astrocyte swelling opens volume-regulated anion channels (VRACs), which release glutamate into the extracellular space (6). In addition, reduced expression of glutamine synthetase (GS) in the epileptic condition (7) elevates cytoplasmic concentration of glutamate in astrocytes, providing more glutamate to be released. Upregulation of metabotropic glutamate receptors (mGluRs) in reactive astrocytes could enhance AQP4-dependent swelling and swelling-evoked release of glutamate through VRACs (8). Astrocytically-released glutamate can then bind to extrasynaptic NMDA receptors (NMDARs) (9), generating slow inward currents (SICs) and potentially interictal and ictal (seizure-like) discharges (10). Facilitated by the close proximity of adjacent cellular membranes during cell swelling, Eph receptor (EphR) – ephrin (Eph) ligand interactions may further enhance the stimulation of NMDA receptors (11). EphRs, ephrins, and certain NMDA receptor subunits are upregulated after neural injury on different cell types, including reactive astrocytes and neurons. Reduced excitatory amino transporter 2 (EAAT2) expression in epileptic tissue may lead to delayed clearance of glutamate from the extrasynaptic space (12). All of the above mechanisms may contribute to astrocyte control of neuronal excitability. This figure was reproduced, with permission, from (Hubbard, Hsu et al. 2013).

above 1 mM and those levels decay within milliseconds (Clements, Lester et al. 1992).

Accumulation of glutamate in the extracellular space can lead to cell excitotoxicity. Therefore, the brain must have a powerful protective system to maintain glutamate homeostasis in the brain. First, the blood brain barrier (BBB) helps create an isolated environment that prevents circulating glutamate from entering the brain. Second, at synaptic clefts, neurons are surrounded by astrocytes that have such a high glutamate uptake activity that the healthy, non-compromised brain is remarkably resistant to glutamate toxicity. Third, a number of metabolic enzymes exist that allow for the synthesis and metabolism of glutamate. Finally, a well-established system between neurons and astrocytes, called glutamate-glutamine cycling, allows for the rapid uptake and conversion of glutamate into a non-toxic compound in astrocytes followed by its release into the extracellular space for uptake by neurons. All of these mechanisms are required to prevent neuronal excitotoxicity and all are possible with the aid of astrocytes. Here I will focus on glutamate transporters at the synapse.

1.4.1 Glutamate transporters

Glutamate transporters play a major role in clearing glutamate from the extracellular space. Five excitatory amino acid transporters (EAAT1-5) help clear

glutamate from the extracellular space to help resist glutamate toxicity. The rodent homologs to EAAT1-5 are glutamate aspartate transporter (GLAST), glutamate transporter-1 (GLT1), excitatory amino acid carrier-1 (EAAC1), EAAT4, and EAAT5, respectively. GLAST and GLT1 are primarily found on astrocytes whereas EAAC1, EAAT4, and EAAT5 are predominantly expressed by neurons. These transporters co-transport three Na^+ and one H^+ into the cell along with glutamate in exchange for the release of one K^+. GLAST, GLT1, and EAAC1 are efficient glutamate transporters with small associated macroscopic anion currents whereas EAAT4 and EAAT5 are low-capacity transporters that have a predominant anion (Cl^-) conductance (Jensen, Fahlke et al. 2015). GLAST expression is most prominent in the cerebellum with only moderate levels in the forebrain whereas GLT1 expression is most abundant in the forebrain and low within the cerebellum. EAAC1 is expressed at low levels throughout the brain. EAAT4 is only found in the cerebellum whereas EAAT5 is only found in the retina.

At the tripartite synapse, the pre- and post-synaptic neurons are surrounded by astrocytes that abundantly express glutamate transporters. GLT1 is responsible for the majority of glutamate clearance after synaptic activity and is essential in glutamate uptake. Although the cycle time of glutamate transport has been measured to be slow, ranging from 11-80 ms (Danbolt 2001), it is possible that the highly efficient removal of glutamate from the extracellular space may be due

to both the ability of the transporters to quickly bind glutamate and their sheer abundance. Recently, it was discovered that even though GLT1 is anchored to the membrane at synapses, it can become untethered after glutamate is released into the extracellular space and can perform rapid, activity-regulated surface diffusion (Murphy-Royal, Dupuis et al. 2015; Al Awabdh, Gupta-Agarwal et al. 2016). Therefore, GLT1 can readily move between synaptic and nonsynaptic sites to ensure glutamate clearance and effectively shape excitatory postsynaptic currents.

1.4.2 Glial glutamate transporter expression

GLAST and GLT1 are found throughout the CNS and are almost exclusively expressed on astrocytes. Previous studies have only found GLT1 mRNA, but not protein, in neurons of the healthy adult CNS (Danbolt 2001) but more recent studies have reported functional GLT1 protein in excitatory nerve terminals (Chen, Mahadomrongkul et al. 2004; Furness, Dehnes et al. 2008; Petr, Sun et al. 2015). GLT1 protein is also transiently expressed in several neuronal populations during development in the rodent and sheep brain, however this expression disappears on maturation. GLAST is the dominant glutamate transporter in the cerebellum, expressed most densely on the Bergmann glia (Lehre, Levy et al. 1995), and GLT1 is the predominant glutamate transporter in the forebrain, expressed most heavily in the hippocampus. GLAST levels are

estimated to be 3,200 and 18,000 per μm^3 tissue in the young adult rat stratum radiatum in the hippocampus (CA1) and the cerebellar molecular layer, respectively (Lehre and Danbolt 1998). The number of GLT1 in the young adult rat stratum radiatum of the hippocampus (CA1) was measured to be 12,000 per μm^3 tissue and only 2,800 per μm^3 in the cerebellar molecular layer (Lehre and Danbolt 1998).

1.4.3 Neuronal glutamate transporter expression

EAAC1 concentration is lower than that of the other EAATs and is mostly expressed in neurons. Unlike GLT1 and GLAST, EAAC1 is mostly intracellular and can transport cysteine. It is most abundantly expressed in the hippocampus, cerebellum, and basal ganglia (Danbolt 2001) and is found in a variety of neurons. Although it is predominantly expressed by neurons in the healthy CNS, EAAC1 has also been found in oligodendrocytes and, in the injured brain, in microglia (Bianchi, Bardelli et al. 2014). Administration of EAAC1 antisense oligonucleotide in rats has been shown to produce mild neurotoxicity and seizures in less than a week of treatment (Rothstein, Dykes-Hoberg et al. 1996). The expression of EAAT4 is predominantly cerebellar, but low levels have been detected in the forebrain. It is most extensively found on the Purkinje cell plasma membrane and the highest levels are found perisynaptically (Dehnes, Chaudhry et al. 1998). The average concentration of EAAT4 in the molecular layer of adult

rats is estimated to be 1,900 molecules per μm^3 tissue. Even though EAAT4 shares a similar mechanism to EAAT1-3, it operates 5-10 times more slowly (Mim, Balani et al. 2005). Unlike EAAT1-3, both EAAT4 and EAAT5 are highly associated with Cl^- conductance. EAAT5 is only found in the retina and is considered a low-capacity and low-affinity glutamate transporter (Schneider, Cordeiro et al. 2014).

1.5 Glial glutamate transporters in epilepsy

It is widely accepted that delayed clearance of extracellular glutamate is implicated in seizure development and spread (During and Spencer 1993; Glass and Dragunow 1995; Tanaka, Watase et al. 1997; Campbell and Hablitz 2004; Hubbard, Hsu et al. 2013). During and Spencer (1993) used microdialysis probes to record glutamate levels in the hippocampus before and during a seizure in human patients with complex partial epilepsy refractory to medical treatment. The dialysate concentration of glutamate rose before the occurrence of a seizure, which was followed by a sustained increase, potentially to neurotoxic levels, during a seizure in the epileptic hippocampus (During and Spencer 1993). Elevated levels of extracellular glutamate have been reported in patients with various epilepsies, which could potentially be a consequence of altered expression or activity of glutamate transporters.

1.5.1 Glial glutamate transporters in animal models of epilepsy

Glial glutamate transporters are essential in maintaining low extracellular glutamate concentrations. GLT1-deficient mice suffered from lethal spontaneous seizure due to the elevated extracellular glutamate levels in the brain (Tanaka, Watase et al. 1997). Deletion (Tanaka, Watase et al. 1997) or antisense oligonucleotide-mediate inhibition of synthesis (Rothstein, Dykes-Hoberg et al. 1996) of GLT1 in rodents revealed that it is the major contributor to glutamate uptake from the extracellular space. Intraventricular administration of GLT1 antisense oligonucleotide in rats resulted in a 32-fold rise in extracellular glutamate, measured by a microdialysis probe in the striatum. In addition, this treatment resulted in a progressive motor syndrome that included mildly paretic hindlimbs and dystonic posture (Rothstein, Dykes-Hoberg et al. 1996). Overexpression of GLT1 in transgenic mice, on the other hand, attenuated epileptogenesis and reduced chronic seizure frequency in a pilocarpine model of epilepsy (Kong, Takahashi et al. 2012). Without GLT1, glutamate levels rise enough to cause neurotoxicity and seizures whereas overexpression of GLT1 can offer neuroprotective effects.

Mice lacking GLAST showed increased cerebellar damage after brain injury and motor discoordination (Watase, Hashimoto et al. 1998). In the amygdala kindling model, duration of generalized seizures was prolonged by about 35% in GLAST-

deficient mice (Watanabe, Morimoto et al. 1999). GLAST-deficient mice also showed a shorter latency period and more severe stages of pentylenetetrazol (PTZ)-induced seizures compared to wild-type mice (Watanabe, Morimoto et al. 1999). The inhibition of synthesis of GLAST by antisense oligonucleotides in rats resulted in a 13-fold rise in extracellular glutamate dialysate in the striatum and a progressive motor syndrome (Rothstein, Dykes-Hoberg et al. 1996). Like GLT1, GLAST plays a role in modulating extracellular glutamate levels and deletion of it may result in neurotoxicity.

Reduced levels of GLT1 (Sakurai, Kurokawa et al. 2015; Hubbard, Szu et al. 2016) and GLAST (Ueda, Doi et al. 2001) have been reported in kainic acid and pilocarpine (Lopes, Soares et al. 2013) models of epilepsy. GLT1 has also been reported to be downregulated in genetic (Akbar, Rattray et al. 1998; Ingram, Wiseman et al. 2001; Dutuit, Touret et al. 2002) and post-traumatic (Samuelsson, Kumlien et al. 2000) models of epilepsy. Similarly, GLAST has been reported to be downregulated in the electrical kindling (Miller, Levey et al. 1997), genetic (Dutuit, Touret et al. 2002; Guo, Sun et al. 2010), and post-traumatic (Ueda and Willmore 2000) models of epilepsy. The results, however, are controversial. For example, increased expression of GLT1 has been reported in the kainic acid (Simantov, Crispino et al. 1999), post-traumatic (Ueda and Willmore 2000), and various genetic (Ingram, Tessler et al. 2000; Guo, Sun et al. 2010) models of epilepsy. Similarly, increased levels of GLAST were reported in the kainic acid

(Nonaka, Kohmura et al. 1998) and genetic (Ingram, Tessler et al. 2000) models of epilepsy. To complicate this topic even further, both GLAST and GLT1 levels have been reported as unchanged in the electrical kindling (Akbar, Torp et al. 1997; Miller, Levey et al. 1997), post-traumatic (Samuelsson, Kumlien et al. 2000; Ueda and Willmore 2000), and various genetic models (Ingram, Wiseman et al. 2001; Dutuit, Touret et al. 2002) of epilepsy. These discrepancies can be explained by the different models used, brain regions explored, time points examined, and evaluation of mRNA versus protein. Therefore, this field would greatly benefit from more thorough analyses of mRNA, protein, and immunohistochemical changes of these crucial glial glutamate transporters at various time points in a chronic epilepsy model.

1.5.2 Glial glutamate transporters in human epilepsy

Reduced EAAT2 expression has been reported in the sclerotic hippocampus of human patients with TLE but either no change or increased EAAT2 immunoreactivity has been found in non-HS tissue (Mathern, D. et al. 1999; Tessler, Danbolt et al. 1999; Crino, Jin et al. 2002; Proper, Hoogland et al. 2002; Eid, Thomas et al. 2004; van der Hel, Notenboom et al. 2005; Bjørnsen, Eid et al. 2007). Equivocal results on EAAT1 expression include reports of upregulated (Mathern, D. et al. 1999) and downregulated (Proper, Hoogland et al. 2002)

expression in HS and unaltered (Mathern, D. et al. 1999) or slightly reduced (Tessler, Danbolt et al. 1999) expression in non-HS in TLE patients.

In studies examining the dysplastic tissue of human patients with focal cortical dysplasia (FCD), decreased immunoreactivity and more diffuse pattern of EAAT1 and EAAT2 expression were observed (Ulu, Tanriverdi et al. 2010; González-Martínez, Ying et al. 2011). No changes were found in EAAT2 mRNA in the epileptic foci compared to the nonepileptic regions of human neocortical epilepsy tissue, bur EAAT2 protein expression was reduced (Rakhade and Loeb 2008). Support of these findings was found in a freeze-induced rat model of cortical dysplasia. The non-selective glutamate transporter antagonist DL-threo-β-benzyloxyaspartic acid (TBOA) prolonged postsynaptic currents (PSCs) and decreased the threshold for evoking epileptiform activity in lesioned cortex compared to controls (Campbell and Hablitz 2008). This effect could be mimicked with the specific GLT1 antagonist dihydrokainate (DHK), suggesting a role of GLT1 in regulating network excitability.

1.6 Ceftriaxone

It is clear that glutamate is the principal excitatory neurotransmitter in the brain and that it is critical to maintain at low extracellular concentrations. GLT1 is responsible for at least 90% of glutamate clearance in the forebrain (Kim, Lee et

al. 2011). GLT1 has also been reported as downregulated in a number of neurological disorders including in amyotrophic lateral sclerosis (Rothstein, Van Kammen et al. 1995), Alzheimer's disease (Li, Mallory et al. 1997), and in a model of temporal lobe epilepsy (Hubbard, Szu et al. 2016). Therefore, a pharmacological tool to restore GLT1 levels would be beneficial for a wide range of patients.

In 2005, Rothstein *et al.* (2005) screened 1,040 compounds and discovered that the cephalosporin (β-lactam) antibiotic ceftriaxone could increase GLT1 expression (Rothstein, Patel et al. 2005). This discovery was revolutionary not only because it could modulate the expression of possibly the most abundant protein in the brain, but it was also a cheap, readily available, and FDA approved drug. In addition, ceftriaxone had the potential to offer neuroprotection in a wide variety of diseases. In fact, ceftriaxone-induced GLT1 expression has shown to have beneficial effects in models of ethanol and drug addiction (Sari, Smith et al. 2009; Sari, Sakai et al. 2011; Fischer, Houston et al. 2013; Lee, Ruby et al. 2013; Qrunfleh, Alazizi et al. 2013; Sari, Franklin et al. 2013; Sari, Sreemantula et al. 2013; Abulseoud, Camsari et al. 2014; Alhaddad, Das et al. 2014; Rao and Sari 2014; Dodman, Featherstone et al. 2015; Sari, Toalston et al. 2016), ALS (Rothstein, Patel et al. 2005), post-traumatic epilepsy (Goodrich, Kabakov et al. 2013), visceral pain (Lin, Tian et al. 2009; Ackerman, Jellison et al. 2015), neuropathic pain (Inquimbert, Bartels et al. 2012), hypoxia (Jagadapillai, Mellen

et al. 2014), ischemia (Chu, Lee et al. 2007), Huntington's disease (Miller, Dorner et al. 2008; Sari, Prieto et al. 2010), prepulse inhibition of the acoustic startle reflex (Bellesi, Melone et al. 2009), subarachnoid hemorrhage (Feng, Wang et al. 2014), spinal muscular atrophy (Nizzardo, Nardini et al. 2011), traumatic brain injury (Wei, Pan et al. 2012; Goodrich, Kabakov et al. 2013), thiamine deficiency (Jhala, Wang et al. 2011), and memory deficits in aquaporin-4 knockout mice (Li, Wang et al. 2012; Yang, Li et al. 2013). The proposed mechanism of GLT1 regulation was through induction of the nuclear factor-κB pathway.

The effects of ceftriaxone have been equivocal. Ceftriaxone failed to regulate GLT1 expression in a more recent drug screen study (Carbone, Duty et al. 2012) and failed to have any clinical efficacy in a stage 3 ALS study (Cudkowicz, Titus et al. 2014). Ceftriaxone did not alter GLT1 levels in an animal model of myelin oligodendrocyte glycoprotein-induced experimental autoimmune encephalomyelitis (EAE) (Melzer, Meuth et al. 2008), stroke (Thöne-Reineke, Neumann et al. 2008), and perinatal hypoxic-ischemic encephalopathy (Lai, Huang et al. 2011). In all of these cases, however, ceftriaxone offered therapeutic benefits through other means such as modulation of the inflammatory process (Melzer, Meuth et al. 2008) or upregulation of neurotrophins (Thöne-Reineke, Neumann et al. 2008). Other proposed effects of ceftriaxone include increased expression of the cystine/glutamate exchange transporter (Alhaddad,

Das et al. 2014; Rao and Sari 2014) and upregulation of several transcription factors (Nizzardo, Nardini et al. 2011).

Ceftriaxone may also upregulate GLT1 in a region- or cell-specific manner (Jhala, Wang et al. 2011; Lai, Huang et al. 2011). For example, ceftriaxone failed to increase GLT1 in the corpus callosum, hippocampus, and striatum in neonatal rats but did increase GLT1 in the cortex (Lai, Huang et al. 2011). In a model of thiamine deficiency, ceftriaxone increased GLT1 in the inferior colliculus but not the thalamus or frontal cortex (Jhala, Wang et al. 2011).

Studies involving models of ischemic cortical lesions (Kim and Jones 2013), neuropathic pain (Amin, Hajhashemi et al. 2012; Hajhashemi, Hosseinzadeh et al. 2013), and seizures (Jelenkovic, Jovanovic et al. 2008; Rawls, Karaca et al. 2010) demonstrated that ceftriaxone could alleviate symptoms of the disease, but did not directly examine the effect on GLT1 expression levels. Therefore, it is possible that other mechanisms, such as neuroinflammatory modulation, alleviated symptoms instead of (or in addition to) increased GLT1 expression. Ceftriaxone and two other β-lactam drugs, clavulanic acid and tazobactam, reduced seizure-like activity in an invertebrate model (Rawls, Karaca et al. 2010). The therapeutic potential of increased GLT1 expression has already been demonstrated in a chronic epilepsy model using transgenic mice with a 1.5-2 fold increase in GLT1 levels; the transgenic mice had decreased pilocarpine-induced

seizure frequency, neuronal degeneration, mossy fiber sprouting, and SE-induced death (Kong, Takahashi et al. 2012). Ceftriaxone and other β-lactam drugs, however, have never been tested in a chronic model of TLE.

1.7 Aquaporins

The aquaporins (AQPs) are a family of water channels responsible for fluid transport in response to changes in the osmotic gradient. AQPs are expressed in different tissues and cell types. At least 13 AQPs have been identified, but only a subset of them have been found in the brain (Badaut, Fukuda et al. 2014). Among them is aquaporin-4 (AQP4), an astrocyte-specific protein expressed throughout the CNS. The expression of AQP4 is polarized with high expression at sites of fluid transport, such as pial and ependymal surfaces in contact with CSF, subarachnoid space, the ventricular system, and astrocytic end-feet around capillaries (Nielsen, Nagelhus et al. 1997; Rash, Yasumura et al. 1998; Nagelhus, Mathiisen et al. 2004; Oshio, Binder et al. 2004; Costa, Tortosa et al. 2007). Not surprisingly, AQP4 participates in fluid exchange between both the blood and CSF compartments in the brain (Nagelhus, Mathiisen et al. 2004). AQP4 knockout mice were originally created in the Verkman laboratory using a targeting vector for homologous recombination (Ma, Yang et al. 1997). The initial study found that in general, AQP4 knockout mice exhibited normal development, survival, growth, blood chemistry, and neuromuscular function. Mice did,

however, exhibit a minor urinary concentration deficit (Ma, Yang et al. 1997). Later on, it was discovered that blood-brain barrier function, baseline intracranial pressure, and intracranial compliance were also unaltered (Manley, Fujimura et al. 2000; Papadopoulos, Manley et al. 2004) but astrocyte water permeability was decreased (Solenov, Watanabe et al. 2004). AQP4 knockout mice also suffer from a hearing deficit (Li and Verkman 2001) and mild impairment in retinal function (Li, Patil et al. 2002). Thanks to these knockout mice, it is now known that AQP4 plays a role in K^+ homeostasis (Binder, Yao et al. 2006) the regulation of the brain extracellular space volume (Binder, Papadopoulos et al. 2004), synaptic plasticity (Skucas, Mathews et al. 2011), spatial memory (Zhang, Li et al. 2013), astrocyte migration (Saadoun, Papadopoulos et al. 2005), and cell adhesion (Hiroaki, Tani et al. 2006).

1.7.1 Aquaporin-4 in epilepsy

Aquaporin-4 knockout mice exhibit different seizure phenotypes compared to their wild-type counterparts. Intraperitoneal injections of 40 mg/kg PTZ was sufficient to induce seizures in 100% of wild-type mice but only induced seizures in 1 out of 7 AQP4 knockout mice (Binder, Oshio et al. 2004). At the higher dose of 50 mg/kg, all mice exhibited seizures, but the latency to seizures was increased in the knockout mice (Binder, Oshio et al. 2004). AQP4 knockout mice also had higher seizure threshold but prolonged seizure duration in an electrical

stimulation model of seizures (Binder, Yao et al. 2006). In the IHKA model of epilepsy, AQP4 knockout mice also exhibited an increased number of seizures compared to wild-type mice (Lee, Hsu et al. 2012). Therefore, although it is harder to induce seizures in AQP4 knockout mice, once that threshold is reached, these mice seem to have a worsened seizure phenotype (increased number and duration of seizures) compared to wild-type mice.

AQP4 expression is altered in various models of epilepsy. After pilocarpine-induced SE, AQP4-deleted areas were detected in the piriform cortex but not the hippocampus (Kim, Yeo et al. 2010). Several weeks after pilocarpine-induced SE (in the chronic phase), AQP4 immunoreactivity was significant decreased in vacuolized CA1 astrocytes but increased in non-vacuolized astrocytes (Kim, Ryu et al. 2009). In the intrahippocampal kainic acid model, AQP4 immunoreactivity was immediately downregulated in the hippocampus with only partial recovery over time (Lee, Hsu et al. 2012). Reduced AQP4 adluminal expression with stable or slightly increased abluminal expression was reported in the intraperitoneal kainic acid rat model (Alvestad, Hammer et al. 2013). A similar mislocalization of AQP4 expression with an overall increase in AQP4 levels was found in the sclerotic hippocampus in human TLE (Lee, Eid et al. 2004; Eid, Lee et al. 2005) and focal cortical dysplasia type IIB (Medici, Frassoni et al. 2011). Taken together, AQP4 is likely reduced in regions of the brain that would reduce fluid homeostasis. More detailed studies investigating the expression changes

during epileptogenesis would increase our understanding of the role of AQP4 in epilepsy. This would aid in the discovery of drugs that could modify AQP4 expression. One study has demonstrated that ceftriaxone can also increase AQP4 expression in the caudate-putamen, but this was done in type 1 equilibrative nucleoside transporter (ENT1) knockout mice (Lee, Ruby et al. 2013). The efficacy of modulating AQP4 expression by β-lactam drugs needs to be investigated further.

1.8 Summary

In summary, both GLT1 and AQP4 clearly play a vital role in both the healthy and epileptic brain. Although they have both been studied in epilepsy models, the data are both ambivalent and incomplete. A region-specific investigation of both mRNA and protein expression changes during epileptogenesis in a chronic epilepsy model would greatly benefit the field. In this dissertation, I will describe histological characteristics of the intrahippocampal kainic acid model of TLE with a focus on astrocytes. I will then describe the expression patterns of AQP4 in the healthy and epileptic rodent brain. Next, I will discuss GLT1 changes that occur after IHKA-induced epilepsy. After that, I will discuss the lack of effects that β-lactam drugs have on regulating both AQP4 and GLT1 expression. I will then describe the pattern of co-localization, but lack of a strong physical interaction, between AQP4 and GLT1 in both C57BL/6 and CD1 mice. Since GLT1 is only

one of the two glial glutamate transporters, I will then discuss the regulation of GLAST in the IHKA model in the penultimate chapter. Finally, I will conclude with a brief chapter discussing the implications of my findings and describing the potential future directions.

1.9 References

Abulseoud, O. A., U. M. Camsari, C. L. Ruby, A. Kasasbeh, S. Choi and D. S. Choi (2014). "Attenuation of ethanol withdrawal by ceftriaxone-induced upregulation of glutamate transporter EAAT2." Neuropsychopharmacology **39**(7): 1674-1684.

Ackerman, A. L., F. C. Jellison, U. J. Lee, S. Bradesi and L. V. Rodriguez (2015). "Glt1 glutamate receptor mediates the establishment and perpetuation of chronic visceral pain in an animal model of stress-induced bladder hyperalgesia." Am J Physiol Renal Physiol: ajprenal 00297 02015.

Akbar, M. T., M. Rattray, R. J. Williams, N. W. Chong and B. S. Meldrum (1998). "Reduction of GABA and glutamate transporter messenger RNAs in the severe-seizure genetically epilepsy-prone rat." Neuroscience **85**(4): 1235-1251.

Akbar, M. T., R. Torp, N. C. Danbolt, L. M. Levy, B. S. Meldrum and O. P. Ottersen (1997). "Expression of glial glutamate transporters GLT-1 and GLAST is unchanged in the hippocampus in fully kindled rats." Neuroscience **78**(2): 351-359.

Al Awabdh, S., S. Gupta-Agarwal, D. F. Sheehan, J. Muir, R. Norkett, A. E. Twelvetrees, L. D. Griffin and J. T. Kittler (2016). "Neuronal activity mediated regulation of glutamate transporter GLT-1 surface diffusion in rat astrocytes in dissociated and slice cultures." Glia **64**(7): 1252-1264.

Aldenkamp, A. P., M. De Krom and R. Reijs (2003). "Newer antiepileptic drugs and cognitive issues." Epilepsia **44**: 21-29.

Alhaddad, H., S. C. Das and Y. Sari (2014). "Effects of ceftriaxone on ethanol intake: a possible role for xCT and GLT-1 isoforms modulation of glutamate levels in P rats." Psychopharmacology (Berl) **231**(20): 4049-4057.

Alvestad, S., J. Hammer, E. H. Hoddevik, O. Skare, U. Sonnewald, M. Amiry-Moghaddam and O. P. Ottersen (2013). "Mislocalization of AQP4 precedes chronic seizures in the kainate model of temporal lobe epilepsy." Epilepsy Res **105**(1-2): 30-41.

Amin, B., V. Hajhashemi, H. Hosseinzadeh and K. Abnous (2012). "Antinociceptive evaluation of ceftriaxone and minocycline alone and in combination in a neuropathic pain model in rat." Neuroscience **224**: 15-25.

Anderson, C. M. and R. A. Swanson (2000). "Astrocyte glutamate transport: review of properties, regulation, and physiological functions." Glia **32**(1): 1-14.

Arabadzisz, D., K. Antal, F. Parpan, Z. Emri and J. M. Fritschy (2005). "Epileptogenesis and chronic seizures in a mouse model of temporal lobe epilepsy are associated with distinct EEG patterns and selective neurochemical alterations in the contralateral hippocampus." Exp Neurol **194**(1): 76-90.

Babb, T. L., J. Pereira-Leite, G. W. Mathern and J. K. Pretorius (1995). "Kainic acid induced hippocampal seizures in rats: comparisons of acute and chronic seizures using intrahippocampal versus systemic injections." Ital J Neurol Sci **16**(1-2): 39-44.

Badaut, J., A. M. Fukuda, A. Jullienne and K. G. Petry (2014). "Aquaporin and brain diseases." Biochim Biophys Acta **1840**(5): 1554-1565.

Bellesi, M., M. Melone, A. Gubbini, S. Battistacci and F. Conti (2009). "GLT-1 upregulation impairs prepulse inhibition of the startle reflex in adult rats." Glia **57**(7): 703-713.

Berg, A. T. (2009). "Identification of pharmacoresistant epilepsy." Neurol Clin **27**(4): 1003-1013.

Berg, A. T., S. F. Berkovic, M. J. Brodie, J. Buchhalter, J. H. Cross, W. van Emde Boas, J. Engel, J. French, T. A. Glauser, G. W. Mathern, S. L. Moshe, D. Nordli, P. Plouin and I. E. Scheffer (2010). "Revised terminology and concepts for organization of seizures and epilepsies: report of the ILAE Commission on Classification and Terminology, 2005-2009." Epilepsia **51**(4): 676-685.

Bianchi, M. G., D. Bardelli, M. Chiu and O. Bussolati (2014). "Changes in the expression of the glutamate transporter EAAT3/EAAC1 in health and disease." Cell Mol Life Sci **71**(11): 2001-2015.

Binder, D. K., E. A. Nagelhus and O. P. Ottersen (2012). "Aquaporin-4 and epilepsy." Glia **60**(8): 1203-1214.

Binder, D. K., K. Oshio, T. Ma, A. S. Verkman and G. T. Manley (2004). "Increased seizure threshold in mice lacking aquaporin-4 water channels." Neuroreport **15**(2): 259-262.

Binder, D. K., M. C. Papadopoulos, P. M. Haggie and A. S. Verkman (2004). "In vivo measurement of brain extracellular space diffusion by cortical surface photobleaching." J Neurosci **24**(37): 8049-8056.

Binder, D. K. and C. Steinhäuser (2006). "Functional changes in astroglial cells in epilepsy." Glia **54**(5): 358-368.

Binder, D. K., X. Yao, Z. Zador, T. J. Sick, A. S. Verkman and G. T. Manley (2006). "Increased seizure duration and slowed potassium kinetics in mice lacking aquaporin-4 water channels." Glia **53**(6): 631-636.

Bjørnsen, L. P., T. Eid, S. Holmseth, N. C. Danbolt, D. D. Spencer and N. C. de Lanerolle (2007). "Changes in glial glutamate transporters in human epileptogenic hippocampus: inadequate explanation for high extracellular glutamate during seizures." Neurobiol Dis **25**(2): 319-330.

Blümcke, I., H. Beck, A. A. Lie and O. D. Wiestler (1999). "Molecular neuropathology of human mesial temporal lobe epilepsy." Epilepsy Res **36**(2-3): 205-223.

Blümcke, I., M. Thom, E. Aronica, D. D. Armstrong, F. Bartolomei, A. Bernasconi, N. Bernasconi, C. G. Bien, F. Cendes, R. Coras, J. H. Cross, T. S. Jacques, P. Kahane, G. W. Mathern, H. Miyata, S. L. Moshé, B. Oz, Ç. Özkara, E. Perucca, S. Sisodiya, S. Wiebe and R. Spreafico (2013). "International consensus classification of hippocampal sclerosis in temporal lobe epilepsy: a Task Force report from the ILAE Commission on Diagnostic Methods." Epilepsia **54**(7): 1315-1329.

Bouilleret, V., V. Ridoux, A. Depaulis, C. Marescaux, A. Nehlig and G. Le Gal La Salle (1999). "Recurrent seizures and hippocampal sclerosis following intrahippocampal kainate injection in adult mice: electroencephalography, histopathology and synaptic reorganization similar to mesial temporal lobe epilepsy." Neuroscience **89**(3): 717-729.

Bushong, E. A., M. E. Martone, Y. Z. Jones and M. H. Ellisman (2002). "Protoplasmic astrocytes in CA1 stratum radiatum occupy separate anatomical domains." J Neurosci **22**(1): 183-192.

Butt, A. M., K. Colquhoun, M. Tutton and M. Berry (1994). "Three-dimensional morphology of astrocytes and oligodendrocytes in the intact mouse optic nerve." J Neurocytol **23**(8): 469-485.

Campbell, S. L. and J. J. Hablitz (2004). "Glutamate transporters regulate excitability in local networks in rat neocortex." Neuroscience **127**: 625-635.

Campbell, S. L. and J. J. Hablitz (2008). "Decreased glutamate transport enhances excitability in a rat model of cortical dysplasia." Neurobiol Dis **32**(2): 254-261.

Carbone, M., S. Duty and M. Rattray (2012). "Riluzole elevates GLT-1 activity and levels in striatal astrocytes." Neurochem Int **60**(1): 31-38.

Chen, W., V. Mahadomrongkul, U. V. Berger, M. Bassan, T. DeSilva, K. Tanaka, N. Irwin, C. Aoki and P. A. Rosenberg (2004). "The glutamate transporter GLT1a is expressed in excitatory axon terminals of mature hippocampal neurons." J Neurosci **24**(5): 1136-1148.

Chu, K., S. T. Lee, D. I. Sinn, S. Y. Ko, E. H. Kim, J. M. Kim, S. J. Kim, D. K. Park, K. H. Jung, E. C. Song, S. K. Lee, M. Kim and J. K. Roh (2007). "Pharmacological Induction of Ischemic Tolerance by Glutamate Transporter-1 (EAAT2) Upregulation." Stroke **38**(1): 177-182.

Clasadonte, J. and P. G. Haydon (2012). Astrocytes and Epilepsy. Jasper's Basic Mechanisms of the Epilepsies. J. L. Noebels, M. Avoli, M. A. Rogawski, R. W. Olsen and A. V. Delgado-Escueta. Bethesda (MD).

Clasadonte, J. and P. G. Haydon (2012). Astrocytes and epilepsy. Jasper's Basic Mechanisms of the Epilepsies. J. L. Noebles, Avoli, M., Rogawski, M.A., Olsen, R.W., Delgado-Escueta, A.V.**:** 19.

Clements, J. D., R. A. Lester, G. Tong, C. E. Jahr and G. L. Westbrook (1992). "The time course of glutamate in the synaptic cleft." Science **258**(5087): 1498-1501.

Cockerell, O. C., A. L. Johnson, J. W. Sander, Y. M. Hart and S. D. Shorvon (1995). "Remission of epilepsy: results from the National General Practice Study of Epilepsy." Lancet **346**(8968): 140-144.

Costa, C., R. Tortosa, A. Domenech, E. Vidal, M. Pumarola and A. Bassols (2007). "Mapping of aggrecan, hyaluronic acid, heparan sulphate proteoglycans and aquaporin 4 in the central nervous system of the mouse." J Chem Neuroanat **33**(3): 111-123.

Coulter, D. A. and C. Steinhauser (2015). "Role of astrocytes in epilepsy." Cold Spring Harb Perspect Med **5**(3): a022434.

Crawford, P. (2005). "Best practice guidelines for the management of women with epilepsy." Epilepsia **46**(Suppl. 9): 117-124.

Crino, P. B., H. Jin, M. D. Shumate, M. B. Robinson, D. A. Coulter and A. R. Brooks-Kayal (2002). "Increased expression of the neuronal glutamate transporter (EAAT3/EAAC1) in hippocampal and neocortical epilepsy." Epilepsia **43**(3): 211-218.

Cudkowicz, M. E., S. Titus, M. Kearney, H. Yu, A. Sherman, D. Schoenfeld, D. Hayden, A. Shui, B. Brooks, R. Conwit, D. Felsenstein, D. J. Greenblatt, M. Keroack, J. T. Kissel, R. Miller, J. Rosenfeld, J. D. Rothstein, E. Simpson, N. Tolkoff-Rubin, L. Zinman and J. M. Shefner (2014). "Safety and efficacy of ceftriaxone for amyotrophic lateral sclerosis: a multi-stage, randomised, double-blind, placebo-controlled trial." Lancet Neurol **13**(11): 1083-1091.

Danbolt, N. C. (2001). "Glutamate uptake." Progress in Neurobiology **65**: 1-105.

de Lanerolle, N. C. and T. Lee (2005). "New facets of the neuropathology and molecular profile of human temporal lobe epilepsy." Epilepsy & Behavior **7**: 190-203.

de Lanerolle, N. C., T. S. Lee and D. D. Spencer (2012). Histopathology of Human Epilepsy. Jasper's Basic Mechanisms of the Epilepsies. J. L. Noebels, M. Avoli, M. A. Rogawski, R. W. Olsen and A. V. Delgado-Escueta. Bethesda (MD).

Dehnes, Y., F. A. Chaudhry, K. Ullensvang, K. P. Lehre, J. Storm-Mathisen and N. C. Danbolt (1998). "The glutamate transporter EAAT4 in rat cerebellar Purkinje cells: a glutamate-gated chloride channel concentrated near the synapse in parts of the dendritic membrane facing astroglia." J Neurosci **18**(10): 3606-3619.

Devinsky, O., A. Vezzani, S. Najjar, N. C. De Lanerolle and M. A. Rogawski (2013). "Glia and epilepsy: excitability and inflammation." Trends Neurosci **36**(3): 174-184.

Devinsky, O., B. G. Vickrey, J. Cramer, K. Perrine, B. Hermann, K. Meador and R. D. Hays (1995). "Development of the quality of life in epilepsy inventory." Epilepsia **36**(11): 1089-1104.

Dodman, K., R. E. Featherstone, J. Bang, Y. Liang and S. J. Siegel (2015). "Ceftriaxone reverses ketamine-induced lasting EEG and astrocyte alterations in juvenile mice." Drug Alcohol Depend **156**: 14-20.

During, M. J. and D. D. Spencer (1993). "Extracellular hippocampal glutamate and spontaneous seizure in the conscious human brain." The Lancet **341**(8861): 1607-1610.

Dutuit, M., M. Touret, R. Szymocha, A. Nehlig, M. F. Belin and M. Didier-Bazes (2002). "Decreased expression of glutamate transporters in genetic absence epilepsy rats before seizure occurrence." J Neurochem **80**(6): 1029-1038.

Eid, T., T. S. Lee, M. J. Thomas, M. Amiry-Moghaddam, L. P. Bjornsen, D. D. Spencer, P. Agre, O. P. Ottersen and N. C. de Lanerolle (2005). "Loss of perivascular aquaporin 4 may underlie deficient water and K+ homeostasis in the human epileptogenic hippocampus." Proc Natl Acad Sci U S A **102**(4): 1193-1198.

Eid, T., M. J. Thomas, D. D. Spencer, E. Runden-Pran, J. C. Lai, G. V. Malthankar, J. H. Kim, N. C. Danbolt, O. P. Ottersen and N. C. de Lanerolle (2004). "Loss of glutamine synthetase in the human epileptogenic hippocampus: possible mechanism for raised extracellular glutamate in mesial temporal lobe epilepsy." Lancet **363**(9402): 28-37.

Engel, J. (2006). "Report of the ILAE Classification Core Group." Aktuelle Neurologie **33**(8): 442-452.

Engel, J., Jr. (2001). "A proposed diagnostic scheme for people with epileptic seizures and with epilepsy: report of the ILAE Task Force on Classification and Terminology." Epilepsia **42**(6): 796-803.

Engel, J., Jr. (2006). "ILAE classification of epilepsy syndromes." Epilepsy Res **70 Suppl 1**: S5-10.

Eyo, U. B., M. Murugan and L. J. Wu (2016). "Microglia-Neuron Communication in Epilepsy." Glia.

Farina, C., F. Aloisi and E. Meinl (2007). "Astrocytes are active players in cerebral innate immunity." Trends Immunol **28**(3): 138-145.

Feng, D., W. Wang, Y. Dong, L. Wu, J. Huang, Y. Ma, Z. Zhang, S. Wu, G. Gao and H. Qin (2014). "Ceftriaxone alleviates early brain injury after subarachnoid hemorrhage by increasing excitatory amino acid transporter

2 expression via the PI3K/Akt/NF-kappaB signaling pathway." Neuroscience **268**: 21-32.

Fischer, K. D., A. C. Houston and G. V. Rebec (2013). "Role of the major glutamate transporter GLT1 in nucleus accumbens core versus shell in cue-induced cocaine-seeking behavior." J Neurosci **33**(22): 9319-9327.

Fisher, R. S., C. Acevedo, A. Arzimanoglou, A. Bogacz, J. H. Cross, C. E. Elger, J. Engel, Jr., L. Forsgren, J. A. French, M. Glynn, D. C. Hesdorffer, B. I. Lee, G. W. Mathern, S. L. Moshe, E. Perucca, I. E. Scheffer, T. Tomson, M. Watanabe and S. Wiebe (2014). "ILAE official report: a practical clinical definition of epilepsy." Epilepsia **55**(4): 475-482.

Furness, D. N., Y. Dehnes, A. Q. Akhtar, D. J. Rossi, M. Hamann, N. J. Grutle, V. Gundersen, S. Holmseth, K. P. Lehre, K. Ullensvang, M. Wojewodzic, Y. Zhou, D. Attwell and N. C. Danbolt (2008). "A quantitative assessment of glutamate uptake into hippocampal synaptic terminals and astrocytes: new insights into a neuronal role for excitatory amino acid transporter 2 (EAAT2)." Neuroscience **157**(1): 80-94.

Glass, M. and M. Dragunow (1995). "Neurochemical and morphological changes associated with human epilepsy." Brain Research Reviews **21**: 29-41.

González-Martínez, J. A., Z. Ying, R. Prayson, W. Bingaman and I. Najm (2011). "Glutamate clearance mechanism in resected cortical dysplasia." Journal of Neurosurgery **114**: 1195-1202.

Goodrich, G. S., A. Y. Kabakov, M. Q. Hameed, S. C. Dhamne, P. A. Rosenberg and A. Rotenberg (2013). "Ceftriaxone treatment after traumatic brain injury restores expression of the glutamate transporter, GLT-1, reduces regional gliosis, and reduces post-traumatic seizures in the rat." J Neurotrauma **30**(16): 1434-1441.

Guo, F., F. Sun, J. L. Yu, Q. H. Wang, D. Y. Tu, X. Y. Mao, R. Liu, K. C. Wu, N. Xie, L. Y. Hao and J. Q. Cai (2010). "Abnormal expressions of glutamate transporters and metabotropic glutamate receptor 1 in the spontaneously epileptic rat hippocampus." Brain Res Bull **81**(4-5): 510-516.

Hajhashemi, V., H. Hosseinzadeh and B. Amin (2013). "Antiallodynia and antihyperalgesia effects of ceftriaxone in treatment of chronic neuropathic pain in rats." Acta Neuropsychiatr **25**(1): 27-32.

Halassa, M. M., T. Fellin and P. G. Haydon (2007). "The tripartite synapse: roles for gliotransmission in health and disease." Trends Mol Med **13**(2): 54-63.

Heinemann, U., G. R. Jauch, J. K. Schulze, A. Kivi, A. Eilers, R. Kovacs and T. N. Lehmann (2000). "Alterations of glial cell functions in temporal lobe epilepsy." Epilepsia **41**(Suppl. 6): S285-S189.

Hesdorffer, D. C., G. Logroscino, E. K. Benn, N. Katri, G. Cascino and W. A. Hauser (2011). "Estimating risk for developing epilepsy: a population-based study in Rochester, Minnesota." Neurology **76**(1): 23-27.

Hinterkeuser, S., W. Schröder, G. Hager, G. Seifert, I. Blümcke, C. E. Elger, J. Schramm and C. Steinhäuser (2000). "Astrocytes in the hippocampus of patients with temporal lobe epilepsy display changes in potassium conductances." European Journal of Neuroscience **12**: 2087-2096.

Hiroaki, Y., K. Tani, A. Kamegawa, N. Gyobu, K. Nishikawa, H. Suzuki, T. Walz, S. Sasaki, K. Mitsuoka, K. Kimura, A. Mizoguchi and Y. Fujiyoshi (2006). "Implications of the aquaporin-4 structure on array formation and cell adhesion." J Mol Biol **355**(4): 628-639.

Hubbard, J. A. and D. K. Binder (2016). Astrocytes and Epilepsy. Amsterdam, Netherlands, Elsevier, in press.

Hubbard, J. A., M. S. Hsu, T. A. Fiacco and D. K. Binder (2013). "Glial cell changes in epilepsy: overview of the clinical problem and therapeutic opportunities." Neurochem Int **63**(7): 638-651.

Hubbard, J. A., J. I. Szu, J. M. Yonan and D. K. Binder (2016). "Regulation of astrocyte glutamate transporter-1 (GLT1) and aquaporin-4 (AQP4) expression in a model of epilepsy." Exp Neurol.

ILAE (1989). "Proposal for revised classification of epilepsies and epileptic syndromes. Commission on Classification and Terminology of the International League Against Epilepsy." Epilepsia **30**(4): 389-399.

Ingram, E. M., S. Tessler, N. G. Bowery and P. C. Emson (2000). "Glial glutamate transporter mRNAs in the genetically absence epilepsy rat from Strasbourg." Brain Res Mol Brain Res **75**(1): 96-104.

Ingram, E. M., J. W. Wiseman, S. Tessler and P. C. Emson (2001). "Reduction of glial glutamate transporters in the parietal cortex and hippocampus of the EL mouse." J Neurochem **79**(3): 564-575.

Inquimbert, P., K. Bartels, O. B. Babaniyi, L. B. Barrett, I. Tegeder and J. Scholz (2012). "Peripheral nerve injury produces a sustained shift in the balance

between glutamate release and uptake in the dorsal horn of the spinal cord." Pain **153**(12): 2422-2431.

Jacoby, A., D. Snape, S. Lane and G. A. Baker (2015). "Self-reported anxiety and sleep problems in people with epilepsy and their association with quality of life." Epilepsy Behav **43**: 149-158.

Jagadapillai, R., N. M. Mellen, L. R. Sachleben, Jr. and E. Gozal (2014). "Ceftriaxone preserves glutamate transporters and prevents intermittent hypoxia-induced vulnerability to brain excitotoxic injury." PLoS One **9**(7): e100230.

Jelenkovic, A. V., M. D. Jovanovic, D. D. Stanimirovic, D. D. Bokonjic, G. G. Ocic and B. S. Boskovic (2008). "Beneficial effects of ceftriaxone against pentylenetetrazole-evoked convulsions." Exp Biol Med (Maywood) **233**(11): 1389-1394.

Jensen, A. A., C. Fahlke, W. E. Bjorn-Yoshimoto and L. Bunch (2015). "Excitatory amino acid transporters: recent insights into molecular mechanisms, novel modes of modulation and new therapeutic possibilities." Curr Opin Pharmacol **20C**: 116-123.

Jhala, S. S., D. Wang and A. S. Hazell (2011). "Loss of the glutamate transporter splice-variant GLT-1b in inferior colliculus and its prevention by ceftriaxone in thiamine deficiency." Neurochem Int **58**(5): 558-563.

Kandratavicius, L., P. A. Balista, C. Lopes-Aguiar, R. N. Ruggiero, E. H. Umeoka, N. Garcia-Cairasco, L. S. Bueno-Junior and J. P. Leite (2014). "Animal models of epilepsy: use and limitations." Neuropsychiatr Dis Treat **10**: 1693-1705.

Kim, J. E., H. J. Ryu, S. I. Yeo, C. H. Seo, B. C. Lee, I. G. Choi, D. S. Kim and T. C. Kang (2009). "Differential expressions of aquaporin subtypes in astroglia in the hippocampus of chronic epileptic rats." Neuroscience **163**(3): 781-789.

Kim, J. E., S. I. Yeo, H. J. Ryu, M. J. Kim, D. S. Kim, S. M. Jo and T. C. Kang (2010). "Astroglial loss and edema formation in the rat piriform cortex and hippocampus following pilocarpine-induced status epilepticus." J Comp Neurol **518**(22): 4612-4628.

Kim, K., S. G. Lee, T. P. Kegelman, Z. Z. Su, S. K. Das, R. Dash, S. Dasgupta, P. M. Barral, M. Hedvat, P. Diaz, J. C. Reed, J. L. Stebbins, M. Pellecchia, D. Sarkar and P. B. Fisher (2011). "Role of excitatory amino acid

transporter-2 (EAAT2) and glutamate in neurodegeneration: opportunities for developing novel therapeutics." J Cell Physiol **226**(10): 2484-2493.

Kim, S. Y. and T. A. Jones (2013). "The effects of ceftriaxone on skill learning and motor functional outcome after ischemic cortical damage in rats." Restor Neurol Neurosci **31**(1): 87-97.

Kivi, A., T. N. Lehmann, R. Kovács, A. Eilers, R. Jauch, H. J. Meencke, A. von Deimling, U. Heinemann and S. Gabriel (2000). "Effects of barium on stimulus-induced rises of $[K^+]_o$ in human epileptic non-sclerotic and sclerotic hippocampal area CA1." European Journal of Neuroscience **12**: 2039-2048.

Kong, Q., K. Takahashi, D. Schulte, N. Stouffer, Y. Lin and C. G. Lin (2012). "Increased glial glutamate transporter EAAT2 expression reduces epileptogenic processes following pilocarpine-induced status epilepticus." Neurobiology of Disease **47**: 145-154.

Kong, Q., K. Takahashi, D. Schulte, N. Stouffer, Y. Lin and C. L. Lin (2012). "Increased glial glutamate transporter EAAT2 expression reduces epileptogenic processes following pilocarpine-induced status epilepticus." Neurobiol Dis **47**(2): 145-154.

Kwan, P., A. Arzimanoglou, A. T. Berg, M. J. Brodie, W. Allen Hauser, G. Mathern, S. L. Moshe, E. Perucca, S. Wiebe and J. French (2010). "Definition of drug resistant epilepsy: consensus proposal by the ad hoc Task Force of the ILAE Commission on Therapeutic Strategies." Epilepsia **51**(6): 1069-1077.

Kwan, P., S. C. Schachter and M. J. Brodie (2011). "Drug-resistant epilepsy." N Engl J Med **365**(10): 919-926.

Lai, P. C., Y. T. Huang, C. C. Wu, C. J. Lai, P. J. Wang and T. H. Chiu (2011). "Ceftriaxone attenuates hypoxic-ischemic brain injury in neonatal rats." J Biomed Sci **18**: 69.

Lee, D. J., M. S. Hsu, M. M. Seldin, J. L. Arellano and D. K. Binder (2012). "Decreased expression of the glial water channel aquaporin-4 in the intrahippocampal kainic acid model of epileptogenesis." Exp Neurol **235**(1): 246-255.

Lee, M. R., C. L. Ruby, D. J. Hinton, S. Choi, C. A. Adams, N. Young Kang and D. S. Choi (2013). "Striatal adenosine signaling regulates EAAT2 and

astrocytic AQP4 expression and alcohol drinking in mice." Neuropsychopharmacology **38**(3): 437-445.

Lee, T. S., T. Eid, S. Mane, J. H. Kim, D. D. Spencer, O. P. Ottersen and N. C. de Lanerolle (2004). "Aquaporin-4 is increased in the sclerotic hippocampus in human temporal lobe epilepsy." Acta Neuropathol **108**(6): 493-502.

Lehre, K. P. and N. C. Danbolt (1998). "The number of glutamate transporter subtype molecules at glutamatergic synapses: chemical and stereological quantification in young adult rat brain." J Neurosci **18**(21): 8751-8757.

Lehre, K. P., L. M. Levy, O. P. Ottersen, J. Storm-Mathisen and N. C. Danbolt (1995). "Differential expression of two glial glutamate transporters in the rat brain: quantitative and immunocytochemical observations." J Neurosci **15**(3 Pt 1): 1835-1853.

Li, J., R. V. Patil and A. S. Verkman (2002). "Mildly abnormal retinal function in transgenic mice without Muller cell aquaporin-4 water channels." Invest Ophthalmol Vis Sci **43**(2): 573-579.

Li, J. and A. S. Verkman (2001). "Impaired hearing in mice lacking aquaporin-4 water channels." J Biol Chem **276**(33): 31233-31237.

Li, S., M. Mallory, M. Alford, S. Tanaka and E. Masliah (1997). "Glutamate transporter alterations in Alzheimer disease are possibly associated with abnormal APP expression." J Neuropathol Exp Neurol **56**(8): 901-911.

Li, Y. K., F. Wang, W. Wang, Y. Luo, P. F. Wu, J. L. Xiao, Z. L. Hu, Y. Jin, G. Hu and J. G. Chen (2012). "Aquaporin-4 deficiency impairs synaptic plasticity and associative fear memory in the lateral amygdala: involvement of downregulation of glutamate transporter-1 expression." Neuropsychopharmacology **37**(8): 1867-1878.

Lin, Y., G. Tian, K. Roman, C. Handy, J. B. Travers, C. L. Lin and R. L. Stephens, Jr. (2009). "Increased glial glutamate transporter EAAT2 expression reduces visceral nociceptive response in mice." Am J Physiol Gastrointest Liver Physiol **296**(1): G129-134.

Lopes, M. W., F. M. Soares, N. de Mello, J. C. Nunes, A. G. Cajado, D. de Brito, F. M. de Cordova, R. M. da Cunha, R. Walz and R. B. Leal (2013). "Time-dependent modulation of AMPA receptor phosphorylation and mRNA expression of NMDA receptors and glial glutamate transporters in the rat

hippocampus and cerebral cortex in a pilocarpine model of epilepsy." Exp Brain Res **226**(2): 153-163.

Ma, T., B. Yang, A. Gillespie, E. J. Carlson, C. J. Epstein and A. S. Verkman (1997). "Generation and phenotype of a transgenic knockout mouse lacking the mercurial-insensitive water channel aquaporin-4." J Clin Invest **100**(5): 957-962.

Manley, G. T., M. Fujimura, T. Ma, N. Noshita, F. Filiz, A. W. Bollen, P. Chan and A. S. Verkman (2000). "Aquaporin-4 deletion in mice reduces brain edema after acute water intoxication and ischemic stroke." Nat Med **6**(2): 159-163.

Margerison, J. H. and J. A. Corsellis (1966). "Epilepsy and the temporal lobes. A clinical, electroencephalographic and neuropathological study of the brain in epilepsy, with particular reference to the temporal lobes." Brain **89**(3): 499-530.

Martin, D. L. (1992). "Synthesis and release of neuroactive substances by glial cells." Glia **5**(2): 81-94.

Mathern, G. W., M. D., A. Lozado, J. K. Pretorius, Y. Dehnes, N. C. Danbolt, N. Nelson, J. P. Leite, L. Chimelli, D. E. Born, A. C. Sakamoto, J. A. Assirati, I. Fried, W. J. Peacock, G. A. Ojemann and P. D. Adelson (1999). "Hippocampal GABA and glutamate transporter immunoreactivity in patients with temporal lobe epilepsy." Neurology **52**(3): 453-472.

Mathern, G. W., J. K. Pretorius and T. L. Babb (1995). "Quantified patterns of mossy fiber sprouting and neuron densities in hippocampal and lesional seizures." J Neurosurg **82**(2): 211-219.

McCagh, J., J. E. Fisk and G. A. Baker (2009). "Epilepsy, psychosocial and cognitive functioning." Epilepsy Res **86**(1): 1-14.

Medici, V., C. Frassoni, L. Tassi, R. Spreafico and R. Garbelli (2011). "Aquaporin 4 expression in control and epileptic human cerebral cortex." Brain Res **1367**: 330-339.

Melzer, N., S. G. Meuth, D. Torres-Salazar, S. Bittner, A. L. Zozulya, C. Weidenfeller, A. Kotsiari, M. Stangel, C. Fahlke and H. Wiendl (2008). "A beta-lactam antibiotic dampens excitotoxic inflammatory CNS damage in a mouse model of multiple sclerosis." PLoS One **3**(9): e3149.

Miller, B. R., J. L. Dorner, M. Shou, Y. Sari, S. J. Barton, D. R. Sengelaub, R. T. Kennedy and G. V. Rebec (2008). "Up-regulation of GLT1 expression increases glutamate uptake and attenuates the Huntington's disease phenotype in the R6/2 mouse." Neuroscience **153**(1): 329-337.

Miller, H. P., A. I. Levey, J. D. Rothstein, A. V. Tzingounis and P. J. Conn (1997). "Alterations in glutamate transporter protein levels in kindling-induced epilepsy." J Neurochem **68**(4): 1564-1570.

Mim, C., P. Balani, T. Rauen and C. Grewer (2005). "The glutamate transporter subtypes EAAT4 and EAATs 1-3 transport glutamate with dramatically different kinetics and voltage dependence but share a common uptake mechanism." J Gen Physiol **126**(6): 571-589.

Moussawi, K., A. Riegel, S. Nair and P. W. Kalivas (2011). "Extracellular glutamate: functional compartments operate in different concentration ranges." Front Syst Neurosci **5**: 94.

Mulligan, S. J. and B. A. MacVicar (2004). "Calcium transients in astrocyte endfeet cause cerebrovascular constrictions." Nature **431**(7005): 195-199.

Murphy-Royal, C., J. P. Dupuis, J. A. Varela, A. Panatier, B. Pinson, J. Baufreton, L. Groc and S. H. Oliet (2015). "Surface diffusion of astrocytic glutamate transporters shapes synaptic transmission." Nat Neurosci **18**(2): 219-226.

Nagelhus, E. A., T. M. Mathiisen and O. P. Ottersen (2004). "Aquaporin-4 in the central nervous system: cellular and subcellular distribution and coexpression with KIR4.1." Neuroscience **129**(4): 905-913.

Nedergaard, M. (1994). "Direct signaling from astrocytes to neurons in cultures of mammalian brain cells." Science **263**(5154): 1768-1771.

Nielsen, S., E. A. Nagelhus, M. Amiry-Moghaddam, C. Bourque, P. Agre and O. P. Ottersen (1997). "Specialized membrane domains for water transport in glial cells: high-resolution immunogold cytochemistry of aquaporin-4 in rat brain." J Neurosci **17**(1): 171-180.

Nizzardo, M., M. Nardini, D. Ronchi, S. Salani, C. Donadoni, F. Fortunato, G. Colciago, M. Falcone, C. Simone, G. Riboldi, A. Govoni, N. Bresolin, G. P. Comi and S. Corti (2011). "Beta-lactam antibiotic offers neuroprotection in a spinal muscular atrophy model by multiple mechanisms." Exp Neurol **229**(2): 214-225.

Nonaka, M., E. Kohmura, T. Yamashita, S. Shimada, K. Tanaka, T. Yoshimine, M. Tohyama and T. Hayakawa (1998). "Increased transcription of glutamate-aspartate transporter (GLAST/GluT-1) mRNA following kainic acid-induced limbic seizure." Brain Res Mol Brain Res **55**(1): 54-60.

Oberheim, N. A., X. Wang, S. Goldman and M. Nedergaard (2006). "Astrocytic complexity distinguishes the human brain." Trends Neurosci **29**(10): 547-553.

Oshio, K., D. K. Binder, B. Yang, S. Schecter, A. S. Verkman and G. T. Manley (2004). "Expression of aquaporin water channels in mouse spinal cord." Neuroscience **127**(3): 685-693.

Papadopoulos, M. C., G. T. Manley, S. Krishna and A. S. Verkman (2004). "Aquaporin-4 facilitates reabsorption of excess fluid in vasogenic brain edema." FASEB J **18**(11): 1291-1293.

Parpura, V., T. A. Basarsky, F. Liu, K. Jeftinija, S. Jeftinija and P. G. Haydon (1994). "Glutamate-mediated astrocyte-neuron signalling." Nature **369**(6483): 744-747.

Perea, G., M. Sur and A. Araque (2014). "Neuron-glia networks: integral gear of brain function." Front Cell Neurosci **8**: 378.

Perucca, E. (2005). "An introduction to antiepileptic drugs." Epilepsia **46**(Suppl. 4).

Perucca, P. and F. G. Gilliam (2012). "Adverse effects of antiepileptic drugs." The Lancet Neurology **11**(9): 792-802.

Petr, G. T., Y. Sun, N. M. Frederick, Y. Zhou, S. C. Dhamne, M. Q. Hameed, C. Miranda, E. A. Bedoya, K. D. Fischer, W. Armsen, J. Wang, N. C. Danbolt, A. Rotenberg, C. J. Aoki and P. A. Rosenberg (2015). "Conditional deletion of the glutamate transporter GLT-1 reveals that astrocytic GLT-1 protects against fatal epilepsy while neuronal GLT-1 contributes significantly to glutamate uptake into synaptosomes." J Neurosci **35**(13): 5187-5201.

Picot, M. C., M. Baldy-Moulinier, J. P. Daures, P. Dujols and A. Crespel (2008). "The prevalence of epilepsy and pharmacoresistant epilepsy in adults: a population-based study in a Western European country." Epilepsia **49**(7): 1230-1238.

Proper, E. A., G. Hoogland, S. M. Kappen, G. H. Jansen, M. G. Rensen, L. H. Schrama, C. W. van Veelen, P. C. van Rijen, O. van Nieuwenhuizen, W. H. Gispen and P. N. de Graan (2002). "Distribution of glutamate transporters in the hippocampus of patients with pharmaco-resistant temporal lobe epilepsy." Brain **125**(Pt 1): 32-43.

Qrunfleh, A. M., A. Alazizi and Y. Sari (2013). "Ceftriaxone, a beta-lactam antibiotic, attenuates relapse-like ethanol-drinking behavior in alcohol-preferring rats." J Psychopharmacol **27**(6): 541-549.

Rakhade, S. N. and J. A. Loeb (2008). "Focal reduction of neuronal glutamate transporters in human neocortical epilepsy." Epilepsia **49**(2): 226-236.

Rao, P. S. and Y. Sari (2014). "Effects of ceftriaxone on chronic ethanol consumption: a potential role for xCT and GLT1 modulation of glutamate levels in male P rats." J Mol Neurosci **54**(1): 71-77.

Raol, Y. H. and A. R. Brooks-Kayal (2012). "Experimental models of seizures and epilepsies." Prog Mol Biol Transl Sci **105**: 57-82.

Rash, J. E., T. Yasumura, C. S. Hudson, P. Agre and S. Nielsen (1998). "Direct immunogold labeling of aquaporin-4 in square arrays of astrocyte and ependymocyte plasma membranes in rat brain and spinal cord." Proc Natl Acad Sci U S A **95**(20): 11981-11986.

Rawls, S. M., F. Karaca, I. Madhani, V. Bhojani, R. L. Martinez, M. Abou-Gharbia and R. B. Raffa (2010). "beta-lactamase inhibitors display anti-seizure properties in an invertebrate assay." Neuroscience **169**(4): 1800-1804.

Riban, V., V. Bouilleret, B. T. Pham-Le, J. M. Fritschy, C. Marescaux and A. Depaulis (2002). "Evolution of hippocampal epileptic activity during the development of hippocampal sclerosis in a mouse model of temporal lobe epilepsy." Neuroscience **112**(1): 101-111.

Rogawski, M. A. and W. Löscher (2004). "The neurobiology of antiepileptic drugs." Nat Rev Neurosci **5**(7): 553-564.

Rothstein, J. D., M. Dykes-Hoberg, C. A. Pardo, L. A. Bristol, L. Jin, R. W. Kuncl, Y. Kanai, M. A. Hediger, Y. F. Wang, J. P. Schielke and D. F. Welty (1996). "Knockout of glutamate transporters reveals a major role for astroglial transport in excitotoxicity and clearance of glutamate." Neuron **16**: 675-686.

Rothstein, J. D., S. Patel, M. R. Regan, C. Haenggeli, Y. H. Huang, D. E. Bergles, L. Jin, M. Dykes Hoberg, S. Vidensky, D. S. Chung, S. V. Toan, L. I. Bruijn, Z. Z. Su, P. Gupta and P. B. Fisher (2005). "Beta-lactam antibiotics offer neuroprotection by increasing glutamate transporter expression." Nature **433**(7021): 73-77.

Rothstein, J. D., M. Van Kammen, A. I. Levey, L. J. Martin and R. W. Kuncl (1995). "Selective loss of glial glutamate transporter GLT-1 in amyotrophic lateral sclerosis." Ann Neurol **38**(1): 73-84.

Saadoun, S., M. C. Papadopoulos, H. Watanabe, D. Yan, G. T. Manley and A. S. Verkman (2005). "Involvement of aquaporin-4 in astroglial cell migration and glial scar formation." J Cell Sci **118**(Pt 24): 5691-5698.

Sakurai, M., H. Kurokawa, A. Shimada, K. Nakamura, H. Miyata and T. Morita (2015). "Excitatory amino acid transporter 2 downregulation correlates with thalamic neuronal death following kainic acid-induced status epilepticus in rat." Neuropathology **35**(1): 1-9.

Samuelsson, C., E. Kumlien, R. Flink, D. Lindholm and E. Ronne-Engstrom (2000). "Decreased cortical levels of astrocytic glutamate transport protein GLT-1 in a rat model of posttraumatic epilepsy." Neurosci Lett **289**(3): 185-188.

Sari, Y., K. M. Franklin, A. Alazizi, P. S. Rao and R. L. Bell (2013). "Effects of ceftriaxone on the acquisition and maintenance of ethanol drinking in peri-adolescent and adult female alcohol-preferring (P) rats." Neuroscience **241**: 229-238.

Sari, Y., A. L. Prieto, S. J. Barton, B. R. Miller and G. V. Rebec (2010). "Ceftriaxone-induced up-regulation of cortical and striatal GLT1 in the R6/2 model of Huntington's disease." J Biomed Sci **17**: 62.

Sari, Y., M. Sakai, J. M. Weedman, G. V. Rebec and R. L. Bell (2011). "Ceftriaxone, a beta-lactam antibiotic, reduces ethanol consumption in alcohol-preferring rats." Alcohol Alcohol **46**(3): 239-246.

Sari, Y., K. D. Smith, P. K. Ali and G. V. Rebec (2009). "Upregulation of GLT1 attenuates cue-induced reinstatement of cocaine-seeking behavior in rats." J Neurosci **29**(29): 9239-9243.

Sari, Y., S. N. Sreemantula, M. R. Lee and D. S. Choi (2013). "Ceftriaxone treatment affects the levels of GLT1 and ENT1 as well as ethanol intake in alcohol-preferring rats." J Mol Neurosci **51**(3): 779-787.

Sari, Y., J. E. Toalston, P. S. Rao and R. L. Bell (2016). "Effects of ceftriaxone on ethanol, nicotine or sucrose intake by alcohol-preferring (P) rats and its association with GLT-1 expression." Neuroscience **326**: 117-125.

Scheffer, I. E., S. F. Berkovic, P. Capovilla and e. al. (2014). "The organization of the epilepsies: report of the ILAE Commission on Classification and Terminology." ILAE website.

Schneider, N., S. Cordeiro, J. P. Machtens, S. Braams, T. Rauen and C. Fahlke (2014). "Functional properties of the retinal glutamate transporters GLT-1c and EAAT5." J Biol Chem **289**(3): 1815-1824.

Seifert, G., G. Carmignoto and C. Steinhäuser (2010). "Astrocyte dysfunction in epilepsy." Brain Research Reviews **63**: 212-221.

Seifert, G., K. Schilling and C. Steinhäuser (2006). "Astrocyte dysfunction in neurological disorders: a molecular perspective." Nature Reviews Neuroscience **7**(194-206).

Sharma, A. K., R. Y. Reams, W. H. Jordan, M. A. Miller, H. L. Thacker and P. W. Snyder (2007). "Mesial temporal lobe epilepsy: pathogenesis, induced rodent models and lesions." Toxicol Pathol **35**(7): 984-999.

Simantov, R., M. Crispino, W. Hoe, G. Broutman, G. Tocco, J. D. Rothstein and M. Baudry (1999). "Changes in expression of neuronal and glial glutamate transporters in rat hippocampus following kainate-induced seizure activity." Brain Res Mol Brain Res **65**(1): 112-123.

Simard, M. and M. Nedergaard (2004). "The neurobiology of glia in the context of water and ion homeostasis." Neuroscience **129**(4): 877-896.

Skucas, V. A., I. B. Mathews, J. Yang, Q. Cheng, A. Treister, A. M. Duffy, A. S. Verkman, B. L. Hempstead, M. A. Wood, D. K. Binder and H. E. Scharfman (2011). "Impairment of select forms of spatial memory and neurotrophin-dependent synaptic plasticity by deletion of glial aquaporin-4." J Neurosci **31**(17): 6392-6397.

Solenov, E., H. Watanabe, G. T. Manley and A. S. Verkman (2004). "Sevenfold-reduced osmotic water permeability in primary astrocyte cultures from AQP-4-deficient mice, measured by a fluorescence quenching method." Am J Physiol Cell Physiol **286**(2): C426-432.

Steinhäuser, C. and G. Seifert (2002). "Glial membrane channels and receptors in epilepsy: imact for generation and spread of seizure activity." European Journal of Pharmacology **447**: 227-237.

Takano, T., G. F. Tian, W. Peng, N. Lou, W. Libionka, X. Han and M. Nedergaard (2006). "Astrocyte-mediated control of cerebral blood flow." Nat Neurosci **9**(2): 260-267.

Tanaka, K., K. Watase, T. Manabe, K. Yamada, M. Watanabe, K. Takahashi, H. Iwama, T. Nishikawa, N. Ichihara, T. Kikuchi, S. Okuyama, N. Kawashima, S. Hori, M. Takimoto and K. Wada (1997). "Epilepsy and exacerbation of brain injury in mice lacking the glutamate transporter GLT-1." Science **276**: 1699-1702.

Tessler, S., N. C. Danbolt, R. L. Faull, J. Storm-Mathisen and P. C. Emson (1999). "Expression of the glutamate transporters in human temporal lobe epilepsy." Neuroscience **88**(4): 1083-1091.

Thöne-Reineke, C., C. Neumann, P. Namsolleck, K. Schmerbach, M. Krikov, J. H. Schefe, K. Lucht, H. Hörtnagl, M. Godes, S. Muller, K. Rumschüssel, H. Funke-Kaiser, A. Villringer, U. M. Steckelings and T. Unger (2008). "The beta-lactam antibiotic, ceftriaxone, dramatically improves survival, increases glutamate uptake and induces neurotrophins in stroke." J Hypertens **26**(12): 2426-2435.

Tian, G., H. Azmi, T. Takano, Q. Xu, W. Peng, J. Lin, N. Oberheim, N. Lou, R. Zielke, J. Kang and M. Nedergaard (2005). "An astrocytic basis of epilepsy." Nature Medicine **11**(9): 973-981.

Trinka, E., H. Cock, D. Hesdorffer, A. O. Rossetti, I. E. Scheffer, S. Shinnar, S. Shorvon and D. H. Lowenstein (2015). "A definition and classification of status epilepticus--Report of the ILAE Task Force on Classification of Status Epilepticus." Epilepsia **56**(10): 1515-1523.

Ueda, Y., T. Doi, J. Tokumaru, H. Yokoyama, A. Nakajima, Y. Mitsuyama, H. Ohya-Nishiguchi, H. Kamada and L. J. Willmore (2001). "Collapse of extracellular glutamate regulation during epileptogenesis: down-regulation and functional failure of glutamate transporter function in rats with chronic seizures induced by kainic acid." J Neurochem **76**(3): 892-900.

Ueda, Y. and L. J. Willmore (2000). "Sequential changes in glutamate transporter protein levels during Fe(3+)-induced epileptogenesis." Epilepsy Res **39**(3): 201-209.

Ulu, M. O., T. Tanriverdi, B. Oz, H. Biceroglu, C. Isler, B. S. Eraslan, C. Ozkara, E. Ozyurt and M. Uzan (2010). "The expression of astroglial glutamate transporters in patients with focal cortical dysplasia: an immunohistochemical study." Acta Neuropathologica **152**: 845-853.

van der Hel, W. S., R. G. Notenboom, I. W. Bos, P. C. van Rijen, C. W. van Veelen and P. N. de Graan (2005). "Reduced glutamine synthetase in hippocampal areas with neuron loss in temporal lobe epilepsy." Neurology **64**(2): 326-333.

Ventura, R. and K. M. Harris (1999). "Three-dimensional relationships between hippocampal synapses and astrocytes." J Neurosci **19**(16): 6897-6906.

Volterra, A. and J. Meldolesi (2005). "Astrocytes, from brain glue to communication elements: the revolution continues." Nat Rev Neurosci **6**(8): 626-640.

Watanabe, T., K. Morimoto, T. Hirao, H. Suwaki, K. Watase and K. Tanaka (1999). "Amygdala-kindled and pentylenetetrazole-induced seizures in glutamate transporter GLAST-deficient mice." Brain Res **845**(1): 92-96.

Watase, K., K. Hashimoto, M. Kano, K. Yamada, M. Watanabe, Y. Inoue, S. Okuyama, T. Sakagawa, S. Ogawa, N. Kawashima, S. Hori, M. Takimoto, K. Wada and K. Tanaka (1998). "Motor discoordination and increased susceptibility to cerebellar injury in GLAST mutant mice." Eur J Neurosci **10**(3): 976-988.

Wei, J., X. Pan, Z. Pei, W. Wang, W. Qiu, Z. Shi and G. Xiao (2012). "The beta-lactam antibiotic, ceftriaxone, provides neuroprotective potential via anti-excitotoxicity and anti-inflammation response in a rat model of traumatic brain injury." J Trauma Acute Care Surg **73**(3): 654-660.

Wetherington, J., G. Serrano and R. Dingledine (2008). "Astrocytes in the epileptic brain." Neuron **58**(2): 168-178.

Wiebe, S. (2000). "Epidemiology of temporal lobe epilepsy." Can J Neurol Sci **27 Suppl 1**: S6-10; discussion S20-11.

Wilcox, K. S., J. M. Gee, M. B. Gibbons, P. Tvrdik and J. A. White (2015). "Altered structure and function of astrocytes following status epilepticus." Epilepsy Behav **49**: 17-19.

Wilhelmsson, U., E. A. Bushong, D. L. Price, B. L. Smarr, V. Phung, M. Terada, M. H. Ellisman and M. Pekny (2006). "Redefining the concept of reactive

astrocytes as cells that remain within their unique domains upon reaction to injury." Proc Natl Acad Sci U S A **103**(46): 17513-17518.

Wlodarczyk, B. J., A. M. Palacios, T. M. George and R. H. Finnell (2012). "Antiepileptic drugs and pregnancy outcomes." American Journal of Medical Genetics **158A**(8): 2071-2090.

Yang, J., M. X. Li, Y. Luo, T. Chen, J. Liu, P. Fang, B. Jiang, Z. L. Hu, Y. Jin, J. G. Chen and F. Wang (2013). "Chronic ceftriaxone treatment rescues hippocampal memory deficit in AQP4 knockout mice via activation of GLT-1." Neuropharmacology **75**: 213-222.

Zhang, J., Y. Li, Z. G. Chen, H. Dang, J. H. Ding, Y. Fan and G. Hu (2013). "Glia protein aquaporin-4 regulates aversive motivation of spatial memory in Morris water maze." CNS Neurosci Ther **19**(12): 937-944.

Ziebell, J. M., P. D. Adelson and J. Lifshitz (2015). "Microglia: dismantling and rebuilding circuits after acute neurological injury." Metab Brain Dis **30**(2): 393-400.

Zonta, M., M. C. Angulo, S. Gobbo, B. Rosengarten, K. A. Hossmann, T. Pozzan and G. Carmignoto (2003). "Neuron-to-astrocyte signaling is central to the dynamic control of brain microcirculation." Nat Neurosci **6**(1): 43-50.

Chapter 2: Characterization of the intrahippocampal kainic acid (IHKA) model of epilepsy

Portions of this chapter were modified and/or reproduced, with permission from Elsevier, from: Hubbard, J.A., Szu, J.I., Yonan, J.M., Binder, D.K. (2016). "Regulation of astrocyte glutamate transporter-1 (GLT1) and aquaporin-4 (AQP4) expression in a model of epilepsy. *Exp Neurol*, 283: 85-96. Copyright 2016.

2.1 Abstract

Epilepsy is a group of disorders characterized by the unpredictable occurrence of seizures and unconsciousness. The most common form of epilepsy is temporal lobe epilepsy (TLE), which is frequently accompanied by a sclerotic hippocampus. Characterized by gliosis, neuronal cell dispersion, and cell loss, the sclerotic hippocampus may be a focal point of seizures. Due to ethical limitations, human tissue cannot be used to determine physiological changes that result in the conversion of a healthy brain to an epileptic one (a process known as epileptogenesis). Therefore, an accurate and reproducible animal model of temporal lobe epilepsy is necessary to study early time points during epileptogenesis. In this study, I characterized morphological changes that occurred in the intralhippocampal kainic acid (IHKA) model of epilepsy. I used video-EEG recordings, immunohistochemistry, Western blotting, and real time

polymerase chain reaction (RT-PCR) to characterize glial cell changes involved in epileptogenesis. In this model, I observed reproducible seizure activity as well as histological changes characteristic of a sclerotic hippocampus. In addition, I found changes in glial immunoreactivity in the non-sclerotic hippocampus. Finally, I detected increased GFAP immunoreactivity, protein, and mRNA levels in this model of epilepsy. Overall, I have shown that the IHKA model is an excellent model that mimics pathological features seen in human TLE.

2.2 Introduction

Epilepsy is a group of neurological syndromes characterized by the unpredictable occurrence of seizures. This disorder affects over 70 million people worldwide and has a much higher rate in developing countries than in developed regions (Ngugi, Bottomley et al. 2010). People who suffer from this infliction have a decreased quality of life (Thurman, Beghi et al. 2011) and experience impaired cognitive abilities, difficulty maintaining steady employment, limited access to a driver's license, and impaired socioeconomic integration (Hubbard, Hsu et al. 2013). Temporal lobe epilepsy (TLE) is the most common form of epilepsy. Although the true frequency of TLE is unknown, it is estimated to affect up to two thirds of epilepsy patients (Wiebe 2000).

It has been well established that neuronal excitability is a major contributor to epilepsy, but more recent evidence suggests that changes in glial cells contribute to the development of epilepsy (Tian, Azmi et al. 2005; Binder and Steinhäuser 2006; Seifert, Schilling et al. 2006; Seifert, Carmignoto et al. 2010; Clasadonte and Haydon 2012; Devinsky, Vezzani et al. 2013; Hubbard, Hsu et al. 2013; Coulter and Steinhauser 2015; Wilcox, Gee et al. 2015; Ziebell, Adelson et al. 2015; Eyo, Murugan et al. 2016; Hubbard and Binder 2016). Glial cells play several crucial roles in the central nervous system. Astrocytes are now considered an integral part of the tripartite synapse (Araque, Parpura et al. 1999) and participate in a variety of brain functions including synaptic network formation (Ransom, Behar et al. 2003), modulation of synaptic transmission (Volterra and Meldolesi 2005; Halassa and Haydon 2010; Murphy-Royal, Dupuis et al. 2015), ion homeostasis, and metabolism (Ransom and Ransom 2012). Microglia are the resident immune cells in the brain and are important for initiating the inflammatory response after injury or infection (Davis, Foster et al. 1994). In addition to playing a major role in the immune response, microglia can also modulate neurotransmission, prune synapses, and regulate neurogenesis and survival (Eyo, Murugan et al. 2016). In the injured brain, both astrocytes and microglia can become “reactive”, changing in shape and function, as measured by levels of the intermediate filament glial fibrillary acidic protein (GFAP) and the ionized calcium-binding adapter molecule-1 (Iba1), respectively. This pathological feature is called “gliosis” and can be further subdivided into

astrogliosis (reactive astrocytes) and micorgliosis (reactive microglia). The morphological alterations in these cells are also accompanied by functional and expression changes of channels and receptors. Therefore, reactive astrocytes and microglia may contribute to increased neuronal excitability and the development of epilepsy (Binder and Steinhäuser 2006; Hubbard, Hsu et al. 2013; Eyo, Murugan et al. 2016; Robel and Sontheimer 2016).

The most common histopathological feature of TLE in humans is hippocampal sclerosis. It is primarily characterized by a pronounced loss of pyramidal neurons, granule cell dispersion, and severe gliosis (Margerison and Corsellis 1966; Mathern, Pretorius et al. 1995; Blümcke, Beck et al. 1999; Clasadonte and Haydon 2012; de Lanerolle, Lee et al. 2012). When present, the sclerotic hippocampus may be the focus of seizure origin (Babb, Lieb et al. 1984). Patients with hippocampal sclerosis often undergo epilepsy surgery and the majority of patients (over 80%) have a favorable outcome (Tugcu, Gungor et al. 2016). In fact, about 68% of patients remain seizure free several years after surgery completion (Tugcu, Gungor et al. 2016). Surgery is not an option for all patients, however, and a greater understanding of the pathophysiology of epilepsy is necessary to find alternative treatment methods.

Critical to understanding the various forms of epilepsy is the use of animal models. Several different models of epilepsy are used today, including

chemoconvulsants, electrical kindling, injury-induced, hyperthermia-induced, and genetic models (Sharma, Reams et al. 2007; Kandratavicius, Balista et al. 2014; Hubbard and Binder 2016). The most common TLE models are intrahippocampal or intraperitoneal injections of either kainic acid or pilocarpine. Kainic acid is a kainate receptor agonist whereas pilocarpine is a muscarinic acetylcholine receptor agonist. Both models are highly reproducible and immediately induce status epilepticus (SE), a prolonged state of continuous seizures, in rodents. This is followed by a seizure-free latency period before the occurrence of spontaneous seizures. Furthermore, both models mimic several of the histopathological changes seen in human TLE, including hippocampal sclerosis. Kainic acid causes injuries restricted to the hippocampus whereas pilocarpine, which may cause lesions in the neocortex (Sharma, Reams et al. 2007). Although the use of both chemoconvulsants results in neuropathologic alterations that mirror the human condition, kainic acid is considered one of the best models of TLE (Sharma, Reams et al. 2007).

Systemic administration of chemoconvulsants often result in variable seizure severity, longer latency periods, widespread damage, and a high mortality rate (Babb, Pereira-Leite et al. 1995). Intrahippocampal injections, on the other hand, result in more consistent seizure severity, shorter latency periods, focal damage, and a reduced mortality rate. Common pathological features of the sclerotic hippocampus, including mossy fiber sprouting, are observed after

intrahippocampal kainic aid injections (Leite, Babb et al. 1996). In this study, I characterized some of the histopathological changes that occur in the intrahippocampal kainic acid (IHKA) model of TLE. Specifically, I used video-EEG recordings to confirm the presence of seizures in animals. I then used immunohistochemistry to characterize changes in neurons, microglia, and astrocytes in this epilepsy model. Finally, I used Western blotting and real-time polymerase chain reaction (RT-PCR) to further characterize GFAP protein and mRNA changes. In this model, I observed clear cellular changes characteristic of a sclerotic hippocampus, including CA1 pyramidal cell death, granule cell dispersion, astrocytic and microglial activation, and increased GFAP protein and mRNA expression. It is clear that both neurons and glial cells undergo extensive morphological and expression changes in the IHKA model of TLE.

2.3 Methods

2.3.1 Animals

All experiments were conducted in accordance with the National Institutes of Health guidelines and were approved by the University of California, Riverside Institutional Animal Care and Use Committee (IACUC). Only CD1 male mice, 6-8 weeks old, were used for these experiments. The mice were housed under

controlled conditions (12 hour light/12 hour dark) with food and water provided *ad libitum*.

2.3.2 Intrahippocampal kainic acid surgery and EEG implants

CD1 male mice were anesthetized with an intraperitoneal (i.p.) injection of an 80mg/kg ketamine and 10 mg/kg xylazine mixture. Mice were then mounted in a stereotaxic frame and an incision was made to expose the skull and locate bregma (Figure 2.1A). Using stereotaxic coordinates of the hippocampus (Paxinos and Franklin 2001), a 0.6 mm burr hole was made 1.8 mm posterior and 1.6 mm lateral from bregma with a high-speed drill (Drummond Scientific). A microinjector (Nanoject, Drummond Scientific) was then placed into the right dorsal hippocampus and lowered to the dorsoventral coordinate of 1.9 mm. Mice were injected with either 74 nL of a 20 mM solution of kainic acid or an equal volume of 0.9% saline over a period of 4 minutes (Figure 2.1B). In initial experiments, Nissl staining was performed to confirm the accuracy of the injection site (Figure 2.1C).

In preliminary experiments, the presence of epileptiform activity was verified in 100% of animals using video-EEG recordings. Three-channel twisted bipolar stainless steel electrodes (Plastics One) were prepared by cutting the recording and ground electrodes to the appropriate lengths to end up in CA3 of the

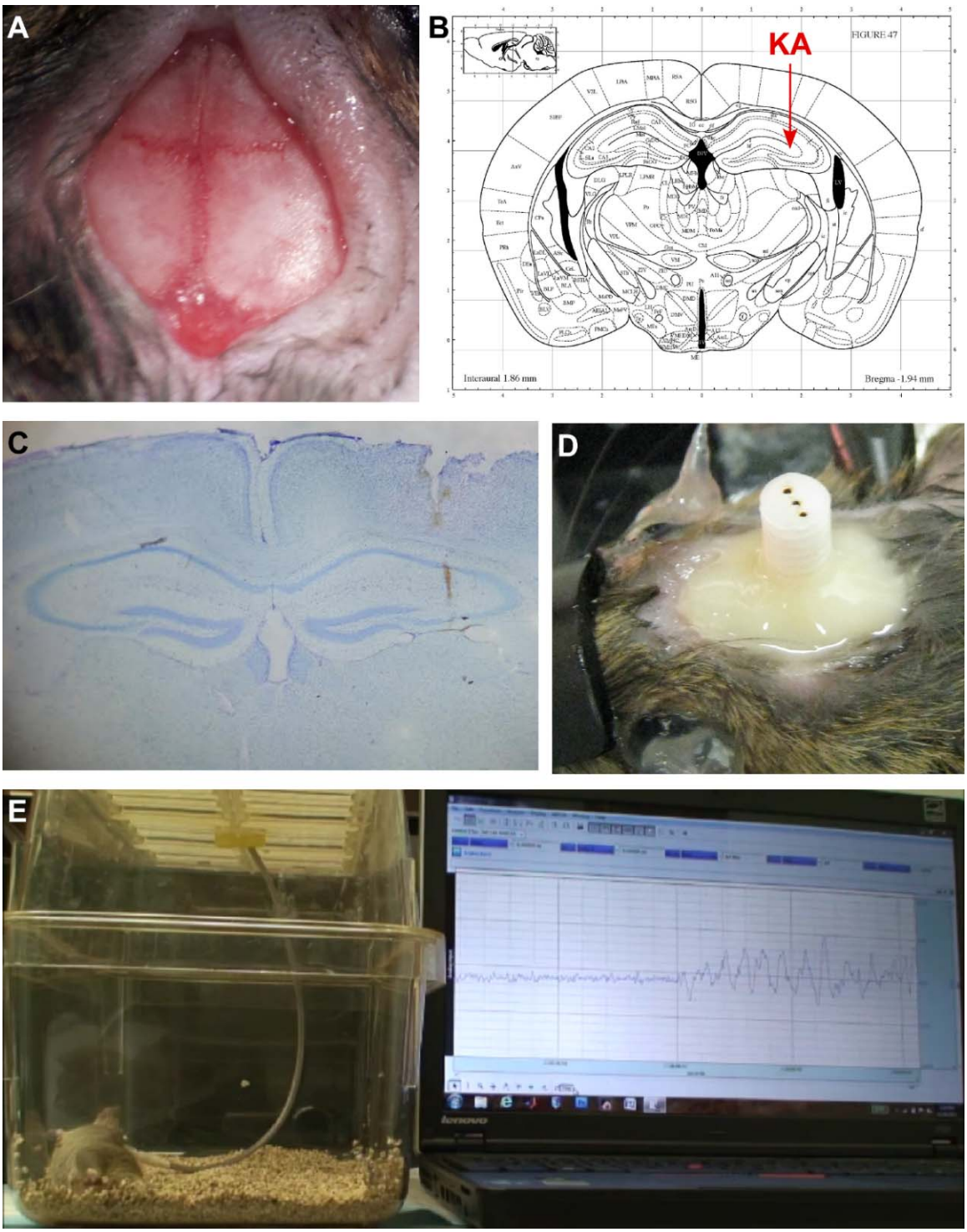

A
B
KA
FIGURE 47
Interaural 1.86 mm
Bregma -1.94 mm
C
D
E

Figure 2.1. Intrahippocampal kainic acid (IHKA) injections and video-EEG recording in a mouse.
A. An exposed skull in a mouse with clear visualization of bregma, the region on the skull where the sagittal and coronal sutures are joined. **B.** A page from (Paxinos and Franklin 2001), which was used to stereotaxically locate the hippocampus. The red arrow indicates the approximate location where a small hole was drilled in the skull and a microinjector was used to inject kainic acid (KA) or saline into the CA3 region of the hippocampus. **C.** A representative Nissl stain of a coronal hippocampal slice 1 day after KA-induced status epilepticus to confirm correct location of injections. Nissl stain was performed on mounted slices by dipping them in 100% EtOH, 95% EtOH, and 70% EtOH for 1 minute each followed by 3 minutes in water. Slices were then incubated in Cresyl violet, washed, and imaged using a Carton microscope. **D.** In a subset of animals, electrodes were implanted in the mouse brain and held into place with a bonding agent and cement**. E.** After electrode implantation, mice were connected to an EEG acquisition system through a commutator, allowing mice to move freely. Behavioral and electrographic seizures were monitored with this continuous video-EEG recording set up.

hippocampus and the dura, respectively. After intrahippocampal injections of kainic acid, the skull was etched and the electrode was lowered into the injection site. The electrode implant was secured into place using dual-cure bonding agent (Clearfil Photo Bond, Kuraray) and permanent cement (Clearfil SA Cement, Kuraray, Figure 2.1D). Mice implanted with electrodes were connected to an EEG acquisition system (MP150, Biopac Systems inc., and AcqKnowledge 4.0 software) through a commutator (Figure 2.1E). Animals were freely moving and monitored using a digital video camera (Sony HDR-HC5, Sony Electronics).

2.3.3 Kainic acid-induced status epilepticus

After kainic acid injections, all mice experienced status epilepticus (SE). This has been confirmed with video-EEG monitoring previously by our lab (Lee, Hsu et al. 2012) and in preliminary studies (Figure 2.2). Within 30 minutes of IHKA injections, mice experienced SE for several hours, which spontaneously subsided. In this model, mice exhibited spontaneous recurrent seizures in both hippocampi (Figure 2.3).

For the current studies, I wished to avoid electrode damage to the brain and therefore proceeded without the use of EEG implantation. Instead, I monitored animals for behavioral seizures. All animals experienced continuous (3 or more hours) Racine stage 3-5 seizures (Racine 1972), characterized by forelimb and

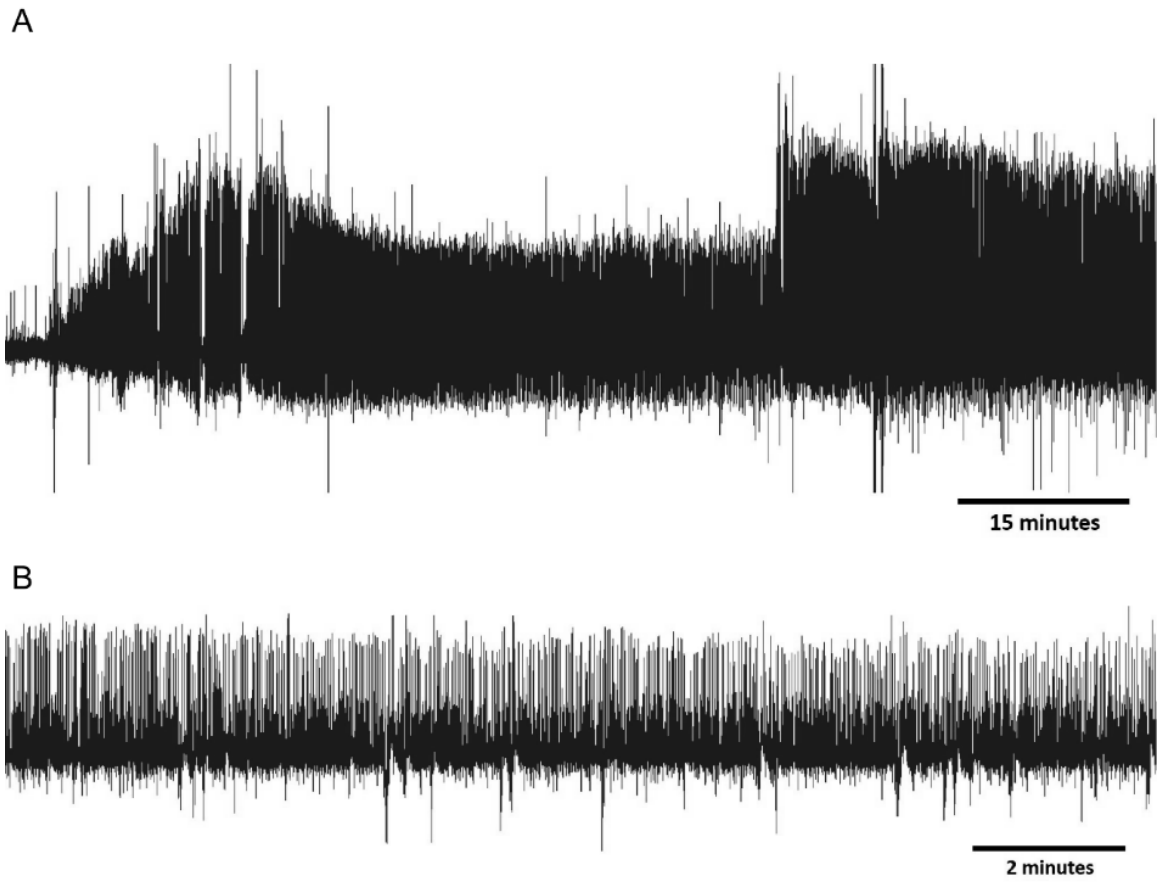


Figure 2.2. EEG recording of status epilepticus immediately after intrahippocampal kainic acid (IHKA) injections.
A. A. An example of an EEG recording during status epilepticus (SE). Shortly after kainic acid injections, mice developed electrographic and behavioral SE lasting several hours. Scale bar = 15 minutes. **B.** Another EEG recording of kainic acid-induced SE with a different time scale. Scale bar = 2 minutes. These recordings indicate electrographic status epilepticus.

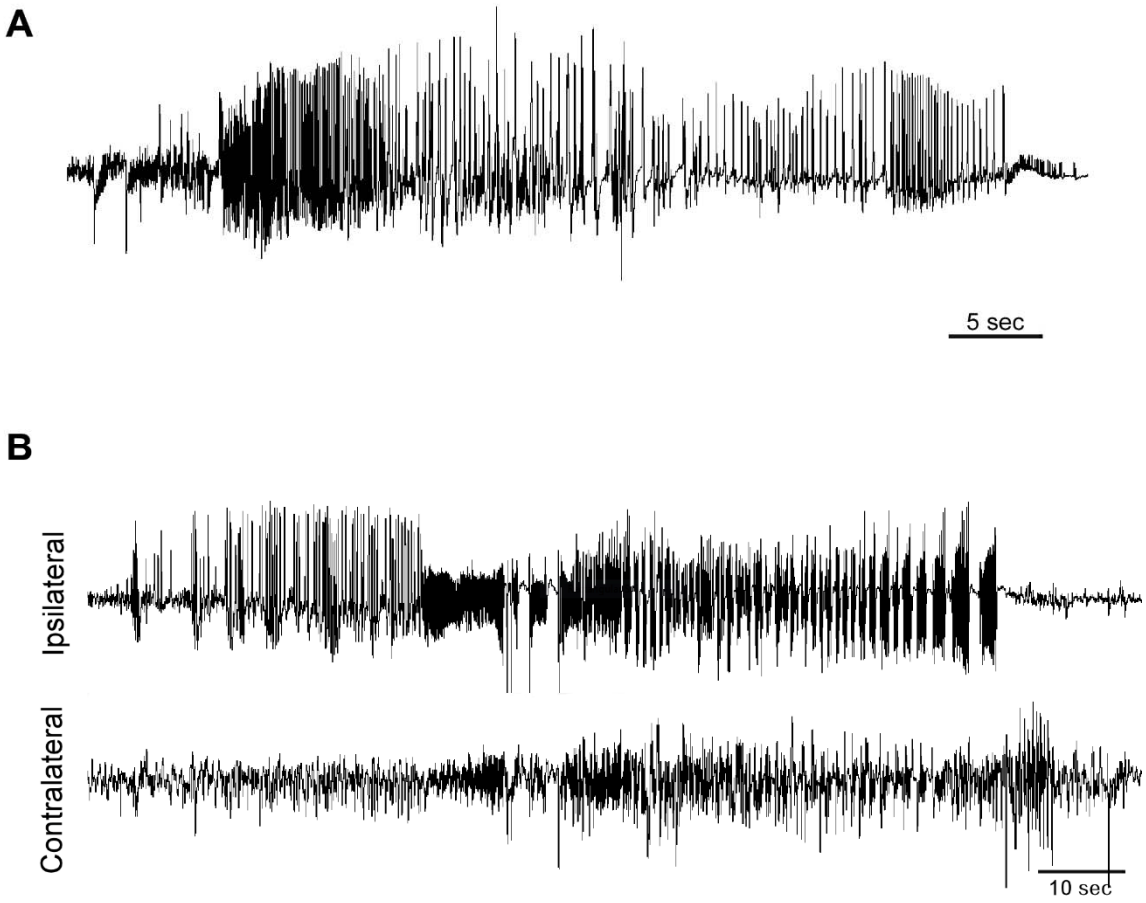


Figure 2.3. EEG recordings in intrahippocampal kainic acid model. **A.** Example of an EEG recording of a spontaneous seizure 7 days after SE. **B.** Example of simultaneous bilateral recordings of spontaneous seizures 8 days after SE. In this example, the seizure begins in the hippocampus ipsilateral to injection (*upper trace*) and then propagates into the contralateral hippocampus (*lower trace*).

hindlimb clonus, rearing, and falling (Table 2.1). Animals that died due to SE were excluded from the study. Otherwise, animals were euthanized with fatal plus (Western Medical Supply), perfused, and processed at various time points post IHKA injections.

Stage	Description of seizures
1	Immobility; mouth and facial clonus
2	Head nodding; rigid posture; tail extension
3	Forelimb and/or hindlimb clonus; repetitive movements
4	Rearing; limb clonus with rearing
5	Rearing and falling; jumping; severe tonic-clonic seizures

Table 2.1. The Racine scale modified for rodent seizures (Racine 1972). Physical characteristics of observable rodent seizures classified by severity.

2.3.4 Immunohistochemistry

Mice were transcardially perfused with ice-cold phosphate buffered saline (PBS, pH 7.4) followed by 4% paraformaldehyde, pH 7.4. Brains were quickly removed and postfixed in 4% paraformaldehyde overnight at 4°C followed by two days of cryoprotection in 30% sucrose in PBS at 4°C. Brains were then flash frozen with dry ice-cold isopentane, cut into 50 µm coronal sections using a cryostat (Leica CM 1950, Leica Microsytems, Bannockburn, IL), and then stored in PBS at 4°C. For each experiment, slices were processed simultaneously. Slices were blocked for 1 hour with 5% normal goat serum in PBS and then incubated with primary antibodies (Table 2.2) overnight at 4°C in 0.3% Triton X-100. After

washing slices with PBS, sections were incubated with species-specific secondary antibody conjugated with Alexa 488, 594, or 647 for visualization. Slices were mounted in Vectashield with DAPI (Vector Laboratories) and 10x images were taken using a fluorescence microscope (Leica DFC345 FX).

Target	Dilution	Catalog Number	Company
GFAP	1:200	MAB5804	Millipore
Iba1	1:200	019-19741	Wako
NeuN	1:200	MAB377	Millipore

Table 2.2. Antibodies used for immunohistochemistry.
Antibodies to glial fibrillary acidic protein (GFAP), ionized calcium-binding adapter molecule 1 (Iba1), and neuronal specific nuclear protein (NeuN) were used to immunohistochemically label astrocytes, microglia, and neurons, respectively. The dilutions used, catalog number, and the company from which each antibody was purchased are listed.

Quantification of GFAP immunoreactivity was performed using the Leica Application Suite (LAS) X Lite software. Fluorescent images of the hippocampus were captured at 10x magnification under identical settings. A box delineating the region of interest (ROI) was drawn on the DAPI channel either around all layers of the hippocampus or at the center of each layer of the hippocampus: stratum (S.) oriens, S. pyramidale, S. radiatum, S. lacunosum moleculare (SLM), molecular layer, granule cell layer (GCL), and hilus (Figure 2.4A). In the CA3 region of the hippocampus, ROIs around the S. lucidum, S. pyramidale, and S. oriens were drawn (Figure 2.4B). The mean pixel (gray) value within each ROI was obtained for analysis. For each time point, 4 slices from each animal (n=5) were used.

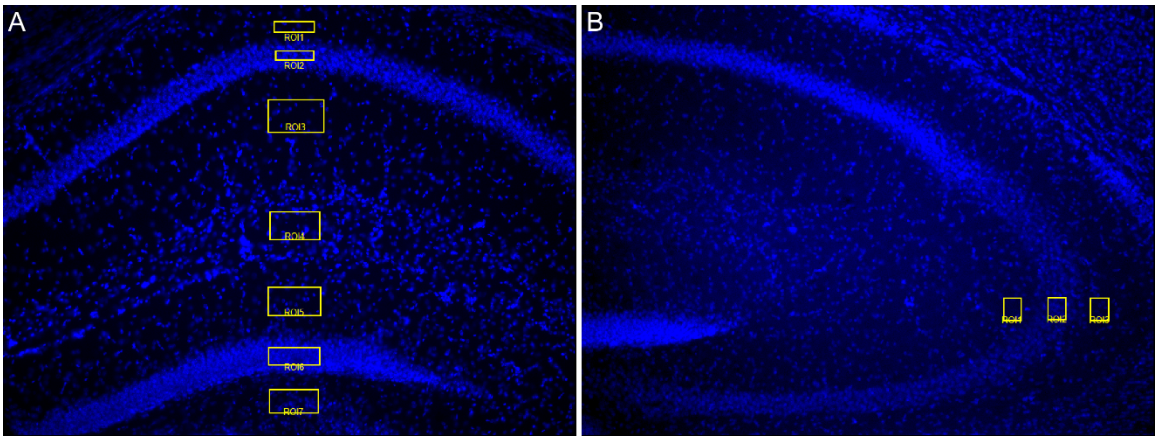


Figure 2.4. Method for analysis of hippocampal immunoreactivity.
A. Boxes delineating the region of interest (ROI) were drawn on the DAPI channel. From top to bottom, ROI1-7 correspond to the Stratum (S.) oriens, S. pyramidale, S. radiatum, S. lacunosum moleculare (SLM), molecular layer, granule cell layer (GCL), and hilus, respectively. A final box was drawn around the entire image to quantify "all layers" of the hippocampus. B. Boxes delineating the ROIs in the CA3 area of the hippocampus. From left to right, ROI1-3 correspond to the S. lucidum, S. pyramidale, and S. oriens, respectively.

2.3.5 Western blot

Whole hippocampal tissue was microdissected from the mouse brain at 1, 4, 7, and 30 days post IHKA or saline injections (n = 5 for saline control and all time points post kainic acid-induced SE). Harvested tissue was homogenized using the Bullet Blender (Next Advance) in radioimmunoprecipitation assay (RIPA) buffer (Sigma) containing complete protease inhibitors (Roche). Protein concentrations were assayed via Bradford and protein was resolved by SDS-PAGE (10% polyacrylamide) and transferred to a nitrocellulose membrane. The membranes were then probed for GFAP (1:5,000, Millipore MAB5804) and β-actin (1:5,000, Sigma A1978) as an internal control. Bands were visualized and

quantified using the Li-COR Odyssey Fc Western Imaging System and GFAP protein levels were normalized to internal β-actin levels.

2.3.6 RT-PCR

Hippocampal tissue was microdissected from the mouse brain at 1, 4, 7, and 30 days post IHKA or saline injections (n = 5 for all time points). Harvested tissue was homogenized using the Bullet Blender (Next Advance). RNA was isolated using the Direct-Zol RNA mini prep kit (Zymo Research) and quantified using a nanodrop (Thermo Scientific NanoDrop 2000c Spectrophotometer). Both cDNA synthesis and RT-PCR were performed using the Bioline SensiFAST SYBR NO-ROX Kit and the CFX-96 detection system (Bio-Rad). Primers for GFAP and 18s RNA (Table 2.3) were purchased from Integrated DNA Technologies. The reaction conditions were as follows: 1 cycle for 10 min at 45°C, 1 cycle for 2 min at 95°C, 40 cycles for 5s at 95°C, and 1 cycle for 20s at 60°C. Results were quantified using the differential CT method representing the fold change in target gene expression. Both a no template control (NTC) and a no reverse

Target Gene	Forward Primer Sequence	Reverse Primer Sequence
GFAP	ATCGAGATCGCCACCTACAG	CTTCTTTGGTGCTTTTGCCCC
18s RNA	CTCAACACGGGAAACCTCAC	CGCTCCACCAACTAAGAACG

Table 2.3. Primers used for RT-PCR experiments.
All primers are listed in the 5' → 3' direction.

transcriptase (NRT) control were included in each assay to detect any contamination or non-specific replication.

2.3.7 Statistical analysis

Statistical analysis was performed using a one-way ANOVA with *post-hoc* Bonferroni multiple comparisons test. All error bars are presented as the mean ± standard error of the mean (SEM). A comparison to saline control was denoted statistically significance by a p-value < 0.05, < 0.01 or < 0.001 and denoted with *, **, or ***, respectively. Any statistically significant differences between other time points were not indicated for the purpose of clarity.

2.4 Results

2.4.1 Histological confirmation and characterization of the sclerotic hippocampus

In a healthy hippocampus, distinct laminar-specific organization of the hippocampus exists (Figure 2.5A). NeuN revealed highly organized, dense layers of granule and pyramidal cell neurons. Microglia and astrocytes displayed normal morphology, determined by Iba1 and GFAP immunoreactivity,

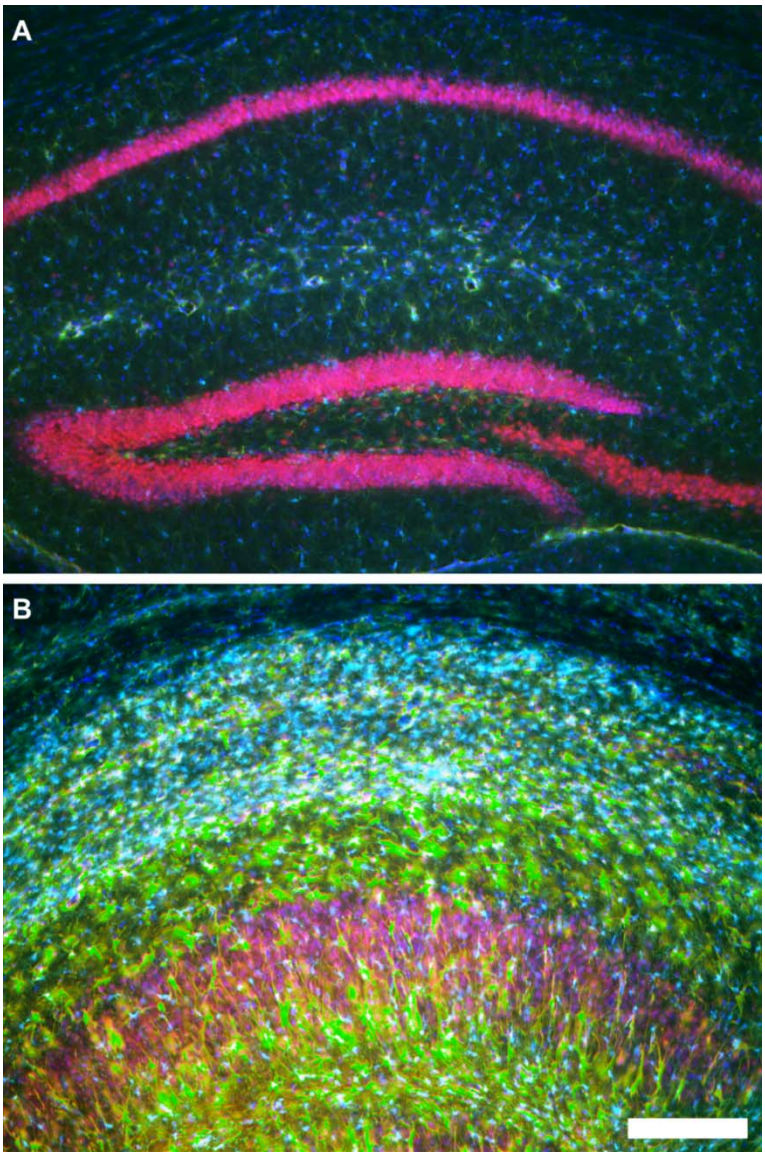


Figure 2.5. Marked histological changes occur during epileptogenesis in the mouse hippocampus.
10x images of cell nuclei (DAPI, dark blue), neurons (NeuN, red), astrocytes (GFAP, green) and microglia (Iba1, cyan) in **A.** the healthy hippocampus and **B.** 21 days post IHKA-induced status epilepticus. Neurons occupy organized cell layers (dentate gyrus, CA1-CA3) in the healthy hippocampus, but marked neuronal loss (*e.g.* loss of CA1 pyramidal cells) and cell layer disorganization (*e.g.* dentate granule cell dispersion) in the epileptic hippocampus. Astrocytes and microglia display normal morphology in the healthy hippocampus but develop markedly abnormal "reactive" morphology in epilepsy. These changes together account for "hippocampal sclerosis", a hallmark of temporal lobe epilepsy. Scale bar = 200 μm.

respectively. Mice developed sclerosis in the hippocampus ipsilateral to IHKA injections, characterized by neuronal disorganization, cell death, and gliosis (Figure 2.5B). More specifically, NeuN staining revealed significant neuronal dispersion of dentate granule cells. Furthermore, a significant loss of pyramidal neurons in the CA1 area of the hippocampus was observed. Microglia and astrocytes became ramified in the sclerotic hippocampus. Together, these changes account for hippocampal sclerosis.

2.4.2 Histological characterization of the microglial marker, Iba1

Iba1 immunoreactivity in the hippocampus (n = 3; Figure 2.6) was imaged in naïve mice, 1 day after saline injections, as well as 1 and 30 days post IHKA injections. In the naïve hippocampus, microglia presented with a healthy morphology. One day after intrahippocampal saline injections, however, astrocytes became slightly ramified in the ipsilateral hippocampus. Microglia in the contralateral hippocampus, however, displayed normal morphology. A single day after kainic acid-induced SE, microglia became activated (ramified) in both the ipsilateral and contralateral hippocampi. In the contralateral hippocampus, microglia returned to fairly normal morphology by 30 days post SE. Microglia in the ipsilateral hippocampus remained reactive at 30 days post SE.

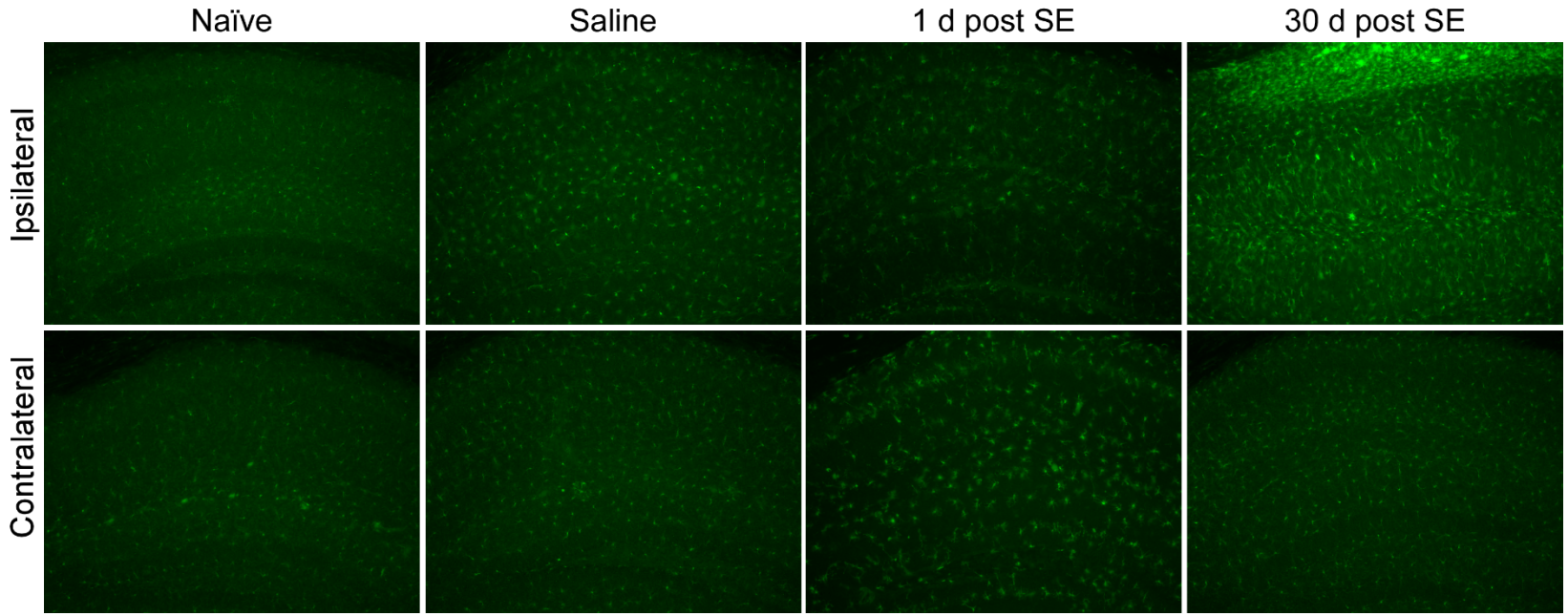


Figure 2.6. Iba1 immunoreactivity in the hippocampus of naïve, saline injected, and kainic acid injected mice.

Iba1 immunoreactivity in naïve mice, 1 day after intrahippocampal saline injections, and 1 and 30 days post IHKA-induced SE in the ipsilateral (top panels) and contralateral (bottom panels) hippocampi. In naïve mice, microglia exhibited a healthy morphology. One day after intrahippocampal saline injections, microglia became slightly ramified in the ipsilateral, but not the contralateral hippocampus to injections. One day post IHKA-induced SE, microglia exhibited atrophic (reactive) morphology in both the ipsilateral and contralateral hippocampi to injections. By 30 days post SE, microglia in the contralateral hippocampus returned to a healthy morphology. Microgliosis was prominent in the ipsilateral hippocampus 30 days post SE. For each time point, 2 slices from each animal (n = 3) were used. Scale bar = 200 µm.

Iba1 immunoreactivity in the cortex was imaged in naïve mice, 1 day after intrahippocampal saline injections, and 1 and 30 days post IHKA-induced SE (n = 3; Figure 2.7). A single day after saline injections, microglia retained a morphology similar to that seen in naïve mice. Microglia presented with reactive morphology in both the ipsilateral and contralateral cortices 1 day after IHKA-induced SE. By 30 days post SE, however, microglia reactivity was diminished and resembled the morphology of microglia seen in naïve mice.

Next, I wanted to determine whether microglial scarring occurred at the injection site after IHKA injections. Therefore, I imaged microglia immunoreactivity around the injection site in both the hippocampus and the cortex (n = 3, Figure 2.8). One day after IHKA injections, no microglia clustered around the injection site in the hippocampus or the cortex. Instead, ramified microglia were observed evenly throughout the tissue. Therefore, microglial activation was a global response rather than a local response. Furthermore, the ramification of microglia was most prominently seen in the hippocampus ipsilateral to IHKA injections when the hippocampus is considered sclerotic.

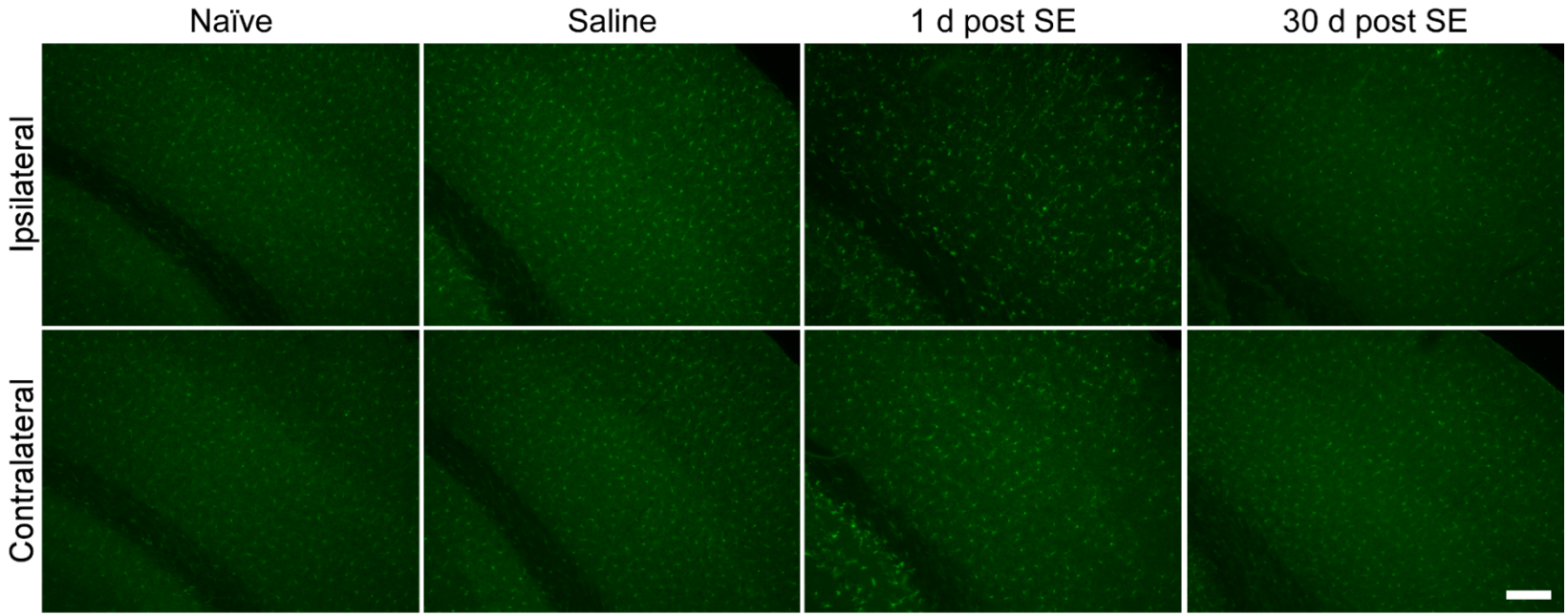


Figure 2.7. Iba1 immunoreactivity in the cortex of naïve, saline injected, and kainic acid injected mice

Iba1 immunoreactivity in naïve mice, 1 day after intrahippocampal saline injections, and 1 and 30 days post IHKA-induced SE in the ipsilateral (top panels) and contralateral (bottom panels) cortices. In naïve mice, microglia exhibited a healthy morphology. Microglia retained this morphology 1 day after intrahippocampal saline injections. One day post IHKA-induced SE, microglia exhibited reactivity in both the ipsilateral and contralateral cortices to injections. By 30 days post SE, microglia returned to a morphology similar to that seen in naïve mice. For each time point, 2 slices from each animal (n = 3) were used. Scale bar = 200 μm.

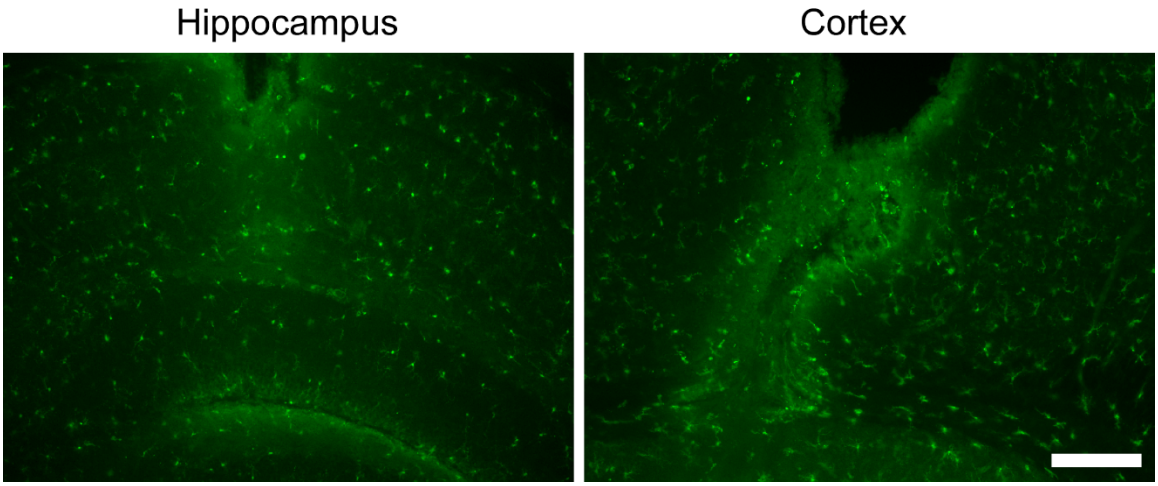


Figure 2.8. Microglia (Iba1) immunoreactivity 1 day after intrahippocampal kainic acid-induced status epilepticus.
Iba1 reactivity was observed throughout the hippocampus (left panel) and cortex (right panel) 1 day after IHKA-induced SE. Two slices from each animal (n = 3) were used. Scale bar = 200 μm.

2.4.3 Increased expression of the astrocyte marker, GFAP

GFAP immunoreactivity was imaged in naïve mice and 1 day post intrahippocampal saline injections (n = 3; Figure 2.9). GFAP immunoreactivity in both the ipsilateral and contralateral hippocampi to saline injections were similar to naïve levels. Therefore, I only used intrahippocampal saline injected brains as controls for all experiments. Furthermore, GFAP immunoreactivity 1, 4, 7, and 30 days after intrahippocampal saline injections (n = 3 for each time point) were imaged (Figure 2.10). GFAP levels remained constant at all time points, so only brains from 7 days post saline injections were used as controls for the remainder of experiments.

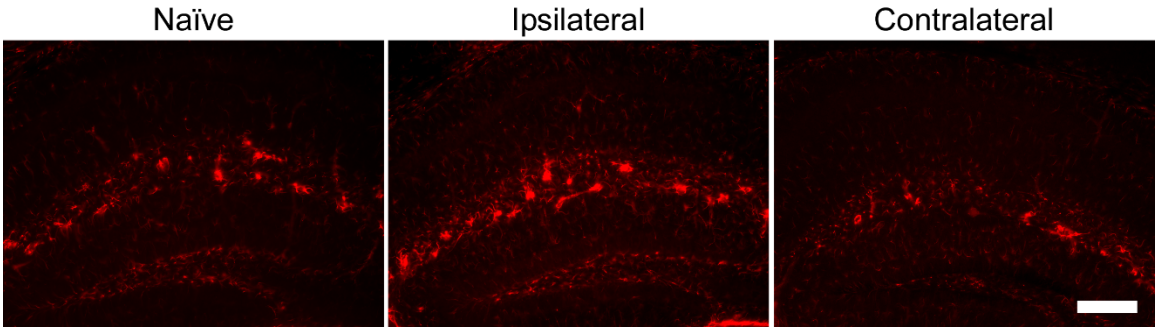


Figure 2.9. Astrocyte (GFAP) immunoreactivity in naïve mice and 1 day after intrahippocampal saline injections.
Similar astrocyte morphology was observed in naïve mice (left panel) and in the ipsilateral (middle panel) and contralateral (right panel) hippocampi 1 day after intrahippocampal saline injections. For each time point, 3 slices from each animal (n = 3) were used. Scale bar = 200 μm.

Hippocampal GFAP and DAPI immunoreactivity were imaged 7 days after saline injections (control) and at 1, 4, 7, and 30 days post kainic acid-induced SE. Analysis of GFAP immunoreactivity revealed a progressive increase in GFAP in the hippocampus ipsilateral to kainic acid injection (Figure 2.11). GFAP immunoreactivity was markedly elevated at 4, 7, and 30 days post kainic acid-induced SE compared to the saline control in every layer of the hippocampus except in the stratum (S.) radiatum and stratum lacunosum moleculare (SLM) at 4 days post SE. At 1 day post SE, no difference from the saline control was observed. A similar progressive increase in GFAP immunoreactivity was observed in the CA3 region of the ipsilateral hippocampus (Figure 2.12). GFAP levels in the S. oriens and S. pyramidale layers at 4, 7, and 30 days post SE

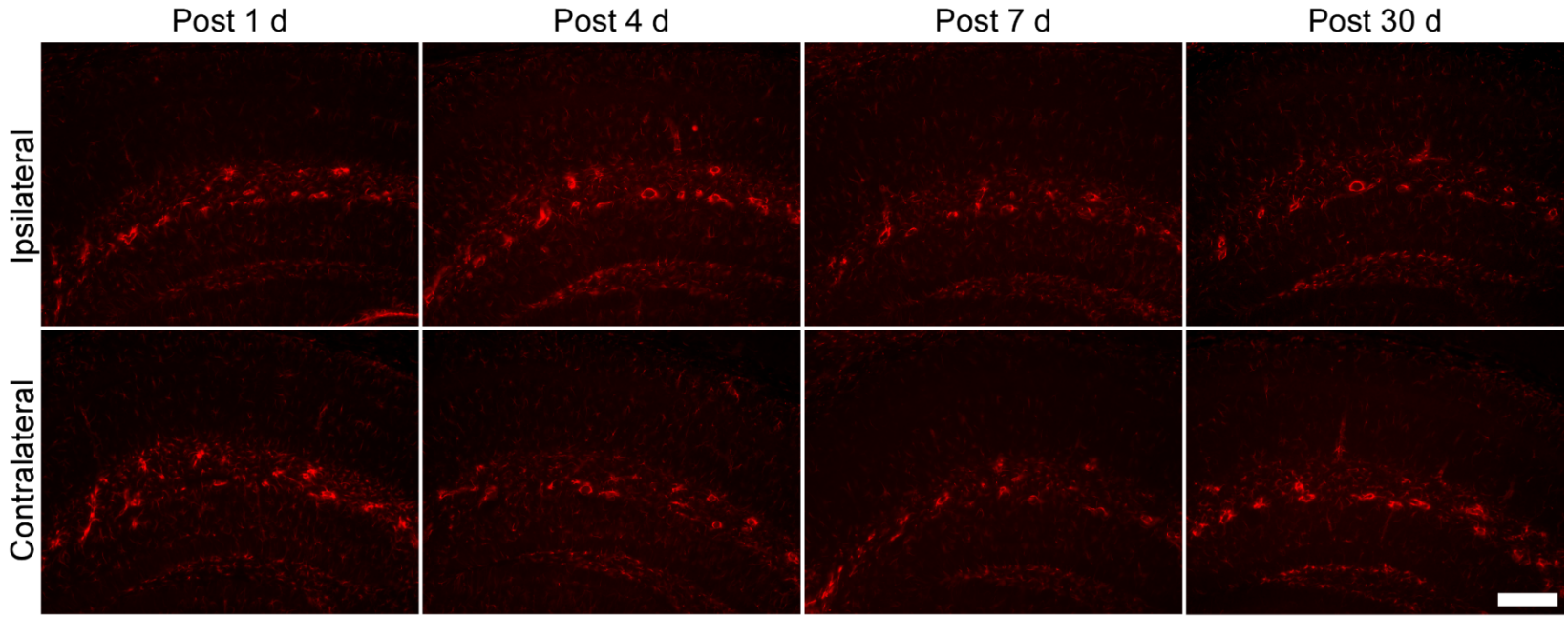
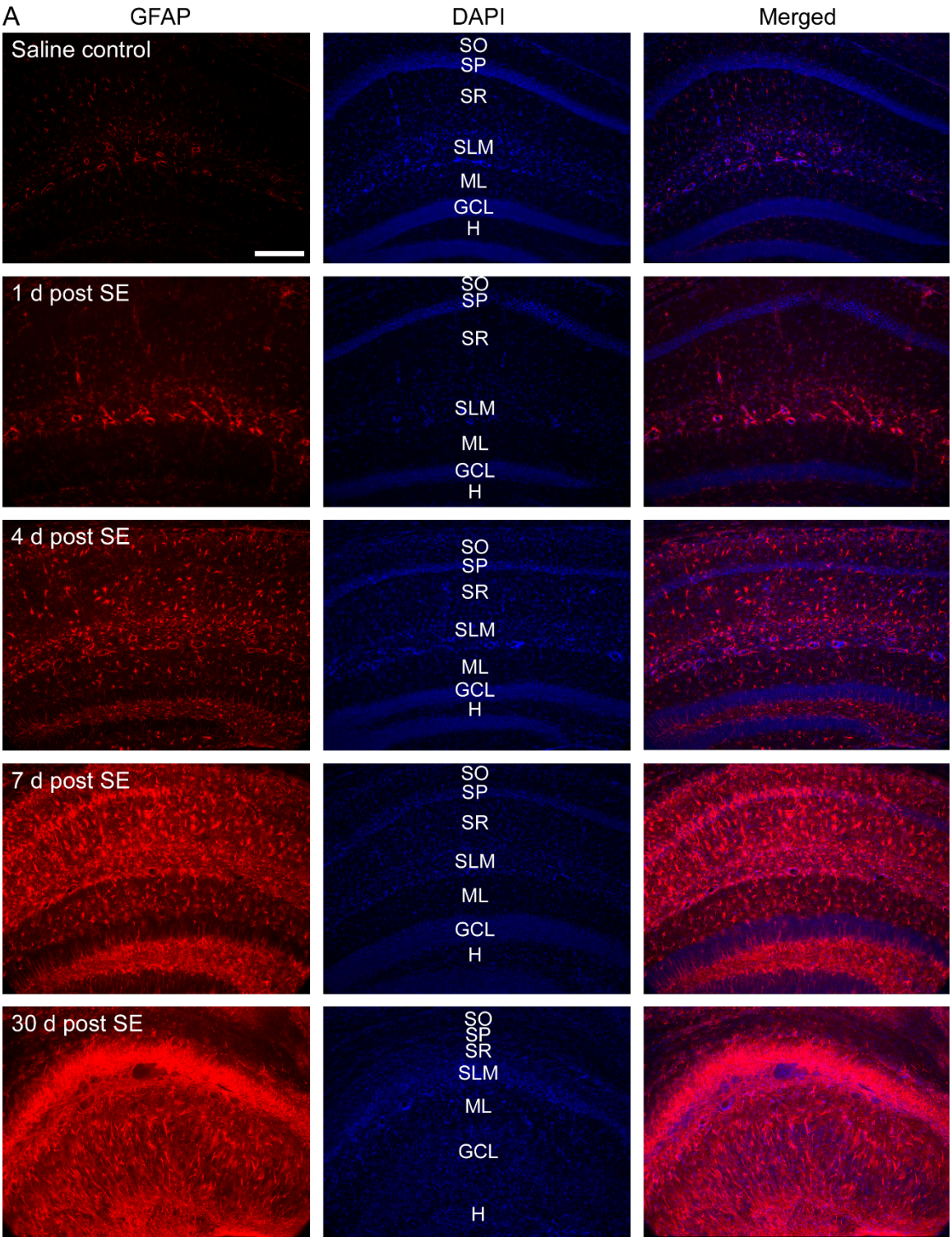


Figure 2.10. Astrocyte (GFAP) immunoreactivity after intrahippocampal saline injections.

Representative 10x images of GFAP immunoreactivity in the ipsilateral (top panel) and contralateral (bottom panel) hippocampi at 1, 4, 7, and 30 days post intrahippocampal saline injections. For each time point, 3-5 slices from each animal (n = 3) were used. Scale bar = 200 μm.


A
GFAP
DAPI
Merged
Saline control
1 d post SE
4 d post SE
7 d post SE
30 d post SE
SO
SP
SR
SLM
ML
GCL
H

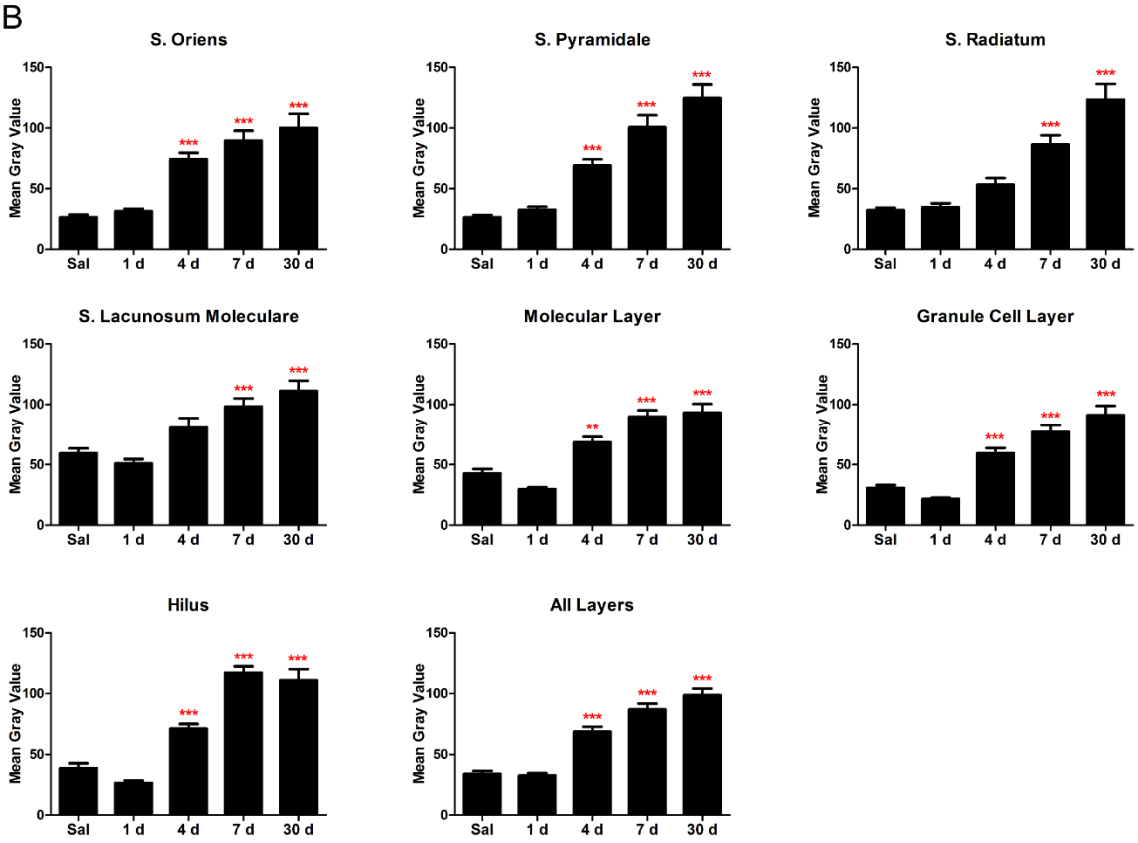
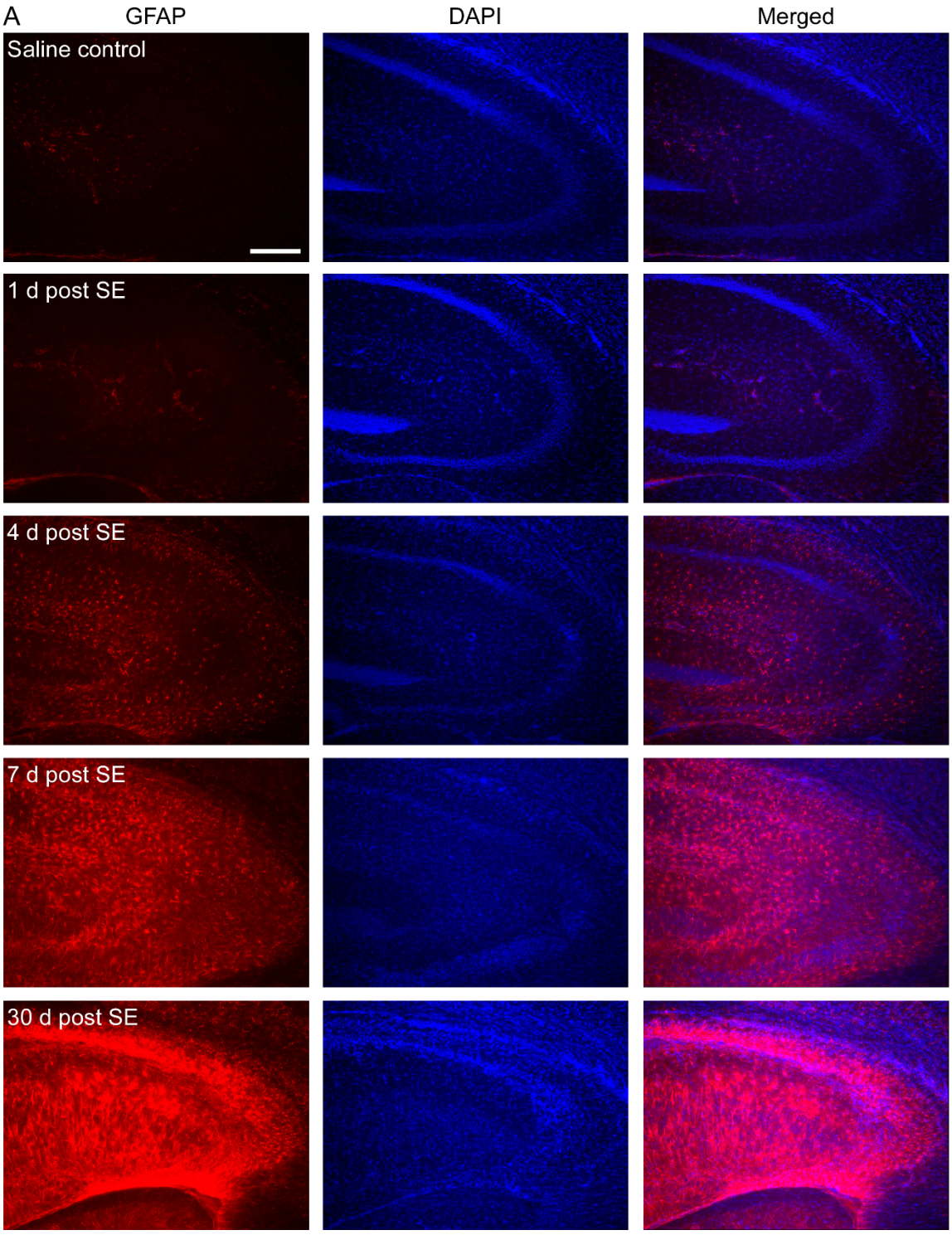


Figure 2.11. Glial fibrillary acidic protein (GFAP) immunoreactivity in the ipsilateral hippocampus after kainic acid-induced status epilepticus (SE). **A.** 10x images of GFAP (red), DAPI (blue), and merged immunoreactivity of the ipsilateral hippocampus after saline injections (Saline control) and 1, 4, 7, and 30 days (d) post SE. **B.** Quantification of GFAP immunoreactivity in the various layers of the hippocampus. ** indicates $p < 0.01$ and *** indicates $p < 0.001$ when compared to saline control. For each time point, 4 slices from each animal ($n = 5$) were used. Scale bar = 200 μm. SO = stratum oriens; SP = stratum pyramidale; SR = stratum radiatum; SLM = stratum lacunosum moleculare; ML = molecular layer; GCL = granule cell layer; H = hilus.


A
GFAP
DAPI
Merged
Saline control
1 d post SE
4 d post SE
7 d post SE
30 d post SE

B

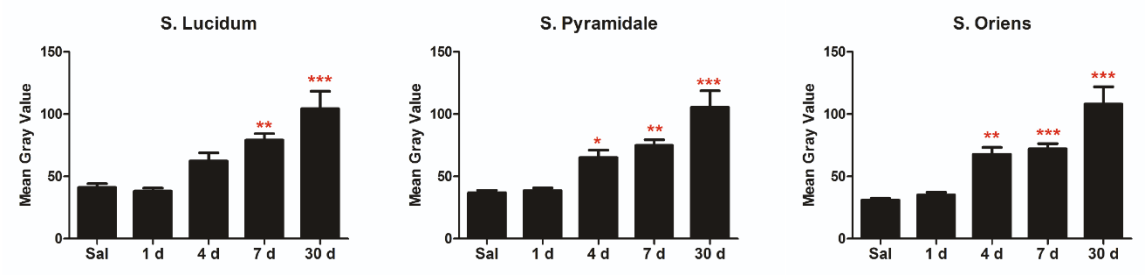
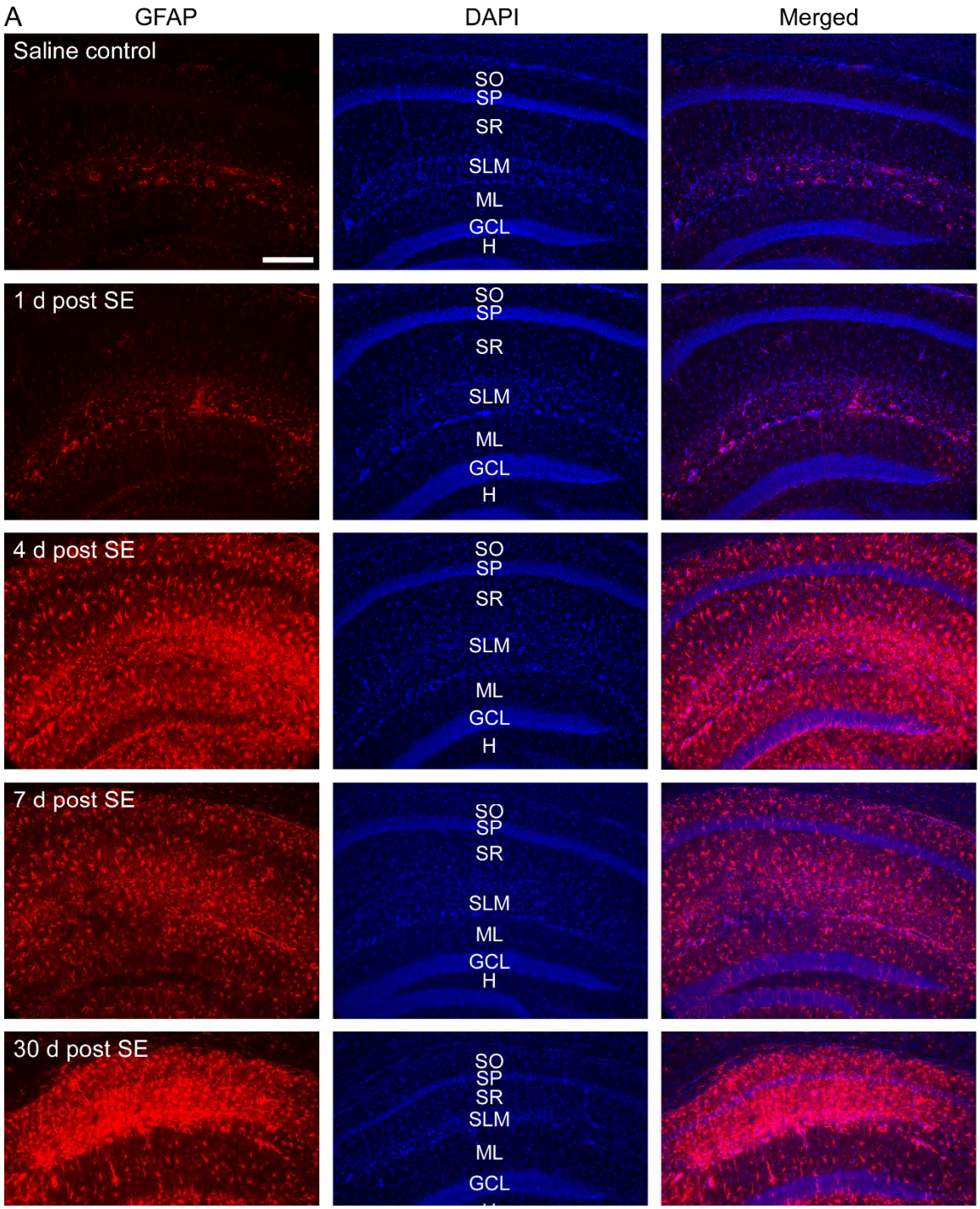


Figure 2.12. Glial fibrillary acidic protein (GFAP) immunoreactivity in the ipsilateral CA3 region of the hippocampus after kainic acid-induced status epilepticus (SE).
A. 10x images of GFAP (red), (blue), and merged immunoreactivity of the ipsilateral CA3 region of the hippocampus after saline injections (Saline control) and 1, 4, 7, and 30 days (d) post SE. **B.** Quantification of GFAP immunoreactivity in the various layers of CA3. * indicates $p < 0.05$, ** indicates $p < 0.01$, and *** indicates $p < 0.001$ when compared to saline control. For each time point, 4 slices from each animal (n = 5) were used. Scale bar = 200 μm.

were elevated compared to saline controls. Increased levels were also observed in the S. lucidum at 7 and 30 days post SE. Again, no difference between saline controls and 1 day post SE were observed.

Increased GFAP immunoreactivity was also observed in the contralateral hippocampus. More specifically, increased GFAP levels were observed 4, 7, and 30 days post SE in all layers quantified (Figure 2.13). No difference between the saline controls and 1 day post IHKA injections was observed. Interestingly, GFAP expression on the contralateral side remained constantly elevated after and including 4 days post IHKA injections in certain hippocampal layers (S. pyramidale, S. radiatum, SLM) but seemed to slightly recover over time in the


A
GFAP
DAPI
Merged
Saline control
1 d post SE
4 d post SE
7 d post SE
30 d post SE
SO
SP
SR
SLM
ML
GCL
H

B

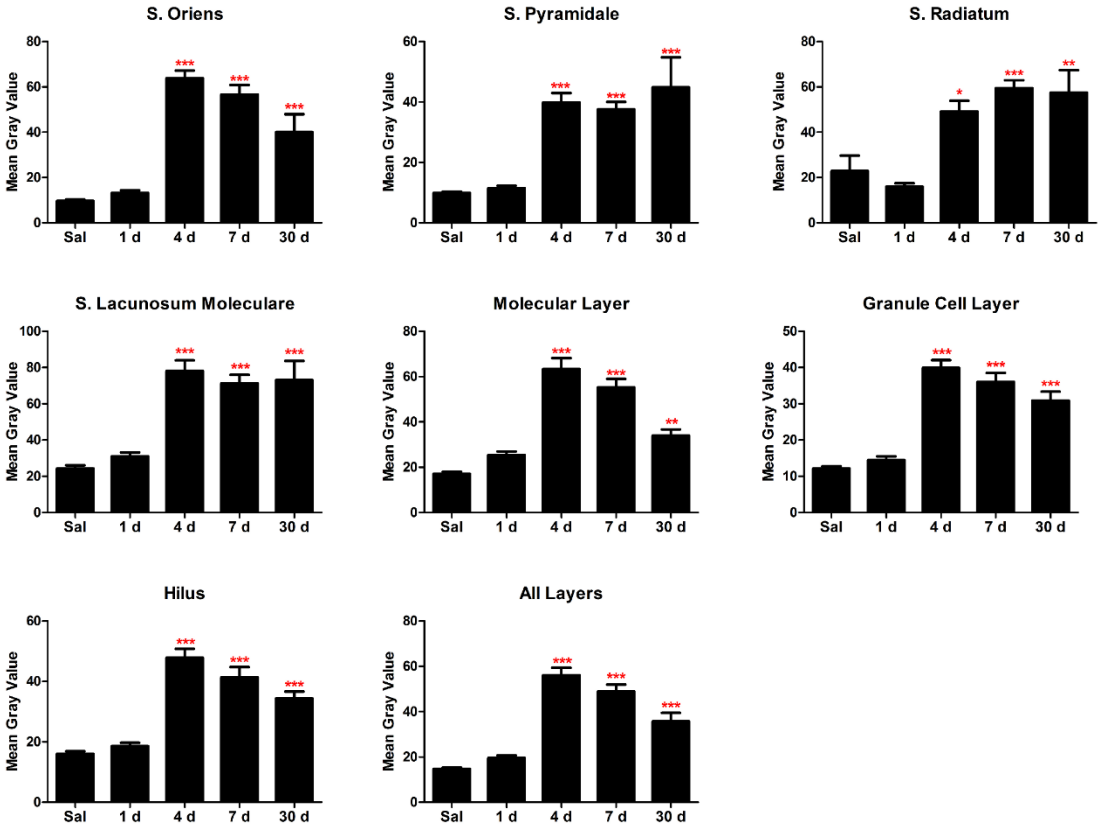
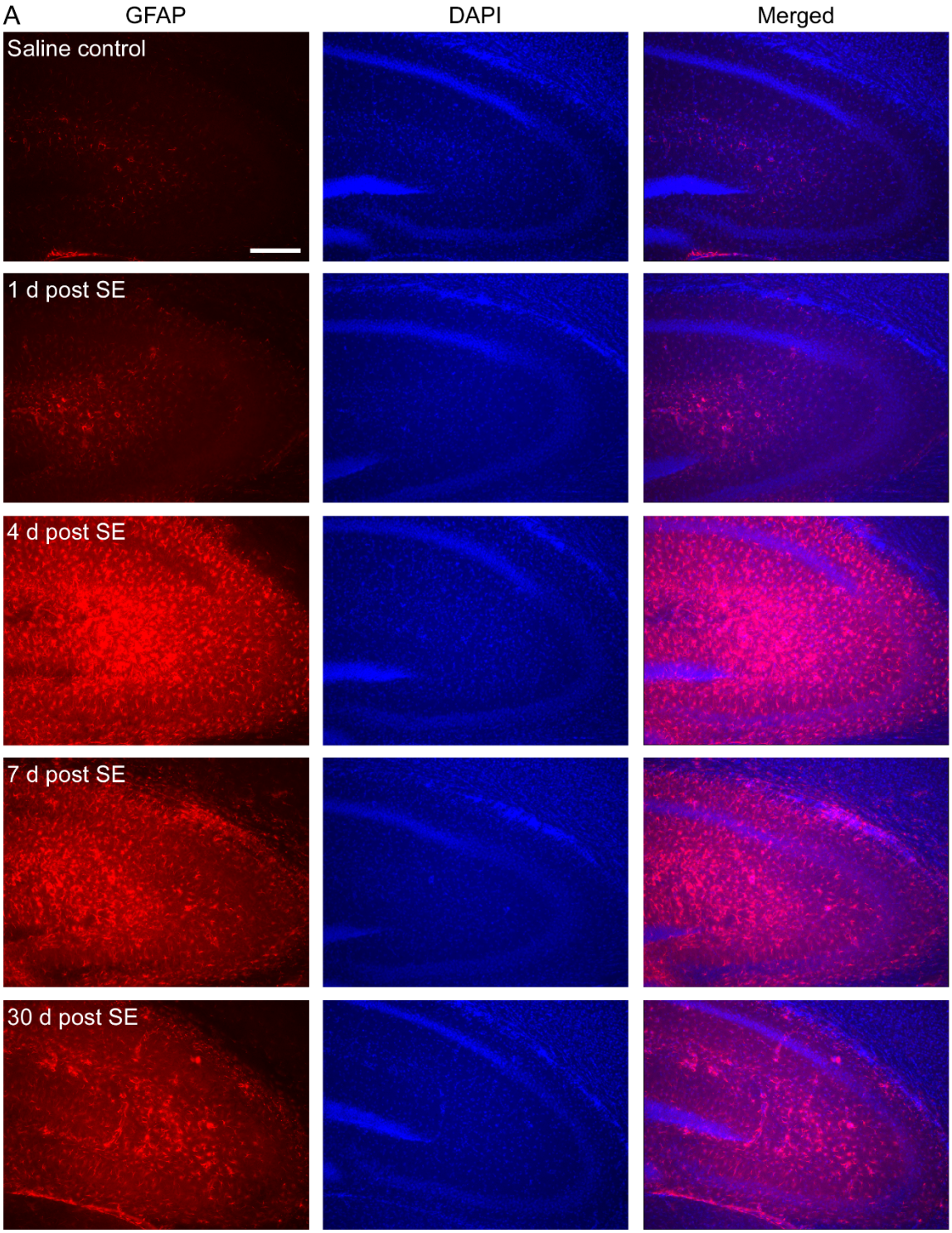


Figure 2.13. Glial fibrillary acidic protein (GFAP) immunoreactivity in the contralateral hippocampus after kainic acid-induced status epilepticus (SE).

A. 10x images of GFAP (red), DAPI (blue), and merged immunoreactivity of the contralateral hippocampus after saline injections (Saline control) and 1, 4, 7, and 30 days (d) post SE. **B.** Quantification of GFAP immunoreactivity in the various layers of the hippocampus. * indicates $p < 0.05$, ** indicates $p < 0.01$, and *** indicates $p < 0.001$ when compared to saline control. For each time point, 4 slices from each animal (n = 5) were used. Scale bar = 200 µm. SO = stratum oriens; SP = stratum pyramidale; SR = stratum radiatum; SLM = stratum lacunosum moleculare; ML = molecular layer; GCL = granule cell layer; H = hilus.


A
GFAP
DAPI
Merged
Saline control
1 d post SE
4 d post SE
7 d post SE
30 d post SE

B

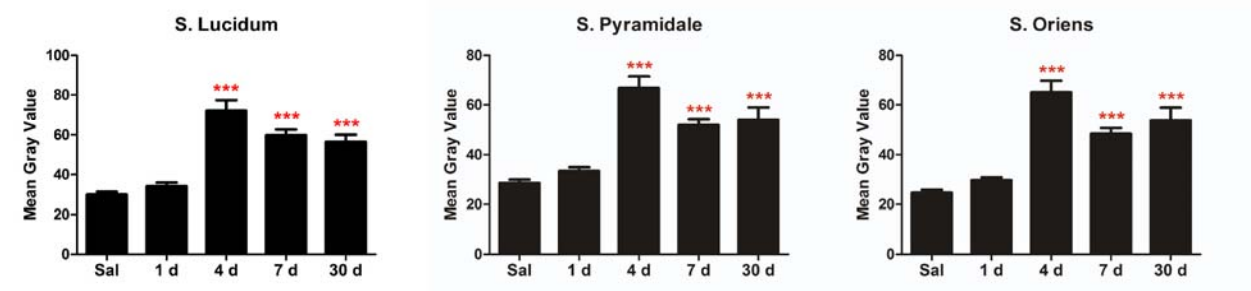


Figure 2.14. Glial fibrillary acidic protein (GFAP) immunoreactivity in the contralateral CA3 region of the hippocampus after kainic acid-induced status epilepticus (SE).
A. 10x images of GFAP (red), (blue), and merged immunoreactivity of the contralateral CA3 region of the hippocampus after saline injections (Saline control) and 1, 4, 7, and 30 days (d) post SE. **B.** Quantification of GFAP immunoreactivity in the various layers of CA3. * indicates $p < 0.05$, ** indicates $p < 0.01$, and *** indicates $p < 0.001$ when compared to saline control. For each time point, 4 slices from each animal (n = 5) were used. Scale bar = 200 μm.

remainder of hippocampal layers (although GFAP immunoreactivity was still elevated to statistically significant levels compared to saline controls). Increased GFAP immunoreactivity was also observed in the S. lucidum, S. pyramidale, and S. oriens in the CA3 region of the hippocampus 4, 7, and 30 days post IHKA-induced SE (Figure 2.14).

I next used Western blot and RT-PCR to investigate changes in GFAP hippocampal protein and mRNA levels, respectively (Figure 2.15). A progressive increase in GFAP protein levels in both the ipsilateral (Figure 2.15A-B) and contralateral (Figure 2.15D-E) hippocampi were noted. Specifically, no changes in GFAP protein expression were observed 1 day post SE, but a trend towards increased protein was observed 4 days post SE with a significant and persistent

increase at 7 and 30 days post SE. GFAP mRNA, on the other hand, showed a significant increase in expression at 1 and 4 days post SE in the ipsilateral hippocampus (Figure 2.15C) but only an increase at 1 day post SE in the contralateral hippocampus (Figure 2.15F). Taken together, these results

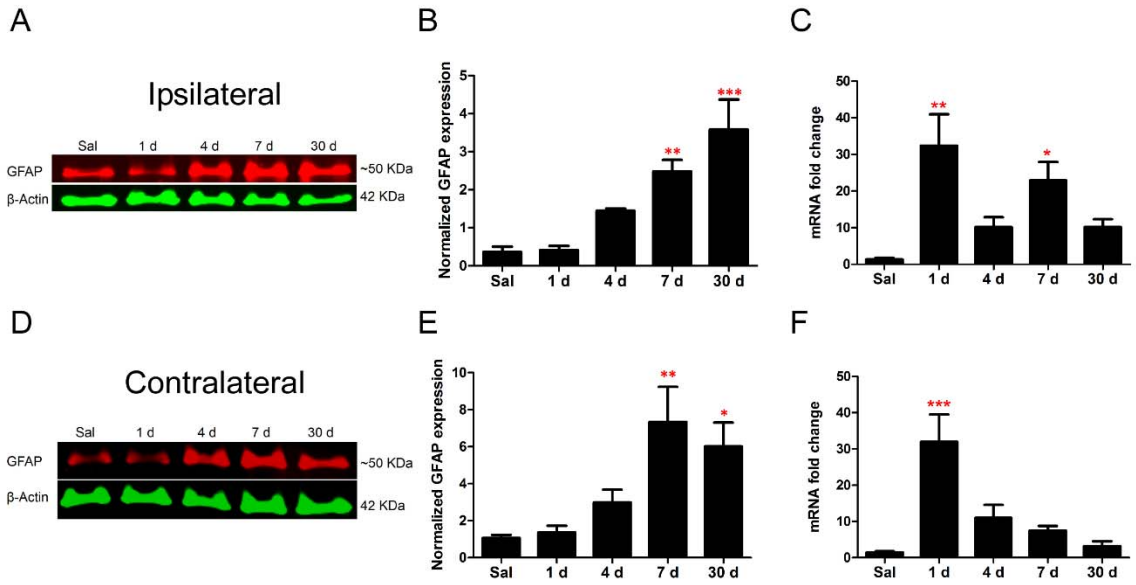


Figure 2.15 Hippocampal protein and mRNA quantification of glial fibrillary acidic protein (GFAP) after kainic acid-induced status epilepticus (SE). **A.** Representative Western blot of GFAP (red) and β-actin (green) protein from the ipsilateral hippocampus of a saline control (Sal) and 1, 4, 7, and 30 days (d) after kainic acid-induced SE. **B.** Quantification of GFAP band intensities normalized to β-actin at each time point in the ipsilateral hippocampus. **C.** Fold change in GFAP mRNA levels in the ipsilateral hippocampal tissue from saline controls (Sal) and in tissue collected 1, 4, 7, and 30 days (d) post SE. **D.** Representative Western blot of GFAP (red) and β-actin (green) protein from the contralateral hippocampus from a saline control (Sal) and 1, 4, 7, and 30 days (d) post SE. **E.** Quantification of contralateral GFAP protein normalized to β-actin in each group. **F.** Quantification of GFAP mRNA levels in the contralateral hippocampus of saline controls (Sal) and various time points post SE. * indicates $p < 0.05$, ** indicates $p < 0.01$, and *** indicates $p < 0.001$ when compared to saline control and $n = 5$ for each time point.

suggest that both GFAP mRNA and protein were significantly increased during epileptogenesis in the IHKA model.

2.5 Discussion

The IHKA model of epilepsy is an excellent model of TLE. Our lab has shown that 100% of mice that survived after SE went on to develop several spontaneous seizures per day (Lee, Hsu et al. 2012). The survival rate for this surgery was about 80%. In this model, I observed hippocampal sclerosis, the most common pathological feature found in patients with TLE. Hippocampal sclerosis has been found in 30-58% of temporal lobe cases in autopsy studies (Margerison and Corsellis 1966; de Lanerolle, Kim et al. 2003; Binder and Steinhäuser 2006). Like others (Margerison and Corsellis 1966; Blümcke, Beck et al. 1999; Clasadonte and Haydon 2012; de Lanerolle, Lee et al. 2012), I observed dispersion of granule cell neurons, death of pyramidal neurons in CA1, microgliosis, and astrogliosis. Furthermore, I observed glial cell changes in both the ipsilateral and contralateral hippocampi to injection, suggesting that this feature is not exclusive to hippocampal sclerosis. Finally, I demonstrated a progressive increase in GFAP protein and transient increases in GFAP mRNA during the development of epilepsy in both the ipsilateral and contralateral hippocampus. Therefore, seizure activity propagated from the ipsilateral (injected) hippocampus to the contralateral hippocampus and caused a subset of

histopathological changes, including gliosis, but not granule cell dispersion or CA1 pyramidal cell death. This study is unique in that it carefully examined ipsilateral vs. contralateral effects of IHKA injections on the hippocampus whereas many previous studies have not. Changes in other astrocyte-specific molecules during the development of epilepsy will be discussed in later chapters.

In other studies, both astrogliosis and microgliosis has been observed in tissue from epileptic patients (Najjar, Pearlman et al. 2011), including in the sclerotic hippocampus of patients with TLE (Sheng, Boop et al. 1994; Beach, Woodhurst et al. 1995; Crespel, Coubes et al. 2002; Aronica, Boer et al. 2007; Ravizza, Gagliardi et al. 2008; Choi, Nordli et al. 2009; Zattoni, Mura et al. 2011) and in focal cortical dysplasia (FCD) (Boer, Spliet et al. 2006; Choi, Nordli et al. 2009; Iyer, Zurolo et al. 2010), as well as in a number of animal models of epilepsy (Ravizza, Rizzi et al. 2005; Somera-Molina, Robin et al. 2007; Ravizza, Gagliardi et al. 2008; Abraham, Fox et al. 2012; Kaur, Patro et al. 2015). The release of proinflammatory molecules from these reactive cells may alter interactions between glial cells and neurons, particularly targeting astrocytes, which may lead to seizure generation and spread (Aronica, Ravizza et al. 2012). In addition, reactive astrocytes in the hippocampus of patients with mesial TLE overexpressed NFκB-p65, a transcription factor known to activate the transcription of numerous proinflammatory genes (Crespel, Coubes et al. 2002). Therefore, gliosis and inflammation may be key components to epileptogenesis.

Microgliosis has been observed in epilepsy patients with Rasmussen's encephalitis (Bauer, Elger et al. 2007; Wirenfeldt, Clare et al. 2009) and hippocampal sclerosis (Blanc, Martinian et al. 2011). It has also been observed in the kainic acid (Sharma, Jordan et al. 2008; Abraham, Fox et al. 2012), pilocarpine (Estrada, Hernandez et al. 2012), and Theiler murine encephalomyelitis virus (Loewen, Barker-Haliski et al. 2016) models of epilepsy, but not in the corneal kindled mouse model (Loewen, Barker-Haliski et al. 2016). Recently, it was shown that the ionotropic purinergic receptor $P2X_7$ activation mediated microglial activation and the release of interleukin 1β (IL-1β); antagonism of this receptor reduced microglial activation (Henshall and Engel 2015). Therefore, the mechanism of microglial activation may involve both neuroinflammation and purinergic signaling.

Significant increases in GFAP gene expression have been observed in both the latent and chronic stages of epilepsy (Lukasiuk and Pitkänen 2004). My findings also match previous studies that demonstrated increased GFAP expression in the electrical kindling (Torre, Lothman et al. 1993; Stringer 1996; Miyazaki, Miyamoto et al. 2003), pentylenetetrazol (PTZ) (Torre, Lothman et al. 1993), kainic acid (Bendotti, Guglielmetti et al. 2000; Lee, Hsu et al. 2012), pilocarpine (Estrada, Hernandez et al. 2012), and frequent repetitive febrile seizures (FRFS) (Yang, Li et al. 2009) models of epilepsy. Although astrogliosis in epilepsy is well established, the mechanism of GFAP upregulation remains unknown. One study

has suggested transcriptional activation of GFAP by the neuropeptide galanin and calcitonin gene-related peptide (CGRP) in cultured astrocytes (Priller, Haas et al. 1998). More recently, it was observed that IL-1β regulated cortical reorganization of F-actin through Rho GTPase-Rho kinase pathway (John, Chen et al. 2004). In a murine corticectomy model of CNS lesion, GFAP transcript elevation immediately followed the early rise in IL-1β mRNA (Herx and Yong 2001). Interestingly, IL-1β knockout mice did not exhibit injury-induced upregulation of GFAP mRNA and protein 2-3 days after injury, although GFAP immunoreactivity was not different between wild-type and knockout mice by 5-7 days after lesion induction (Herx and Yong 2001). A recent study has shown that mice with conditional deletion of β1-integrin developed widespread reactive astrogliosis, spontaneous seizures and impaired glutamate uptake (Robel, Buckingham et al. 2015). Whether astrogliosis itself contributes to epileptogenesis, however, remains unclear.

In summary, I observed neuronal, microglial, and astrocytic changes in the IHKA model of epilepsy. The IHKA model proved to be a reproducible, reliable, and accurate model of the human epileptic condition and it presented with the common pathological feature of hippocampal sclerosis. I focused on the expression changes of the astrocyte marker GFAP and found increases in immunoreactivity, protein, and mRNA levels during the development of epilepsy. Although the exact mechanisms of gliosis are unknown, they likely involves

neuroinflammatory molecules such as IL-1β. Future studies should focus on elucidating the mechanism of gliosis so it can be targeted in novel antiepileptogenic strategies.

2.6 References

Abraham, J., P. D. Fox, C. Condello, A. Bartolini and S. Koh (2012). "Minocycline attenuates microglia activation and blocks the long-term epileptogenic effects of early-life seizures." Neurobiol Dis **46**(2): 425-430.

Araque, A., V. Parpura, R. P. Sanzgiri and P. G. Haydon (1999). "Tripartite synapses: glia, the unacknowledged partner." Trends Neurosci **22**(5): 208-215.

Aronica, E., K. Boer, E. A. van Vliet, S. Redeker, J. C. Baayen, W. G. Spliet, P. C. van Rijen, D. Troost, F. H. da Silva, W. J. Wadman and J. A. Gorter (2007). "Complement activation in experimental and human temporal lobe epilepsy." Neurobiol Dis **26**(3): 497-511.

Aronica, E., T. Ravizza, E. Zurolo and A. Vezzani (2012). "Astrocyte immune responses in epilepsy." Glia **60**(8): 1258-1268.

Babb, T. L., J. P. Lieb, W. J. Brown, J. Pretorius and P. H. Crandall (1984). "Distribution of pyramidal cell density and hyperexcitability in the epileptic human hippocampal formation." Epilepsia **25**(6): 721-728.

Babb, T. L., J. Pereira-Leite, G. W. Mathern and J. K. Pretorius (1995). "Kainic acid induced hippocampal seizures in rats: comparisons of acute and chronic seizures using intrahippocampal versus systemic injections." Ital J Neurol Sci **16**(1-2): 39-44.

Bauer, J., C. E. Elger, V. H. Hans, J. Schramm, H. Urbach, H. Lassmann and C. G. Bien (2007). "Astrocytes are a specific immunological target in Rasmussen's encephalitis." Ann Neurol **62**(1): 67-80.

Beach, T. G., W. B. Woodhurst, D. B. MacDonald and M. W. Jones (1995). "Reactive microglia in hippocampal sclerosis associated with human temporal lobe epilepsy." Neurosci Lett **191**(1-2): 27-30.

Bendotti, C., F. Guglielmetti, M. Tortarolo, R. Samanin and W. D. Hirst (2000). "Differential expression of S100beta and glial fibrillary acidic protein in the hippocampus after kainic acid-induced lesions and mossy fiber sprouting in adult rat." Exp Neurol **161**(1): 317-329.

Binder, D. K. and C. Steinhäuser (2006). "Functional changes in astroglial cells in epilepsy." Glia **54**(5): 358-368.

Blanc, F., L. Martinian, I. Liagkouras, C. Catarino, S. M. Sisodiya and M. Thom (2011). "Investigation of widespread neocortical pathology associated with hippocampal sclerosis in epilepsy: a postmortem study." Epilepsia **52**(1): 10-21.

Blümcke, I., H. Beck, A. A. Lie and O. D. Wiestler (1999). "Molecular neuropathology of human mesial temporal lobe epilepsy." Epilepsy Res **36**(2-3): 205-223.

Boer, K., W. G. Spliet, P. C. van Rijen, S. Redeker, D. Troost and E. Aronica (2006). "Evidence of activated microglia in focal cortical dysplasia." J Neuroimmunol **173**(1-2): 188-195.

Choi, J., D. R. Nordli, Jr., T. D. Alden, A. DiPatri, Jr., L. Laux, K. Kelley, J. Rosenow, S. U. Schuele, V. Rajaram and S. Koh (2009). "Cellular injury and neuroinflammation in children with chronic intractable epilepsy." J Neuroinflammation **6**: 38.

Clasadonte, J. and P. G. Haydon (2012). Astrocytes and Epilepsy. Jasper's Basic Mechanisms of the Epilepsies. J. L. Noebels, M. Avoli, M. A. Rogawski, R. W. Olsen and A. V. Delgado-Escueta. Bethesda (MD).

Clasadonte, J. and P. G. Haydon (2012). Astrocytes and epilepsy. Jasper's Basic Mechanisms of the Epilepsies. J. L. Noebles, Avoli, M., Rogawski, M.A., Olsen, R.W., Delgado-Escueta, A.V.**:** 19.

Coulter, D. A. and C. Steinhauser (2015). "Role of astrocytes in epilepsy." Cold Spring Harb Perspect Med **5**(3): a022434.

Crespel, A., P. Coubes, M. C. Rousset, C. Brana, A. Rougier, G. Rondouin, J. Bockaert, M. Baldy-Moulinier and M. Lerner-Natoli (2002). "Inflammatory reactions in human medial temporal lobe epilepsy with hippocampal sclerosis." Brain Res **952**(2): 159-169.

Davis, E. J., T. D. Foster and W. E. Thomas (1994). "Cellular forms and functions of brain microglia." Brain Res Bull **34**(1): 73-78.

de Lanerolle, N. C., J. H. Kim, A. Williamson, S. S. Spencer, H. P. Zaveri, T. Eid and D. D. Spencer (2003). "A retrospective analysis of hippocampal pathology in human temporal lobe epilepsy: evidence for distinctive patient subcategories." Epilepsia **44**(5): 677-687.

de Lanerolle, N. C., T. S. Lee and D. D. Spencer (2012). Histopathology of Human Epilepsy. Jasper's Basic Mechanisms of the Epilepsies. J. L.

Noebels, M. Avoli, M. A. Rogawski, R. W. Olsen and A. V. Delgado-Escueta. Bethesda (MD).

Devinsky, O., A. Vezzani, S. Najjar, N. C. De Lanerolle and M. A. Rogawski (2013). "Glia and epilepsy: excitability and inflammation." Trends Neurosci **36**(3): 174-184.

Estrada, F. S., V. S. Hernandez, E. Lopez-Hernandez, A. A. Corona-Morales, H. Solis, A. Escobar and L. Zhang (2012). "Glial activation in a pilocarpine rat model for epileptogenesis: a morphometric and quantitative analysis." Neurosci Lett **514**(1): 51-56.

Eyo, U. B., M. Murugan and L. J. Wu (2016). "Microglia-Neuron Communication in Epilepsy." Glia.

Halassa, M. M. and P. G. Haydon (2010). "Integrated brain circuits: astrocytic networks modulate neuronal activity and behavior." Annu Rev Physiol **72**: 335-355.

Henshall, D. C. and T. Engel (2015). "P2X purinoceptors as a link between hyperexcitability and neuroinflammation in status epilepticus." Epilepsy Behav **49**: 8-12.

Herx, L. M. and V. W. Yong (2001). "Interleukin-1 beta is required for the early evolution of reactive astrogliosis following CNS lesion." J Neuropathol Exp Neurol **60**(10): 961-971.

Hubbard, J. A. and D. K. Binder (2016). Astrocytes and Epilepsy. Amsterdam, Netherlands, Elsevier, in press.

Hubbard, J. A., M. S. Hsu, T. A. Fiacco and D. K. Binder (2013). "Glial cell changes in epilepsy: overview of the clinical problem and therapeutic opportunities." Neurochem Int **63**(7): 638-651.

Iyer, A., E. Zurolo, W. G. Spliet, P. C. van Rijen, J. C. Baayen, J. A. Gorter and E. Aronica (2010). "Evaluation of the innate and adaptive immunity in type I and type II focal cortical dysplasias." Epilepsia **51**(9): 1763-1773.

John, G. R., L. Chen, M. A. Rivieccio, C. V. Melendez-Vasquez, A. Hartley and C. F. Brosnan (2004). "Interleukin-1beta induces a reactive astroglial phenotype via deactivation of the Rho GTPase-Rock axis." J Neurosci **24**(11): 2837-2845.

Kandratavicius, L., P. A. Balista, C. Lopes-Aguiar, R. N. Ruggiero, E. H. Umeoka, N. Garcia-Cairasco, L. S. Bueno-Junior and J. P. Leite (2014). "Animal models of epilepsy: use and limitations." Neuropsychiatr Dis Treat **10**: 1693-1705.

Kaur, H., I. Patro, K. Tikoo and R. Sandhir (2015). "Curcumin attenuates inflammatory response and cognitive deficits in experimental model of chronic epilepsy." Neurochem Int **89**: 40-50.

Lee, D. J., M. S. Hsu, M. M. Seldin, J. L. Arellano and D. K. Binder (2012). "Decreased expression of the glial water channel aquaporin-4 in the intrahippocampal kainic acid model of epileptogenesis." Exp Neurol **235**(1): 246-255.

Lee, D. J., M. S. Hsu, M. M. Seldin, J. L. Arellano and D. K. Binder (2012). "Decreased expression of the glial water channel aquaporin-4 in the intrahippocampal kainic acid model of epileptogenesis." Experimental Neurology **235**(1): 246-255.

Leite, J. P., T. L. Babb, J. K. Pretorius, P. A. Kuhlman, K. M. Yeoman and G. W. Mathern (1996). "Neuron loss, mossy fiber sprouting, and interictal spikes after intrahippocampal kainate in developing rats." Epilepsy Res **26**(1): 219-231.

Loewen, J. L., M. L. Barker-Haliski, E. J. Dahle, H. S. White and K. S. Wilcox (2016). "Neuronal Injury, Gliosis, and Glial Proliferation in Two Models of Temporal Lobe Epilepsy." J Neuropathol Exp Neurol **75**(4): 366-378.

Lukasiuk, K. and A. Pitkänen (2004). "Large-scale analysis of gene expression in epilepsy research: is synthesis already possible?" Neurochem Res **29**(6): 1169-1178.

Margerison, J. H. and J. A. Corsellis (1966). "Epilepsy and the temporal lobes. A clinical, electroencephalographic and neuropathological study of the brain in epilepsy, with particular reference to the temporal lobes." Brain **89**(3): 499-530.

Mathern, G. W., J. K. Pretorius and T. L. Babb (1995). "Quantified patterns of mossy fiber sprouting and neuron densities in hippocampal and lesional seizures." J Neurosurg **82**(2): 211-219.

Miyazaki, T., O. Miyamoto, N. A. Janjua, T. Hata, F. Takahashi and T. Itano (2003). "Reactive gliosis in areas around third ventricle in association with epileptogenesis in amygdaloid-kindled rat." Epilepsy Res **56**(1): 5-15.

Murphy-Royal, C., J. P. Dupuis, J. A. Varela, A. Panatier, B. Pinson, J. Baufreton, L. Groc and S. H. Oliet (2015). "Surface diffusion of astrocytic glutamate transporters shapes synaptic transmission." Nat Neurosci **18**(2): 219-226.

Najjar, S., D. Pearlman, D. C. Miller and O. Devinsky (2011). "Refractory epilepsy associated with microglial activation." Neurologist **17**(5): 249-254.

Ngugi, A. K., C. Bottomley, I. Kleinschmidt, J. W. Sander and C. R. Newton (2010). "Estimation of the burden of active and life-time epilepsy: a meta-analytic approach." Epilepsia **51**(5): 883-890.

Paxinos, G. and K. B. J. Franklin (2001). The mouse brain in stereotaxic coordinates. San Diego, CA, Academic Press.

Priller, J., C. A. Haas, M. Reddington and G. W. Kreutzberg (1998). "Cultured astrocytes express functional receptors for galanin." Glia **24**(3): 323-328.

Racine, R. J. (1972). "Modification of seizure activity by electrical stimulation. II. Motor seizure." Electroencephalogr Clin Neurophysiol **32**(3): 281-294.

Ransom, B., T. Behar and M. Nedergaard (2003). "New roles for astrocytes (stars at last)." Trends Neurosci **26**(10): 520-522.

Ransom, B. R. and C. B. Ransom (2012). "Astrocytes: multitalented stars of the central nervous system." Methods Mol Biol **814**: 3-7.

Ravizza, T., B. Gagliardi, F. Noe, K. Boer, E. Aronica and A. Vezzani (2008). "Innate and adaptive immunity during epileptogenesis and spontaneous seizures: evidence from experimental models and human temporal lobe epilepsy." Neurobiol Dis **29**(1): 142-160.

Ravizza, T., M. Rizzi, C. Perego, C. Richichi, J. Veliskova, S. L. Moshe, M. G. De Simoni and A. Vezzani (2005). "Inflammatory response and glia activation in developing rat hippocampus after status epilepticus." Epilepsia **46 Suppl 5**: 113-117.

Robel, S., S. C. Buckingham, J. L. Boni, S. L. Campbell, N. C. Danbolt, T. Riedemann, B. Sutor and H. Sontheimer (2015). "Reactive astrogliosis causes the development of spontaneous seizures." J Neurosci **35**(8): 3330-3345.

Robel, S. and H. Sontheimer (2016). "Glia as drivers of abnormal neuronal activity." Nat Neurosci **19**(1): 28-33.

Seifert, G., G. Carmignoto and C. Steinhäuser (2010). "Astrocyte dysfunction in epilepsy." Brain Research Reviews **63**: 212-221.

Seifert, G., K. Schilling and C. Steinhäuser (2006). "Astrocyte dysfunction in neurological disorders: a molecular perspective." Nature Reviews Neuroscience **7**(194-206).

Sharma, A. K., W. H. Jordan, R. Y. Reams, D. G. Hall and P. W. Snyder (2008). "Temporal profile of clinical signs and histopathologic changes in an F-344 rat model of kainic acid-induced mesial temporal lobe epilepsy." Toxicol Pathol **36**(7): 932-943.

Sharma, A. K., R. Y. Reams, W. H. Jordan, M. A. Miller, H. L. Thacker and P. W. Snyder (2007). "Mesial temporal lobe epilepsy: pathogenesis, induced rodent models and lesions." Toxicol Pathol **35**(7): 984-999.

Sheng, J. G., F. A. Boop, R. E. Mrak and W. S. Griffin (1994). "Increased neuronal beta-amyloid precursor protein expression in human temporal lobe epilepsy: association with interleukin-1 alpha immunoreactivity." J Neurochem **63**(5): 1872-1879.

Somera-Molina, K. C., B. Robin, C. A. Somera, C. Anderson, C. Stine, S. Koh, H. A. Behanna, L. J. Van Eldik, D. M. Watterson and M. S. Wainwright (2007). "Glial activation links early-life seizures and long-term neurologic dysfunction: evidence using a small molecule inhibitor of proinflammatory cytokine upregulation." Epilepsia **48**(9): 1785-1800.

Stringer, J. L. (1996). "Repeated seizures increase GFAP and vimentin in the hippocampus." Brain Res **717**(1-2): 147-153.

Thurman, D. J., E. Beghi, C. E. Begley, A. T. Berg, J. R. Buchhalter, D. Ding, D. C. Hesdorffer, W. A. Hauser, L. Kazis, R. Kobau, B. Kroner, D. Labiner, K. Liow, G. Logroscino, M. T. Medina, C. R. Newton, K. Parko, A. Paschal, P. M. Preux, J. W. Sander, A. Selassie, W. Theodore, T. Tomson and S. Wiebe (2011). "Standards for epidemiologic studies and surveillance of epilepsy." Epilepsia **52 Suppl 7**: 2-26.

Tian, G., H. Azmi, T. Takano, Q. Xu, W. Peng, J. Lin, N. Oberheim, N. Lou, R. Zielke, J. Kang and M. Nedergaard (2005). "An astrocytic basis of epilepsy." Nature Medicine **11**(9): 973-981.

Torre, E. R., E. Lothman and O. Steward (1993). "Glial response to neuronal activity: GFAP-mRNA and protein levels are transiently increased in the hippocampus after seizures." Brain Res **631**(2): 256-264.

Tugcu, B., A. Gungor, A. Akpinar, D. Kinay, D. Y. Kuscu, G. Gul, N. Kayrak, C. Keskinkilic, H. Akdemir and E. Emel (2016). "Outcome of surgical treatment of hippocampal sclerosis from relatively new epilepsy surgery center." J Neurosurg Sci **60**(2): 159-168.

Volterra, A. and J. Meldolesi (2005). "Astrocytes, from brain glue to communication elements: the revolution continues." Nat Rev Neurosci **6**(8): 626-640.

Wiebe, S. (2000). "Epidemiology of temporal lobe epilepsy." Can J Neurol Sci **27 Suppl 1**: S6-10; discussion S20-11.

Wilcox, K. S., J. M. Gee, M. B. Gibbons, P. Tvrdik and J. A. White (2015). "Altered structure and function of astrocytes following status epilepticus." Epilepsy Behav **49**: 17-19.

Wirenfeldt, M., R. Clare, S. Tung, A. Bottini, G. W. Mathern and H. V. Vinters (2009). "Increased activation of Iba1+ microglia in pediatric epilepsy patients with Rasmussen's encephalitis compared with cortical dysplasia and tuberous sclerosis complex." Neurobiol Dis **34**(3): 432-440.

Yang, L., F. Li, H. Zhang, W. Ge, C. Mi, R. Sun and C. Liu (2009). "Astrocyte activation and memory impairment in the repetitive febrile seizures model." Epilepsy Res **86**(2-3): 209-220.

Zattoni, M., M. L. Mura, F. Deprez, R. A. Schwendener, B. Engelhardt, K. Frei and J. M. Fritschy (2011). "Brain infiltration of leukocytes contributes to the pathophysiology of temporal lobe epilepsy." J Neurosci **31**(11): 4037-4050.

Ziebell, J. M., P. D. Adelson and J. Lifshitz (2015). "Microglia: dismantling and rebuilding circuits after acute neurological injury." Metab Brain Dis **30**(2): 393-400.

Chapter 3: Expression of aquaporin-4 in the mouse brain

This chapter was reproduced and modified, with permission, from: Hubbard, J. A., Hsu, M. S., Seldin M.M., and Binder, D.K. (2015). "Expression of the Astrocyte Water Channel Aquaporin-4 in the Mouse Brain." *ASN Neuro* 7(5). For the Creative Commons license, please see the following link: http://creativecommons.org/licenses/by/3.0/legalcode

3.1 Abstract

Aquaporin-4 (AQP4) is a bidirectional water channel that is found on astrocytes throughout the CNS. Expression is particularly high around areas in contact with cerebrospinal fluid (CSF), suggesting that AQP4 plays a role in fluid exchange between the CSF compartments and the brain. Despite its significant role in the brain, the overall spatial and region-specific distribution of AQP4 has yet to be fully characterized. In this chapter, I used Western blotting and immunohistochemical techniques to characterize AQP4 expression and localization throughout the mouse brain. I observed AQP4 expression throughout the forebrain, subcortical areas and brainstem. AQP4 protein levels were highest in the cerebellum with lower expression in the cortex and hippocampus. I found that AQP4 immunoreactivity was profuse on glial cells bordering ventricles, blood vessels and subarachnoid space. Throughout the

brain, AQP4 was expressed on astrocytic endfeet surrounding blood vessels but was also heterogeneously expressed in brain tissue parenchyma and neuropil, often with striking laminar specificity. In the cerebellum, I showed that AQP4 colocalized with the proteoglycan brevican, which is synthesized by and expressed on cerebellar astrocytes. Despite the high abundance of AQP4 in the cerebellum, its functional significance has yet to be investigated. Given the known role of AQP4 in synaptic plasticity in the hippocampus, the widespread and region-specific expression pattern of AQP4 suggests involvement not only in fluid balance and ion homeostasis but also local synaptic plasticity and function in distinct brain circuits.

3.2 Introduction

The aquaporins (AQPs) are a family of at least 13 molecular water channels that are expressed throughout various mammalian tissues. A number of these proteins have been found in the brain, including AQP1, AQP3, AQP4, AQP5, AQP6, AQP8, AQP9 and AQP12 (Badaut, Fukuda et al. 2014). Aquaporin-4 (AQP4) is the main water channel in the neuropil of the CNS and is highly polarized in expression (Nielsen, Nagelhus et al. 1997). It is primarily found on astrocytes, particularly on the astrocytic end-feet surrounding capillaries and the blood-brain barrier as well as the glia limitans (Nagelhus, Mathiisen et al. 2004; Oshio, Binder et al. 2004; Costa, Tortosa et al. 2007). AQP4 is highly abundant

at sites of fluid transport, including pial and ependymal surfaces in contact with CSF, subarachnoid space, and the ventricular system (Nielsen, Nagelhus et al. 1997; Rash, Yasumura et al. 1998). Based on its location and expression, it was hypothesized that AQP4 is involved in bidirectional fluid exchange between both the blood and CSF compartments and the brain (Nagelhus, Mathiisen et al. 2004).

Studies using AQP4 null mice have helped elucidate the role of AQP4 in brain function. Initially generated in 1997 using targeted gene distribution (Ma, Yang et al. 1997), AQP4 knockout mice appear normal in phenotype, growth, tissue morphology, neuromuscular function, blood brain barrier function, baseline intracranial pressure (ICP), and intracranial compliance (Ma, Yang et al. 1997; Manley, Fujimura et al. 2000; Papadopoulos, Manley et al. 2004). However, these mice exhibited decreased astrocyte water permeability (Solenov, Watanabe et al. 2004) and a mild urine concentrating deficit (Ma, Yang et al. 1997). The use of these knockout mice have revealed that AQP4 is involved in a variety of brain functions including normal cognitive function (Skucas, Mathews et al. 2011; Scharfman and Binder 2013), spatial memory (Zhang, Li et al. 2013), K^+ buffering (Binder, Yao et al. 2006), astrocyte migration (Saadoun, Papadopoulos et al. 2005), cell adhesion (Hiroaki, Tani et al. 2006), and regulation of brain extracellular space (Binder, Papadopoulos et al. 2004).

Abnormalities in water balance play a crucial role in the pathophysiology of several neurological disorders, including cerebral edema, stroke, and epilepsy. Due to impaired AQP4-dependent water clearance, AQP4 knockout mice had higher ICP and accelerated neurological deterioration in a model of vasogenic edema compared to wild type mice (Papadopoulos, Manley et al. 2004). Interestingly, AQP4-deficient mice have increased survival and reduced swelling in models of cytotoxic (cellular) edema (Manley, Fujimura et al. 2000). In the rodent stroke model of transient occlusion of the middle cerebral artery, AQP4 immunoreactivity was rapidly reduced, primarily in regions with vascular damage (Friedman, Schachtrup et al. 2009). However, AQP4 expression changes depend on the model used; for example, in the rodent model of transient focal brain ischemia, peaks of swelling and AQP4 expression, particularly the M1 isoform, were observed at 1- and 48-hours after ischemia (Ribeiro Mde, Hirt et al. 2006; Hirt, Ternon et al. 2009). In an animal model of temporal lobe epilepsy, hippocampal AQP4 immunoreactivity was downregulated with partial recovery over time (Lee, Hsu et al. 2012). In addition, AQP4 knockout mice exhibited prolonged seizure duration and slowed K^+ kinetics, but increased seizure latency, in response to hippocampal electrical stimulation (Binder, Yao et al. 2006). Despite the clear functional significance of AQP4 in both the healthy and diseased brain, AQP4 expression patterns in distinct brain areas have been incompletely defined.

Determining the overall spatial distribution of AQP4 throughout the brain could enhance our understanding of the functional relationship between AQP4 and specific regions in the brain. Thus far, the location and abundance of AQP4 protein in the brain has only been partially described and only in certain brain areas (Nielsen, Nagelhus et al. 1997; Rash, Yasumura et al. 1998; Wen, Nagelhus et al. 1999; Nagelhus, Mathiisen et al. 2004; Oshio, Binder et al. 2004; Vitellaro-Zuccarello, Mazzetti et al. 2005; Costa, Tortosa et al. 2007; Hsu, Seldin et al. 2011). Therefore, I developed sensitive and specific Western blotting and immunohistochemical techniques to provide a comprehensive description of AQP4 expression and localization throughout the entire mouse brain. I found that highest AQP4 protein levels were found in the cerebellum while significantly lower levels were in the cortex and hippocampus. Throughout the brain, AQP4 does not only display targeted expression on glial endfeet surrounding blood vessels, but marked region-specific parenchymal expression was also observed.

3.3 Methods

3.3.1 Animals

All experiments were conducted in accordance with the guidelines set forth by the National Institutes of Health and were approved by the University of California, Riverside Institutional Animal Care and Use Committee (IACUC).

Animals were housed under controlled conditions (12 hour light/12 hour dark) and had access to food and water *ad libitum*. Six week old wild-type or AQP4 knockout mice on a CD1 background were used for all experiments.

3.3.2 Western blot

CD1 mice (n=5) were deeply anesthetized with an intraperitoneal injection of sodium pentobarbital (200 mg/kg) and were transcardially perfused with ice-cold phosphate-buffered saline (PBS) containing protease inhibitors (Roche). Brains were quickly removed from the skull and the cerebral cortex, diencephalon, hippocampus, cerebellum and brainstem were rapidly microdissected according to the mouse brain atlas of Paxinos and Watson (Paxinos and Franklin 2001). Tissue was mechanically homogenized in ice-cold radioimmunoprecipitation assay (RIPA) buffer (Sigma) containing a protease inhibitor cocktail (Roche) using a glass dounce tissue grinder (Wheaton). Lysates were centrifuged at 10,000g for 5 minutes and the supernatant extracted. Protein concentrations were determined using Bio-Rad BSA detection system and Bio-Tek plate reader. Briefly, 15 µg of protein were electrophoresed through a 12% SDS-PAGE gel with 0.2% SDS with 8M urea. Samples were then transferred to a nitrocellulose membrane and incubated overnight in a 5% milk in tris-buffered saline with Tween (TBST) blocking solution with rabbit anti-AQP4 (1:1,000; EMD Millipore AB3594 and ABN411) and mouse anti-β-actin (1:5,000, Calbiochem). Specificity

of Millipore anti-AQP4 AB3594 antibody was determined previously with the use of AQP4 knockout mice (Binder, Yao et al. 2006) and specificity of Millipore anti-AQP4 ABN411 is shown in the following chapter. The next day, membranes were washed and incubated for two hours at room temperature with peroxidase-conjugated goat anti-rabbit and goat anti-mouse secondary antibodies. After several washes, membranes were visualized with ECL chemiluminescence (Pierce) and captured on Hyblot film (Denville). Band intensities were determined using densitometry (ImageJ) and AQP4 levels were normalized to β-actin. Statistical analysis was performed with GraphPad Prism 5 using a one-way ANOVA with *post-hoc* Tukey pairs of columns comparison test. Statistical significance was determined by a p-value < 0.05, 0.01 or 0.001.

3.3.3 Immunohistochemistry

Mice were euthanized with 200 mg/kg sodium pentobarbital and transcardially perfused with ice-cold phosphate-buffered saline (PBS) followed by 4% paraformaldehyde (PFA). Brains were then post-fixed overnight in 4% PFA followed by cryoprotection in 30% sucrose in PBS, both at 4°C. Tissue was frozen in dry ice-cold isopentane and stored at -80°C until sectioning. Tissue was cut into either coronal (n=3 mice) or sagittal (n = 3 wild-type mice and n = 3 AQP4 knockout mice) 50 µm thick sections using a cryostat (Leica CM1950). Two sections from every animal of each brain region examined were used, for a

total of n = 6 slices per experiment. In addition, both hemispheres were imaged in coronal slices. Sections were quenched in 3% peroxidase for one hour, blocked with 5% normal goat serum (NGS) in PBS for one hour, and incubated with rabbit anti-AQP4 (1:200; EMD Millipore) in 0.3% Triton-X-100 overnight at 4°C. The next day, sections were washed and incubated with HRP-conjugated goat anti-rabbit and tyramide from a TSA kit (Molecular Probes/Invitrogen). Slices were washed and mounted on frosted slides (Fisher) with Vectashield (Vector laboratories).

Double immunofluorescence labeling of AQP4 with the cerebellar astrocyte marker brevican was carried out using mouse anti-brevican (1:200, BD Transduction Laboratories) overnight concurrently with rabbit anti-AQP4. Following tyramide development the next day, sections were washed and incubated with Alexa Fluor 594-conjugated anti-mouse IgG (1:100, Invitrogen) for two hours at room temperature. Sections were then washed and counterstained with fluorescent Nissl dye for 10 minutes. After a final wash, sections were mounted with Vectashield.

3.3.4 Confocal microscopy

Fluorescent images were obtained using a fluorescent microscope (BX-51, Olympus) with the 10x objective. Confocal microscope images of various brain

regions were generated using either the 63x objective and the Zeiss LSM 510 Meta or the 2x objective on the Olympus BX61. Image processing was done using the LSM 510 imaging software (Zeiss) or Slidebook 4.2. Merged images were created using Photoshop CS4 with the photomerge reposition feature.

3.4 Results

3.4.1 Differential expression of AQP4 in the mouse brain

Western blot analysis revealed an approximately 150 KDa monomeric band representing AQP4 in the brain. To determine the relative expression levels of AQP4 throughout the brain, protein was isolated from the cortex, diencephalon, hippocampus, cerebellum, and brainstem, separated by SDS-PAGE and probed for AQP4 (Figure 3.1A). Highest expression of AQP4 was found in the cerebellum with a significantly lower amount of AQP4 protein in the hippocampus, diencephalon, and cortex (Figure 3.1B). One-way ANOVA demonstrated a significant difference between the amount of AQP4 protein in the cerebellum compared to the cortex ($p < 0.001$), diencephalon ($p < 0.001$), hippocampus ($p < 0.001$), and brainstem ($p < 0.05$). The brainstem demonstrated significantly higher AQP4 levels than both the cortex and hippocampus ($p < 0.01$), but not the diencephalon. No statistically significant difference between the cortex, diencephalon, and hippocampus was observed.

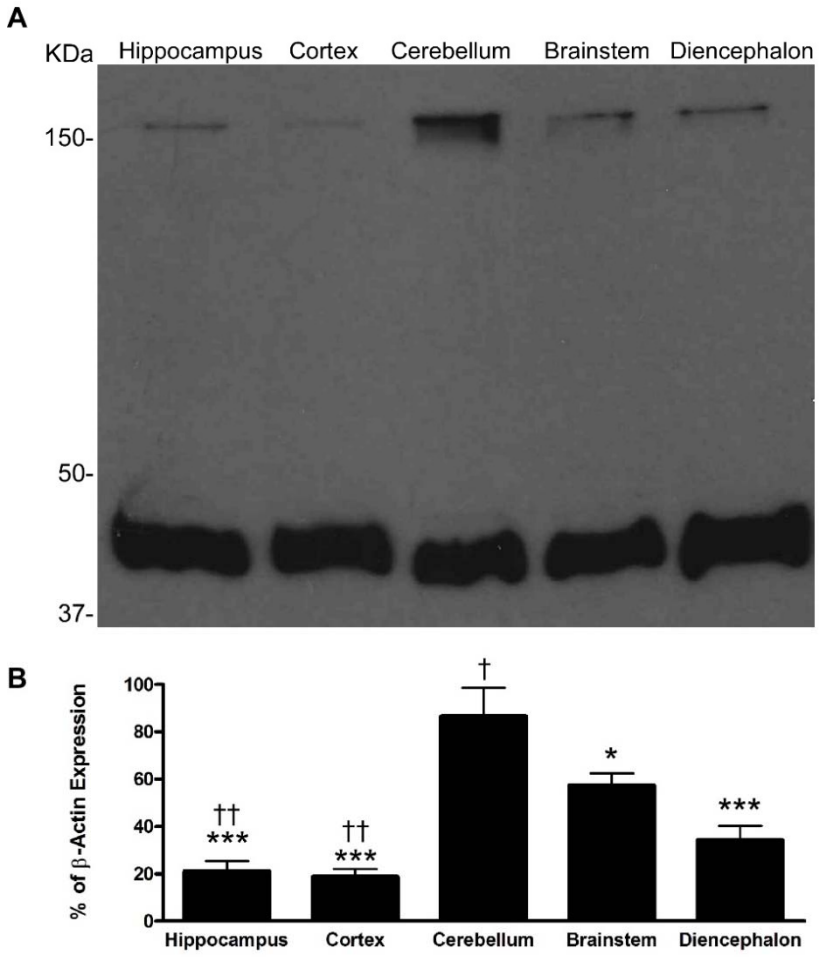


Figure 3.1. Western blot analysis of various brain regions.
A. Representative blot of AQP4 tetramers (~150 Kd, upper band) and β-actin (~43-45 Kd, lower band) protein in the hippocampus, cortex, cerebellum, brainstem, and diencephalon of the mouse brain. **B.** AQP4 band intensities were scanned, quantified, and normalized to the corresponding β-actin band intensities within each brain region (n = 5). * indicates $p < 0.05$ and *** indicates $p < 0.001$ when compared to the cerebellum. † indicates $p < 0.05$ and †† indicates $p < 0.01$ relative to the brainstem.

3.4.2 AQP4 expression in the wild-type and knockout mouse brain

Consistent with the Western blot data, AQP4 immunoreactivity was highest in the cerebellum and high in various regions of the brainstem relative to the levels

seen in the hippocampus and throughout the cortex (Figure 3.2A). The hypothalamus and thalamus exhibited AQP4 labeling similar to that of the hippocampus and cortex. Most notably, AQP4 was uniformly distributed on astrocytic end-feet surrounding capillaries throughout the entire brain and any region associated with cerebrospinal fluid (CSF) including ependymal and glia limitans. Expression was homogenous throughout the cortex but exhibited heterogeneous sublayer-specific expression in other brain regions, such as the hippocampus and cerebellum. AQP4 knockout mice exhibited no AQP4 immunoreactivity (Figure 3.2B).

3.4.3 AQP4 expression in the mouse forebrain

In the most rostral part of the brain, the olfactory bulb, AQP4 immunoreactivity was richly expressed in the glomerular layer (Figure 3.3A). Both astrocytic processes and end-feet surrounding the capillaries within the glomerular layer densely expressed AQP4. Other layers of the olfactory bulb demonstrated much less parenchymal AQP4 immunoreactivity, although AQP4 was homogenously expressed around blood vessels throughout all layers of the olfactory bulb.

The medial olfactory area, the septal nuclei, receives several reciprocal connections from various brain regions including the olfactory bulb and the hippocampus. In the lateral septal nucleus, bush-like networks of AQP4

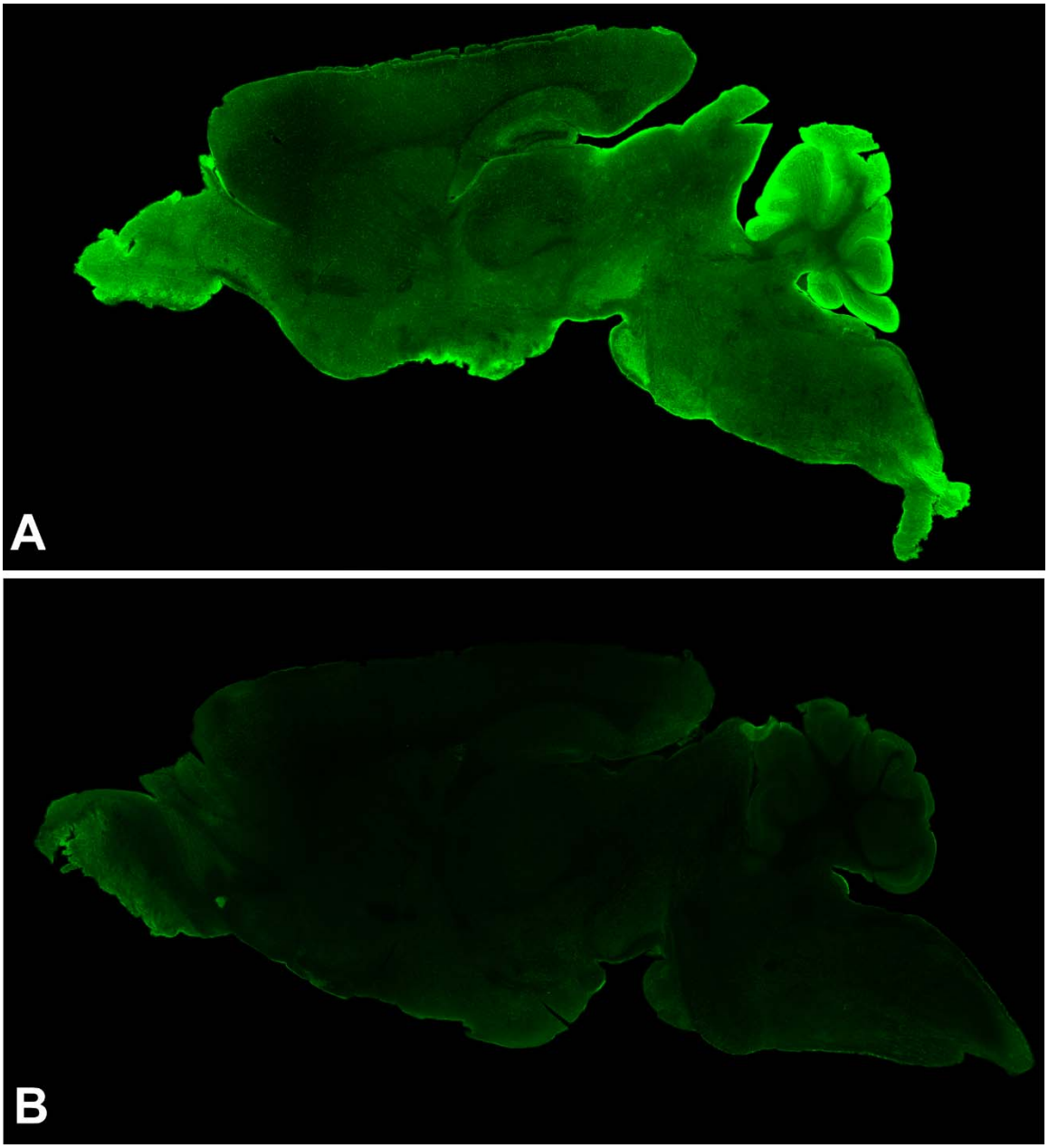


Figure 3.2. AQP4 immunoreactivity in the wild-type and AQP4 knockout mouse whole brain.
2x confocal images from sagittal brain slices were merged together to form a whole brain image of the mouse brain. **A**. AQP4 immunoreactivity in a sagittal slice from a wild-type mouse brain. **B**. AQP4 immunoreactivity in an AQP4 knockout mouse.

immunoreactivity were observed throughout, suggesting that astrocytic processes were well labeled with AQP4 (Figure 3.3B). Similarly, AQP4 staining was pronounced on the astrocyte processes within the thalamic nuclei, with rich AQP4 stain found in particular within the reticular thalamic nucleus (Figure 3.3C), a diencephalic GABAergic structure.

The habenula is a region of the brain that is reciprocally connected to the pineal gland and is thought to play a role in behavioral choices and responses to pain, stress, anxiety, sleep, and reward (Hikosaka 2010). In the medial habenula (MH), by far the most intense AQP4 immunoreactivity was observed around the ependymal cells lining the third ventricle with substantial immunoreactivity also seen in the adjacent glial cell processes within the habenular nucleus (Figure 3.3D). Intense staining outlined the cells in the MH suggesting cell membrane AQP4 expression.

The hippocampus exhibited laminar specific AQP4 immunoreactivity (Figure 3.3E) as previously observed (Hsu, Seldin et al. 2011). In the CA1 region, AQP4 was intensely stained across the hippocampal fissure and within the stratum lacunosum moleculare (SLM). The dentate gyrus was largely absent of AQP4 staining with the exception of astrocytic end-feet and astrocytic processes that protruded into this neuronal layer. The CA1 stratum radiatum and hilus of the dentate gyrus both exhibited bush-like networks of AQP4 staining on astrocytes,

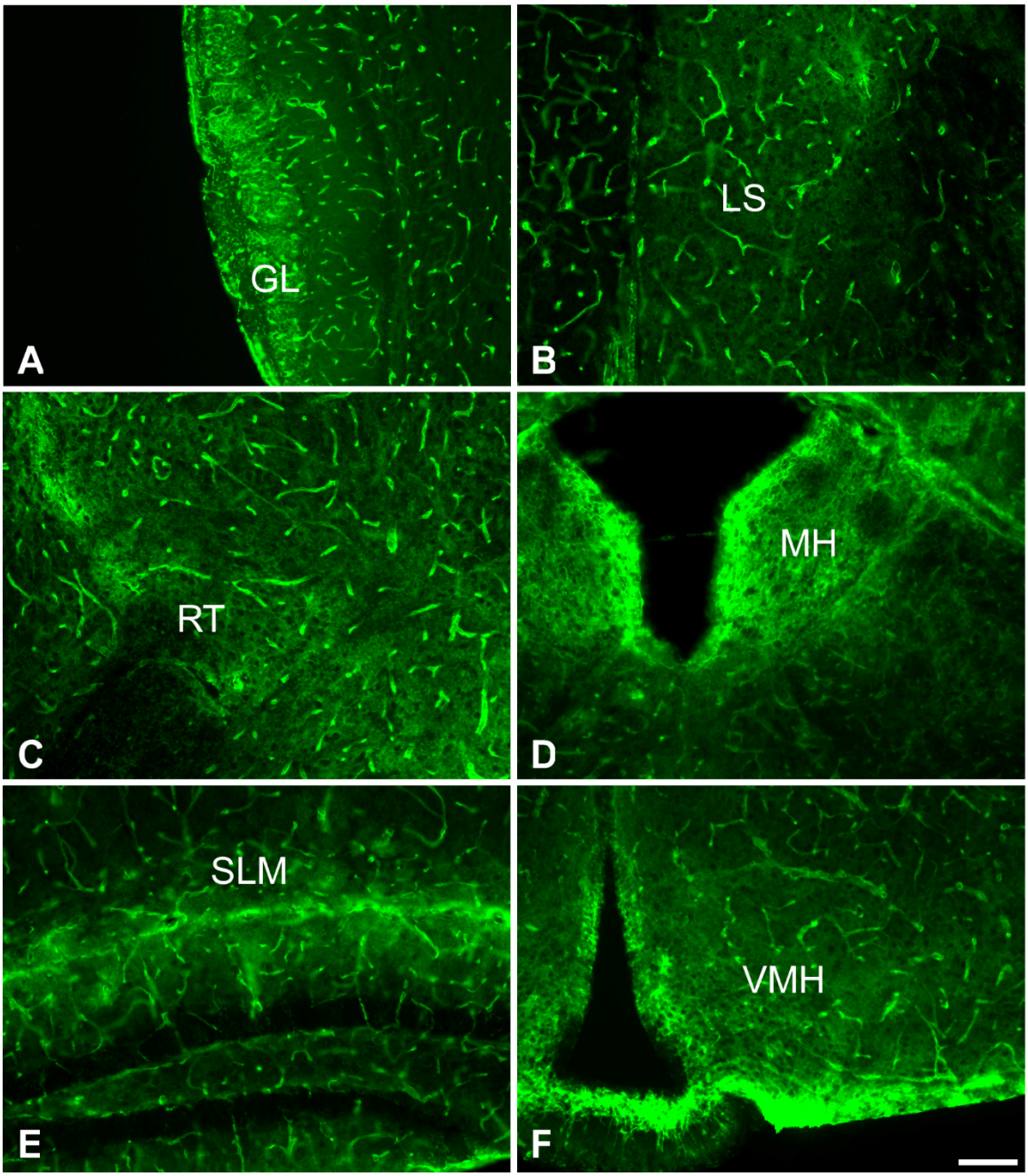


Figure 3.3. AQP4 immunoreactivity within forebrain regions, 10x images. **A**. Glomerular layer of the olfactory bulb (GL). **B**. Lateral septal nucleus (LS). **C**. Reticular thalamic nucleus (RT). **D**. Medial habenula (MH). **E**. Stratum lacunosum moleculare (SLM) of the hippocampus. **F**. Ventromedial hypothalamus (VMH). Scale bar = 100 μm.

although it was not as pronounced as that seen in the CA1 SLM. Of note, the staining of blood vessels throughout the hippocampus was not laminar-specific but, instead, was uniformly distributed throughout all layers.

Similar to what was observed in the medial habenula, AQP4 staining was intense around the third ventricle and the glia limitans in the ventromedial hypothalamus (Figure 3.3F). Throughout the hypothalamus, a structure central to neuroendocrine function, AQP4 immunoreactivity was evident on astrocytic processes and end-feet surrounding capillaries. This staining, however, was not as prominent as the staining seen on glial cells lining the third ventricle.

3.4.4 AQP4 expression in the mouse brainstem

Within the midbrain regions, AQP4 expression was prominent in cells surrounding ventricular and cisternal spaces (Figure 3.4). The substantia nigra of the basal ganglia exhibits robust AQP4 expression among the astrocytic end-feet surrounding the capillaries, astrocytic membranes and the branched processes (Figure 3.4A). Of note, intense astrocytic AQP4 immunoreactivity is seen throughout the substantia nigra pars reticulata (SNr). In the substantia nigra pars compacta (SNc), AQP4 staining is not as intense, but it is still present on both the capillaries and the astrocytic membranes and processes. Interestingly, the substantia nigra is known to be involved in processes

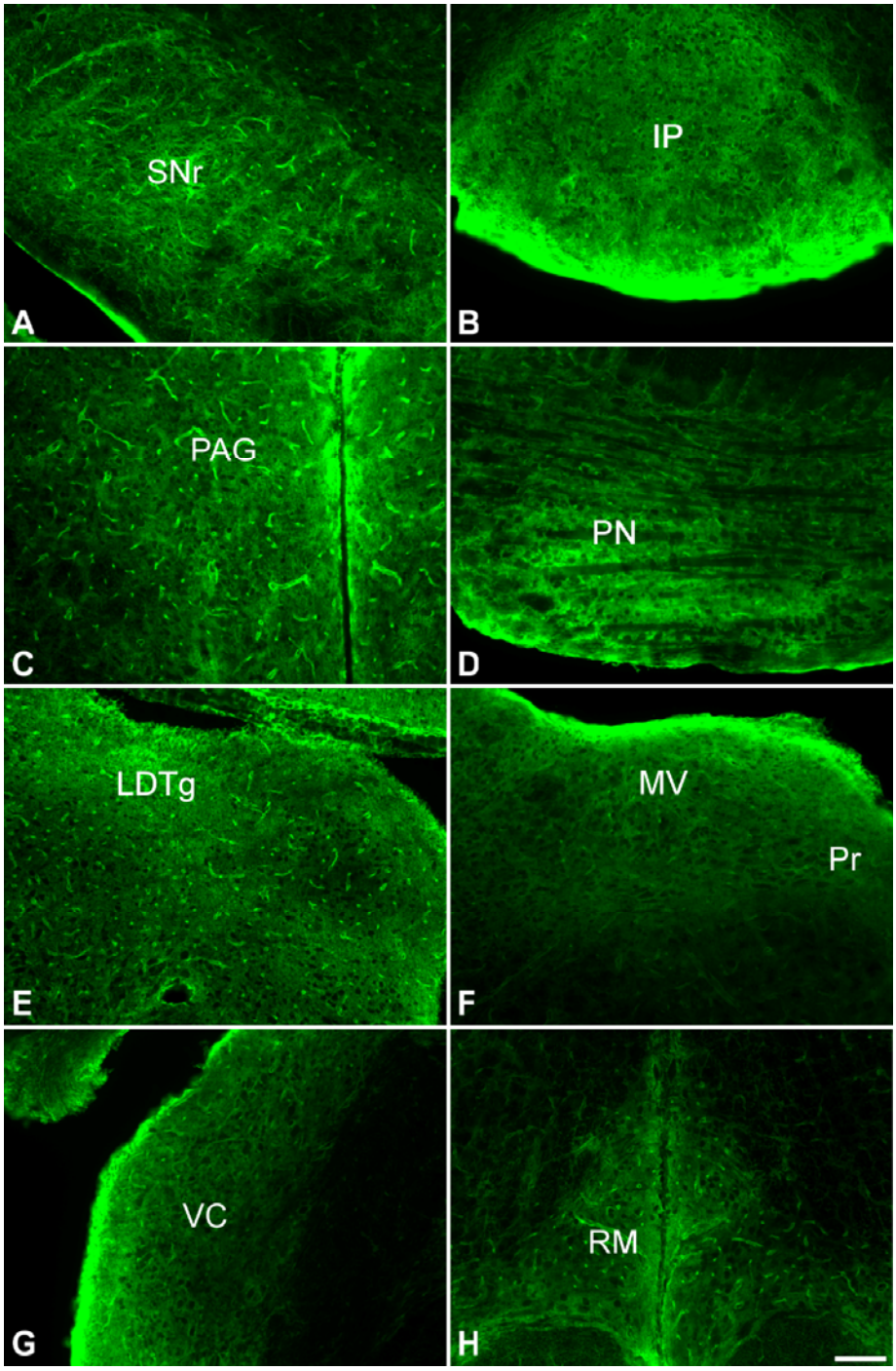


Figure 3.4. AQP4 immunoreactivity within the brainstem, 10x images. **A**. Substantia nigra pars reticulata (SNr). **B**. Interpeduncular nucleus (IP). **C**. Periaqueductal gray (PAG). **D**. Pons (PN). **E**. Lateral dorsal tegmental nucleus (LDTg). **F**. Medial vestibular nucleus (MV) and nucleus prepositus (Pr). **G**. Ventral cochlear nucleus (VC). **H**. Raphe magnus (RM). Scale bar = 100 μm.

associated with movement, reward, addiction and degeneration of the SNc is a hallmark of Parkinson's disease.

Intense AQP4 immunoreactivity was found along the glial limiting membranes lining the caudal edge of the interpeduncular nucleus (Figure 3.4B), an area found at the base of the midbrain tegmentum that is associated with dopamine release and the regulation of rapid eye movement (REM) sleep. Within this region, homogenous AQP4 staining was found on astrocytes, with distinct branch-like processes seen throughout. Compared to other regions of the midbrain, fewer capillaries were observed in the interpeduncular nucleus, determined by the relatively low abundance of AQP4-positive astrocytic end-feet.

AQP4 labeling was densely along the cerebral aqueduct within the periaqueductal gray (Figure 3.4C), a brainstem region associated with pain modulation. Along the aqueduct, astrocytic membranes, processes and end-feet were all intensely labeled with AQP4. Lateral to that, AQP4-postive astrocytic bush-like processes and blood vessels were present, however, they were less prominent.

In the pons, intense AQP4 immunoreactivity was interspersed with patches of little to no AQP4 immunoreactivity (Figure 3.4D). This streak-like staining, in conjunction with the lack of capillaries, was unique to this region of the brain.

The appearance suggests dark nonstained white matter pathways known to cross the pons and pockets of intense AQP4 immunoreactivity outlining cells (likely pontine reticular formation nuclei). This is in contrast to the robust staining seen in the lateral dorsal tegmental nucleus (LDTg) (Figure 3.4E), a part of the brain that, like the interpeduncular nucleus, is associated with the modulation of REM sleep. In the LDTg, capillaries were prominent and branch-like processes labeled with AQP4 were clearly present throughout.

Marked AQP4 staining in the hindbrain was seen along the ependymal surfaces lining the fourth ventricle in the medial vestibular nucleus and nucleus prepositus (Figure 3.4F), regions associated with eye movement and gaze holding, respectively. The glia limitans coating the lateral edge of the ventral cochlear nucleus (Figure 3.4G), closest to the flocculus, featured equally as prominent AQP4 immunoreactivity. Striking AQP4 staining was seen throughout the vestibular nucleus, but very little AQP4 stain was observed more medial to the ventral cochlear nucleus. Along the raphe magnus, another region associated with pain modulation, AQP4 is brightly stained (Figure 3.4H).

3.4.5 Cerebellar expression of AQP4

The unique architecture of the cerebellum makes AQP4 immunoreactivity look distinct from any other brain region (Figure 5A). AQP4 immunoreactivity was rich

in the granule cell layer and prominent surrounding the blood vessels within the cerebellum. The Purkinje cell layer was nearly devoid of AQP4 staining except for some astrocytic processes extending from the granule cell layer. The molecular layer had abundant astrocytic AQP4 staining. In both the granule cell and molecular layers, AQP4 was seen on astrocyte cell membranes and their branched processes.

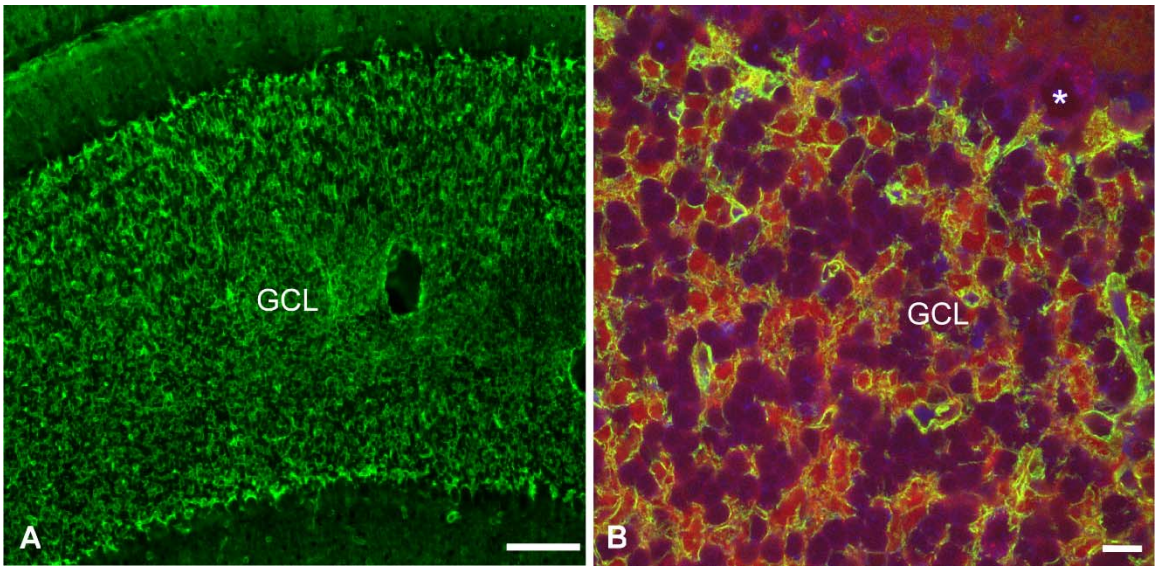


Figure 3.5. AQP4 and brevican immunoreactivity within the cerebellum. **A.** Strong AQP4 signal is observed in the cerebellar granule cell layer (GCL) (10x). Scale bar = 100 µm. **B**. Higher-power image of AQP4 (green), brevican (red) and Nissl (blue) labeling in the cerebellum (63x). Example of a Purkinje cell denoted with an asterisk (*). Scale bar = 10 µm.

Brevican is a chondroitin sulfate proteoglycan that has previously been shown to be synthesized by and expressed on cerebellar astrocytes (Yamada, Fredette et al. 1997). Confocal triple-labeled immunohistochemistry for AQP4 (green), brevican (red) and Nissl (blue) clearly demonstrated co-localization of AQP4 and

brevican on cerebellar astrocytes (Figure 5B). Again, AQP4 was absent from Purkinje cells, but was abundant throughout the granule cell layer.

3.5 Discussion

In this chapter, I used Western blotting and immunohistochemistry to elucidate the expression pattern of AQP4 throughout the mouse brain. Prior studies have demonstrated AQP4 expression in various regions of the brain (Nielsen, Nagelhus et al. 1997; Rash, Yasumura et al. 1998; Wen, Nagelhus et al. 1999; Frigeri, Nicchia et al. 2001; Nagy, Szekeres et al. 2002; Amiry-Moghaddam, Otsuka et al. 2003; Amiry-Moghaddam, Frydenlund et al. 2004; Costa, Tortosa et al. 2007; Hsu, Seldin et al. 2011) and spinal cord (Rash, Yasumura et al. 1998; Oshio, Binder et al. 2004; Vitellaro-Zuccarello, Mazzetti et al. 2005), however, this is the first comprehensive neuroanatomical study of AQP4 localization and protein levels in the rodent brain. I also demonstrate marked expression and co-localization of AQP4 with brevican, a proteoglycan found on the surface of astrocytes in the cerebellum.

The expression pattern of AQP4 suggests a specialized role in mediating the water movement between glial cells and cavities containing CSF and the intravascular space. I, like others, have found highly polarized AQP4 expression, with intense immunoreactivity on glia limitans boarding the subarachnoid space

and ventricles, subpopulations of ependymocytes, pia and perivascular glial end-feet surrounding capillaries (Nielsen, Nagelhus et al. 1997; Amiry-Moghaddam, Otsuka et al. 2003; Goren, Adorjan et al. 2006). Although AQP4 has been found on ependymal cells (Badaut, Verbavatz et al. 2000), it was completely absent from tanycytes, a class of ependymal cells found in the 3rd ventricle of the internal median eminence that contact hypothalamic neurons and blood vessels (Badaut, Lasbennes et al. 2002). AQP4 null mice lack the ability to properly maintain water homeostasis and therefore are more prone to neurological decline in vasogenic edema (Papadopoulos, Manley et al. 2004).

In previous studies, AQP4 immunoreactivity has been found close to blood vessels and on astrocyte processes in the corpus callosum (Badaut, Verbavatz et al. 2000; Badaut, Lasbennes et al. 2002; Badaut, Fukuda et al. 2014). AQP4, like AQP9, has also been found on other white matter tracts such as the anterior commissure and optic chiasm (Badaut, Lasbennes et al. 2002). AQP9 exhibited a similar distribution to AQP4 and is thought to play a role in aiding AQP4 function. Both AQP4 and AQP9 have been found on astrocytic processes in periventricular regions of parenchyma and in glia limitans bordering subarachnoid space (Badaut, Lasbennes et al. 2002). More recently, however, studies of AQ9 knockout mice revealed that in addition to astrocytes and ependymal cells, AQP9 is also expressed on catecholaminergic neurons (Mylonakou, Petersen et al. 2009; Badaut, Fukuda et al. 2014).

I have demonstrated a region specific expression pattern of AQP4. Robust staining was found on astrocytic membranes and processes in the lateral septal nuclei, reticular thalamic nucleus, hippocampal fissure, and stratum lacunosum moleculare layer of CA1, substantia nigra pars reticulata, interpeduncular nucleus and throughout the granule cell layer of the cerebellum. Very little AQP4 immunoreactivity was found medial to the ventral cochlear nucleus and in predominantly neuronal areas, such as the dentate granule cell layer of the hippocampus and the Purkinje cell layer of the cerebellum.

The heterogeneous pattern of AQP4 expression throughout the brain suggests various functional roles for AQP4 in addition to its role in water movement across cell membranes. For example, I observed robust AQP4 staining in the ventral cochlear nuclei. Previously, AQP4-null mice were found to have impaired hearing (Li and Verkman 2001; Mhatre, Stern et al. 2002), which was interpreted as suggesting a role for AQP4 in ion and water homeostasis in the inner ear. However, our findings suggest that deficiency of AQP4 in the ventral cochlear nuclei and/or central auditory pathways could also play a role. Similarly, in the olfactory bulb, AQP4 expression was highest in the glomerular layer, the characteristic multicellular synaptic unit of the olfactory bulb, which agrees with previous findings (Sorbo, Moe et al. 2007). Interestingly, AQP4-null mice exhibit impaired olfaction (Lu, Zhang et al. 2008), which was interpreted as a deficit in the olfactory epithelium, but our results suggest that deficiency of AQP4 in the

glomerular layer of the olfactory bulb may be responsible for this phenotype. The septal nucleus is connected to both the olfactory bulb and the hippocampus, a structure associated with learning and memory formation. Here I have shown abundant AQP4 expression in the septal nuclei, hippocampus and glomerular layer of the olfactory bulb. A correlation between AQP4 and olfactory learning has not been shown, but would be interesting to explore. It is of interest that AQP4 expression is particularly high in the thalamic reticular nucleus (TRN), a structure hypothesized to be important in selective attention and other functions related to consciousness (Crick 1984; Pinault 2004).

The hippocampus is a structure critical to cognitive function and long-term memory formation. Our current findings agree with previous results suggesting laminar-specific expression of AQP4 in the hippocampus, with highest levels of AQP4 staining near the hippocampal fissure and in the stratum lacunosum moleculare (Costa, Tortosa et al. 2007; Hsu, Seldin et al. 2011). Previous studies have shown a role for AQP4 in synaptic plasticity. Specifically, AQP4-deficient mice exhibit impaired long-term potentiation (LTP) and long-term depression (LTD) without any change in basal transmission (Skucas, Mathews et al. 2011; Scharfman and Binder 2013). Furthermore, marked AQP4 downregulation has been observed in an animal model of temporal lobe epilepsy (Lee, Hsu et al. 2012) and AQP4-deficient mice have slowed K^+ kinetics and increased seizure duration (Binder, Yao et al. 2006). It is well known that

patients with temporal lobe epilepsy often exhibit cognitive deficits, particularly in hippocampal-dependent tasks such as spatial memory (Bell, Lin et al. 2011; Amlerova, Laczo et al. 2013; Brooks-Kayal, Bath et al. 2013; Chin and Scharfman 2013). These data, together with recent findings that AQP4 modulates extracellular [K^+] during synaptic stimulation in the hippocampus (Haj-Yasein, Bugge et al. 2014), suggest that AQP4 is essential for synaptic plasticity.

The hypothalamic magnocellular neurosecretory system has been implicated in both neuronal and glial plasticity (Hatton 1986). A previous study has demonstrated that AQP4 staining is abundant in the rat magnocellular hypothalamic nuclei (Badaut, Nehlig et al. 2000). In addition, high AQP4 mRNA levels have been observed in thalamic and hypothalamic regions (Venero, Vizuete et al. 1999). Future studies should examine subregions of the hypothalamus that have distinct important roles in neuroendocrine regulation and plasticity. The polysialylated embryonic form of neural cell adhesion molecule (PSA-NCAM) has been shown to be required for the induction of synaptic plasticity (Muller, Wang et al. 1996). It would be of interest to examine the distribution of PSA-NCAM in hypothalamus subregions and its colocalization with AQP4 to determine its role in plasticity.

The periaqueductal gray (PAG) plays a major role in pain and analgesia. I found abundant levels of AQP4 expressed throughout this region. Mice lacking AQP4

have increased pain thresholds to thermal and chemical stimulation, but not mechanical stimulation (Bao, Chen et al. 2010). Further supporting a role for AQP4 in pain modulation, Nesic *et. al.* (2005) found increased levels of AQP4 mRNA and protein in rats exhibiting central neuropathic pain (Nesic, Lee et al. 2005). It would be interesting for future studies to further explore the role of AQP4 in brain regions associated with pain modulation, such as the periaqueductal gray or the raphe magnus, in which AQP4 immunoreactivity is also prominent.

Similar to AQP4, AQP1 has also been implicated in pain perception. AQP1 knockout mice exhibited reduced thermal, inflammatory, chemical and cold pain perception, but did not differ in response to mechanical stimuli (Oshio, Watanabe et al. 2006; Zhang and Verkman 2010). Although AQP1 has been considered the major water transport protein of the choroid plexus and is thought to play a role in the secretion of CSF (Bondy, Chin et al. 1993; Nielsen, Smith et al. 1993; Hasegawa, Lian et al. 1994; Badaut, Lasbennes et al. 2002; Oshio, Song et al. 2003; Longatti, Basaldella et al. 2004; Oshio, Watanabe et al. 2005; Fukuda, Pop et al. 2012), it was also been found on dorsal root ganglion (DRG) neurons (Zhang and Verkman 2010; Zhang and Verkman 2015). Recent studies have implicated AQP1 in DRG axonal growth and regeneration as well as osmotic water permeability in isolated DRG neurons (Zhang and Verkman 2010; Zhang and Verkman 2015).

Several anatomical regions of the brain are associated with reward and addiction pathways, including the ventral tegmental area (VTA), medial prefrontal cortex, hippocampus, ventral striatum (including the nucleus accumbens) and the amygdala (Luthi and Luscher 2014). Projections connecting these various brain regions are dopaminergic in nature. Previous studies have shown that dopamine can decrease AQP4 water permeability (Zelenina, Zelenin et al. 2002) and AQP4 protein expression (Kuppers, Gleiser et al. 2008). It has also been shown that AQP4 deficiency can increase K^+-stimulated release of striatal dopamine (Ding, Sha et al. 2007). Recent studies have shown that AQP4-deficient mice have attenuated morphine tolerance, inhibited development of morphine physical dependence and impaired morphine analgesia (Wu, Lu et al. 2008; Chen, Bao et al. 2010). In addition, chronic treatment with morphine decreased spinal AQP4 expression in a rodent model (Chen, Bao et al. 2010). An interesting study examining cocaine-induced locomotion found that AQP4 knockout mice exhibited attenuated locomotor activity in response to cocaine stimulation (Li, Gao et al. 2006). Of note, whereas the VTA is associated with reward and addiction, the substantia nigra of the midbrain, which exhibits robust AQP4 immunoreactivity and utilizes dopamine, is associated with movement as well as reward and addiction. These studies, taken together, suggest the involvement of AQP4 in addictive behavior.

Of all brain regions, AQP4 was most abundantly expressed in the cerebellum, which is associated with motor control and motor learning (Therrien and Bastian 2015). I have shown intense AQP4 immunoreactivity throughout the cerebellum; however, very little is known about the relationship between cerebellar AQP4 and motor control. Given the findings in the hippocampus that AQP4-deficient mice exhibit impaired synaptic plasticity (Skucas, Mathews et al. 2011; Scharfman and Binder 2013), it would be interesting to analyze the physiology of cerebellar slices from AQP4-deficient mice for alterations in cerebellar synaptic plasticity (*e.g.* cerebellar LTD), and more generally to assess AQP4-deficient mice for deficits in cerebellar learning paradigms.

Brevican, an extracellular matrix proteoglycan, is synthesized by astrocytes and retained on their surface throughout the adult rodent brain, but its highest level of expression and spatial organization is within the cerebellar cortex (Yamada, Fredette et al. 1997). Brevican has been shown to parallel the gliotic response in CNS injury, suggesting a role of brevican in reactive gliosis (Jaworski, Kelly et al. 1999; Thon, Haas et al. 2000). I demonstrated co-localization of brevican and AQP4 in the cerebellum. Together with other studies demonstrating co-localization of AQP4 and astrocyte markers (GFAP, S-100β) (Hsu, Seldin et al. 2011), our current data clearly indicate cell-type specificity of AQP4 expression in astrocytes.

It is well known that AQP4 is tethered to the membrane by α-syntrophin, a component of the dystrophin protein complex. Mice deficient in α-syntrophin exhibited reversed polarized subcellular localization of AQP4, with reduced expression on perivascular astrocytic endfeet membranes and increased levels on membranes facing the neuropil (Neely, Amiry-Moghaddam et al. 2001; Amiry-Moghaddam, Xue et al. 2004). Dystrophin-independent pools of AQP4 have been found in the granular cell layer of the cerebellum, the subpial endfoot layer, and in ependymal cells (Nicchia, Rossi et al. 2008). In addition, AQP4 and α-syntrophin frequently colocalized at astrocytic membranes, particularly at perivascular astrocyte endfoot processes, suggesting a linkage between these two molecules (Inoue, Wakayama et al. 2002; Masaki, Wakayama et al. 2010). Complimentary to these findings, deletion of the dystroglycan gene resulted in a reduction of AQP4 perivascular expression and a loss of the formation of orthogonal arrays of particles (OAPs) (Noell, Wolburg-Buchholz et al. 2011). The proteoglycan agrin has been implicated in the polarized distrubtion of AQP4, specifically restricting OAPs to endfeet membranes (Warth, Kroger et al. 2004; Noell, Fallier-Becker et al. 2007; Noell, Fallier-Becker et al. 2009). Studies of agrin knockout mice have demonstrated that AQP4 expression was not altered, but the formation of OAPs was decreased (Noell, Fallier-Becker et al. 2009). More recently, a study involving endothelial-astrocyte co-cultures demonstrated that application of agrin gave rise to a pronounced polarization and membrane compartmentalization of AQP4 (Camassa, Lunde et al. 2015). Taken together,

these data suggest that dystrophin and agrin proteins may be responsible for the clustering of AQP4 around blood vessels.

In summary, AQP4 was densely expressed on astrocyte processes surrounding blood vessels (astrocyte endfeet) and in regions of the brain associated with CSF flow, including ventricles, subarachnoid space and ependymal cells. Regionally, AQP4 protein expression was highest in the cerebellum where it was strongly expressed on the dense astrocyte network throughout the granule cell layer. Throughout the entire brain, AQP4 not only demonstrated region specificity but also laminar specificity within individual structures, further supporting the developing concept of astrocyte heterogeneity (Matyash and Kettenmann 2010; Hoft, Griemsmann et al. 2014; Bayraktar, Fuentealba et al. 2015). Reduced levels of AQP4 are associated with a number of functional defects, such as impaired hearing and olfaction, and neurological disorders, including edema, epilepsy and stroke. Thus, investigation of the local functional relationship between AQP4 expression and specific anatomical regions and circuits could offer new insight into the diverse roles of AQP4 in the brain.

3.6 References

Amiry-Moghaddam, M., D. S. Frydenlund and O. P. Ottersen (2004). "Anchoring of aquaporin-4 in brain: molecular mechanisms and implications for the physiology and pathophysiology of water transport." Neuroscience **129**(4): 999-1010.

Amiry-Moghaddam, M., T. Otsuka, P. D. Hurn, R. J. Traystman, F. M. Haug, S. C. Froehner, M. E. Adams, J. D. Neely, P. Agre, O. P. Ottersen and A. Bhardwaj (2003). "An alpha-syntrophin-dependent pool of AQP4 in astroglial end-feet confers bidirectional water flow between blood and brain." Proc Natl Acad Sci U S A **100**(4): 2106-2111.

Amiry-Moghaddam, M., R. Xue, F. M. Haug, J. D. Neely, A. Bhardwaj, P. Agre, M. E. Adams, S. C. Froehner, S. Mori and O. P. Ottersen (2004). "Alpha-syntrophin deletion removes the perivascular but not endothelial pool of aquaporin-4 at the blood-brain barrier and delays the development of brain edema in an experimental model of acute hyponatremia." FASEB J **18**(3): 542-544.

Amlerova, J., J. Laczo, K. Vlcek, A. Javurkova, R. Andel and P. Marusic (2013). "Risk factors for spatial memory impairment in patients with temporal lobe epilepsy." Epilepsy Behav **26**(1): 57-60.

Badaut, J., A. M. Fukuda, A. Jullienne and K. G. Petry (2014). "Aquaporin and brain diseases." Biochim Biophys Acta **1840**(5): 1554-1565.

Badaut, J., F. Lasbennes, P. J. Magistretti and L. Regli (2002). "Aquaporins in brain: distribution, physiology, and pathophysiology." J Cereb Blood Flow Metab **22**(4): 367-378.

Badaut, J., A. Nehlig, J. Verbavatz, M. Stoeckel, M. J. Freund-Mercier and F. Lasbennes (2000). "Hypervascularization in the magnocellular nuclei of the rat hypothalamus: relationship with the distribution of aquaporin-4 and markers of energy metabolism." J Neuroendocrinol **12**(10): 960-969.

Badaut, J., J. M. Verbavatz, M. J. Freund-Mercier and F. Lasbennes (2000). "Presence of aquaporin-4 and muscarinic receptors in astrocytes and ependymal cells in rat brain: a clue to a common function?" Neurosci Lett **292**(2): 75-78.

Bao, F., M. Chen, Y. Zhang and Z. Zhao (2010). "Hypoalgesia in mice lacking aquaporin-4 water channels." Brain Res Bull **83**(6): 298-303.

Bayraktar, O. A., L. C. Fuentealba, A. Alvarez-Buylla and D. H. Rowitch (2015). "Astrocyte development and heterogeneity." Cold Spring Harb Perspect Biol **7**(1): a020362.

Bell, B., J. J. Lin, M. Seidenberg and B. Hermann (2011). "The neurobiology of cognitive disorders in temporal lobe epilepsy." Nat Rev Neurol **7**(3): 154-164.

Binder, D. K., M. C. Papadopoulos, P. M. Haggie and A. S. Verkman (2004). "In vivo measurement of brain extracellular space diffusion by cortical surface photobleaching." J Neurosci **24**(37): 8049-8056.

Binder, D. K., X. Yao, Z. Zador, T. J. Sick, A. S. Verkman and G. T. Manley (2006). "Increased seizure duration and slowed potassium kinetics in mice lacking aquaporin-4 water channels." Glia **53**(6): 631-636.

Bondy, C., E. Chin, B. L. Smith, G. M. Preston and P. Agre (1993). "Developmental gene expression and tissue distribution of the CHIP28 water-channel protein." Proc Natl Acad Sci U S A **90**(10): 4500-4504.

Brooks-Kayal, A. R., K. G. Bath, A. T. Berg, A. S. Galanopoulou, G. L. Holmes, F. E. Jensen, A. M. Kanner, T. J. O'Brien, V. H. Whittemore, M. R. Winawer, M. Patel and H. E. Scharfman (2013). "Issues related to symptomatic and disease-modifying treatments affecting cognitive and neuropsychiatric comorbidities of epilepsy." Epilepsia **54 Suppl 4**: 44-60.

Camassa, L. M., L. K. Lunde, E. H. Hoddevik, M. Stensland, H. B. Boldt, G. A. De Souza, O. P. Ottersen and M. Amiry-Moghaddam (2015). "Mechanisms underlying AQP4 accumulation in astrocyte endfeet." Glia.

Chen, M. L., F. Bao, Y. Q. Zhang and Z. Q. Zhao (2010). "Effects of aquaporin 4 deficiency on morphine analgesia and chronic tolerance: a study at spinal level." J Mol Neurosci **42**(2): 140-144.

Chin, J. and H. E. Scharfman (2013). "Shared cognitive and behavioral impairments in epilepsy and Alzheimer's disease and potential underlying mechanisms." Epilepsy Behav **26**(3): 343-351.

Costa, C., R. Tortosa, A. Domenech, E. Vidal, M. Pumarola and A. Bassols (2007). "Mapping of aggrecan, hyaluronic acid, heparan sulphate

proteoglycans and aquaporin 4 in the central nervous system of the mouse." J Chem Neuroanat **33**(3): 111-123.

Crick, F. (1984). "Function of the thalamic reticular complex: the searchlight hypothesis." Proc Natl Acad Sci U S A **81**(14): 4586-4590.

Ding, J. H., L. L. Sha, J. Chang, X. Q. Zhou, Y. Fan and G. Hu (2007). "Alterations of striatal neurotransmitter release in aquaporin-4 deficient mice: An in vivo microdialysis study." Neurosci Lett **422**(3): 175-180.

Friedman, B., C. Schachtrup, P. S. Tsai, A. Y. Shih, K. Akassoglou, D. Kleinfeld and P. D. Lyden (2009). "Acute vascular disruption and aquaporin 4 loss after stroke." Stroke **40**(6): 2182-2190.

Frigeri, A., G. P. Nicchia, B. Nico, F. Quondamatteo, R. Herken, L. Roncali and M. Svelto (2001). "Aquaporin-4 deficiency in skeletal muscle and brain of dystrophic mdx mice." FASEB J **15**(1): 90-98.

Fukuda, A. M., V. Pop, D. Spagnoli, S. Ashwal, A. Obenaus and J. Badaut (2012). "Delayed increase of astrocytic aquaporin 4 after juvenile traumatic brain injury: possible role in edema resolution?" Neuroscience **222**: 366-378.

Goren, O., I. Adorjan and M. Kalman (2006). "Heterogeneous occurrence of aquaporin-4 in the ependyma and in the circumventricular organs in rat and chicken." Anat Embryol (Berl) **211**(2): 155-172.

Haj-Yasein, N. N., C. E. Bugge, V. Jensen, I. Ostby, O. P. Ottersen, O. Hvalby and E. A. Nagelhus (2014). "Deletion of aquaporin-4 increases extracellular K concentration during synaptic stimulation in mouse hippocampus." Brain Struct Funct.

Hasegawa, H., S. C. Lian, W. E. Finkbeiner and A. S. Verkman (1994). "Extrarenal tissue distribution of CHIP28 water channels by in situ hybridization and antibody staining." Am J Physiol **266**(4 Pt 1): C893-903.

Hatton, G. I. (1986). "Plasticity in the hypothalamic magnocellular neurosecretory system." Fed Proc **45**(9): 2328-2333.

Hikosaka, O. (2010). "The habenula: from stress evasion to value-based decision-making." Nat Rev Neurosci **11**(7): 503-513.

Hiroaki, Y., K. Tani, A. Kamegawa, N. Gyobu, K. Nishikawa, H. Suzuki, T. Walz, S. Sasaki, K. Mitsuoka, K. Kimura, A. Mizoguchi and Y. Fujiyoshi (2006).

"Implications of the aquaporin-4 structure on array formation and cell adhesion." J Mol Biol **355**(4): 628-639.

Hirt, L., B. Ternon, M. Price, N. Mastour, J. F. Brunet and J. Badaut (2009). "Protective role of early aquaporin 4 induction against postischemic edema formation." J Cereb Blood Flow Metab **29**(2): 423-433.

Hoft, S., S. Griemsmann, G. Seifert and C. Steinhauser (2014). "Heterogeneity in expression of functional ionotropic glutamate and GABA receptors in astrocytes across brain regions: insights from the thalamus." Philos Trans R Soc Lond B Biol Sci **369**(1654): 20130602.

Hsu, M. S., M. Seldin, D. J. Lee, G. Seifert, C. Steinhauser and D. K. Binder (2011). "Laminar-specific and developmental expression of aquaporin-4 in the mouse hippocampus." Neuroscience **178**: 21-32.

Inoue, M., Y. Wakayama, J. W. Liu, M. Murahashi, S. Shibuya and H. Oniki (2002). "Ultrastructural localization of aquaporin 4 and alpha1-syntrophin in the vascular feet of brain astrocytes." Tohoku J Exp Med **197**(2): 87-93.

Jaworski, D. M., G. M. Kelly and S. Hockfield (1999). "Intracranial injury acutely induces the expression of the secreted isoform of the CNS-specific hyaluronan-binding protein BEHAB/brevican." Exp Neurol **157**(2): 327-337.

Kuppers, E., C. Gleiser, V. Brito, B. Wachter, T. Pauly, B. Hirt and S. Grissmer (2008). "AQP4 expression in striatal primary cultures is regulated by dopamine--implications for proliferation of astrocytes." Eur J Neurosci **28**(11): 2173-2182.

Lee, D. J., M. S. Hsu, M. M. Seldin, J. L. Arellano and D. K. Binder (2012). "Decreased expression of the glial water channel aquaporin-4 in the intrahippocampal kainic acid model of epileptogenesis." Exp Neurol **235**(1): 246-255.

Li, J. and A. S. Verkman (2001). "Impaired hearing in mice lacking aquaporin-4 water channels." J Biol Chem **276**(33): 31233-31237.

Li, Z., L. Gao, Q. Liu, C. Cao, X. L. Sun, J. H. Ding and G. Hu (2006). "Aquaporin-4 knockout regulated cocaine-induced behavior and neurochemical changes in mice." Neurosci Lett **403**(3): 294-298.

Longatti, P. L., L. Basaldella, E. Orvieto, A. Fiorindi and A. Carteri (2004). "Choroid plexus and aquaporin-1: a novel explanation of cerebrospinal fluid production." Pediatr Neurosurg **40**(6): 277-283.

Lu, D. C., H. Zhang, Z. Zador and A. S. Verkman (2008). "Impaired olfaction in mice lacking aquaporin-4 water channels." FASEB J **22**(9): 3216-3223.

Luthi, A. and C. Luscher (2014). "Pathological circuit function underlying addiction and anxiety disorders." Nat Neurosci **17**(12): 1635-1643.

Ma, T., B. Yang, A. Gillespie, E. J. Carlson, C. J. Epstein and A. S. Verkman (1997). "Generation and phenotype of a transgenic knockout mouse lacking the mercurial-insensitive water channel aquaporin-4." J Clin Invest **100**(5): 957-962.

Manley, G. T., M. Fujimura, T. Ma, N. Noshita, F. Filiz, A. W. Bollen, P. Chan and A. S. Verkman (2000). "Aquaporin-4 deletion in mice reduces brain edema after acute water intoxication and ischemic stroke." Nat Med **6**(2): 159-163.

Masaki, H., Y. Wakayama, H. Hara, T. Jimi, A. Unaki, S. Iijima, H. Oniki, K. Nakano, K. Kishimoto and Y. Hirayama (2010). "Immunocytochemical studies of aquaporin 4, Kir4.1, and alpha1-syntrophin in the astrocyte endfeet of mouse brain capillaries." Acta Histochem Cytochem **43**(4): 99-105.

Matyash, V. and H. Kettenmann (2010). "Heterogeneity in astrocyte morphology and physiology." Brain Res Rev **63**(1-2): 2-10.

Mhatre, A. N., R. E. Stern, J. Li and A. K. Lalwani (2002). "Aquaporin 4 expression in the mammalian inner ear and its role in hearing." Biochem Biophys Res Commun **297**(4): 987-996.

Muller, D., C. Wang, G. Skibo, N. Toni, H. Cremer, V. Calaora, G. Rougon and J. Z. Kiss (1996). "PSA-NCAM is required for activity-induced synaptic plasticity." Neuron **17**(3): 413-422.

Mylonakou, M. N., P. H. Petersen, E. Rinvik, A. Rojek, E. Valdimarsdottir, S. Zelenin, T. Zeuthen, S. Nielsen, O. P. Ottersen and M. Amiry-Moghaddam (2009). "Analysis of mice with targeted deletion of AQP9 gene provides conclusive evidence for expression of AQP9 in neurons." J Neurosci Res **87**(6): 1310-1322.

Nagelhus, E. A., T. M. Mathiisen and O. P. Ottersen (2004). "Aquaporin-4 in the central nervous system: cellular and subcellular distribution and coexpression with KIR4.1." Neuroscience **129**(4): 905-913.

Nagy, G., G. Szekeres, K. Kvell, T. Berki and P. Nemeth (2002). "Development and characterisation of a monoclonal antibody family against aquaporin 1 (AQP1) and aquaporin 4 (AQP4)." Pathol Oncol Res **8**(2): 115-124.

Neely, J. D., M. Amiry-Moghaddam, O. P. Ottersen, S. C. Froehner, P. Agre and M. E. Adams (2001). "Syntrophin-dependent expression and localization of Aquaporin-4 water channel protein." Proc Natl Acad Sci U S A **98**(24): 14108-14113.

Nesic, O., J. Lee, K. M. Johnson, Z. Ye, G. Y. Xu, G. C. Unabia, T. G. Wood, D. J. McAdoo, K. N. Westlund, C. E. Hulsebosch and J. Regino Perez-Polo (2005). "Transcriptional profiling of spinal cord injury-induced central neuropathic pain." J Neurochem **95**(4): 998-1014.

Nicchia, G. P., A. Rossi, M. G. Mola, G. Procino, A. Frigeri and M. Svelto (2008). "Actin cytoskeleton remodeling governs aquaporin-4 localization in astrocytes." Glia **56**(16): 1755-1766.

Nielsen, S., E. A. Nagelhus, M. Amiry-Moghaddam, C. Bourque, P. Agre and O. P. Ottersen (1997). "Specialized membrane domains for water transport in glial cells: high-resolution immunogold cytochemistry of aquaporin-4 in rat brain." J Neurosci **17**(1): 171-180.

Nielsen, S., B. L. Smith, E. I. Christensen and P. Agre (1993). "Distribution of the aquaporin CHIP in secretory and resorptive epithelia and capillary endothelia." Proc Natl Acad Sci U S A **90**(15): 7275-7279.

Noell, S., P. Fallier-Becker, C. Beyer, S. Kroger, A. F. Mack and H. Wolburg (2007). "Effects of agrin on the expression and distribution of the water channel protein aquaporin-4 and volume regulation in cultured astrocytes." Eur J Neurosci **26**(8): 2109-2118.

Noell, S., P. Fallier-Becker, U. Deutsch, A. F. Mack and H. Wolburg (2009). "Agrin defines polarized distribution of orthogonal arrays of particles in astrocytes." Cell Tissue Res **337**(2): 185-195.

Noell, S., K. Wolburg-Buchholz, A. F. Mack, A. M. Beedle, J. S. Satz, K. P. Campbell, H. Wolburg and P. Fallier-Becker (2011). "Evidence for a role of dystroglycan regulating the membrane architecture of astroglial endfeet." Eur J Neurosci **33**(12): 2179-2186.

Oshio, K., D. K. Binder, B. Yang, S. Schecter, A. S. Verkman and G. T. Manley (2004). "Expression of aquaporin water channels in mouse spinal cord." Neuroscience **127**(3): 685-693.

Oshio, K., Y. Song, A. S. Verkman and G. T. Manley (2003). "Aquaporin-1 deletion reduces osmotic water permeability and cerebrospinal fluid production." Acta Neurochir Suppl **86**: 525-528.

Oshio, K., H. Watanabe, Y. Song, A. S. Verkman and G. T. Manley (2005). "Reduced cerebrospinal fluid production and intracranial pressure in mice lacking choroid plexus water channel Aquaporin-1." FASEB J **19**(1): 76-78.

Oshio, K., H. Watanabe, D. Yan, A. S. Verkman and G. T. Manley (2006). "Impaired pain sensation in mice lacking Aquaporin-1 water channels." Biochem Biophys Res Commun **341**(4): 1022-1028.

Papadopoulos, M. C., G. T. Manley, S. Krishna and A. S. Verkman (2004). "Aquaporin-4 facilitates reabsorption of excess fluid in vasogenic brain edema." FASEB J **18**(11): 1291-1293.

Paxinos, G. and K. B. Franklin (2001). The Mouse Brain in Stereotaxic Coordinates, Academic Press.

Pinault, D. (2004). "The thalamic reticular nucleus: structure, function and concept." Brain Res Brain Res Rev **46**(1): 1-31.

Rash, J. E., T. Yasumura, C. S. Hudson, P. Agre and S. Nielsen (1998). "Direct immunogold labeling of aquaporin-4 in square arrays of astrocyte and ependymocyte plasma membranes in rat brain and spinal cord." Proc Natl Acad Sci U S A **95**(20): 11981-11986.

Ribeiro Mde, C., L. Hirt, J. Bogousslavsky, L. Regli and J. Badaut (2006). "Time course of aquaporin expression after transient focal cerebral ischemia in mice." J Neurosci Res **83**(7): 1231-1240.

Saadoun, S., M. C. Papadopoulos, H. Watanabe, D. Yan, G. T. Manley and A. S. Verkman (2005). "Involvement of aquaporin-4 in astroglial cell migration and glial scar formation." J Cell Sci **118**(Pt 24): 5691-5698.

Scharfman, H. E. and D. K. Binder (2013). "Aquaporin-4 water channels and synaptic plasticity in the hippocampus." Neurochem Int **63**(7): 702-711.

Skucas, V. A., I. B. Mathews, J. Yang, Q. Cheng, A. Treister, A. M. Duffy, A. S. Verkman, B. L. Hempstead, M. A. Wood, D. K. Binder and H. E. Scharfman (2011). "Impairment of select forms of spatial memory and neurotrophin-dependent synaptic plasticity by deletion of glial aquaporin-4." J Neurosci **31**(17): 6392-6397.

Solenov, E., H. Watanabe, G. T. Manley and A. S. Verkman (2004). "Sevenfold-reduced osmotic water permeability in primary astrocyte cultures from AQP-4-deficient mice, measured by a fluorescence quenching method." Am J Physiol Cell Physiol **286**(2): C426-432.

Sorbo, J. G., S. E. Moe and T. Holen (2007). "Early upregulation in nasal epithelium and strong expression in olfactory bulb glomeruli suggest a role for Aquaporin-4 in olfaction." FEBS Lett **581**(25): 4884-4890.

Therrien, A. S. and A. J. Bastian (2015). "Cerebellar damage impairs internal predictions for sensory and motor function." Curr Opin Neurobiol **33**: 127-133.

Thon, N., C. A. Haas, U. Rauch, T. Merten, R. Fassler, M. Frotscher and T. Deller (2000). "The chondroitin sulphate proteoglycan brevican is upregulated by astrocytes after entorhinal cortex lesions in adult rats." Eur J Neurosci **12**(7): 2547-2558.

Venero, J. L., M. L. Vizuete, A. A. Ilundain, A. Machado, M. Echevarria and J. Cano (1999). "Detailed localization of aquaporin-4 messenger RNA in the CNS: preferential expression in periventricular organs." Neuroscience **94**(1): 239-250.

Vitellaro-Zuccarello, L., S. Mazzetti, P. Bosisio, C. Monti and S. De Biasi (2005). "Distribution of Aquaporin 4 in rodent spinal cord: relationship with astrocyte markers and chondroitin sulfate proteoglycans." Glia **51**(2): 148-159.

Warth, A., S. Kroger and H. Wolburg (2004). "Redistribution of aquaporin-4 in human glioblastoma correlates with loss of agrin immunoreactivity from brain capillary basal laminae." Acta Neuropathol **107**(4): 311-318.

Wen, H., E. A. Nagelhus, M. Amiry-Moghaddam, P. Agre, O. P. Ottersen and S. Nielsen (1999). "Ontogeny of water transport in rat brain: postnatal expression of the aquaporin-4 water channel." Eur J Neurosci **11**(3): 935-945.

Wu, N., X. Q. Lu, H. T. Yan, R. B. Su, J. F. Wang, Y. Liu, G. Hu and J. Li (2008). "Aquaporin 4 deficiency modulates morphine pharmacological actions." Neurosci Lett **448**(2): 221-225.

Yamada, H., B. Fredette, K. Shitara, K. Hagihara, R. Miura, B. Ranscht, W. B. Stallcup and Y. Yamaguchi (1997). "The brain chondroitin sulfate proteoglycan brevican associates with astrocytes ensheathing cerebellar glomeruli and inhibits neurite outgrowth from granule neurons." J Neurosci **17**(20): 7784-7795.

Zelenina, M., S. Zelenin, A. A. Bondar, H. Brismar and A. Aperia (2002). "Water permeability of aquaporin-4 is decreased by protein kinase C and dopamine." Am J Physiol Renal Physiol **283**(2): F309-318.

Zhang, H. and A. S. Verkman (2010). "Aquaporin-1 tunes pain perception by interaction with Na(v)1.8 Na+ channels in dorsal root ganglion neurons." J Biol Chem **285**(8): 5896-5906.

Zhang, H. and A. S. Verkman (2015). "Aquaporin-1 water permeability as a novel determinant of axonal regeneration in dorsal root ganglion neurons." Exp Neurol **265**: 152-159.

Zhang, J., Y. Li, Z. G. Chen, H. Dang, J. H. Ding, Y. Fan and G. Hu (2013). "Glia protein aquaporin-4 regulates aversive motivation of spatial memory in Morris water maze." CNS Neurosci Ther **19**(12): 937-944.

Chapter 4: Regulation of aquaporin-4 (AQP4) expression in a model of epilepsy

Parts of this chapter were reproduced, with permission from Elsevier, from: Hubbard, J.A., Szu, J.I., Yonan, J.M., Binder, D.K. (2016). "Regulation of astrocyte glutamate transporter-1 (GLT1) and aquaporin-4 (AQP4) expression in a model of epilepsy. *Exp Neurol*, 283: 85-96. Copyright 2016.

4.1 Abstract

The aquaporins are a family of water channels that regulate water flow in and out of a cell in response to changes in the osmotic gradient. Aquaporin-4 (AQP4) is the most abundant water channel in the central nervous system and is found exclusively on astrocytes. Therefore, astrocytes primarily regulate extracellular water homeostasis through AQP4. Previous studies have demonstrated increased seizure duration and frequency in AQP4 knockout mice. The regulation of AQP4 in epilepsy, however, is not fully understood. In this chapter, I investigated AQP4 expression changes in the intrahippocampal kainic acid (IHKA) model of temporal lobe epilepsy (TLE). I used real-time polymerase chain reaction (RT-PCR), Western blot, and immunohistochemical analysis at 1, 4, 7, and 30 days after IHKA-induced status epilepticus (SE) to determine hippocampal AQP4 expression changes during the development of epilepsy

(epileptogenesis). Following IHKA injections, AQP4 immunoreactivity and dorsal hippocampal protein expression were significantly downregulated at 1 day post SE and was followed by a gradual return to baseline levels. Interestingly, I observed a significant increase in ipsilateral AQP4 protein levels at 30 days post SE. Transient increases in AQP4 mRNA were also observed. My findings suggest that AQP4 could serve as a novel therapeutic target to restore water homeostasis in epilepsy.

4.2 Introduction

Epilepsy is a group of brain conditions characterized by the sporadic and unpredictable occurrence of seizures. It is the fourth most common neurological disorder and is estimated to affect 1 in 26 people in their lifetime (Hesdorffer, Logroscino et al. 2011). The most common form of epilepsy is temporal lobe epilepsy (TLE), which is characterized by seizures that originate in the temporal lobe. Although there are antiepileptic drugs (AEDs) available to patients today, there are at least two major drawbacks. First, current AEDs lead to several adverse effects, including cognitive impairment (Aldenkamp, De Krom et al. 2003), increased risk of teratogenicity (Crawford 2005; Wlodarczyk, Palacios et al. 2012), mood alterations, and suicidality (Perucca and Gilliam 2012). Second, approximately 30% of patients taking AEDs become medically refractory meaning they cannot control their seizures with medication alone. Current AEDs

primarily target neuronal channels or receptors (Rogawski and Löscher 2004). Since these AEDs often cause severe cognitive, developmental, and behavioral side effects, non-neuronal targets for new AEDs has the potential to have fewer deleterious effects. Recent evidence has suggested that in addition to the over-excitation of neurons, changes in astrocytes contribute to epileptogenesis (Tian, Azmi et al. 2005; Binder and Steinhäuser 2006; Seifert, Schilling et al. 2006; Seifert, Carmignoto et al. 2010; Clasadonte and Haydon 2012; Devinsky, Vezzani et al. 2013; Hubbard, Hsu et al. 2013; Coulter and Steinhauser 2015; Wilcox, Gee et al. 2015; Hubbard and Binder 2016).

Astrocytes are a crucial component of the tripartite synapse (Araque, Parpura et al. 1999) and participate in synaptic transmission regulation (Volterra and Meldolesi 2005; Halassa and Haydon 2010; Murphy-Royal, Dupuis et al. 2015; Al Awabdh, Gupta-Agarwal et al. 2016), water and K^+ homeostasis (Binder, Yao et al. 2006), and brain metabolic processes (Ransom and Ransom 2012). Striking astrocytic changes, including altered protein expression, has been reported in epileptic tissue (Steinhäuser and Seifert 2002; Seifert, Schilling et al. 2006). Direct astrocyte stimulation led to synchronization of neurons in epilepsy models (Tian, Azmi et al. 2005). Furthermore, both water and potassium homeostasis are dysregulated in patients and animal models of epilepsy (Binder and Steinhäuser 2006). Therefore, the modulation of fluid homeostasis in the brain may affect seizure susceptibility.

The aquaporins (AQPs) are a family of small, hydrophobic membrane water channels that facilitate water transport in response to osmotic gradients (Agre, King et al. 2002; Amiry-Moghaddam and Ottersen 2003; Verkman 2005; Binder, Nagelhus et al. 2012). Aquaporin-4 (AQP4) is the main water channel in the brain and spinal cord and is expressed by astrocytes, especially at specialized membrane domains including astroglial endfeet in contact with blood vessels and astrocyte membranes that ensheathe glutamatergic synapses (Nielsen, Nagelhus et al. 1997; Rash, Yasumura et al. 1998; Nagelhus, Mathiisen et al. 2004). The creation of AQP4 knockout mice in 1997 (Ma, Yang et al. 1997) helped elucidate the various functions of AQP4 in the brain, including potassium buffering (Binder, Yao et al. 2006), modulation of extracellular space diffusion (Binder, Papadopoulos et al. 2004), and even synaptic plasticity and memory (Skucas, Mathews et al. 2011; Szu and Binder 2016). Mice deficient in AQP4 have increased seizure duration (Binder, Yao et al. 2006) and decreased AQP4 immunoreactivity has been reported during the early epileptogenic phase in mouse models of epilepsy (Lee, Hsu et al. 2012; Alvestad, Hammer et al. 2013). Although AQP4 has been implicated in epilepsy (Eid, Lee et al. 2005; Binder, Yao et al. 2006; Binder, Nagelhus et al. 2012; Lee, Amini et al. 2012; Lee, Hsu et al. 2012), the expression and regulation of AQP4 during epileptogenesis has not been fully characterized.

In this group of experiments, I used the IHKA mouse model of temporal lobe epilepsy (Bouilleret, Ridoux et al. 1999; Riban, Bouilleret et al. 2002; Arabadzisz, Antal et al. 2005) to characterize AQP4 regulation at various time points during epileptogenesis. Specifically, I used RT-PCR, Western blot, and immunohistochemical analysis to determine AQP4 expression changes in the hippocampus. AQP4 dorsal hippocampal protein levels were downregulated at early time points after SE and were upregulated ipsilaterally at 30 days post SE. In addition, mRNA levels were transiently elevated at most time points examined. Reversing the significant downregulation of this critical glial water channel during the early epileptogenic period may serve as a novel therapeutic strategy.

4.3 Methods

4.3.1 Animals

All experiments were conducted in accordance with National Institutes of Health guidelines and were approved by the University of California, Riverside Institutional Animal Care and Use Committee (IACUC). Animals were housed under a 12 hour light/12 hour dark cycle with food and water provided *ad libitum*. 7-8 week-old CD1 male mice from Charles River were used for these experiments.

4.3.2 Surgery

I used IHKA injections to induce epileptogenesis (Bouilleret, Ridoux et al. 1999; Riban, Bouilleret et al. 2002; Arabadzisz, Antal et al. 2005). Briefly, mice were anesthetized with an intraperitoneal injection of an 80mg/kg ketamine and 10 mg/kg xylazine mixture and mounted in a stereotaxic frame. The skull was exposed with an incision and bregma was located. Using stereotaxic coordinates of the hippocampus (Paxinos and Franklin 2001), a 0.6 mm burr hole was made 1.8 mm posterior and 1.6 mm lateral from bregma with a high-speed drill (Drummond Scientific). Mice were injected with either 74 nL of a 20 mM solution of kainic acid or an equal volume of 0.9% saline over a period of 4 minutes using a microinjector (Nanoject, Drummond Scientific) into the right dorsal hippocampus at the dorsoventral coordinate of 1.9 mm.

Animals were then monitored for behavioral seizures. All animals experienced continuous (3 or more hours) Racine stage 3-5 seizures (Racine 1972), described in Table 2.1. Animals that died due to SE were excluded from the study. Otherwise, at each time point n = 5 animals were euthanized with fatal plus (Western Medical Supply), perfused, and processed for each experiment, unless otherwise specified.

4.3.3 Immunohistochemistry

After mice were transcardially perfused with ice-cold phosphate buffered saline (PBS, pH 7.4) followed by 4% paraformaldehyde (PFA), brains were quickly removed and postfixed in 4% PFA overnight at 4°C. Next, brains were cryoprotected in 30% sucrose in PBS at 4°C for two days. Brains were then flash frozen and cut into 50 µm coronal sections using a cryostat (Leica CM 1950, Leica Microsytems) and slices were stored in PBS at 4°C. For each experiment, slices were processed simultaneously. Slices were blocked for 1 hour with 5% normal goat serum in PBS and then incubated with primary antibodies to AQP4 (1:200, Millipore AB3594) overnight at 4°C in 0.3% Triton X-100. After washing slices with PBS, sections were incubated with a species-specific secondary antibody conjugated with Alexa 488. Slices were mounted in Vectashield with DAPI (Vector Laboratories) and 10x images were taken using a fluorescence microscope (Zeiss Axio Observer Inverted Microscope).

4.3.4 Western blot analysis

Dorsal hippocampus was microdissected from the mouse brain at 1, 4, 7, and 30 days post IHKA or intrahippocampal saline injections (n = 5 for saline controls and all other time points). Harvested tissue was homogenized using the Bullet Blender (Next Advance) in radioimmunoprecipitation assay buffer (Sigma)

containing complete protease inhibitors (Roche). Protein concentrations were assayed and protein was resolved by SDS-PAGE, 10% polyacrylamide, and transferred to a nitrocellulose membrane. The membranes were then probed for AQP4 (1:1,000, Millipore ABN411) and β-actin (1:5,000, Sigma A1978) as an internal control. Whole hippocampal tissue was microdissected, processed, and probed for AQP4 (1:1,000, Millipore ABN411) while again using β-actin (1:5,000, Sigma A1978) as an internal control. Bands were visualized and quantified using the Li-COR Odyssey Fc Western Imaging System and protein levels were normalized to internal β-actin levels. The upper (tetrameric) band for AQP4 is shown, was determined to be specific (Figure 4.1), and therefore was used for quantification.

4.3.5 Real-time polymerase chain reaction (RT-PCR) analysis

Dorsal hippocampus was microdissected from the mouse brain at 1, 4, 7, and 30 days post IHKA or intrahippocampal saline injections. Harvested tissue was homogenized in TRIzol using the Bullet Blender (Next Advance). RNA was isolated using the Direct-Zol RNA mini prep kit (Zymo Research) and quantified using a nanodrop (Thermo Scientific NanoDrop 2000c Spectrophotometer). Both cDNA synthesis and RT-PCR were performed using the Bioline SensiFAST SYBR NO-ROX Kit and the CFX-96 detection system (Bio-Rad). Primers for AQP4 and 18s RNA (Table 4.1) were purchased from Integrated DNA

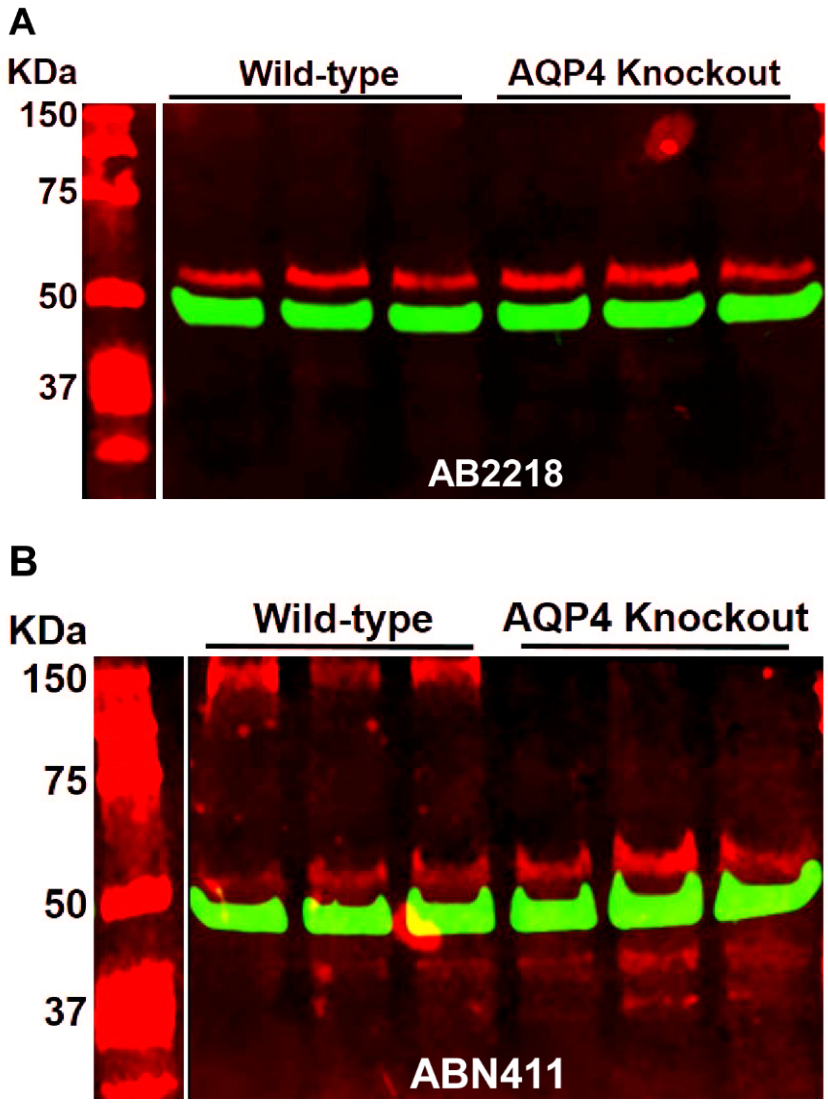


Figure 4.1. Western blot analysis of aquaporin-4 (AQP4) antibodies using wild-type and AQP4 knockout mouse tissue.
Western blots of AQP4 (red) and β-actin (green) protein using hippocampal tissue from CD1 wild-type (first three lanes) and AQP4 knockout (last 3 lanes) mice. **A.** Western blot using the Millipore anti-AQP4 AB2218 antibody. AQP4 bands were observed in both wild-type and knockout tissue. Therefore, the antibody was not used further in this study. **B.** Western blot using Millipore anti-AQP4 ABN411 antibody. Bot monomeric and multimeric bands for AQP4 were observed in the wild-type and knockout tissue and therefore were excluded from analysis. The upper, tetrameric (~150 KDa) band was only found in the wild-type tissue and was used exclusively for analysis in this study.

Technologies. The reaction conditions were as follows: 1 cycle for 10 min at 45°C, 1 cycle for 2 min at 95°C, 40 cycles for 5s at 95°C, and 1 cycle for 20s at 60°C. Results were quantified using the differential CT method representing the fold change in target gene expression. Both a no template control (NTC) and a no reverse transcriptase (NRT) control were included in each assay to detect any contamination or non-specific replication.

Target Gene	Forward Primer Sequence	Reverse Primer Sequence
AQP4	CTGGAGCCAGCATGAATCCAG	TTCTTCTCTTCTCCACGGTCA
18s RNA	CTCAACACGGGAAACCTCAC	CGCTCCACCAACTAAGAACG

Table 4.1. Primers used for RT-PCR experiments.
Primers are listed in the 5' → 3' direction.

4.3.6 Statistical analysis

Statistical analysis was performed using a one-way ANOVA with *post-hoc* Bonferroni multiple comparisons test. All error bars are presented as the mean ± standard error of the mean (SEM). A comparison to saline control was considered statistically significance by a p-value < 0.05, < 0.01 or < 0.001 and denoted with *, **, or ***, respectively. Any statistically significant differences between other time points were not indicated for the purpose of clarity.

4.4 Results

4.4.1 Decreased AQP4 immunoreactivity

Marked downregulation of AQP4 immunoreactivity in the contralateral hippocampus has been previously demonstrated in the IHKA model (Lee, Hsu et al. 2012). Specifically, AQP4 immunoreactivity was downregulated in all layers of the hippocampus except the stratum oriens at 1 and 4 days post IHKA-induced SE. AQP4 remained downregulated up to 30 days post SE with partial recovery in the stratum pyramidale and stratum radiatum. I have demonstrated a similar downregulation of AQP4 immunoreactivity in the ipsilateral hippocampus to IHKA injections (Figure 4.2). An immediate downregulation of AQP4 immunoreactivity was observed at 1 day post IHKA-induced SE in all layers of the hippocampus. Over time, a recovery to at least baseline levels was observed.

4.4.2 Changes in aquaporin-4 (AQP4) expression

I next characterized AQP4 protein and mRNA expression changes using Western blot and RT-PCR, respectively. I found a dramatic downregulation of AQP4 protein 1 day and 4 days post SE in the ipsilateral dorsal hippocampus (Figure 4.3A-B). AQP4 returned to nearly control protein levels by 7 days post SE and significantly increased AQP4 protein levels were observed at 30 days

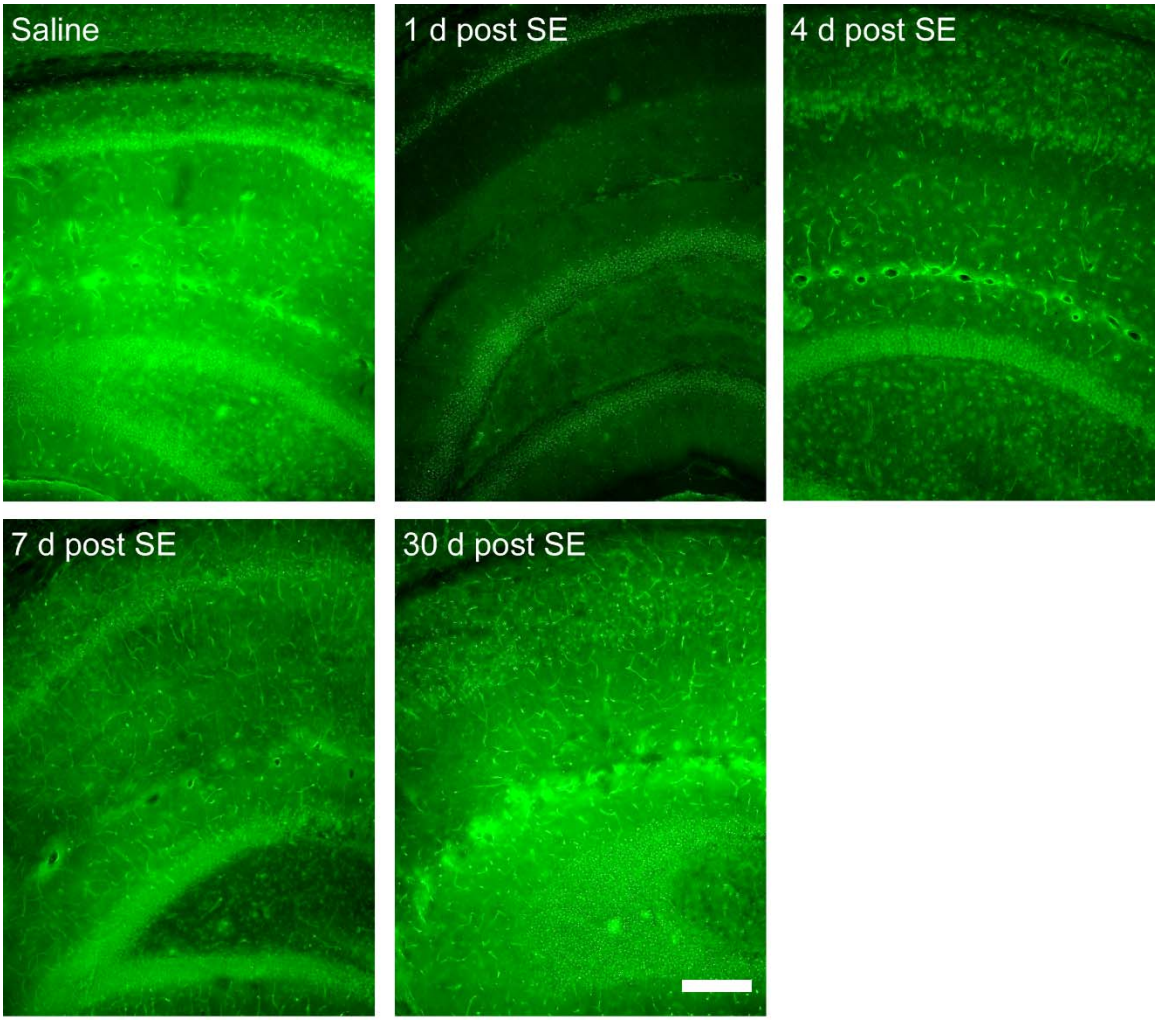


Figure 4.2. Hippocampal aquaporin-4 (AQP4) immunoreactivity following intrahippocampal kainic acid (IHKA)-induced status epilepticus (SE).
A significant reduction in AQP4 immunoreactivity was observed at 1 day (d) post SE with a partial recovery over time (4, 7, and 30 days (d) post SE). One to two slices from each animal (n = 3) were used. Scale bar = 200 μm.

post SE. In the contralateral dorsal hippocampus, AQP4 protein was immediately downregulated by 1 day post SE (Figures 4.3D-E). This was followed by a gradual return to control AQP4 levels. Increased levels of AQP4 mRNA were observed 7 days post SE in both the ipsilateral (Figure 4.3C) and

contralateral (Figure 4.3F) dorsal hippocampi. The highest level of AQP4 mRNA expression, however, was observed 4 days post SE in the ipsilateral dorsal hippocampus. Together, these results suggest that AQP4 regulation in the dorsal hippocampus occurs both at the mRNA and protein level in the IHKA model of epilepsy. Separate analysis of whole hippocampal AQP4 protein

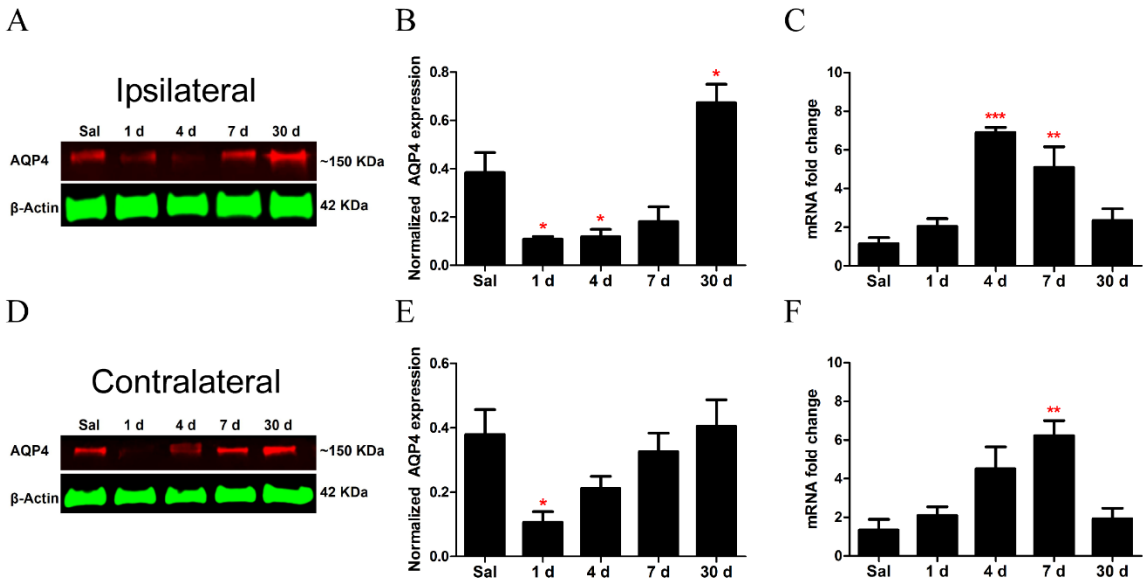


Figure 4.3. Dorsal hippocampal aquaporin-4 (AQP4) protein and mRNA levels after kainic acid-induced status epilepticus (SE).
A. Representative Western blot of AQP4 (red) and β-actin (green) protein from the ipsilateral hippocampus from a saline control (Sal) and 1, 4, 7, and 30 days (d) post SE. **B.** Quantification of AQP4 band intensities normalized to β-actin at each time point from the ipsilateral hippocampus. **C.** Fold change in AQP4 mRNA in the ipsilateral hippocampus from saline controls (Sal) and 1, 4, 7, and 30 days (d) post SE. **D.** Representative Western blot of AQP4 (red) and β-actin (green) protein from the contralateral hippocampus in a saline control (Sal) and 1, 4, 7, and 30 days post kainic acid-induced SE. **E.** Quantification of AQP4 protein from the contralateral hippocampus normalized to β-actin in each group. **F.** Quantification of AQP4 mRNA levels in the contralateral hippocampus in tissue collected from saline controls (Sal) and at various time points post SE. * indicates $p < 0.05$, ** indicates $p < 0.01$, and *** indicates $p < 0.001$ when compared to saline control and $n = 5$ for each time point.

revealed no changes at any time point examined (Figure 4.4). AQP4 mRNA levels, however, were significantly increased in both the ipsilateral and contralateral hippocampi to injection at most time points examined (Figure 4.4).

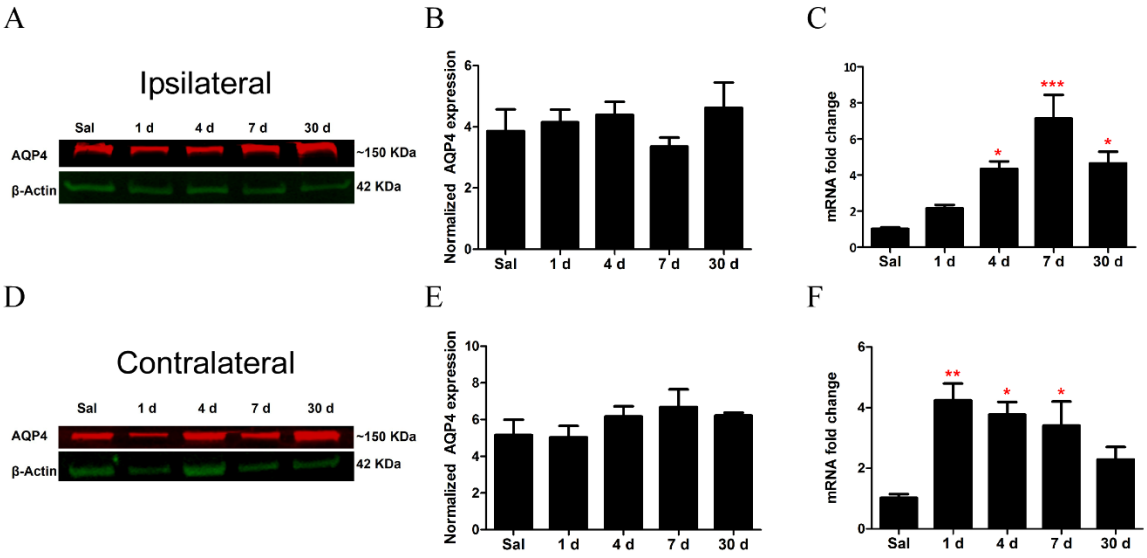


Figure 4.4. Aquaporin-4 (AQP4) protein and mRNA whole hippocampal levels after kainic acid-induced status epilepticus (SE).
A. Representative Western blot of AQP4 (red) and β-actin (green) protein from the ipsilateral hippocampus of a saline control (Sal) and 1, 4, 7, and 30 days (d) post kainic acid-induced SE. **B.** Quantification of AQP4 band intensities normalized to β-actin in each group in the ipsilateral hippocampus. **C.** Fold change in AQP4 mRNA in the ipsilateral hippocampus from saline controls (Sal) and in tissue collected 1, 4, 7, and 30 days (d) post SE. **D.** Representative Western blot of AQP4 (red) and β-actin (green) protein from the contralateral hippocampus of a saline control (Sal) or 1, 4, 7, or 30 days (d) post kainic acid-induced SE. **E.** Quantification of contralateral AQP4 protein normalized to β-actin in each group. **F.** Quantification of AQP4 mRNA levels in the contralateral hippocampus in the saline controls (Sal) and various time points post SE. * indicates $p < 0.05$, ** indicates $p < 0.01$ and *** indicates $p < 0.001$ when compared to saline control and $n = 5$ for each time point.

4.5 Discussion

In this study, I used RT-PCR, Western blot, and immunohistochemistry to examine changes in AQP4 at various time points post SE in the IHKA model of epilepsy. First, I found an immediate downregulation of AQP4 immunoreactivity with partial recovery over time. Second, I observed a parallel change in AQP4 dorsal hippocampal protein levels with increased AQP4 protein levels in the ipsilateral hippocampus at 30 days post SE. Third, mRNA was transiently upregulated at various time points after kainic acid-induced SE. Importantly, significant regulation of AQP4 expression was observed in both the hippocampi ipsilateral and contralateral to IHKA injections. As discussed in Chapter 2, the hippocampus ipsilateral to IHKA injections becomes sclerotic (neuronal dispersion and cell death; gliosis) by 30 days post SE. Therefore, regulation of AQP4 by seizure activity does not appear to require cell death/sclerosis. This time course study is the first to examine mRNA, protein, and immunoreactivity changes of AQP4 in a well-established model of TLE. These results support the hypothesis that intense seizures regulate AQP4 expression and may lead to astrocytic dysregulation of extracellular space, water, and potassium homeostasis during epileptogenesis.

Increasing evidence suggests dysregulation of water and potassium plays a role in epilepsy (Binder and Steinhäuser 2006; Binder, Nagelhus et al. 2012).

Expression and subcellular localization of AQP4 is altered in sclerotic human hippocampi (Lee, Eid et al. 2004), with increased total AQP4 protein but a reduction in perivascular membrane expression (Eid, Lee et al. 2005); this suggests a dysregulation of AQP4 localization. AQP4 knockout mice have significantly prolonged seizure duration associated with a deficit in extracellular K^+ clearance (Binder, Yao et al. 2006; Strohschein, Hüttmann et al. 2011; Haj-Yasein, Bugge et al. 2015). These results together suggest a pro-epileptogenic effect of AQP4 dysregulation (Dudek and Rogawski 2005; Wetherington, Serrano et al. 2008; Binder, Nagelhus et al. 2012). In the current study, I found decreased dorsal AQP4 protein levels in both the ipsilateral and contralateral dorsal hippocampi 1 day post SE. These results closely align with previously observed reductions in AQP4 immunoreactivity early after SE (Lee, Hsu et al. 2012). In the dorsal ipsilateral hippocampus, AQP4 protein levels remained downregulated at 4 days post SE and were found to be upregulated in the chronically epileptic brain (30 days post SE). The changes in AQP4 mRNA levels may have been compensatory to restore AQP4 protein levels after the significant drop in protein at early time points post SE.

Other results also suggest that AQP4 dysregulation may occur early during epileptogenesis. Kim *et al.* studied regulation of various aquaporins in the rat pilocarpine model of epilepsy (Kim, Ryu et al. 2009; Kim, Yeo et al. 2010). In control animals, AQP4 immunoreactivity was detected diffusely in the piriform

cortex and hippocampus, with greatest expression at astrocyte endfeet. Following status epilepticus in this model the authors described an “AQP4-deleted area” in the piriform cortex. However, EEG analysis for timing of spontaneous seizure onset was not investigated. In a distinct model of intraperitoneal kainic acid administration in rats, Alvestad et al. (2013) found mislocalization of AQP4. In particular, using immunogold analysis these investigators demonstrated that AQP4 was reduced in adluminal endfoot membranes but was stable or slightly increased in abluminal endfoot membranes (Alvestad, Hammer et al. 2013). This occurred in the early epileptogenic period prior to the occurrence of spontaneous seizures. AQP4 regulation and subcellular compartmentalization remains to be examined in other models of epilepsy. In particular, distinct epilepsy models in which epileptogenesis occurs in the *absence* of detectable cell death would prove useful in determining the threshold for AQP4 regulation, such as the electrical kindling model.

Alterations in glial molecules during epileptogenesis may play a role in epilepsy-associated cognitive dysfunction. For example, increasing evidence has suggested an important role for AQP4 in the regulation of synaptic plasticity in the hippocampus and amygdala (Szu and Binder 2016). AQP4-deficient mice have been found to have marked deficits in synaptic plasticity, including deficits in long-term potentiation and long-term depression, and impairment in location-specific object memory (Skucas, Mathews et al. 2011). More recent studies from

other groups have confirmed deficits in synaptic plasticity in AQP4-deficient mice (Li, Wang et al. 2012; Fan, Liu et al. 2013; Yang, Li et al. 2013). In human patients with mesial TLE, a correlation between IQ and AQP4 expression was observed (Kandratavicius, Peixoto-Santos et al. 2015). Therefore, a downregulation of AQP4 may lead not only to hyperexcitability but also to broader deficits in synaptic plasticity and cognitive performance which are important comorbidities in patients with epilepsy (Bell, Lin et al. 2011; Brooks-Kayal, Bath et al. 2013).

In conclusion, I found significant changes in AQP4 expression levels during the early epileptic period. Early disruption of astrocytic water and potassium homeostasis could have powerful epileptogenic and cognitive effects. Increased AQP4 expression observed in the ipsilateral (sclerotic) hippocampus at 30 days post SE closely aligns with human tissue studies. Therefore, restoration of AQP4 levels after the initial reduction in the IHKA model may also be accompanied by mislocalization of AQP4. Future studies should focus on elucidating the mechanism of AQP4 dysregulation. In addition, methods to maintain steady AQP4 expression may ameliorate hyperexcitability and provide a new astrocyte-based antiepileptogenic strategy.

4.6 References

Agre, P., L. S. King, M. Yasui, W. B. Guggino, O. P. Ottersen, Y. Fujiyoshi, A. Engel and S. Nielsen (2002). "Aquaporin water channels--from atomic structure to clinical medicine." J Physiol **542**(Pt 1): 3-16.

Al Awabdh, S., S. Gupta-Agarwal, D. F. Sheehan, J. Muir, R. Norkett, A. E. Twelvetrees, L. D. Griffin and J. T. Kittler (2016). "Neuronal activity mediated regulation of glutamate transporter GLT-1 surface diffusion in rat astrocytes in dissociated and slice cultures." Glia **64**(7): 1252-1264.

Aldenkamp, A. P., M. De Krom and R. Reijs (2003). "Newer antiepileptic drugs and cognitive issues." Epilepsia **44**: 21-29.

Alvestad, S., J. Hammer, E. H. Hoddevik, O. Skare, U. Sonnewald, M. Amiry-Moghaddam and O. P. Ottersen (2013). "Mislocalization of AQP4 precedes chronic seizures in the kainate model of temporal lobe epilepsy." Epilepsy Res **105**(1-2): 30-41.

Amiry-Moghaddam, M. and O. P. Ottersen (2003). "The molecular basis of water transport in the brain." Nat Rev Neurosci **4**(12): 991-1001.

Arabadzisz, D., K. Antal, F. Parpan, Z. Emri and J. M. Fritschy (2005). "Epileptogenesis and chronic seizures in a mouse model of temporal lobe epilepsy are associated with distinct EEG patterns and selective neurochemical alterations in the contralateral hippocampus." Exp Neurol **194**(1): 76-90.

Araque, A., V. Parpura, R. P. Sanzgiri and P. G. Haydon (1999). "Tripartite synapses: glia, the unacknowledged partner." Trends Neurosci **22**(5): 208-215.

Bell, B., J. J. Lin, M. Seidenberg and B. Hermann (2011). "The neurobiology of cognitive disorders in temporal lobe epilepsy." Nat Rev Neurol **7**(3): 154-164.

Binder, D. K., E. A. Nagelhus and O. P. Ottersen (2012). "Aquaporin-4 and epilepsy." Glia **60**(8): 1203-1214.

Binder, D. K., M. C. Papadopoulos, P. M. Haggie and A. S. Verkman (2004). "In vivo measurement of brain extracellular space diffusion by cortical surface photobleaching." J Neurosci **24**(37): 8049-8056.

Binder, D. K. and C. Steinhäuser (2006). "Functional changes in astroglial cells in epilepsy." Glia **54**(5): 358-368.

Binder, D. K., X. Yao, Z. Zador, T. J. Sick, A. S. Verkman and G. T. Manley (2006). "Increased seizure duration and slowed potassium kinetics in mice lacking aquaporin-4 water channels." Glia **53**(6): 631-636.

Bouilleret, V., V. Ridoux, A. Depaulis, C. Marescaux, A. Nehlig and G. Le Gal La Salle (1999). "Recurrent seizures and hippocampal sclerosis following intrahippocampal kainate injection in adult mice: electroencephalography, histopathology and synaptic reorganization similar to mesial temporal lobe epilepsy." Neuroscience **89**(3): 717-729.

Brooks-Kayal, A. R., K. G. Bath, A. T. Berg, A. S. Galanopoulou, G. L. Holmes, F. E. Jensen, A. M. Kanner, T. J. O'Brien, V. H. Whittemore, M. R. Winawer, M. Patel and H. E. Scharfman (2013). "Issues related to symptomatic and disease-modifying treatments affecting cognitive and neuropsychiatric comorbidities of epilepsy." Epilepsia **54 Suppl 4**: 44-60.

Clasadonte, J. and P. G. Haydon (2012). Astrocytes and Epilepsy. Jasper's Basic Mechanisms of the Epilepsies. J. L. Noebels, M. Avoli, M. A. Rogawski, R. W. Olsen and A. V. Delgado-Escueta. Bethesda (MD).

Coulter, D. A. and C. Steinhauser (2015). "Role of astrocytes in epilepsy." Cold Spring Harb Perspect Med **5**(3): a022434.

Crawford, P. (2005). "Best practice guidelines for the management of women with epilepsy." Epilepsia **46**(Suppl. 9): 117-124.

Devinsky, O., A. Vezzani, S. Najjar, N. C. De Lanerolle and M. A. Rogawski (2013). "Glia and epilepsy: excitability and inflammation." Trends Neurosci **36**(3): 174-184.

Dudek, F. E. and M. A. Rogawski (2005). "Regulation of brain water: is there a role for aquaporins in epilepsy?" Epilepsy Curr **5**(3): 104-106.

Eid, T., T. S. Lee, M. J. Thomas, M. Amiry-Moghaddam, L. P. Bjornsen, D. D. Spencer, P. Agre, O. P. Ottersen and N. C. de Lanerolle (2005). "Loss of perivascular aquaporin 4 may underlie deficient water and K+ homeostasis in the human epileptogenic hippocampus." Proc Natl Acad Sci U S A **102**(4): 1193-1198.

Fan, Y., M. Liu, X. Wu, F. Wang, J. Ding, J. Chen and G. Hu (2013). "Aquaporin-4 promotes memory consolidation in Morris water maze." Brain Struct Funct **218**(1): 39-50.

Haj-Yasein, N. N., C. E. Bugge, V. Jensen, I. Ostby, O. P. Ottersen, O. Hvalby and E. A. Nagelhus (2015). "Deletion of aquaporin-4 increases extracellular K(+) concentration during synaptic stimulation in mouse hippocampus." Brain Struct Funct **220**(4): 2469-2474.

Halassa, M. M. and P. G. Haydon (2010). "Integrated brain circuits: astrocytic networks modulate neuronal activity and behavior." Annu Rev Physiol **72**: 335-355.

Hesdorffer, D. C., G. Logroscino, E. K. Benn, N. Katri, G. Cascino and W. A. Hauser (2011). "Estimating risk for developing epilepsy: a population-based study in Rochester, Minnesota." Neurology **76**(1): 23-27.

Hubbard, J. A. and D. K. Binder (2016). Astrocytes and Epilepsy. Amsterdam, Netherlands, Elsevier, in press.

Hubbard, J. A., M. S. Hsu, T. A. Fiacco and D. K. Binder (2013). "Glial cell changes in epilepsy: overview of the clinical problem and therapeutic opportunities." Neurochem Int **63**(7): 638-651.

Kandratavicius, L., J. E. Peixoto-Santos, M. R. Monteiro, R. C. Scandiuzzi, C. G. Carlotti, Jr., J. A. Assirati, Jr., J. E. Hallak and J. P. Leite (2015). "Mesial temporal lobe epilepsy with psychiatric comorbidities: a place for differential neuroinflammatory interplay." J Neuroinflammation **12**: 38.

Kim, J. E., H. J. Ryu, S. I. Yeo, C. H. Seo, B. C. Lee, I. G. Choi, D. S. Kim and T. C. Kang (2009). "Differential expressions of aquaporin subtypes in astroglia in the hippocampus of chronic epileptic rats." Neuroscience **163**(3): 781-789.

Kim, J. E., S. I. Yeo, H. J. Ryu, M. J. Kim, D. S. Kim, S. M. Jo and T. C. Kang (2010). "Astroglial loss and edema formation in the rat piriform cortex and hippocampus following pilocarpine-induced status epilepticus." J Comp Neurol **518**(22): 4612-4628.

Lee, D. J., M. Amini, M. J. Hamamura, M. S. Hsu, M. M. Seldin, O. Nalcioglu and D. K. Binder (2012). "Aquaporin-4-dependent edema clearance following status epilepticus." Epilepsy Res **98**(2-3): 264-268.

Lee, D. J., M. S. Hsu, M. M. Seldin, J. L. Arellano and D. K. Binder (2012). "Decreased expression of the glial water channel aquaporin-4 in the intrahippocampal kainic acid model of epileptogenesis." Exp Neurol **235**(1): 246-255.

Lee, T. S., T. Eid, S. Mane, J. H. Kim, D. D. Spencer, O. P. Ottersen and N. C. de Lanerolle (2004). "Aquaporin-4 is increased in the sclerotic hippocampus in human temporal lobe epilepsy." Acta Neuropathol **108**(6): 493-502.

Li, Y. K., F. Wang, W. Wang, Y. Luo, P. F. Wu, J. L. Xiao, Z. L. Hu, Y. Jin, G. Hu and J. G. Chen (2012). "Aquaporin-4 deficiency impairs synaptic plasticity and associative fear memory in the lateral amygdala: involvement of downregulation of glutamate transporter-1 expression." Neuropsychopharmacology **37**(8): 1867-1878.

Ma, T., B. Yang, A. Gillespie, E. J. Carlson, C. J. Epstein and A. S. Verkman (1997). "Generation and phenotype of a transgenic knockout mouse lacking the mercurial-insensitive water channel aquaporin-4." J Clin Invest **100**(5): 957-962.

Murphy-Royal, C., J. P. Dupuis, J. A. Varela, A. Panatier, B. Pinson, J. Baufreton, L. Groc and S. H. Oliet (2015). "Surface diffusion of astrocytic glutamate transporters shapes synaptic transmission." Nat Neurosci **18**(2): 219-226.

Nagelhus, E. A., T. M. Mathiisen and O. P. Ottersen (2004). "Aquaporin-4 in the central nervous system: cellular and subcellular distribution and coexpression with KIR4.1." Neuroscience **129**(4): 905-913.

Nielsen, S., E. A. Nagelhus, M. Amiry-Moghaddam, C. Bourque, P. Agre and O. P. Ottersen (1997). "Specialized membrane domains for water transport in glial cells: high-resolution immunogold cytochemistry of aquaporin-4 in rat brain." J Neurosci **17**(1): 171-180.

Paxinos, G. and K. B. J. Franklin (2001). The mouse brain in stereotaxic coordinates. San Diego, CA, Academic Press.

Perucca, P. and F. G. Gilliam (2012). "Adverse effects of antiepileptic drugs." The Lancet Neurology **11**(9): 792-802.

Racine, R. J. (1972). "Modification of seizure activity by electrical stimulation. II. Motor seizure." Electroencephalogr Clin Neurophysiol **32**(3): 281-294.

Ransom, B. R. and C. B. Ransom (2012). "Astrocytes: multitalented stars of the central nervous system." Methods Mol Biol **814**: 3-7.

Rash, J. E., T. Yasumura, C. S. Hudson, P. Agre and S. Nielsen (1998). "Direct immunogold labeling of aquaporin-4 in square arrays of astrocyte and ependymocyte plasma membranes in rat brain and spinal cord." Proc Natl Acad Sci U S A **95**(20): 11981-11986.

Riban, V., V. Bouilleret, B. T. Pham-Le, J. M. Fritschy, C. Marescaux and A. Depaulis (2002). "Evolution of hippocampal epileptic activity during the development of hippocampal sclerosis in a mouse model of temporal lobe epilepsy." Neuroscience **112**(1): 101-111.

Rogawski, M. A. and W. Löscher (2004). "The neurobiology of antiepileptic drugs." Nature Reviews Neuroscience **5**: 553-564.

Seifert, G., G. Carmignoto and C. Steinhäuser (2010). "Astrocyte dysfunction in epilepsy." Brain Research Reviews **63**: 212-221.

Seifert, G., K. Schilling and C. Steinhäuser (2006). "Astrocyte dysfunction in neurological disorders: a molecular perspective." Nature Reviews Neuroscience **7**(194-206).

Seifert, G., K. Schilling and C. Steinhäuser (2006). "Astrocyte dysfunction in neurological disorders: a molecular perspective." Nat Rev Neurosci **7**(3): 194-206.

Skucas, V. A., I. B. Mathews, J. Yang, Q. Cheng, A. Treister, A. M. Duffy, A. S. Verkman, B. L. Hempstead, M. A. Wood, D. K. Binder and H. E. Scharfman (2011). "Impairment of select forms of spatial memory and neurotrophin-dependent synaptic plasticity by deletion of glial aquaporin-4." J Neurosci **31**(17): 6392-6397.

Steinhäuser, C. and G. Seifert (2002). "Glial membrane channels and receptors in epilepsy: impact for generation and spread of seizure activity." Eur J Pharmacol **447**(2-3): 227-237.

Strohschein, S., K. Hüttmann, S. Gabriel, D. K. Binder, U. Heinemann and C. Steinhäuser (2011). "Impact of aquaporin-4 channels on K+ buffering and gap junction coupling in the hippocampus." Glia **59**(6): 973-980.

Szu, J. I. and D. K. Binder (2016). "The Role of Astrocytic Aquaporin-4 in Synaptic Plasticity and Learning and Memory." Front Integr Neurosci **10**: 8.

Tian, G., H. Azmi, T. Takano, Q. Xu, W. Peng, J. Lin, N. Oberheim, N. Lou, R. Zielke, J. Kang and M. Nedergaard (2005). "An astrocytic basis of epilepsy." Nature Medicine **11**(9): 973-981.

Tian, G. F., H. Azmi, T. Takano, Q. Xu, W. Peng, J. Lin, N. Oberheim, N. Lou, X. Wang, H. R. Zielke, J. Kang and M. Nedergaard (2005). "An astrocytic basis of epilepsy." Nat Med **11**(9): 973-981.

Verkman, A. S. (2005). "More than just water channels: unexpected cellular roles of aquaporins." J Cell Sci **118**(Pt 15): 3225-3232.

Volterra, A. and J. Meldolesi (2005). "Astrocytes, from brain glue to communication elements: the revolution continues." Nat Rev Neurosci **6**(8): 626-640.

Wetherington, J., G. Serrano and R. Dingledine (2008). "Astrocytes in the epileptic brain." Neuron **58**(2): 168-178.

Wilcox, K. S., J. M. Gee, M. B. Gibbons, P. Tvrdik and J. A. White (2015). "Altered structure and function of astrocytes following status epilepticus." Epilepsy Behav **49**: 17-19.

Wlodarczyk, B. J., A. M. Palacios, T. M. George and R. H. Finnell (2012). "Antiepileptic drugs and pregnancy outcomes." American Journal of Medical Genetics **158A**(8): 2071-2090.

Yang, J., M. X. Li, Y. Luo, T. Chen, J. Liu, P. Fang, B. Jiang, Z. L. Hu, Y. Jin, J. G. Chen and F. Wang (2013). "Chronic ceftriaxone treatment rescues hippocampal memory deficit in AQP4 knockout mice via activation of GLT-1." Neuropharmacology **75**: 213-222.

Chapter 5: Regulation of glutamate transporter-1 (GLT1) expression in a model of epilepsy

This chapter was modified and reproduced, with permission from Elsevier, from: Hubbard, J.A., Szu, J.I., Yonan, J.M., Binder, D.K. (2016). "Regulation of astrocyte glutamate transporter-1 (GLT1) and aquaporin-4 (AQP4) expression in a model of epilepsy. *Exp Neurol*, 283: 85-96. Copyright 2016.

5.1 Abstract

Prolonged elevations in extracellular glutamate can lead to neuronal cell death and hyperexcitability. Glutamate transporter-1 (GLT1) is an astrocyte-specific membrane protein that removes glutamate from the extracellular space in the brain. Mice lacking GLT1 develop spontaneous lethal seizures whereas transgenic overexpression of GLT1 in mice offers neuroprotection and anti-seizure effects. The specific regulation of GLT1 in epilepsy, however, is not fully understood. In this chapter, I determined GLT1 expression changes in the intrahippocampal kainic acid (IHKA) model of temporal lobe epilepsy (TLE). Specifically, I used real-time polymerase chain reaction (RT-PCR), Western blot, and immunohistochemical analysis at 1, 4, 7, and 30 days after kainic acid-induced status epilepticus (SE) to determine hippocampal GLT1 expression changes during epileptogenesis. I observed a significant initial increase in dorsal

hippocampal GLT1 immunoreactivity and protein levels 1 day post SE followed by a marked downregulation at 4 and 7 days post SE with a return to near control levels by 30 days post SE. Little changes in hippocampal GLT1 mRNA levels were noted. The restoration of glutamate homeostasis by direct modulation of astrocytic GLT1 protein levels could serve as a novel therapeutic strategy for the prevention of seizures.

5.2 Introduction

Epilepsy, a group of seizure disorders, is a major public health concern estimated to afflict 3.9% of the US population at some point in their lifetime (Hesdorffer, Logroscino et al. 2011). TLE, the most common form of epilepsy, affects over 40 million people worldwide alone (de Lanerolle, Lee et al. 2012). Approximately 30% of patients taking antiepileptic drugs (AEDs), however, do not become seizure-free with existing medications. Current AEDs primarily target neurons and often cause severe cognitive, developmental, and behavioral side effects. Thus, new drugs based on non-neuronal targets may offer an alternative treatment method with fewer adverse effects. One potential target is astrocytes because they are now known to contribute to the development of epilepsy (Hubbard, Hsu et al. 2013; Hubbard and Binder 2016).

Astrocytes were previously thought of as passive cells, but they are now known to regulate ionic homeostasis, energy metabolism (Ransom and Ransom 2012), the formation of synaptic networks (Ransom, Behar et al. 2003), and the modulation of glutamatergic synaptic transmission (Volterra and Meldolesi 2005; Halassa and Haydon 2010; Murphy-Royal, Dupuis et al. 2015; Al Awabdh, Gupta-Agarwal et al. 2016). Striking changes in astrocytic shape and function are observed in "reactive" cells (see Chapter 2). Based on not only morphological alterations but also functional changes in expression of channels and receptors, reactive astrocytes may contribute to increased neuronal excitability (Binder and Steinhäuser 2006; Hubbard, Hsu et al. 2013).

Extracellular glutamate levels determine the extent of neuronal excitability; therefore it is crucial to maintain low glutamate levels in the extracellular space (ECS). Glutamate transporters are responsible for removing glutamate from the ECS. The most prominently expressed glutamate transporter in the mammalian forebrain is GLT1 (Danbolt 2001), found almost exclusively on astrocytes, although neuronal GLT1 has been reported (Chen, Mahadomrongkul et al. 2004; Furness, Dehnes et al. 2008). Deletion (Tanaka, Watase et al. 1997) or antisense oligonucleotide-mediated inhibition of synthesis (Rothstein, Dykes-Hoberg et al. 1996) of GLT1 in rodents revealed that it is the major contributor to extracellular glutamate clearance. Interestingly, deletion of astrocytic GLT1 led to seizures whereas deletion of neuronal GLT1 reduced synaptosomal glutamate

uptake by nearly 40% (Petr, Sun et al. 2015). GLT1-mediated glutamate removal from the tripartite synapse is conducted in an activity-regulated manner, thereby shaping synaptic transmission (Murphy-Royal, Dupuis et al. 2015). Furthermore, homozygous mice deficient in GLT1 developed lethal spontaneous seizures (Tanaka, Watase et al. 1997). Overexpression of GLT1, on the other hand, attenuated epileptogenesis and reduced seizure frequency in transgenic mice (Kong, Takahashi et al. 2012). It is widely accepted that delayed glutamate clearance from the ECS is implicated in seizures (During and Spencer 1993; Glass and Dragunow 1995; Tanaka, Watase et al. 1997; Campbell and Hablitz 2004; Hubbard, Hsu et al. 2013), but whether changes in GLT1 expression or function underlie the development of epilepsy is unknown.

Here, I used the well-established IHKA mouse model of TLE (Bouilleret, Ridoux et al. 1999; Riban, Bouilleret et al. 2002; Arabadzisz, Antal et al. 2005) to fully examine GLT1 regulation during epileptogenesis. I used real-time polymerase chain reaction (RT-PCR), Western blot, and immunohistochemical analysis at 1, 4, 7, and 30 days after IHKA-induced SE to determine hippocampal GLT1 expression changes during epileptogenesis. I found a significant initial increase in dorsal hippocampal GLT1 immunoreactivity and protein levels 1 day post SE and a significant downregulation as early as 4 days post SE. Little change in GLT1 mRNA however, was observed. These results indicate significant

translational or post-translational modulation of this critical glial transporter during the early epileptogenic period in this model.

5.3 Methods

5.3.1 Animals

All experiments were conducted in accordance with National Institutes of Health guidelines and were approved by the University of California, Riverside Institutional Animal Care and Use Committee (IACUC). Animals were housed under a 12 hour light/12 hour dark cycle with food and water provided *ad libitum*. 7-8 week-old CD1 male mice from Charles River were used for these experiments.

5.3.2 Surgery

I used IHKA injections to induce SE (Bouilleret, Ridoux et al. 1999; Riban, Bouilleret et al. 2002; Arabadzisz, Antal et al. 2005). Briefly, mice were anesthetized with an intraperitoneal (i.p.) injection of a mixture of 80mg/kg ketamine and 10 mg/kg xylazine and mounted in a stereotaxic frame. An incision was made to expose and locate bregma. Using stereotaxic coordinates of the hippocampus (Paxinos and Franklin 2001), a 0.6 mm burr hole was made 1.8

mm posterior and 1.6 mm lateral from bregma with a high-speed drill (Drummond Scientific). Mice were injected with either 74 nL of a 20 mM solution of kainic acid or an equal volume of 0.9% saline over a period of 4 minutes using a microinjector (Nanoject, Drummond Scientific) at the dorsoventral coordinate of 1.9 mm. After kainic acid injections, all mice experienced SE, defined by Racine scale stage 3-5 seizures (Table 2.1, Racine 1972) continuously for at least 3 hours until they spontaneously subsided. At each time point n = 5 animals were euthanized with fatal plus (Western Medical Supply), perfused, and processed for each experiment, unless otherwise specified.

5.3.3 Immunohistochemistry

Mice were transcardially perfused with ice-cold PBS, pH 7.4, followed by 4% paraformaldehyde, pH 7.4. Brains were quickly removed, postfixed in 4% paraformaldehyde overnight at 4°C, and then cryoprotected in 30% sucrose in PBS at 4°C for two days. Brains were frozen with ice-cold isopentane and stored at -80°C until they were cut into 50 µm coronal sections using a cryostat (Leica CM 1950, Leica Microsytems, Bannockburn, IL). Slices were stored in PBS at 4°C and all slices were processed simultaneously. Endogenous peroxidase activity was quenched by incubating slices in 3% H_2O_2 for 1 hour at room temperature. This was followed by a 1 hour blocking step with 5% normal goat serum in 0.1 M PBS. Slices were then incubated with primary antibody to GLT1

(1:3,000, AbCam AB41621) and GFAP (1:200, Millipore MAB360) in 0.3% Triton X-100 overnight at 4°C. After washing slices with PBS, sections were incubated with species-specific secondary antibody conjugated with Alexa 488 or Alexa 594 and a tyramide signaling amplification (TSA) kit (Molecular Probes/Invitrogen) for visualization. Slices were mounted in Vectashield with DAPI (Vector Laboratories) and 10x images were taken using a fluorescence microscope (Leica DFC345 FX). Confocal 40x images were taken on the Leica SP5 inverted microscope.

Brains were sliced and processed at 1, 4, 7, and 30 days post kainic acid-induced SE. For controls, I initially determined that GLT1 immunoreactivity 1 day after intrahippocampal saline injections was the same as in naïve mice (n = 3, Figure 5.1). Therefore, only intrahippocampal saline injected mice, and not naïve

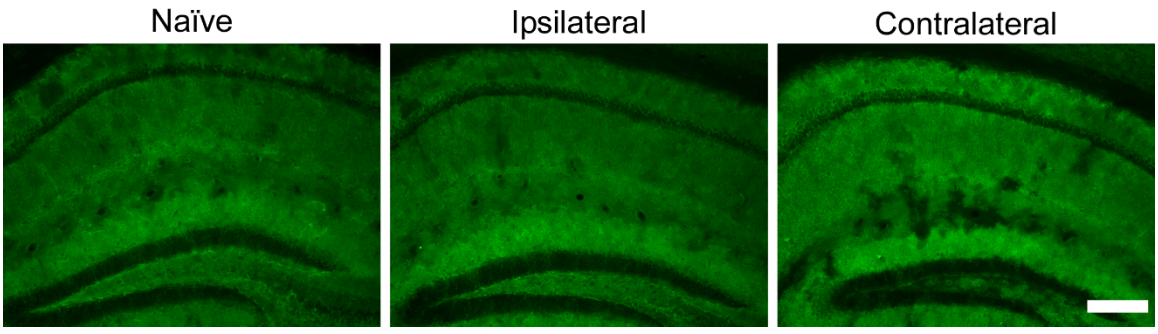


Figure 5.1. Glutamate transporter-1 (GLT1) immunoreactivity in naïve mice and 1 day after intrahippocampal saline injections.
Representative 10x images of GLT1 immunoreactivity in the naïve hippocampus and the ipsilateral and contralateral hippocampi 1 day post intrahippocampal saline injections. For each time point, 3 slices from each animal (n = 3) were used. Scale bar = 200 μm.

mice, were used as controls for the remainder of the study. I next perfused mice at 1, 4, 7, and 30 days post saline injections (n = 3 for each time point). After it was determined that GLT1 levels remained constant at all time points after saline injections (Figure 5.2), I collected brains only at 7 days post saline injections (n = 5) as controls for the remainder of the experiments.

Quantification was performed on 10x fluorescent images of the hippocampus (captured under identical settings) using the Leica Application Suite X Lite software. As described in Chapter 2, a box delineating the region of interest (ROI) was drawn while looking at the DAPI channel either around the whole image of the hippocampus or at the center of each individual layer: stratum (S.) oriens, S. pyramidale, S. radiatum, S. lacunosum moleculare (SLM), molecular layer, granule cell layer (GCL), and hilus (Figure 2.4A). ROIs were drawn around the S. lucidum, S. pyramidale, and S. oriens in the hippocampal CA3 region (Figure 2.4B). The mean pixel (gray) value for each ROI was obtained for analysis. For each time point I used 4 slices from each animal (n = 5).

5.3.4 Western blot analysis

Dorsal hippocampus was microdissected from the mouse brain at 1, 4, 7, and 30 days post IHKA or saline injection (n=7 for 7 days post SE; n = 5 for saline control and all other time points). Harvested tissue was homogenized using the

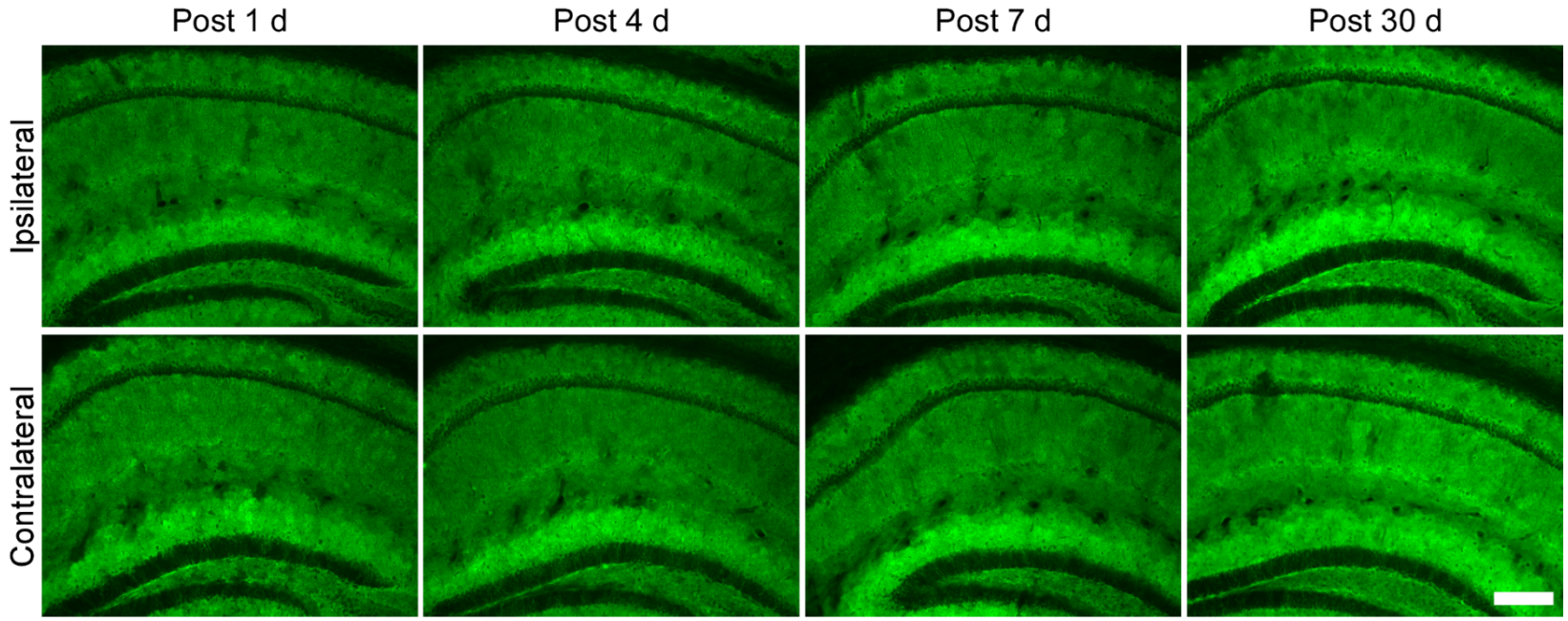


Figure 5.2. Glutamate transporter-1 (GLT1) immunoreactivity after intrahippocampal saline injections.

Representative 10x images of GLT1 immunoreactivity in the ipsilateral (top panel) and contralateral (bottom panel) hippocampi at 1, 4, 7, and 30 days post intrahippocampal saline injections. For each time point, 3-5 slices from each animal (n = 3) were used. Scale bar = 200 µm.

Bullet Blender (Next Advance) in RIPA buffer (Sigma) containing complete protease inhibitors (Roche). Protein concentrations were assayed and protein was resolved by SDS-PAGE, 10% polyacrylamide, and transferred to a nitrocellulose membrane. The membranes were then probed for GLT1 (1:5,000 of a C-terminal polyclonal antibody (Rothstein, Martin et al. 1994)) and β-actin (1:5,000, Sigma A1978) as an internal control. Whole hippocampal tissue was microdissected, processed, and probed for GLT1 (1:10,000, AbCam AB41621; also confirmed with 1:5,000 of the C-terminal polyclonal antibody (Rothstein, Martin et al. 1994)) while again using β-actin (1:5,000, Sigma A1978) as an internal control. Bands were visualized and quantified using the Li-COR Odyssey Fc Western Imaging System and protein levels were normalized to internal β-actin levels. Both the upper and lower bands for GLT1 are shown but only quantification of the lower band was included for simplicity. Similar results, however, were observed when quantifying the upper band.

5.3.5 Real-time polymerase chain reaction (RT-PCR) analysis

Whole or dorsal hippocampus was microdissected from the mouse brain at 1, 4, 7, and 30 days post intrahippocampal kainic acid or saline injections. Harvested tissue was homogenized using the Bullet Blender (Next Advance). RNA was isolated using the Direct-Zol RNA mini prep kit (Zymo Research) and quantified using a nanodrop (Thermo Scientific NanoDrop 2000c Spectrophotometer). Both

cDNA synthesis and RT-PCR were performed using the Bioline SensiFAST SYBR NO-ROX Kit and the CFX-96 detection system (Bio-Rad). Primers for GLT1 and 18s RNA (Table 5.1) were purchased from Integrated DNA Technologies. The reaction conditions were as follows: 1 cycle for 10 min at 45°C, 1 cycle for 2 min at 95°C, 40 cycles for 5s at 95°C, and 1 cycle for 20s at 60°C. Results were quantified using the differential CT method representing the fold change in target gene expression. Both a no template control (NTC) and a no reverse transcriptase (NRT) control were included in each assay to detect any contamination or non-specific replication.

Target Gene	Forward Primer Sequence	Reverse Primer Sequence
GLT1	CTGGTGCAAGCCTGTTTCC	GCCTGTTCACCCATCTTCC
18s RNA	CTCAACACGGGAAACCTCAC	CGCTCCACCAACTAAGAACG

Table 5.1. Primers used for RT-PCR experiments.
All primers are listed in the 5' → 3' direction.

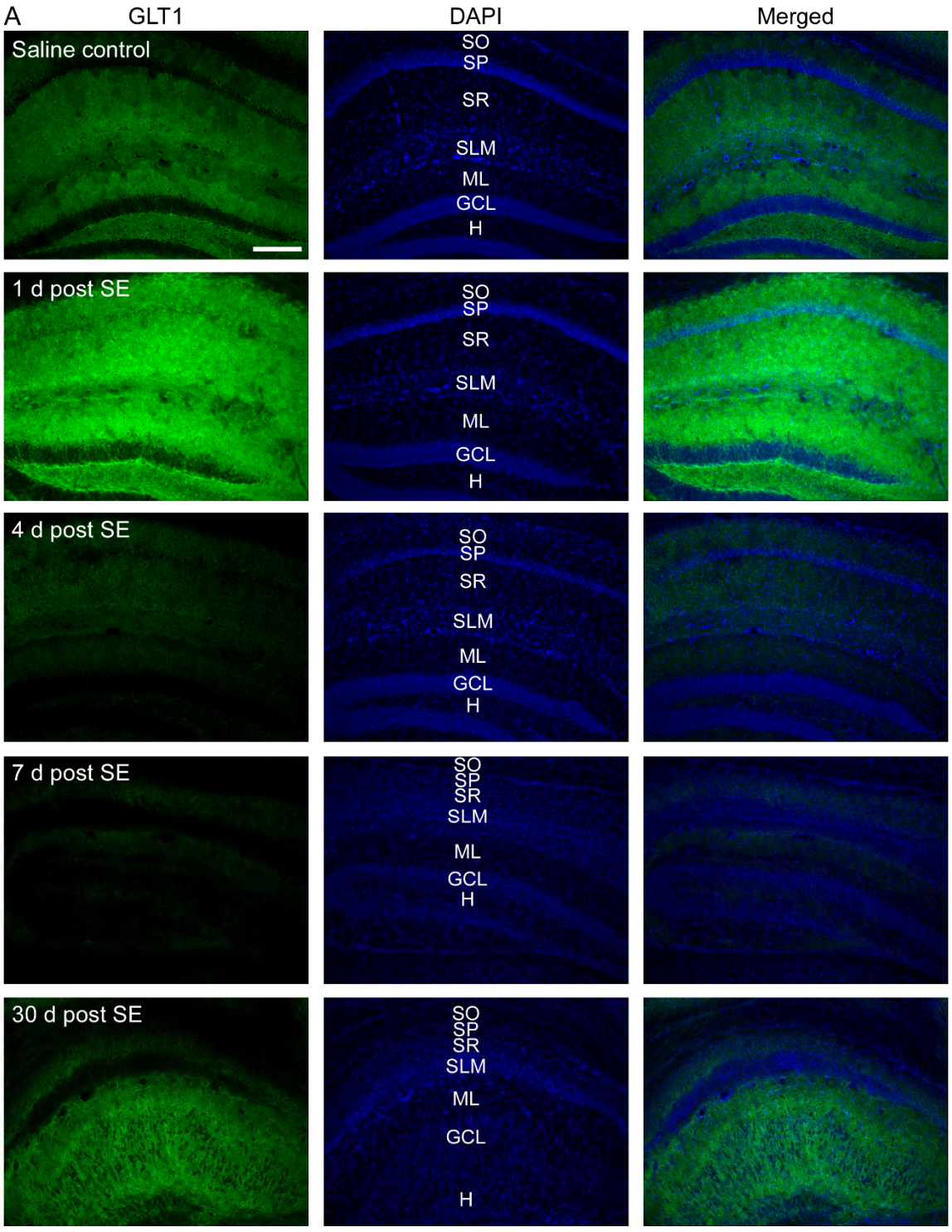
5.3.6 Statistical analysis

Statistical analysis was performed using a one-way ANOVA with *post-hoc* Bonferroni multiple comparisons test. All error bars are presented as the mean ± standard error of the mean (SEM). A comparison to saline control was denoted statistically significance by a p-value < 0.05, < 0.01 or < 0.001 and denoted with *, **, or ***, respectively. Any statistically significant differences between other time points were not indicated for the purpose of clarity.

5.4 Results

5.4.1 Alterations in glutamate transporter-1 (GLT1) immunoreactivity

GLT1 and DAPI immunoreactivity in the hippocampus were imaged after saline injections (control) and at 1, 4, 7, and 30 days post kainic acid-induced SE (Figures 5.3-5.8). Marked changes in GLT1 immunoreactivity were observed in the ipsilateral hippocampus after IHKA injections (Figure 5.3). An initial increase in GLT1 immunoreactivity was observed at 1 day post SE, which subsided by 4 days post SE, was followed by a significant downregulation at 7 days post SE, and returned to near baseline levels by 30 days post SE. More specifically, a significant increase in GLT1 immunoreactivity was observed in all layers of the hippocampus at 1 day post SE (Figure 5.3B). By 4 days post SE, GLT1 immunoreactivity was persistently decreased in the primarily astrocytic layers (S. radiatum, SLM, molecular layer) for the remainder of the time course study. In the hilus, however, GLT1 immunoreactivity was downregulated at 4 and 7 days post SE, but returned to baseline levels by 30 days post SE. The neuronal layers, S. pyramidale and GCL, did not show any downregulation of GLT1 immunoreactivity. In fact, GLT1 levels were elevated at 4 days post SE in the S. pyramidale layer and returned to saline control levels by 7 days post SE. Although GLT1 immunoreactivity was no different from the saline control at 4 and 7 days post SE in the GCL, immunoreactivity was elevated at 30 days post SE.


A
GLT1
DAPI
Merged
Saline control
1 d post SE
4 d post SE
7 d post SE
30 d post SE
SO
SP
SR
SLM
ML
GCL
H

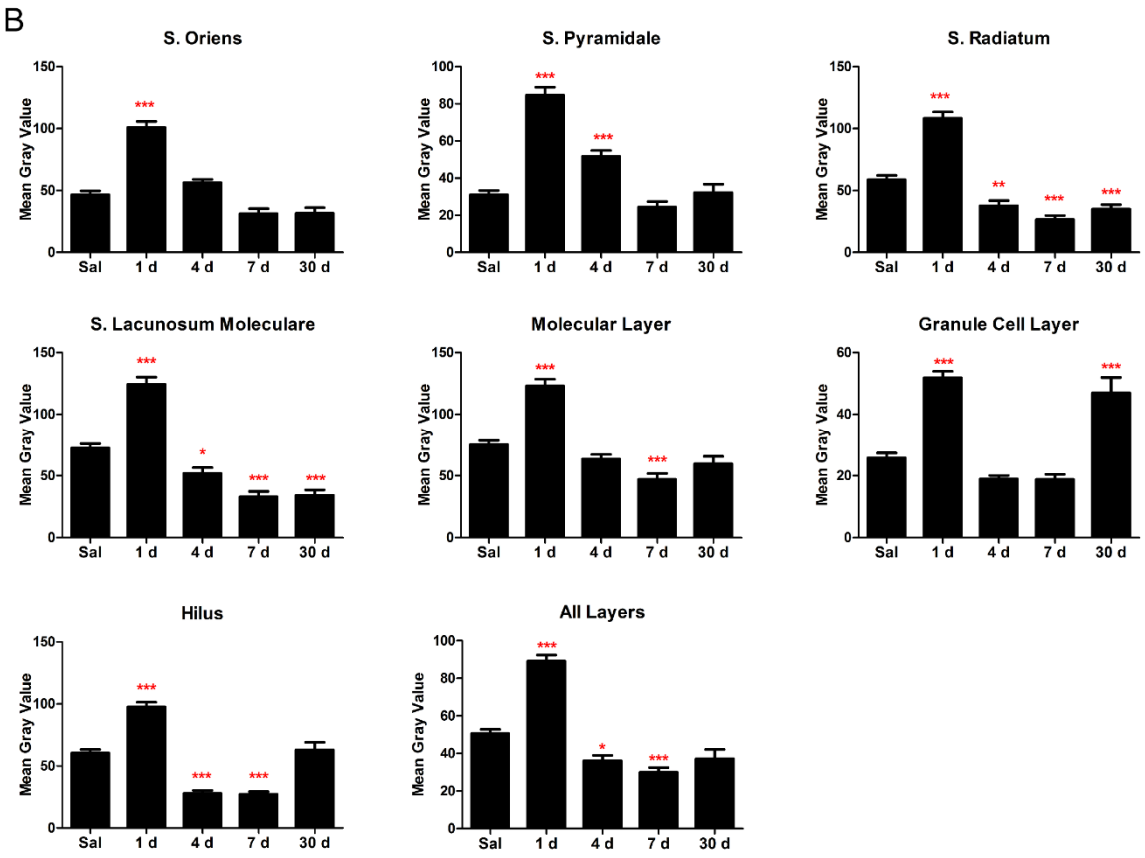


Figure 5.3. Glutamate transporter-1 (GLT1) immunoreactivity in the ipsilateral hippocampus after kainic acid-induced status epilepticus (SE). **A.** 10x images of GLT1 (green), DAPI (blue), and merged immunoreactivity of the ipsilateral hippocampus after saline injections (Saline control) and 1, 4, 7, and 30 days (d) post SE. **B.** Quantification of GLT1 immunoreactivity in the various layers of the hippocampus ipsilateral to kainic acid injections. * indicates $p < 0.05$, ** indicates $p < 0.01$, and *** indicates $p < 0.001$ when compared to saline control. Scale bar = 200 μm. SO = stratum oriens; SP = stratum pyramidale; SR = stratum radiatum; SLM = stratum lacunosum moleculare; ML = molecular layer; GCL = granule cell layer; H = hilus.

This is likely due to reactive astrocytic processes protruding into the dispersed GCL in the sclerotic hippocampus at this time point. Higher magnification (40x) images of GLT1 and GFAP immunoreactivity in the ipsilateral hippocampus can be seen in Figure 5.4. At 1 and 30 days post SE, GLT1 and GFAP are highly colocalized. Notably, at 4 and 7 days post SE, many GLT1-negative/GFAP-positive astrocytes are seen.

Downregulation of GLT1 immunoreactivity was observed at 7 days post SE and returned to control levels by 30 days post SE in all layers analyzed in the CA3 region of the hippocampus ipsilateral to kainic acid injections (Figure 5.5). GLT1 immunoreactivity was upregulated in the S. pyramidale layer 1 day post SE. At 4 and 7 days post SE, GLT1 immunoreactivity was downregulated in the S. lucidum in the ipsilateral hippocampus.

Similar changes in GLT1 immunoreactivity were observed in the contralateral hippocampus (Figure 5.6). Throughout the hippocampal layers, GLT1 was downregulated at 4 and 7 days post SE with the exception of the S. oriens at 4 days post SE (Figure 5.6B). A significant increase in GLT1 immunoreactivity 1 day post SE was only observed in the SLM and hilus of the contralateral hippocampus. A persistent downregulation of GLT1 immunoreactivity out to 30 days post SE was only detected in the SLM. In the CA3 region of the hippocampus, GLT1 immunoreactivity was downregulated at 4 and 7 days post

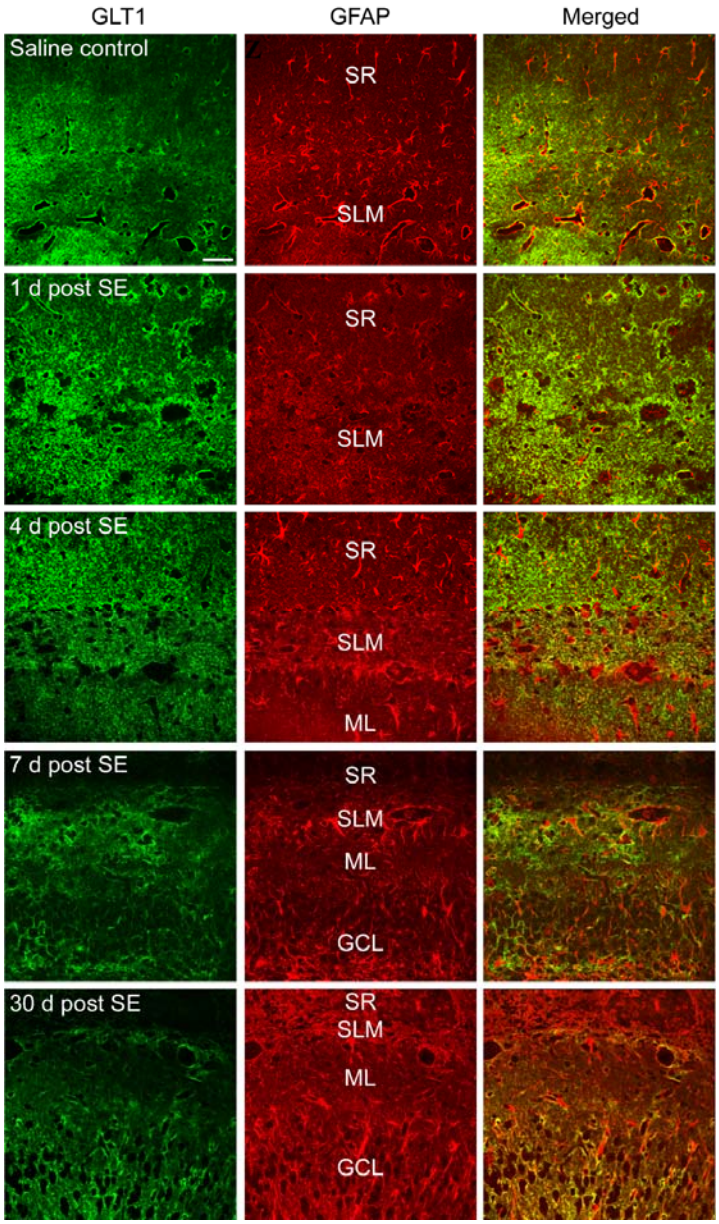
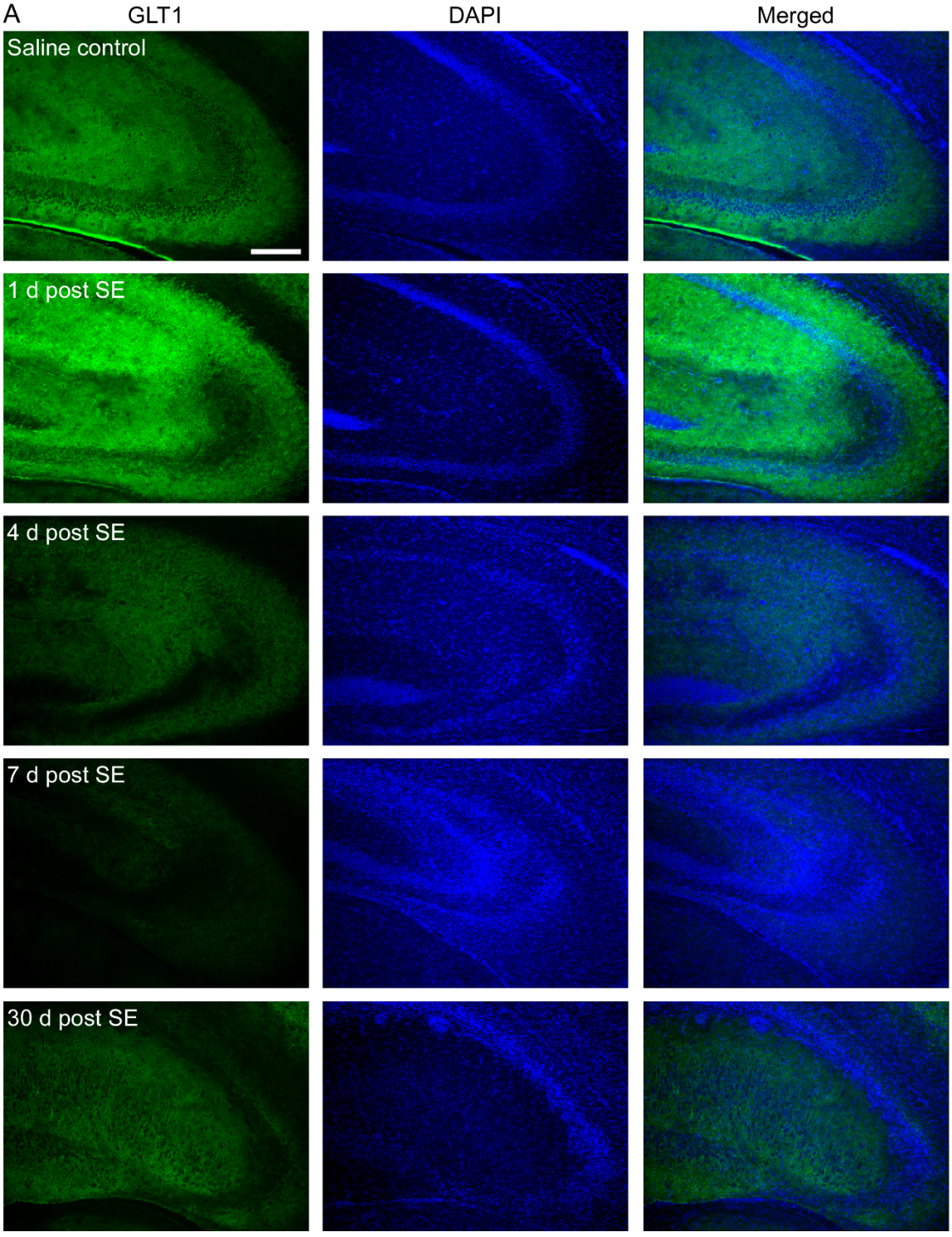


Figure 5.4. Confocal images of glutamate transporter-1 (GLT1) and glial fibrillary acidic protein (GFAP) in the ipsilateral hippocampus after kainic acid-induced status epilepticus (SE).
40x images of GLT1 (green), GFAP (red), and merged immunoreactivity of the stratum radiatum (SR) and surrounding layers of the ipsilateral hippocampus after saline injections (Saline control) and 1, 4, 7, and 30 days (d) post SE. Scale bar = 50 μm. Images were taken under different exposure time settings to maximize structural detail (see Figure 5.3 for quantitation by layer). SR = stratum radiatum; SLM = stratum lacunosum moleculare; ML = molecular layer; GCL = granule cell layer.


A
GLT1
DAPI
Merged
Saline control
1 d post SE
4 d post SE
7 d post SE
30 d post SE

B

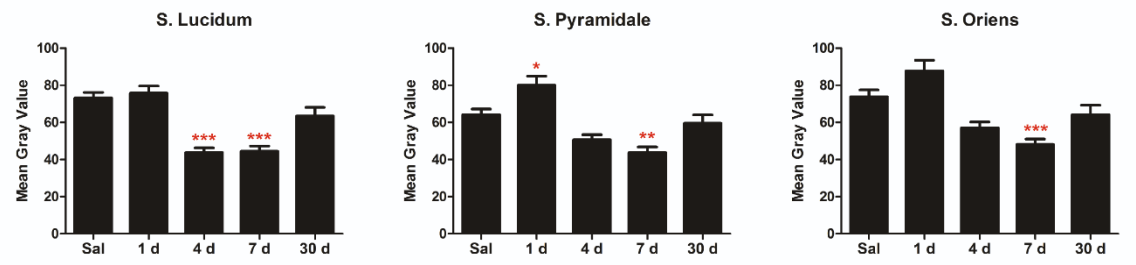
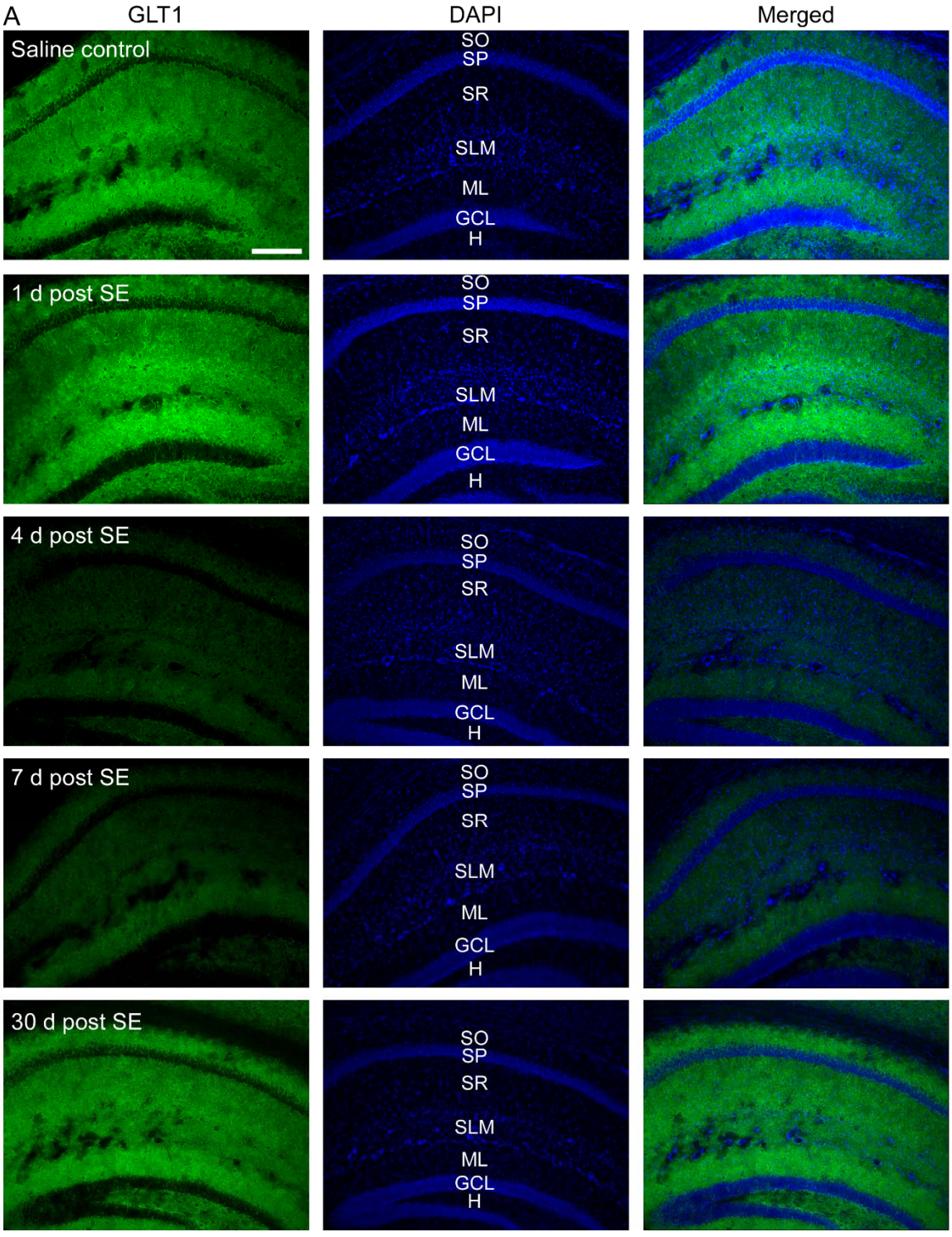


Figure 5.5. Glutamate transporter-1 (GLT1) immunoreactivity in the ipsilateral CA3 region of the hippocampus after kainic acid-induced status epilepticus (SE).
A. 10x images of GLT1 (green), DAPI (blue), and merged immunoreactivity of the ipsilateral CA3 region of the hippocampus after saline injections (Saline control) and 1, 4, 7, and 30 days (d) post SE. **B.** Quantification of GLT1 immunoreactivity in the various layers of CA3. * indicates $p < 0.05$, ** indicates $p < 0.01$, and *** indicates $p < 0.001$ when compared to saline control. Scale bar = 200 μm.

SE in all layers quantified (Figure 5.7). Thus, downregulation of GLT1immunoreactivity was observed in *both* ipsilateral and contralateral hippocampi at 4 and 7 days. Higher magnification images of GLT1 immunoreactivity in the contralateral hippocampus can be seen in Figure 5.8. GLT1 and GFAP were highly colocalized in the saline control and 1 day post SE. At 4 and 7 days post SE, many GLT-negative/GFAP-positive astrocytes are seen.


A
GLT1
DAPI
Merged
Saline control
1 d post SE
4 d post SE
7 d post SE
30 d post SE
SO
SP
SR
SLM
ML
GCL
H

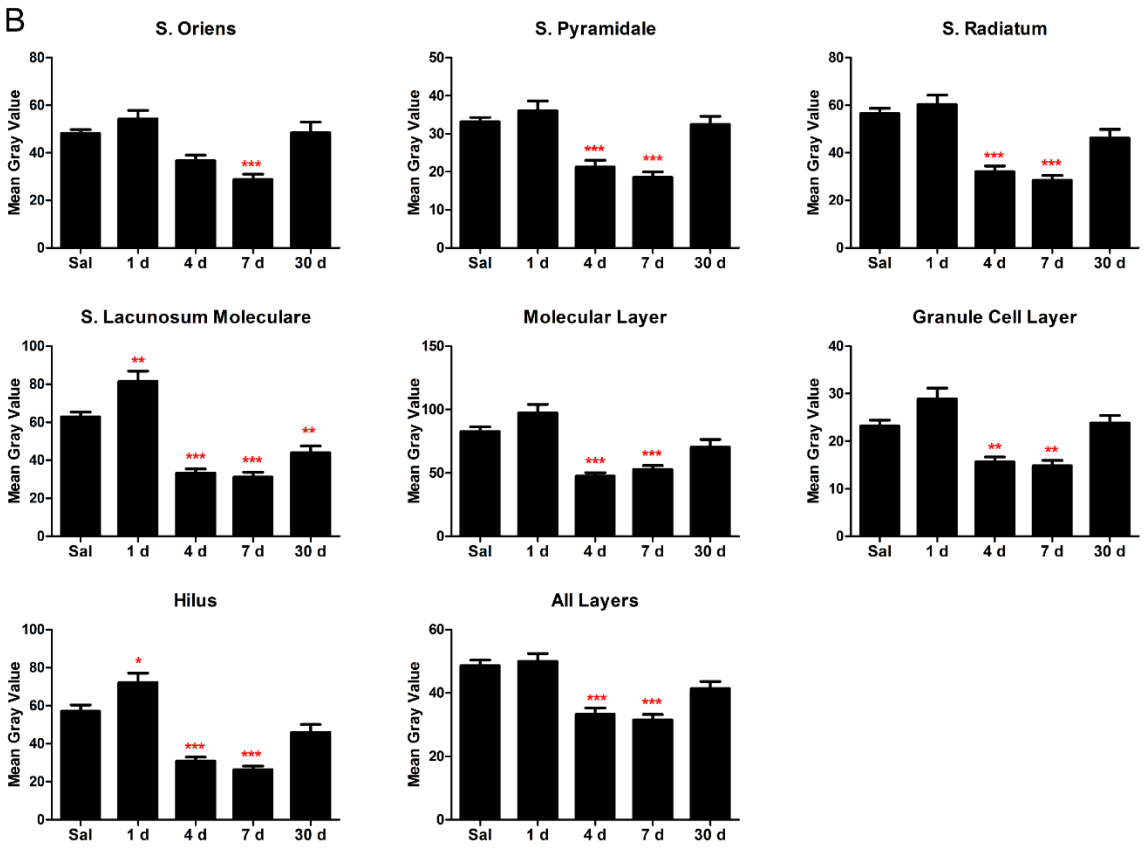
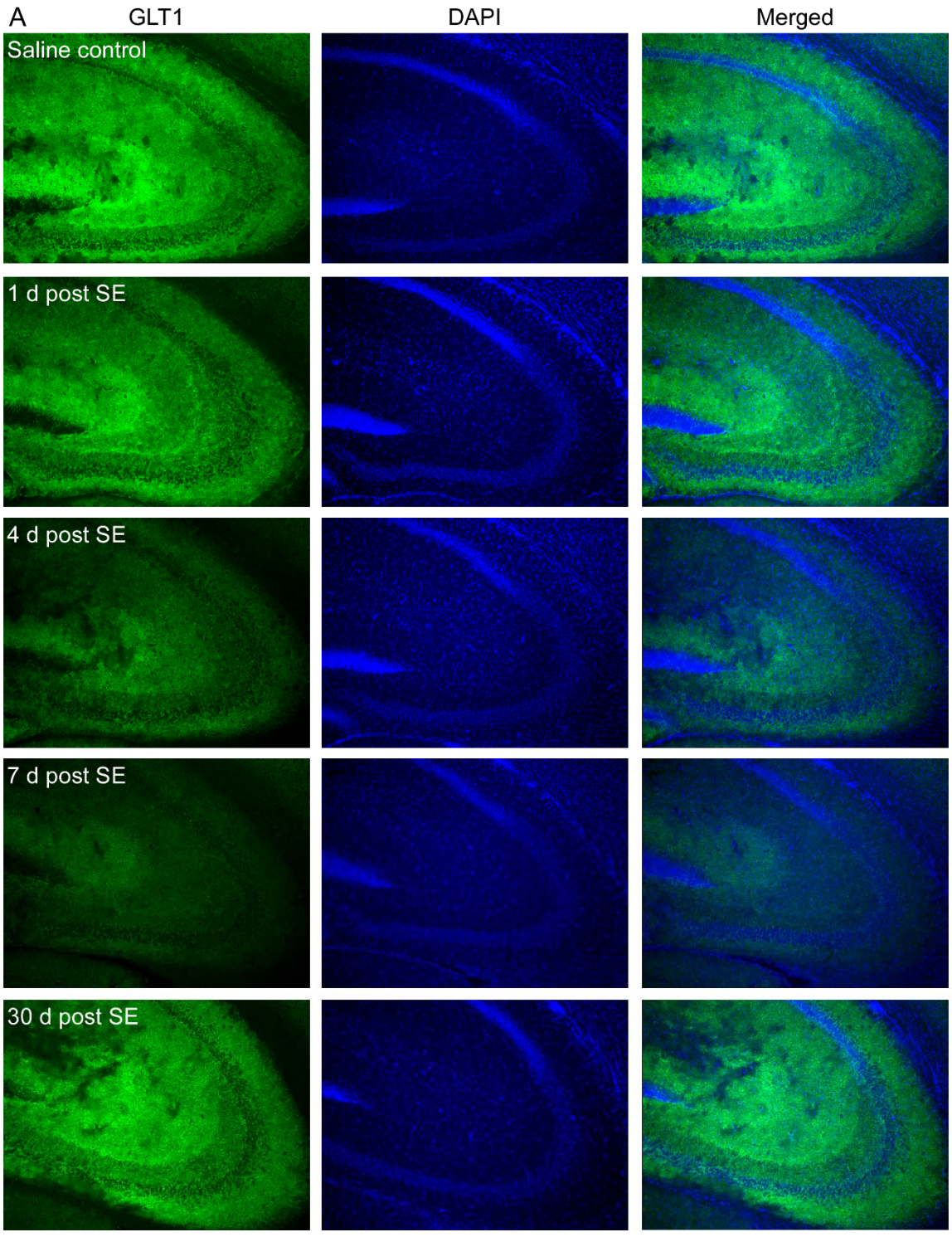


Figure 5.6. Glutamate transporter-1 (GLT1) immunoreactivity in the contralateral hippocampus after kainic acid-induced status epilepticus (SE).

A. 10x images of GLT1 (green), DAPI (blue), and merged immunoreactivity of the contralateral hippocampus after saline injections (Saline control) and 1, 4, 7, and 30 days (d) post SE. **B.** Quantification of GLT1 immunoreactivity in the various layers of the hippocampus contralateral to kainic acid injections. * indicates $p < 0.05$, ** indicates $p < 0.01$, and *** indicates $p < 0.001$ when compared to saline control. Scale bar = 200 µm. SO = stratum oriens; SP = stratum pyramidale; SR = stratum radiatum; SLM = stratum lacunosum moleculare; ML = molecular layer; GCL = granule cell layer; H = hilus.


A
GLT1
DAPI
Merged
Saline control
1 d post SE
4 d post SE
7 d post SE
30 d post SE

B

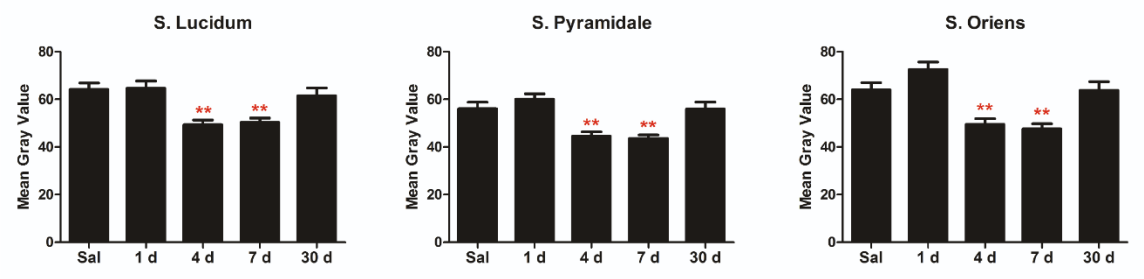


Figure 5.7. Glutamate transporter-1 (GLT1) immunoreactivity in the contralateral CA3 region of the hippocampus after kainic acid-induced status epilepticus (SE).
A. 10x images of GLT1 (green), DAPI (blue), and merged immunoreactivity of the contralateral CA3 region of the hippocampus after saline injections (Saline control) and 1, 4, 7, and 30 days (d) post SE. **B.** Quantification of GLT1 immunoreactivity in the various layers of CA3. ** indicates $p < 0.01$ when compared to saline control. Scale bar = 200 μm.

5.4.2 Alterations in GLT1 protein expression

Western blot analysis revealed a significant increase in dorsal hippocampal GLT1 protein levels at 1 day post SE followed by a significant downregulation of GLT1 protein levels by 7 days post SE in the ipsilateral hippocampus compared to the saline control (Figure 5.9A-B). In the contralateral dorsal hippocampus, a significant downregulation of GLT1 protein was found at 4 and 7 days post SE (Figures 5.9D-E). These results were consistent with the immunohistochemical findings both in direction and time course. Quantitative RT-PCR analysis of GLT1 mRNA revealed no changes in GLT1 mRNA levels in either the ipsilateral (Figure 5.9C) or contralateral (Figure 5.9F) dorsal hippocampus with the exception of an increase in GLT1 mRNA in the ipsilateral hippocampus 7 days

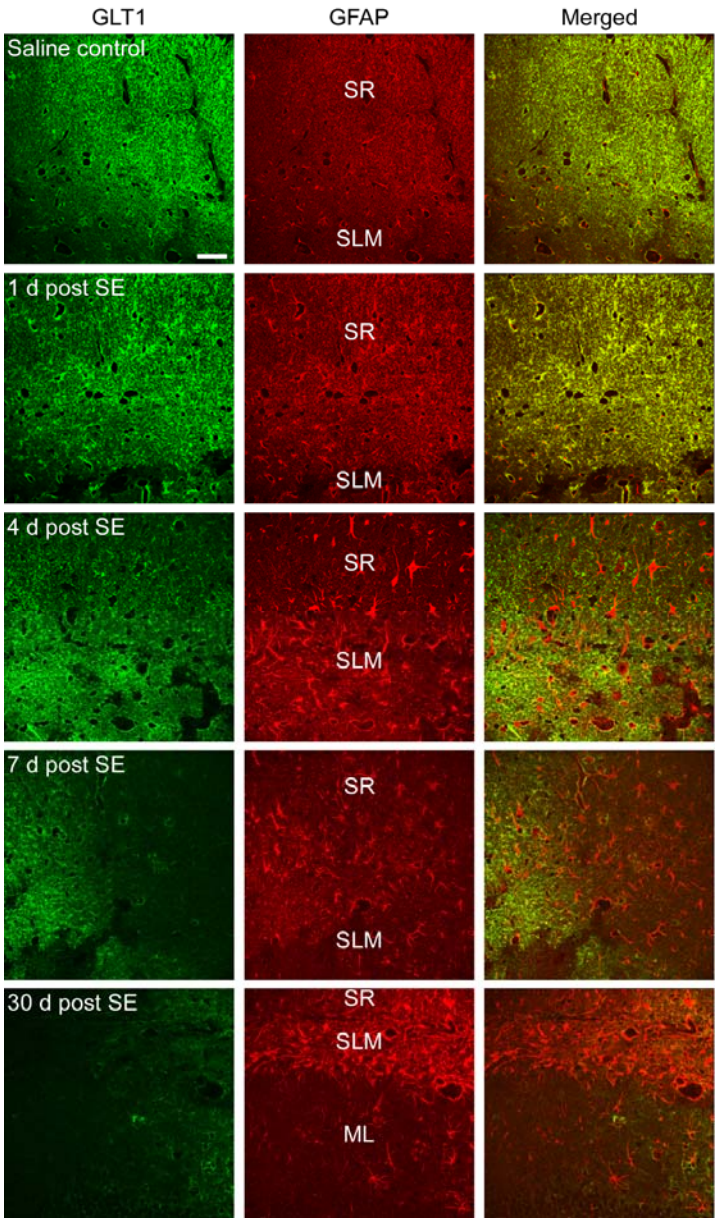


Figure 5.8: Confocal images of glutamate transporter-1 (GLT1) and glial fibrillary acidic protein (GFAP) in the contralateral hippocampus after kainic acid-induced status epilepticus (SE).
40x images of GLT1 (green), GFAP (red), and merged immunoreactivity of the stratum radiatum (SR) and surrounding layers of the contralateral hippocampus after saline injections (Saline control) and 1, 4, 7, and 30 days (d) post SE. Scale bar = 50 μm. Images were taken under different exposure time settings to maximize structural detail (see Figure 5.6 for quantitation by layer). SR = stratum radiatum; SLM = stratum lacunosum moleculare; ML = molecular layer; GCL = granule cell layer.

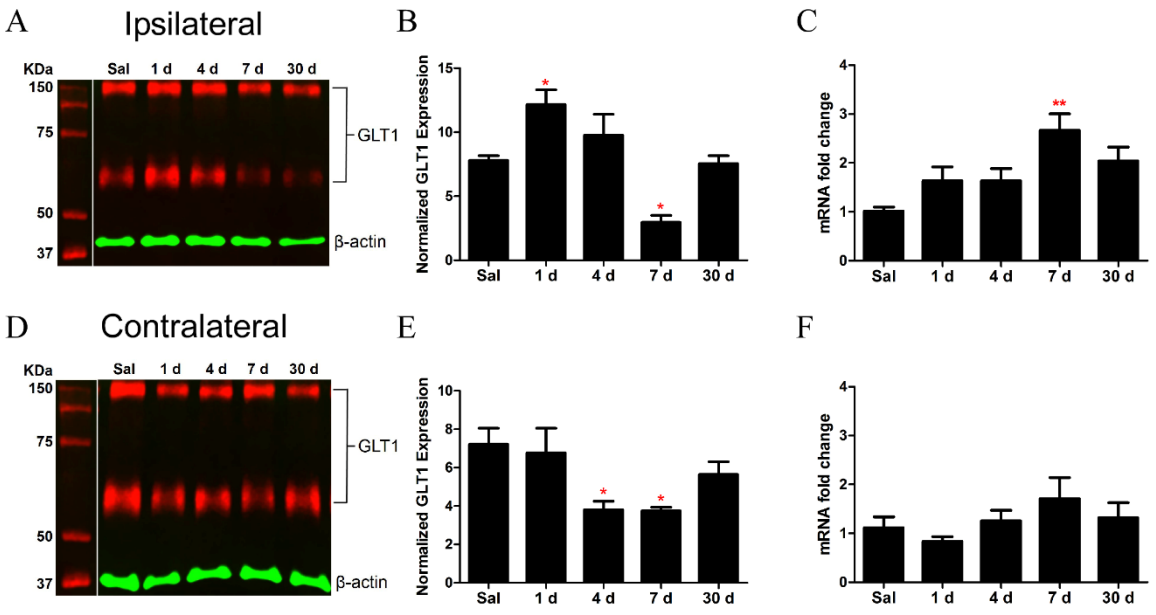


Figure 5.9. Dorsal hippocampal glutamate transporter-1 (GLT1) protein and mRNA levels after kainic acid-induced status epilepticus (SE).
A. Representative Western blot of GLT1 (red) and β-actin (green) protein from the ipsilateral hippocampus of a saline control (Sal) and 1, 4, 7, and 30 days (d) post kainic acid-induced SE. **B.** Quantification of GLT1 lower band intensity normalized to β-actin at each time point in the ipsilateral hippocampus. **C.** Fold change in GLT1 mRNA in the ipsilateral hippocampus from tissue collected from saline controls (Sal) and at 1, 4, 7, and 30 days (d) post kainic acid-induced SE. **D.** Representative Western blot of GLT1 (red) and β-actin (green) protein from the contralateral hippocampus of a saline control (Sal) and 1, 4, 7, and 30 days post SE. **E.** Quantification of contralateral hippocampal GLT1 lower protein band normalized to β-actin in each group. **F.** Quantification of GLT1 mRNA levels in the contralateral hippocampus from tissue collected from saline controls (Sal) and at various time points post kainic acid-induced SE. * indicates $p < 0.05$ and ** indicates $p < 0.01$ when compared to saline control. For each time point, n = 5 except protein for 7 days post SE (n=7).

post SE. Overall, these results indicate a strong regulation of GLT1 dorsal hippocampal protein levels with an increase at 1 day and significant decreases at 4 and 7 days post SE in this model, with little accompanying change in GLT1 mRNA levels. Separate analysis of whole hippocampal GLT1 protein and mRNA

levels revealed no change in protein levels but small decrease in GLT1 mRNA in the ipsilateral hippocampus 1 day post SE and an increase in GLT1 mRNA in the contralateral hippocampus 7 days post SE (Figure 5.10).

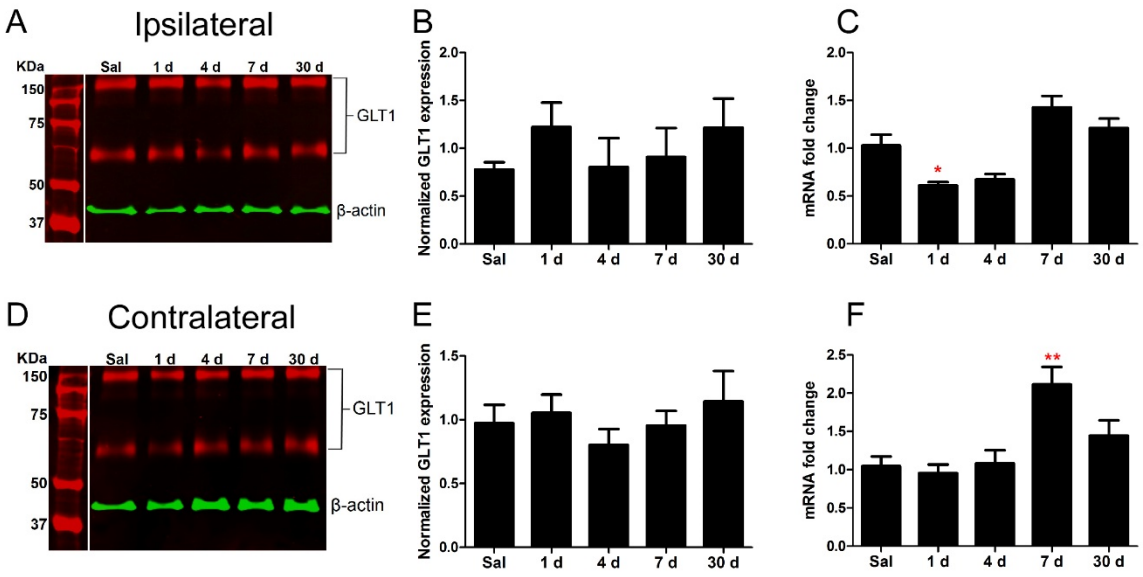


Figure 5.10. Glutamate transporter-1 (GLT1) protein and mRNA whole hippocampal levels after kainic acid-induced status epilepticus (SE). **A.** Representative Western blot of GLT1 (red) and β-actin (green) protein from the ipsilateral hippocampus of a saline control (Sal) and 1, 4, 7, and 30 days (d) post kainic acid-induced SE. **B.** Quantification of GLT1 lower band intensity normalized to β-actin at each time point in the ipsilateral hippocampus. **C.** Fold change in GLT1 mRNA levels in the ipsilateral hippocampus of saline controls (Sal) and in tissue collected 1, 4, 7, and 30 days (d) post kainic acid-induced SE. **D.** Representative Western blot of GLT1 (red) and β-actin (green) protein from the contralateral hippocampus in a saline control (Sal) and 1, 4, 7, and 30 days post kainic acid-induced SE. **E.** Quantification of contralateral GLT1 lower band intensity normalized to β-actin at each time point. **F.** Quantification of GLT1 mRNA levels in the contralateral hippocampus in saline controls (Sal) and various time points after kainic acid-induced SE. * indicates $p < 0.05$ and ** indicates $p < 0.01$ when compared to saline control and $n = 5$ for each time point.

5.5 Discussion

In this study, I used RT-PCR, Western blot, and immunohistochemistry to examine changes in GLT1 expression at various time points post SE in the IHKA model of epilepsy. I observed an upregulation of dorsal hippocampal GLT1 immunoreactivity and protein at 1 day post SE. This was followed by a significant reduction in dorsal hippocampal GLT1 immunoreactivity and protein expression at 4 and 7 days post SE, which returned to near control levels by 30 days post SE. GLT1 hippocampal mRNA levels, however, were rarely altered during the time course of this study. Interestingly, I observed significant regulation of GLT1 in both the contralateral and ipsilateral hippocampi to IHKA injections, suggesting that only seizure spread, and not sclerosis, was sufficient for GLT1 regulation. These results support the hypothesis that intense seizures regulate GLT1 expression and may lead to a functionally relevant astrocytic dysregulation of glutamate uptake during epileptogenesis.

It is well known that extracellular levels of glutamate are elevated during seizures (During and Spencer 1993; Glass and Dragunow 1995; Tanaka, Watase et al. 1997; Campbell and Hablitz 2004; Hubbard, Hsu et al. 2013). Increased levels of glutamate in the ECS are likely due either to increased glutamate release and/or impaired reuptake. GLT1 is responsible for the majority of glutamate uptake from

the ECS (Danbolt 2001) and therefore reduced levels of glutamate uptake by GLT1 could powerfully contribute to hyperexcitability and seizure generation.

Human tissue data have revealed reduced GLT1 (human analog is called excitatory amino acid transporter 2, EAAT2) immunoreactivity in the sclerotic hippocampus (Mathern, Mendoza et al. 1999; Proper, Hoogland et al. 2002; van der Hel, Notenboom et al. 2005) and either no change (Mathern, Mendoza et al. 1999) or increased GLT1/EAAT2 expression in the non-sclerotic hippocampus (Tessler, Danbolt et al. 1999; Eid, Thomas et al. 2004; Bjørnsen, Eid et al. 2007). The use of animal models, on the other hand, have demonstrated equivocal results on the regulation of GLT1 expression in epilepsy. Downregulation (Samuelsson, Kumlien et al. 2000; Ueda, Doi et al. 2001; Lopes, Soares et al. 2013; Sakurai, Kurokawa et al. 2015), upregulation (Simantov, Crispino et al. 1999), or no change (Miller, Levey et al. 1997) in GLT1 have all been reported in a variety of epilepsy models. These differences, however, can be accounted for by several factors, including mRNA *vs.* protein evaluation, distinct models used, brain region examined, and time point(s) used in the study (*e.g.*, latent or chronic phase). For example, I demonstrated an initial increase in GLT1 expression that subsided and subsequently became downregulated in the dorsal hippocampus. This study is the first to examine both early and chronic time points, regional specificity (dorsal *vs.* whole hippocampus and laminar analysis), and combine immunoreactivity with Western blot and RT-PCR analysis.

Recent studies have shown dynamic regulation of astrocyte GLT1. Sakurai *et al.* (2015) demonstrated neuronal cell death was associated with a focal loss of GLT1 immunoreactivity and stronger immunoreactivity for glutamate (Sakurai, Kurokawa et al. 2015). In addition, GLT1 can be untethered from the membrane at synapses after glutamate release and can undergo rapid, activity-regulated surface diffusion between synaptic and non-synaptic sites to ensure effective glutamate clearance (Murphy-Royal, Dupuis et al. 2015; Al Awabdh, Gupta-Agarwal et al. 2016). Since GLT1 may be regulated by the intensity of neuronal activity, its expression may vary during the course of epileptogenesis, as I have shown here. Increased levels were found at 1 day post SE (after a long duration of high intensity seizures) with decreased levels becoming apparent as early as 4 days post SE. The early reduction of GLT1 expression may lead to increased extracellular glutamate levels that consequently contribute to hyperexcitability and neuronal cell death. The loss of GLT1, therefore, could contribute to the transition from a healthy brain to an epileptic one. Further studies will need to characterize (i) mechanisms of regulation of GLT1 by seizures; (ii) subcellular trafficking of GLT1; and (iii) posttranslational modification(s) of GLT1 in epilepsy. Posttranslational modifications such as sumoylation (Foran, Rosenblum et al. 2014) and S-nitrosylation (Raju, Doulias et al. 2015) have been described that may contribute to alterations in plasma membrane *vs.* cytosolic localization of

GLT1. Subcellular trafficking of GLT1 would carry significant implications for the efficacy of glutamate clearance and thus network hyperexcitability.

In conclusion, I demonstrated alterations in GLT1 during the early epileptogenic period. Early disruption of glutamate homeostasis could have powerful epileptogenic and cognitive effects. While there is some apparent partial recovery of overall GLT1 expression at the longest time point studied (30 days), the pattern of expression remains quite distinct. Future studies could examine mechanisms of activity-regulated GLT1 *in vitro* and *in vivo*. In addition, if normalization of GLT1 expression and function ameliorates hyperexcitability, this could provide a new astrocyte-based antiepileptogenic strategy.

5.6 References

Al Awabdh, S., S. Gupta-Agarwal, D. F. Sheehan, J. Muir, R. Norkett, A. E. Twelvetrees, L. D. Griffin and J. T. Kittler (2016). "Neuronal activity mediated regulation of glutamate transporter GLT-1 surface diffusion in rat astrocytes in dissociated and slice cultures." Glia **64**(7): 1252-1264.

Arabadzisz, D., K. Antal, F. Parpan, Z. Emri and J. M. Fritschy (2005). "Epileptogenesis and chronic seizures in a mouse model of temporal lobe epilepsy are associated with distinct EEG patterns and selective neurochemical alterations in the contralateral hippocampus." Exp Neurol **194**(1): 76-90.

Binder, D. K. and C. Steinhäuser (2006). "Functional changes in astroglial cells in epilepsy." Glia **54**(5): 358-368.

Bjørnsen, L. P., T. Eid, S. Holmseth, N. C. Danbolt, D. D. Spencer and N. C. de Lanerolle (2007). "Changes in glial glutamate transporters in human epileptogenic hippocampus: inadequate explanation for high extracellular glutamate during seizures." Neurobiol Dis **25**(2): 319-330.

Bouilleret, V., V. Ridoux, A. Depaulis, C. Marescaux, A. Nehlig and G. Le Gal La Salle (1999). "Recurrent seizures and hippocampal sclerosis following intrahippocampal kainate injection in adult mice: electroencephalography, histopathology and synaptic reorganization similar to mesial temporal lobe epilepsy." Neuroscience **89**(3): 717-729.

Campbell, S. L. and J. J. Hablitz (2004). "Glutamate transporters regulate excitability in local networks in rat neocortex." Neuroscience **127**(3): 625-635.

Chen, W., V. Mahadomrongkul, U. V. Berger, M. Bassan, T. DeSilva, K. Tanaka, N. Irwin, C. Aoki and P. A. Rosenberg (2004). "The glutamate transporter GLT1a is expressed in excitatory axon terminals of mature hippocampal neurons." J Neurosci 24(5): 1136-1148.

Danbolt, N. C. (2001). "Glutamate uptake." Prog Neurobiol **65**(1): 1-105.

de Lanerolle, N. C., T. S. Lee and D. D. Spencer (2012). Histopathology of Human Epilepsy. Jasper's Basic Mechanisms of the Epilepsies. J. L. Noebels, M. Avoli, M. A. Rogawski, R. W. Olsen and A. V. Delgado-Escueta. Bethesda (MD).

During, M. J. and D. D. Spencer (1993). "Extracellular hippocampal glutamate and spontaneous seizure in the conscious human brain." Lancet **341**(8861): 1607-1610.

Eid, T., M. J. Thomas, D. D. Spencer, E. Runden-Pran, J. C. Lai, G. V. Malthankar, J. H. Kim, N. C. Danbolt, O. P. Ottersen and N. C. de Lanerolle (2004). "Loss of glutamine synthetase in the human epileptogenic hippocampus: possible mechanism for raised extracellular glutamate in mesial temporal lobe epilepsy." Lancet **363**(9402): 28-37.

Foran, E., L. Rosenblum, A. Bogush, P. Pasinelli and D. Trotti (2014). "Sumoylation of the astroglial glutamate transporter EAAT2 governs its intracellular compartmentalization." Glia **62**(8): 1241-1253.

Furness, D. N., Y. Dehnes, A. Q. Akhtar, D. J. Rossi, M. Hamann, N. J. Grutle, V. Gundersen, S. Holmseth, K. P. Lehre, K. Ullensvang, M. Wojewodzic, Y. Zhou, D. Attwell and N. C. Danbolt (2008). "A quantitative assessment of glutamate uptake into hippocampal synaptic terminals and astrocytes: new insights into a neuronal role for excitatory amino acid transporter 2 (EAAT2)." Neuroscience 157(1): 80-94.

Glass, M. and M. Dragunow (1995). "Neurochemical and morphological changes associated with human epilepsy." Brain Res Brain Res Rev **21**(1): 29-41.

Halassa, M. M. and P. G. Haydon (2010). "Integrated brain circuits: astrocytic networks modulate neuronal activity and behavior." Annu Rev Physiol **72**: 335-355.

Hesdorffer, D. C., G. Logroscino, E. K. Benn, N. Katri, G. Cascino and W. A. Hauser (2011). "Estimating risk for developing epilepsy: a population-based study in Rochester, Minnesota." Neurology **76**(1): 23-27.

Hubbard, J. A. and D. K. Binder (2016). Astrocytes and Epilepsy. Amsterdam, Netherlands, Elsevier, in press.

Hubbard, J. A., M. S. Hsu, T. A. Fiacco and D. K. Binder (2013). "Glial cell changes in epilepsy: overview of the clinical problem and therapeutic opportunities." Neurochem Int **63**(7): 638-651.

Kong, Q., K. Takahashi, D. Schulte, N. Stouffer, Y. Lin and C. L. Lin (2012). "Increased glial glutamate transporter EAAT2 expression reduces epileptogenic processes following pilocarpine-induced status epilepticus." Neurobiol Dis **47**(2): 145-154.

Mathern, G. W., D. Mendoza, A. Lozada, J. K. Pretorius, Y. Dehnes, N. C. Danbolt, N. Nelson, J. P. Leite, L. Chimelli, D. E. Born, A. C. Sakamoto, J. A. Assirati, I. Fried, W. J. Peacock, G. A. Ojemann and P. D. Adelson (1999). "Hippocampal GABA and glutamate transporter immunoreactivity in patients with temporal lobe epilepsy." Neurology **52**(3): 453-472.

Murphy-Royal, C., J. P. Dupuis, J. A. Varela, A. Panatier, B. Pinson, J. Baufreton, L. Groc and S. H. Oliet (2015). "Surface diffusion of astrocytic glutamate transporters shapes synaptic transmission." Nat Neurosci **18**(2): 219-226.

Paxinos, G. and K. B. J. Franklin (2001). The mouse brain in stereotaxic coordinates. San Diego, CA, Academic Press.

Petr, G. T., Y. Sun, N. M. Frederick, Y. Zhou, S. C. Dhamne, M. Q. Hameed, C. Miranda, E. A. Bedoya, K. D. Fischer, W. Armsen, J. Wang, N. C. Danbolt, A. Rotenberg, C. J. Aoki and P. A. Rosenberg (2015). "Conditional deletion of the glutamate transporter GLT-1 reveals that astrocytic GLT-1 protects against fatal epilepsy while neuronal GLT-1 contributes significantly to glutamate uptake into synaptosomes." J Neurosci **35**(13): 5187-5201.

Proper, E. A., G. Hoogland, S. M. Kappen, G. H. Jansen, M. G. Rensen, L. H. Schrama, C. W. van Veelen, P. C. van Rijen, O. van Nieuwenhuizen, W. H. Gispen and P. N. de Graan (2002). "Distribution of glutamate transporters in the hippocampus of patients with pharmaco-resistant temporal lobe epilepsy." Brain **125**(Pt 1): 32-43.

Racine, R. J. (1972). "Modification of seizure activity by electrical stimulation. II. Motor seizure." Electroencephalogr Clin Neurophysiol **32**(3): 281-294.

Raju, K., P. T. Doulias, P. Evans, E. N. Krizman, J. G. Jackson, O. Horyn, Y. Daikhin, I. Nissim, M. Yudkoff, K. A. Sharp, M. B. Robinson and H. Ischiropoulos (2015). "Regulation of brain glutamate metabolism by nitric oxide and S-nitrosylation." Sci Signal **8**(384): ra68.

Ransom, B., T. Behar and M. Nedergaard (2003). "New roles for astrocytes (stars at last)." Trends Neurosci **26**(10): 520-522.

Ransom, B. R. and C. B. Ransom (2012). "Astrocytes: multitalented stars of the central nervous system." Methods Mol Biol **814**: 3-7.

Riban, V., V. Bouilleret, B. T. Pham-Le, J. M. Fritschy, C. Marescaux and A. Depaulis (2002). "Evolution of hippocampal epileptic activity during the

development of hippocampal sclerosis in a mouse model of temporal lobe epilepsy." Neuroscience **112**(1): 101-111.

Rothstein, J. D., M. Dykes-Hoberg, C. A. Pardo, L. A. Bristol, L. Jin, R. W. Kuncl, Y. Kanai, M. A. Hediger, Y. Wang, J. P. Schielke and D. F. Welty (1996). "Knockout of glutamate transporters reveals a major role for astroglial transport in excitotoxicity and clearance of glutamate." Neuron **16**(3): 675-686.

Rothstein, J. D., L. Martin, A. I. Levey, M. Dykes-Hoberg, L. Jin, D. Wu, N. Nash and R. W. Kuncl (1994). "Localization of neuronal and glial glutamate transporters." Neuron **13**(3): 713-725.

Sakurai, M., H. Kurokawa, A. Shimada, K. Nakamura, H. Miyata and T. Morita (2015). "Excitatory amino acid transporter 2 downregulation correlates with thalamic neuronal death following kainic acid-induced status epilepticus in rat." Neuropathology **35**(1): 1-9.

Tanaka, K., K. Watase, T. Manabe, K. Yamada, M. Watanabe, K. Takahashi, H. Iwama, T. Nishikawa, N. Ichihara, T. Kikuchi, S. Okuyama, N. Kawashima, S. Hori, M. Takimoto and K. Wada (1997). "Epilepsy and exacerbation of brain injury in mice lacking the glutamate transporter GLT-1." Science **276**(5319): 1699-1702.

Tessler, S., N. C. Danbolt, R. L. Faull, J. Storm-Mathisen and P. C. Emson (1999). "Expression of the glutamate transporters in human temporal lobe epilepsy." Neuroscience **88**(4): 1083-1091.

van der Hel, W. S., R. G. Notenboom, I. W. Bos, P. C. van Rijen, C. W. van Veelen and P. N. de Graan (2005). "Reduced glutamine synthetase in hippocampal areas with neuron loss in temporal lobe epilepsy." Neurology **64**(2): 326-333.

Volterra, A. and J. Meldolesi (2005). "Astrocytes, from brain glue to communication elements: the revolution continues." Nat Rev Neurosci **6**(8): 626-640.

Chapter 6: β-lactam antibiotics are an ineffective treatment option for restoration of aquaporin-4 (AQP4) and glutamate transporter-1 (GLT1) in an epilepsy model

6.1 Abstract

Astrocytes primarily regulate glutamate and water homeostasis through the membrane proteins glutamate transporter-1 (GLT1) and aquaporin-4 (AQP4), respectively. GLT1 is responsible for over 90% of glutamate clearance from the extracellular space and AQP4 regulates extracellular space volume and K^+ distribution. Cell swelling and increased extracellular glutamate and K^+ levels can lead to excitotoxicity and can be detrimental to the health of neurons in the brain. For example, reduced expression of AQP4 and GLT1 have been reported in the epileptic brain. Therefore, it is crucial to maintain levels of AQP4 and GLT1, but a therapeutic strategy to do so in a model of epilepsy has not been established. Ceftriaxone, a β-lactam antibiotic, has been shown to increase GLT1 *in vivo.* The effects of ceftriaxone on AQP4, however, have not been well studied. Furthermore, the ability of other β-lactam drugs to increase AQP4 and GLT1 expression has not been investigated. Therefore, I studied the effects of the β-lactam antibiotics ceftriaxone, clavulanic acid, and tazobactam on regulating AQP4 and GLT1 expression in wild-type mice. I then examined the therapeutic potential of ceftriaxone and tazobactam on restoring GLT1 levels and

ameliorating histological changes in the intrahippocampal kainic acid (IHKA) model of temporal lobe epilepsy (TLE). I found that these drugs failed to alter AQP4 or GLT1 expression in wild-type animals at doses that were previously reported to be effective (Rothstein, Patel et al. 2005; Lee, Ruby et al. 2013). Furthermore, ceftriaxone and tazobactam failed to increase GLT1, reduce astrogliosis, and prevent morphological changes in the hippocampus after IHKA injections in multiple, separate groups of experiments at a variety of doses. Therefore, β-lactam antibiotics may not be a promising therapeutic option for the prevention of epileptogenesis.

6.2 Introduction

Excitatory amino acid transporters (EAATs) are a family of 5 membrane proteins that are primarily responsible for the synaptic reuptake of glutamate. The rodent homologs to EAAT1-5 are glutamate aspartate transporter (GLAST) glutamate transporter-1 (GLT1), excitatory amino acid carrier-1 (EAAC1), EAAT4, and EAAT5, respectively. GLAST and GLT1 are predominantly expressed on astrocytes whereas EAAC1, EAAT4, and EAAT5 are largely expressed by neurons. At the tripartite synapse, GLT1 is responsible for the majority of glutamate clearance from the extracellular space (Kim, Lee et al. 2011). Interestingly, the cycle time of glutamate transport is relatively slow, but it was hypothesized that the ability of GLT1 to efficiently remove glutamate from the

extracellular space was due to its ability to quickly bind glutamate and its sheer abundance (Danbolt 2001). More recently, however, it was discovered that GLT1 can diffuse between synaptic and nonsynaptic sites in an activity-dependent manner (Murphy-Royal, Dupuis et al. 2015; Al Awabdh, Gupta-Agarwal et al. 2016). Since extracellular glutamate levels can determine the extent of receptor stimulation, it is critical to maintain low glutamate levels to prevent neurotoxicity.

GLT1 is downregulated in a variety of neurological diseases, including amyotrophic lateral sclerosis (ALS) (Rothstein, Van Kammen et al. 1995), Alzheimer's disease (Li, Mallory et al. 1997), and epilepsy (Hubbard, Szu et al. 2016). It is crucial to maintain GLT1 levels to prevent accumulation of glutamate in the extracellular space. In 2005, it was discovered that ceftriaxone, a β-lactam antibiotic, can increase GLT1 levels *in vitro* and *in vivo* (Rothstein, Patel et al. 2005). Since then, several other research groups have confirmed its effectiveness (Chu, Lee et al. 2007; Miller, Dorner et al. 2008; Bellesi, Melone et al. 2009; Lin, Tian et al. 2009; Sari, Smith et al. 2009; Nizzardo, Nardini et al. 2011; Rasmussen, Baron et al. 2011; Sari, Sakai et al. 2011; Inquimbert, Bartels et al. 2012; Wei, Pan et al. 2012; Feng, Wang et al. 2014), although this remains controversial (Melzer, Meuth et al. 2008; Thöne-Reineke, Neumann et al. 2008; Lai, Huang et al. 2011; Carbone, Duty et al. 2012; Cudkowicz, Titus et al. 2014). Ceftriaxone and the β-lactam drugs clavulanic acid and tazobactam have been

shown to reduce seizure-like activity in an invertebrate model (Rawls, Karaca et al. 2010), but their effects on hippocampal GLT1 restoration in a chronic model of epilepsy have not been investigated. More recently, ceftriaxone has been used to increase GLT1 levels in aquaporin-4 knockout mice (Li, Wang et al. 2012; Yang, Li et al. 2013).

The aquaporins are a family of at least 13 water channels expressed throughout a variety of mammalian tissues. The main water channel in the CNS is aquaporin-4 (AQP4) and it is responsible for the bidirectional fluid exchange in response to changes in the osmotic gradient. AQP4 is primarily found on astrocytic end-feet surrounding capillaries, the blood-brain barrier, and glia limitans (Nielsen, Nagelhus et al. 1997; Nagelhus, Mathiisen et al. 2004; Oshio, Binder et al. 2004; Costa, Tortosa et al. 2007). Mice deficient in AQP4 (Ma, Yang et al. 1997) have been used to determine several different functions of AQP4 including K^+ buffering (Binder, Yao et al. 2006), synaptic plasticity (Skucas, Mathews et al. 2011), and even addictive behavior (Ding, Sha et al. 2007; Wu, Lu et al. 2008; Chen, Bao et al. 2010). Furthermore, reduced levels of AQP4 expression have been reported in several neurological disorders, including a model of temporal lobe epilepsy (Lee, Hsu et al. 2012; Hubbard, Szu et al. 2016). The effects of ceftriaxone, clavulanic acid, and tazobactam on AQP4 expression, however, have not yet to be studied.

In this group of experiments, I used Western blot and immunohistochemistry to examine the effects of β-lactam drugs on GLT1 and AQP4 expression in wild-type mice. I next tested the efficacy of various treatment paradigms involving ceftriaxone and tazobactam in the IHKA model of TLE. In wild-type mice, two weeks of treatment with β-lactam drugs had no effect on AQP4 or GLT1 expression. Furthermore, GLT1 levels were not rescued after IHKA-induced downregulation. No IHKA-induced astrogliosis or hippocampal morphological changes were ameliorated by either ceftriaxone or tazobactam. Several different treatment paradigms were tested. Therefore, β-lactam drugs may not be a promising treatment option for patients with temporal lobe epilepsy.

6.3 Methods

6.3.1 Animals

All experiments were conducted in accordance with the guidelines set forth by the National Institutes of Health and were approved by the University of California, Riverside Institutional Animal Care and Use Committee (IACUC). Animals were housed under controlled conditions (12 hour light/12 hour dark) and had access to food and water *ad libitum*. Adult CD1 male mice were used for all experiments.

6.3.2 Drug Treatment

Ceftriaxone, clavulanic acid, or tazobactam (Table 6.1) were given to mice through intraperitoneal (i.p.) injections. While ceftriaxone and clavulanic acid were given at 200 mg/kg, tazobactam was given at 1/10th the dose. Rothstein *et al.* (2005) previously determined that i.p. injections of 200 mg/kg ceftriaxone per day is both safe and effective (Rothstein, Patel et al. 2005). Clavulanic acid has previously been demonstrated to be effective at a similar concentration to ceftriaxone whereas a significantly lower amount of tazobactam (less than 1/10th the dosage) was required to have the same effect (Rawls, Karaca et al. 2010). Equal volumes of saline (0.9%) were used for the control group. Treatment lasted 1-2 weeks and was given to either wild-type mice (n = 3 for each experimental condition) or during an intrahippocampal kainic acid (IHKA) treatment paradigm (see Table 6.2).

Drug Name	Daily dosage	Company	Catalog number
Ceftriaxone	200 mg/kg	Sigma-Aldrich	1098184
Clavulanic acid	200 mg/kg	Sigma-Aldrich	61177-45-5
Tazobactam	20 mg/kg	LKT Laboratories, Inc.	T0298

Table 6.1. β-lactam drug Information.
Daily dosage and purchasing information for ceftriaxone, clavulanic acid, and tazobactam.

6.3.3 Western blot

After 2 weeks of drug treatment, CD1 wild-type mice (n=3 for each experimental group) were deeply anesthetized with an i.p. injection of sodium pentobarbital (200 mg/kg) and were transcardially perfused with ice-cold PBS containing protease inhibitors (Roche). Brains were quickly removed from the skull and either the cortex or the hippocampus was rapidly microdissected according to the mouse brain atlas of Paxinos and Watson (Paxinos and Franklin 2001). Tissue was mechanically homogenized in ice-cold RIPA buffer (Sigma) containing protease inhibitor cocktail (Roche) using a glass dounce tissue grinder (Wheaton). Lysates were centrifuged at 10,000g for 5 minutes and the supernatant extracted. Protein concentrations were determined using Bio-Rad BSA detection system and Bio-Tek plate reader. Protein was then electrophoresed through a 12% SDS-PAGE gel and transferred to a nitrocellulose membrane. The membranes were then incubated overnight in a 5% milk in tris-buffered saline with tween (TBST) blocking solution with antibodies to either AQP4 (1:1,000; EMD Millipore) or GLT1 (1:5,000, AbCam) and mouse anti-β-actin (1:5,000, Calbiochem). The next day, membranes with cortex protein were washed and incubated for two hours at room temperature with peroxidase-conjugated goat anti-rabbit and goat anti-mouse secondary antibodies. They were then washed, and visualized with ECL chemiluminescence (Pierce) and captured on Hyblot film (Denville). Membranes

with hippocampal protein were washed and incubated with IRDye (Leica) species-specific secondary antibodies. They were then washed and imaged using the Li-COR Odyssey Infrared Western Imaging System. Band intensities were determined using densitometry (ImageJ or Li-COR software) and AQP4 and GLT1 levels were normalized to internal β-actin. Statistical analysis was performed with GraphPad Prism 5 using a one-way ANOVA with *post-hoc* Bonferroni pairs of columns comparison test.

6.3.4 Intrahippocampal kainic acid injections

Epileptogenesis was induced with IHKA injections (Bouilleret, Ridoux et al. 1999; Riban, Bouilleret et al. 2002; Arabadzisz, Antal et al. 2005). Briefly, mice were anesthetized with an i.p. injection of a mixture of 80mg/kg ketamine and 10 mg/kg xylazine and mounted in a stereotaxic frame. The skull was exposed and stereotaxic coordinates (Paxinos and Franklin 2001) were used to drill a 0.6 mm burr hole 1.8 mm posterior and 1.6 mm lateral from bregma with a high-speed drill (Drummond Scientific). Mice were injected with either 74 nL (moderate; amount used for all previous studies) or 110 nL (severe) of a 20 mM solution of kainic acid over a period of 4 minutes using a microinjector (Nanoject, Drummond Scientific) into the right dorsal hippocampus (dorsoventral coordinate 1.9 mm). After kainic acid injections, all mice experienced status epilepticus (SE), defined by Racine scale stage 3-5 seizures (Table 2.1, Racine 1972)

continuously for a period of 3 or more hours, which spontaneously subsided. The survival rate was high (over 80%) for the “moderate” IHKA, but very low (only ~30%) for the “severe” IHKA; animals that died due to SE were excluded from the study.

Before and/or after IHKA injections, animals were treated with either tazobactam or ceftriaxone (see treatment paradigms in Table 6.2). Treatment history was blinded before IHKA injections. After completion of the treatment paradigms, mice were euthanized with fatal plus (Western Medical Supply), perfused, and processed for each experiment. For each different treatment group, n = 2 mice were used. As a control, saline was used in place of β-lactam drugs and treatment length was matched. All tissue in each different paradigm was processed in parallel with the i.p. saline-treated controls.

Treatment paradigm	Description of treatment paradigm
Pre-treatment	7 days of drug treatment with the final day of treatment done on same day as IHKA injections
Pre- and post-treatment	7 days of drug treatment with the final “pre” day of treatment done on same day as IHKA injections; first day of “post” treatment began 1 day after IHKA injections; therefore, 14 consecutive days of treatment total
Post-treatment	7 or 14 days of drug treatment with first day of treatment done on same day as IHKA injections

Table 6.2. Treatment paradigms.
Explanation of ceftriaxone or tazobactam treatment paradigms used in this chapter.

6.3.5 Immunohistochemistry

Mice were transcardially perfused with ice-cold PBS, pH 7.4, followed by 4% paraformaldehyde, pH 7.4. Brains were quickly removed and postfixed in 4% paraformaldehyde overnight at 4°C followed by two days of cryoprotection in 30% sucrose in PBS at 4°C. Brains were frozen with ice-cold isopentane and stored at -80°C until they were cut into 50 µm coronal sections using a cryostat (Leica CM 1950, Leica Microsytems, Bannockburn, IL). Slices were stored in PBS at 4°C and all slices were processed simultaneously. Endogenous peroxidase activity was quenched by incubating slices in 3% H_2O_2 for 1 hour at room temperature. This was followed by a 1 hour blocking step with 5% normal goat serum in 0.1 M PBS. Slices were then incubated with primary antibody to AQP4 (1:200, EMD Millipore), GLT1 (1:3,000, AbCam) and/or GFAP (1:200, EMD Millipore) in 0.3% Triton X-100 overnight at 4°C. After washing slices with PBS, sections were incubated with species-specific secondary antibody conjugated with Alexa 488 or Alexa 594 and a tyramide signaling amplification (TSA) kit (Molecular Probes/Invitrogen) for visualization. Slices were mounted in Vectorshield with DAPI (Vector Laboratories) and 10x images were taken using a fluorescence microscope (Leica DFC345 FX).

6.4 Results

6.4.1 β-lactam drugs do not alter GLT1 expression in wild-type mice

I first wanted to determine the effects, if any, of ceftriaxone (200 mg/kg), clavulanic acid (200 mg/kg), and tazobactam (20 mg/kg) on GLT1 expression in wild-type mice. Mice were treated once a day for 14 days with i.p. injections of the β-lactam drugs or with an equal volume of saline as a control. I found no change in GLT1 cortex protein expression using Western blotting (n = 3, Figure 6.1). This was confirmed immunohistochemically (n = 3, Figure 6.2).

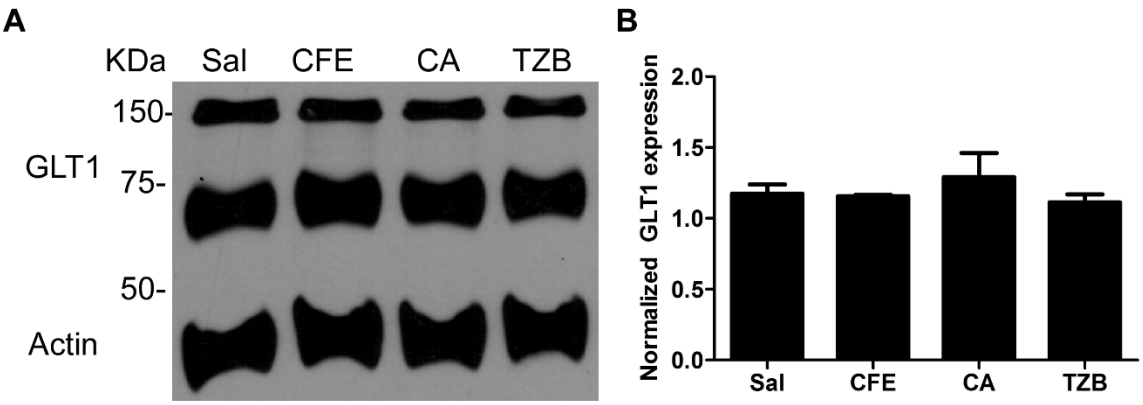


Figure 6.1. No change in wild-type glutamate transporter-1 (GLT1) cortical protein levels after treatment with β-lactam drugs.
A. A representative Western blot image of GLT1 (upper bands) and β-actin (lower band) cortical protein levels in CD1 wild-type male mice after being treated once a day for 2 weeks with i.p. injections of either saline (0.9%), ceftriaxone (CFE, 200 mg/kg), clavulanic acid (CA, 200 mg/kg), or tazobactam (TZB, 20 mg/kg). KDa = kilodaltons. **B.** Quantification of GLT1 cortical protein levels after treatment with saline (control), ceftriaxone, clavulanic acid, or tazobactam. For each treatment group, n = 3.

Furthermore, no structural alterations or change in the staining pattern of GLT1 were noted.

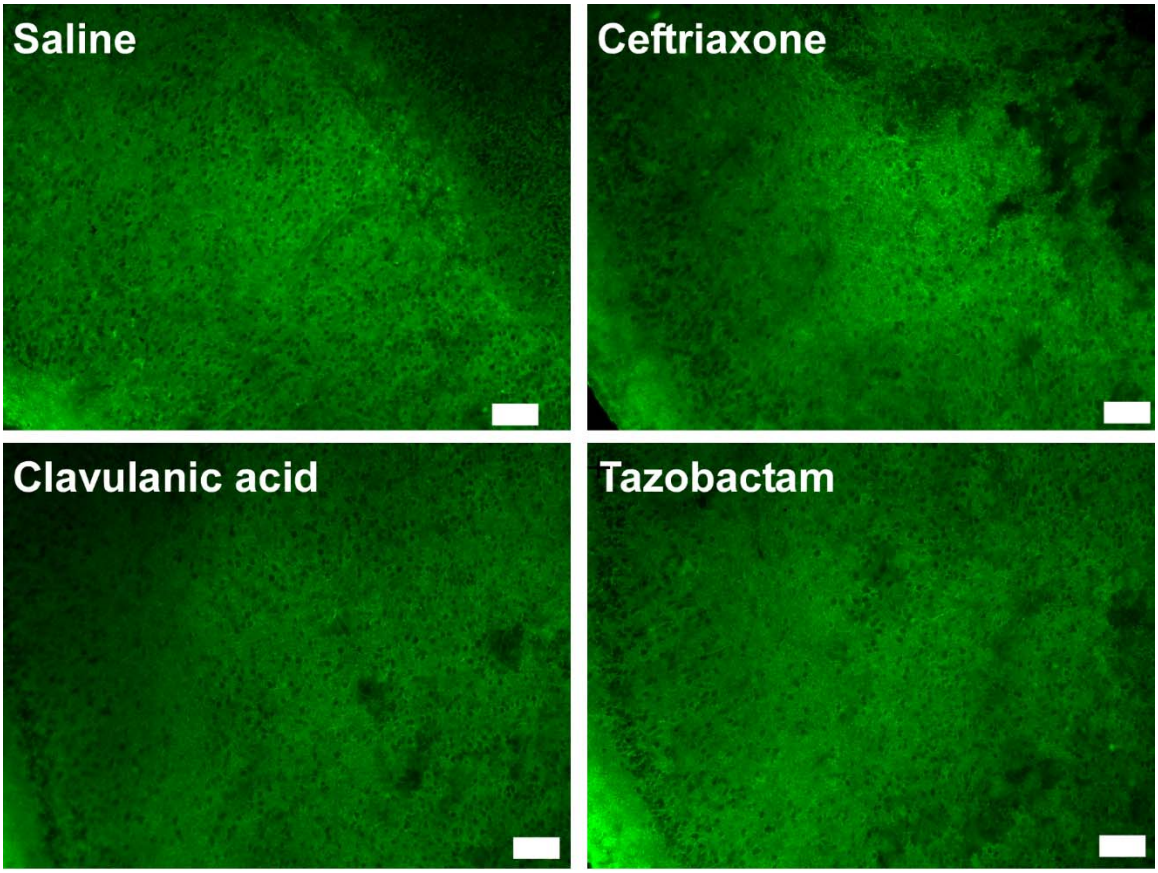


Figure 6.2. No change in wild-type glutamate transporter-1 (GLT1) cortical immunoreactivity after treatment with β-lactam drugs.
GLT1 immunoreactivity in the cortex of CD1 wild-type male mice after being treated once a day for 2 weeks with i.p. injections of either saline (0.9%, upper left), ceftriaxone (200 mg/kg, upper right), clavulanic acid (200 mg/kg, lower left), or tazobactam (20 mg/kg, lower right). For each treatment group, 8-12 slices were taken from each animal (n = 3). Scale bar = 100 μm.

GLT1 is highly expressed in the hippocampus. Therefore, I then wanted to determine whether β-lactam drugs would exhibit different effects on hippocampal GLT1 expression. After 2 weeks of treatment, GLT1 hippocampal protein levels (Figure 6.3) and immunoreactivity (Figure 6.4) were unaltered in the wild-type mice. No alterations in GLT1 hippocampal staining patters were noticed. Therefore, β-lactam drugs do not alter GLT1 protein expression in wild-type mice.

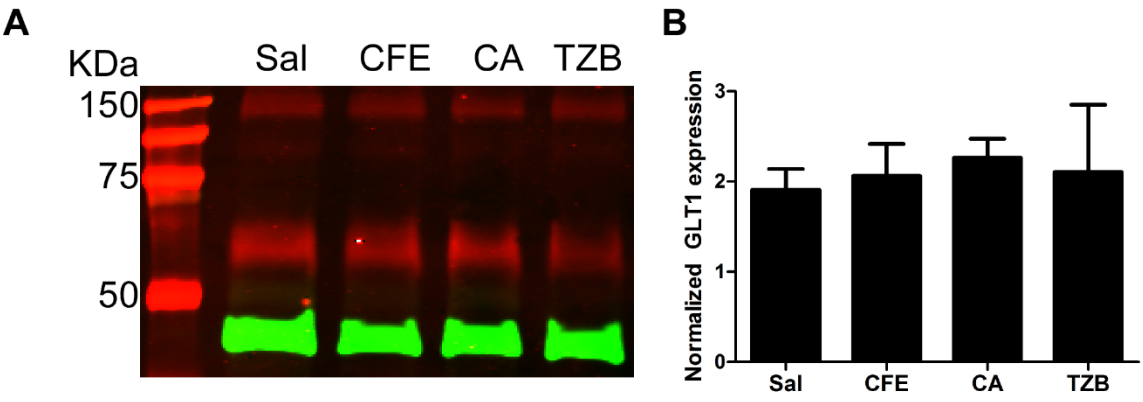


Figure 6.3. No change in wild-type glutamate transporter-1 (GLT1) hippocampal protein levels after treatment with β-lactam drugs.
A. A representative Western blot image of GLT1 (upper red bands) and β-actin (lower green band) hippocampal protein levels in CD1 wild-type male mice after being treated once a day for 2 weeks with i.p. injections of either saline (0.9%), ceftriaxone (CFE, 200 mg/kg), clavulanic acid (CA, 200 mg/kg), or tazobactam (TZB, 20 mg/kg). KDa = kilodaltons. **B.** Quantification of GLT1 hippocampal protein levels after treatment with saline (control), ceftriaxone, clavulanic acid, or tazobactam. For each treatment group, n = 3.

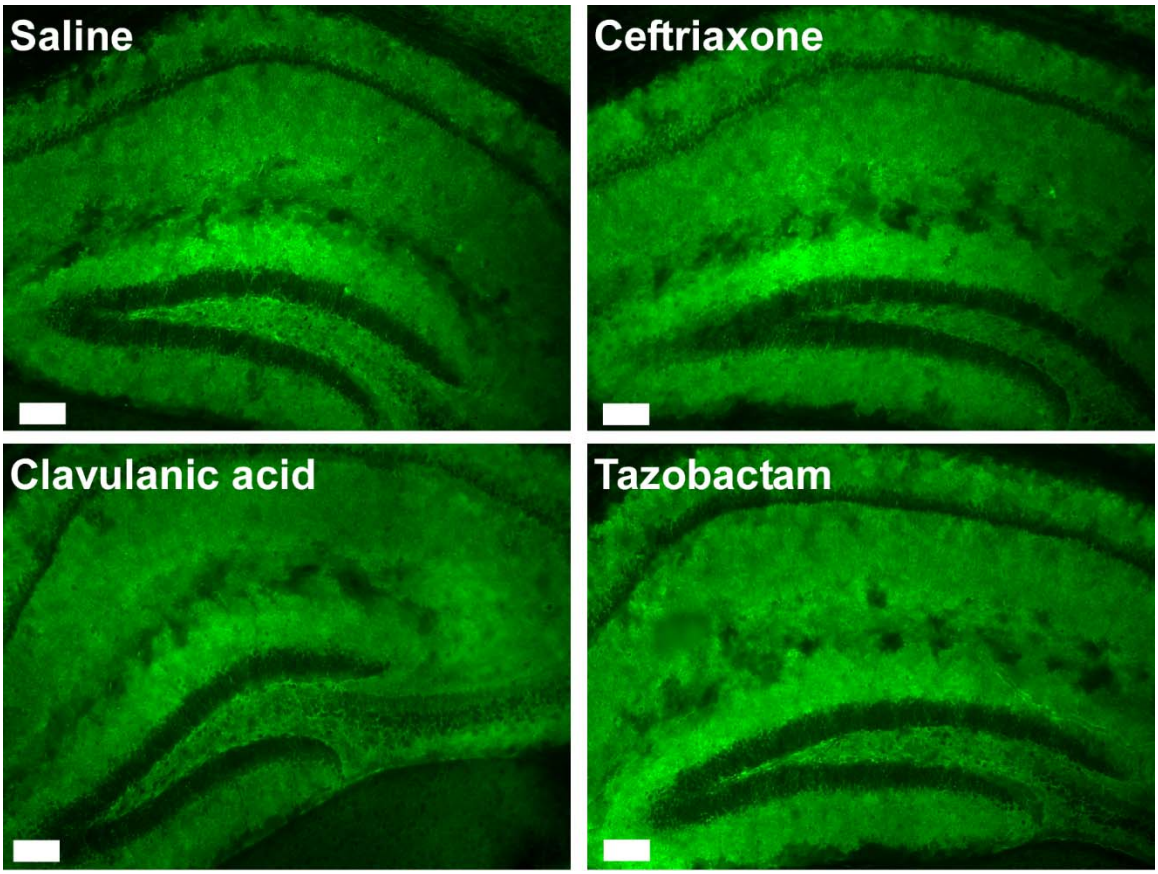


Figure 6.4. No change in wild-type glutamate transporter-1 (GLT1) hippocampal immunoreactivity after treatment with β-lactam drugs. GLT1 immunoreactivity in the hippocampus of CD1 wild-type male mice after being treated once a day for 2 weeks with i.p. injections of either saline (0.9%, upper left), ceftriaxone (200 mg/kg, upper right), clavulanic acid (200 mg/kg, lower left), or tazobactam (20 mg/kg, lower right). For each treatment group, 8-12 slices were taken from each animal (n = 3). Scale bar = 100 μm.

6.4.2 β-lactam drugs do not alter AQP4 expression in wild-type mice

Next I investigated the effects of ceftriaxone (200 mg/kg), clavulanic acid (200 mg/kg), and tazobactam (20 mg/kg) on hippocampal and cortical AQP4 protein expression. Wild-type CD1 male mice were treated once a day for 14 days with

i.p. injections of each β-lactam drug or with equal volumes of saline as an internal control. After this treatment, I found no changes in cortical AQP4 protein expression (Figure 6.5). Similarly, AQP4 immunoreactivity and cortical expression pattern remained unaltered after drug treatment (Figure 6.6).

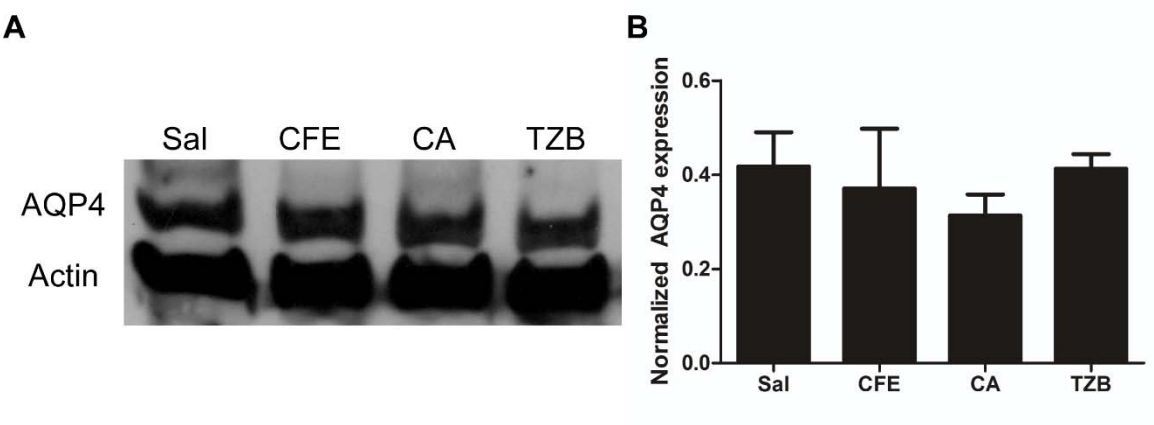


Figure 6.5. No change in wild-type aquaporin-4 (AQP4) cortical protein levels after treatment with β-lactam drugs.
A. A representative Western blot image of AQP4 (upper band, ~60 KDa) and β-actin (lower band, ~42 KDa) cortical protein levels in CD1 wild-type male mice after being treated once a day for 2 weeks with i.p. injections of either saline (0.9%), ceftriaxone (CFE, 200 mg/kg), clavulanic acid (CA, 200 mg/kg), or tazobactam (TZB, 20 mg/kg). KDa = kilodaltons. **B.** Quantification of AQP4 cortical protein levels after treatment with saline (control), ceftriaxone, clavulanic acid, or tazobactam. For each treatment group, n = 3.

Due to the vastly different expression pattern of AQP4 in the cortex and hippocampus (Hubbard, Hsu et al. 2015), I wanted to see whether the β-lactam drugs would have a different effect on hippocampal AQP4 expression. I again discovered no alteration in hippocampal AQP4 protein expression (Figure 6.7) or

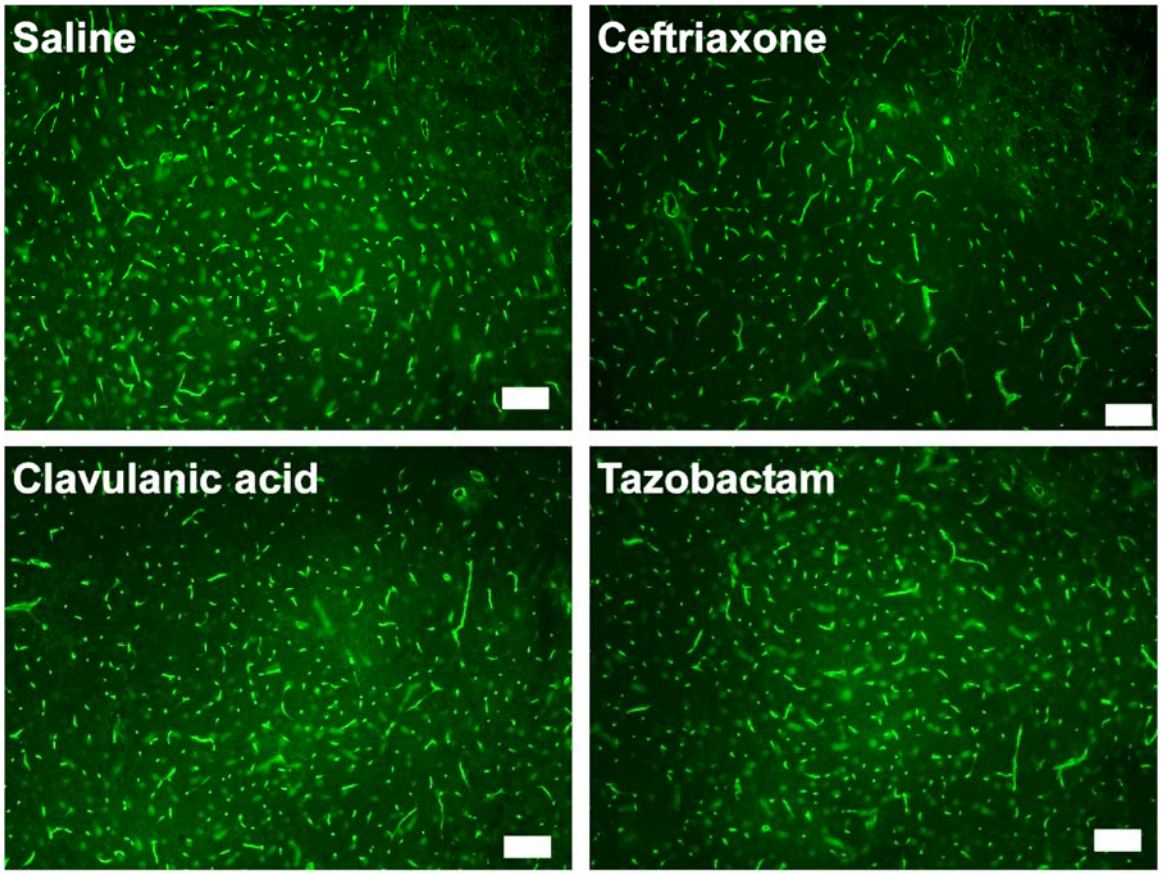


Figure 6.6. No change in wild-type aquaporin-4 (AQP4) cortical immunoreactivity after treatment with β-lactam drugs.
AQP4 immunoreactivity in the cortex of CD1 wild-type male mice after being treated once a day for 2 weeks with i.p. injections of either saline (0.9%, upper left), ceftriaxone (200 mg/kg, upper right), clavulanic acid (200 mg/kg, lower left), or tazobactam (20 mg/kg, lower right). For each treatment group, 8-12 slices were taken from each animal (n = 3). Scale bar = 100 μm.

immunoreactivity (Figure 6.8) after two weeks of treatment. Alterations in AQP4 expression by β-lactam drugs were not apparent and not studied further in this chapter.

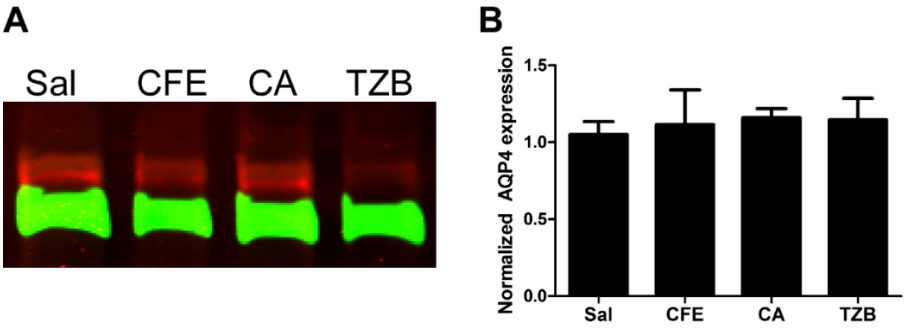


Figure 6.7. No change in wild-type aquaporin-4 (AQP4) hippocampal protein levels after treatment with β-lactam drugs.
A. A representative Western blot image of AQP4 (upper band, ~60 KDa) and β-actin (lower band, ~42 KDa) hippocampal protein levels in CD1 wild-type male mice after being treated once a day for 2 weeks with i.p. injections of either saline (0.9%), ceftriaxone (CFE, 200 mg/kg), clavulanic acid (CA, 200 mg/kg), or tazobactam (TZB, 20 mg/kg). KDa = kilodaltons. **B.** Quantification of AQP4 hippocampal protein levels after treatment with saline (control), ceftriaxone, clavulanic acid, or tazobactam. For each treatment group, n = 3.

6.4.3 Tazobactam does not ameliorate histological changes in the IHKA epilepsy model

It is possible that reductions in GLT1 levels are required for β-lactam antibiotics to be able to rescue GLT1 expression. Therefore, I wanted to investigate the effects of the β-lactam antibiotics in a disease model where GLT1 levels are reduced. I studied only the effects of ceftriaxone and tazobactam (not clavulanic acid, as it had a similar potency as ceftriaxone but was not as well established) in the IHKA model of epilepsy.

I began with a severe model of epilepsy, where mice received an exceptionally high dose of intrahippocampal kainic acid (110 nL of 20 mM kainic acid). All

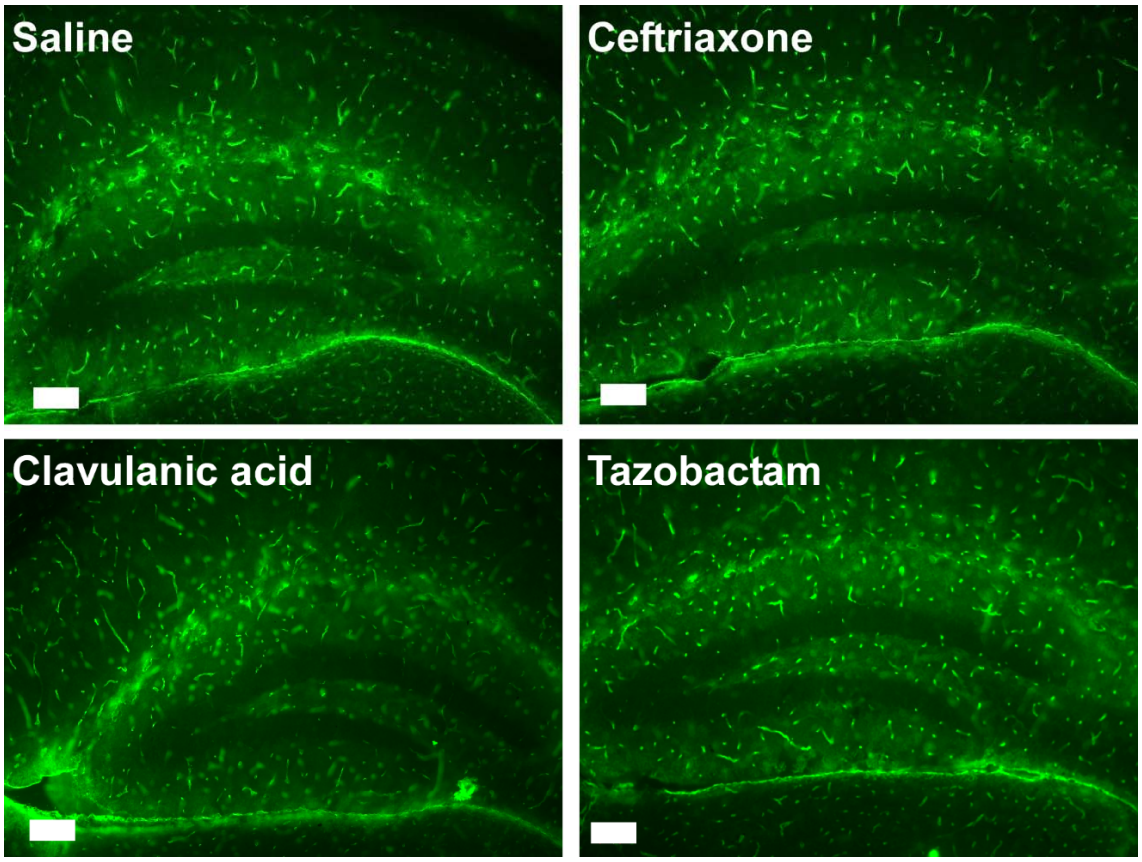


Figure 6.8. No change in wild-type aquaporin-4 (AQP4) cortical immunoreactivity after treatment with β-lactam drugs.
AQP4 immunoreactivity in the hippocampus of CD1 wild-type male mice after being treated once a day for 2 weeks with i.p. injections of either saline (0.9%, upper left), ceftriaxone (200 mg/kg, upper right), clavulanic acid (200 mg/kg, lower left), or tazobactam (20 mg/kg, lower right). For each treatment group, 8-12 slices were taken from each animal (n = 3). Scale bar = 100 μm.

mice experienced severe SE. Beginning immediately after IHKA injections, mice received i.p. injections of either tazobactam (20 mg/kg) or saline every day for 7 days. Immunohistochemical analysis revealed that both GLT1 and GFAP immunoreactivity remained unaltered in the ipsilateral hippocampus to injections after 1 week of treatment (Figure 6.9). Instead, severely reduced levels of GLT1 and increased GFAP expression were observed, as commonly seen at this time

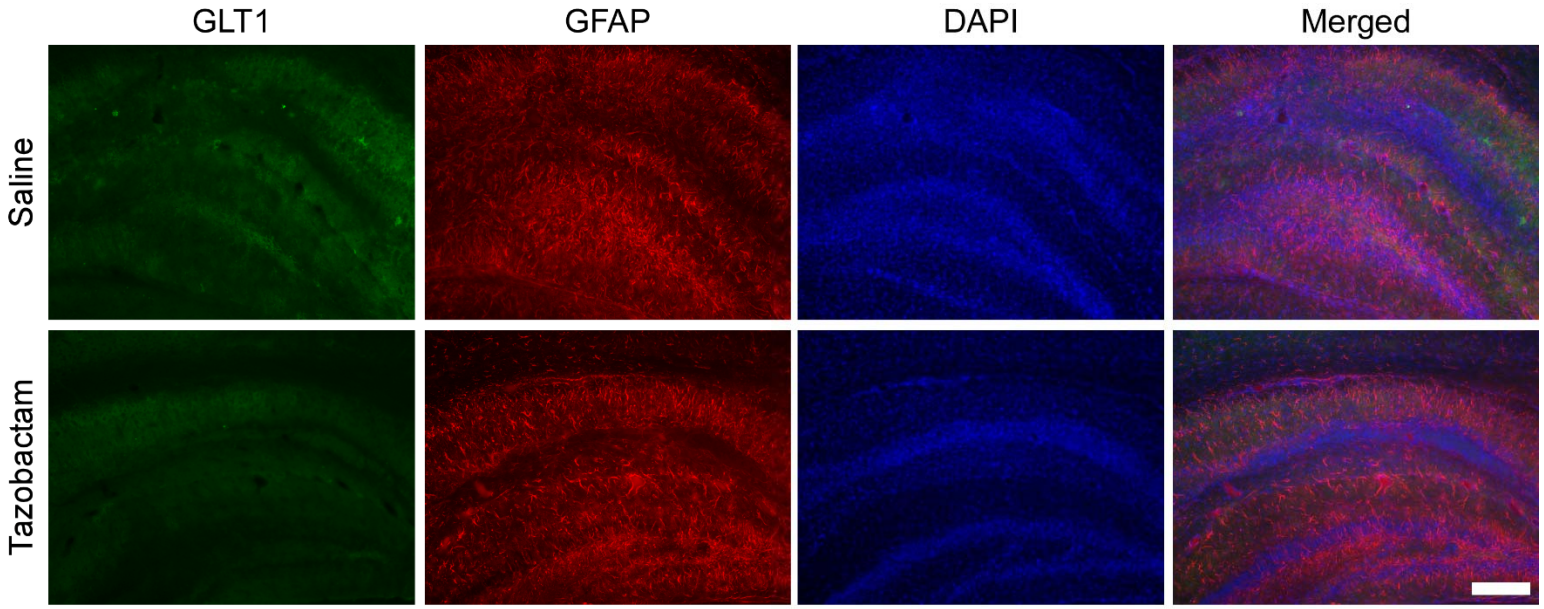


Figure 6.9. Tazobactam failed to ameliorate histological changes in the ipsilateral hippocampus in a severe intrahippocampal kainic acid (IHKA) model of epilepsy.

Glutamate transporter-1 (GLT1), glial fibrillary acidic protein (GFAP), 4,6-diamidino-2-phenylindole (DAPI), and merged immunoreactivity in the ipsilateral hippocampus after a high dose of intrahippocampal kainic acid (110 nL of 20 mM solution) injections. All mice were sacrificed 7 days after IHKA injections. Upper panel: immunoreactivity after 7 days of daily i.p. saline injections. Lower panel: immunoreactivity after 7 days of daily i.p. tazobactam (20 mg/kg) injections. Scale bar = 200 µm.

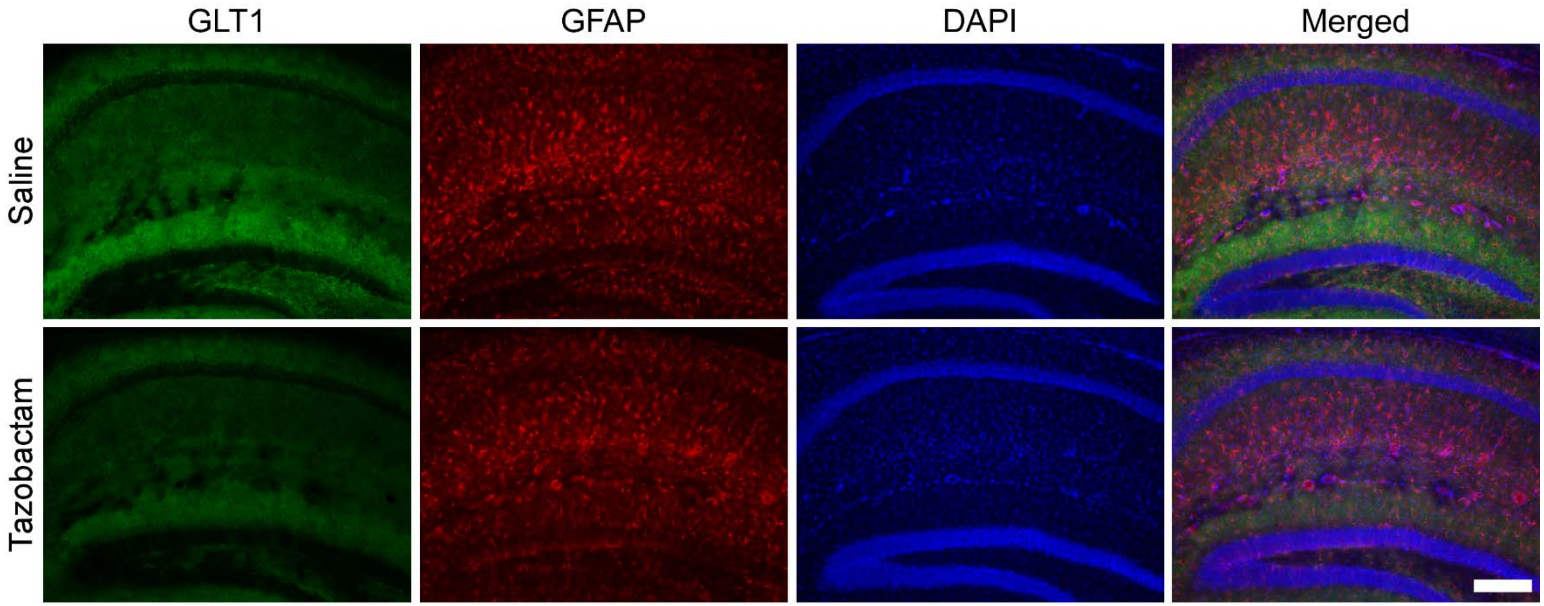


Figure 6.10. Tazobactam failed to ameliorate histological changes in the contralateral hippocampus in a severe intrahippocampal kainic acid (IHKA) model of epilepsy.

Glutamate transporter-1 (GLT1), glial fibrillary acidic protein (GFAP), 4,6-diamidino-2-phenylindole (DAPI), and merged immunoreactivity in the contralateral hippocampus after a high dose of intrahippocampal kainic acid (110 nL of 20 mM solution) injections. All mice were sacrificed 7 days after IHKA injections. Upper panel: immunoreactivity after 7 days of daily i.p. saline injections. Lower panel: immunoreactivity after 7 days of daily i.p. tazobactam (20 mg/kg) injections. Scale bar = 200 μm.

point in the IHKA model (see Chapter 5). DAPI staining also revealed morphological changes in the ipsilateral hippocampus at this time point. In the contralateral hippocampus, GLT1 and GFAP levels also remained similar between the saline-treated and tazobactam-treated animals (Figure 6.10). As expected, no major morphological changes, were noted in the DAPI stain in the contralateral hippocampus to IHKA injections in either treatment paradigm.

Next, I wanted to investigate the effects of tazobactam in the typical (moderate) IHKA model where all mice receive the regular intrahippocampal dose of 74 nL of kainic acid (20 mM). In addition, I tested 3 different treatment paradigms (Table 6.2): 1 week of pre-treatment with tazobactam; 1 week of post-treatment with tazobactam; or 1 week of pre-treatment with tazobactam + 1 week of post-treatment of tazobactam (14 days of tazobactam treatment total). In each treatment paradigm, mice received daily i.p. injections of 20 mg/kg tazobactam. Seven days after IHKA injections, all mice were sacrificed for tissue processing. In the ipsilateral hippocampus to IHKA injections, no difference in GLT1 and GFAP levels were observed between saline post-treated animals and tazobactam-treated (pre-, post-, or pre- and post-treated) animals (Figure 6.11). In all cases, a reduction in GLT1 immunoreactivity from that seen in naïve mice or after intrahippocampal saline levels (Chapter 5) was observed. This reduction, however, was not as drastic as that seen in the severe IHKA model (Figure 6.9). Therefore, GLT1 reduction is kainic acid-dose dependent. Similarly, DAPI

GLT1
GFAP
DAPI
Merged
Saline
Tazobactam Pre-treat
Tazobactam Post-treat
Tazobactam Pre- and post-treat

Figure 6.11. Pre- and post-treatment with tazobactam failed to ameliorate histological changes in the ipsilateral hippocampus in the intrahippocampal kainic acid (IHKA) model of epilepsy.
Glutamate transporter-1 (GLT1), glial fibrillary acidic protein (GFAP), 4,6-diamidino-2-phenylindole (DAPI), and merged immunoreactivity in the ipsilateral hippocampus after intrahippocampal kainic acid (74 nL of 20 mM solution) injections. All animals were perfused 7 days after IHKA injections. Saline: immunoreactivity after 7 days of daily i.p. saline injections. Tazobactam pre-treat: immunoreactivity after 7 days of daily i.p. tazobactam (20 mg/kg) injections before IHKA injections. Tazobactam post-treat: immunoreactivity after 7 days of daily i.p. tazobactam (20 mg/kg) injections after IHKA injections. Tazobactam pre- and post-treat: 7 days of daily i.p. tazobactam injections followed by IHKA injections and 7 more days of daily i.p. tazobatam injections (total of 14 days of treatment). Scale bar = 200 μm.

revealed only minor structural changes (slight dispersion of the granule cell layer) compared to that seen in Figure 6.9 (striking reorganization of the hippocampus). In the contralateral hippocampus to IHKA injections, marked reduction of GLT1 immunoreactivity was observed in all treatment paradigms (Figure 6.12). Similarly, GFAP staining revealed astrocytic ramification in both the saline-treated and tazobactam-treated mice. As expected, DAPI revealed no major structural changes in the contralateral hippocampus after IHKA injections in any treatment group.

Finally, I wanted to test the efficacy of a longer treatment paradigm of tazobactam. Therefore, I treated animals with 20 mg/kg i.p. injections of tazobactam for 14 days after IHKA injections (see “post-treatment” in Table 6.2). Animals were sacrificed 14 days after IHKA injections for tissue processing. Again, no difference in GLT1 or GFAP expression was observed between saline post-treated or tazobactam post-treated animals after 2 weeks in either the ipsilateral (Figure 6.13) or contralateral (Figure 6.14) hippocampus. While structural changes were observed in the ipsilateral hippocampus (DAPI staining, Figure 6.13), the hippocampus maintained laminar organization in the contralateral hippocampus (DAPI, Figure 6.14). Taken together, these results demonstrate that tazobactam does not provide neuroprotective effects in the IHKA model of epilepsy.

GLT1
GFAP
DAPI
Merged
Saline
Tazobactam Pre-treat
Tazobactam Post-treat
Tazobactam Pre- and post-treat

Figure 6.12. Pre- and post-treatment with tazobactam failed to ameliorate histological changes in the contralateral hippocampus in the intrahippocampal kainic acid (IHKA) model of epilepsy.
Glutamate transporter-1 (GLT1), glial fibrillary acidic protein (GFAP), 4,6-diamidino-2-phenylindole (DAPI), and merged immunoreactivity in the contralateral hippocampus after intrahippocampal kainic acid (74 nL of 20 mM solution) injections. All animals were perfused 7 days after IHKA injections. Saline: immunoreactivity after 7 days of daily i.p. saline injections. Tazobactam pre-treat: immunoreactivity after 7 days of daily i.p. tazobactam (20 mg/kg) injections before IHKA injections. Tazobactam post-treat: immunoreactivity after 7 days of daily i.p. tazobactam (20 mg/kg) injections after IHKA injections. Tazobactam pre- and post-treat: 7 days of daily i.p. tazobactam injections followed by IHKA injections and 7 more days of daily i.p. tazobatam injections (total of 14 days of treatment). Scale bar = 200 μm.

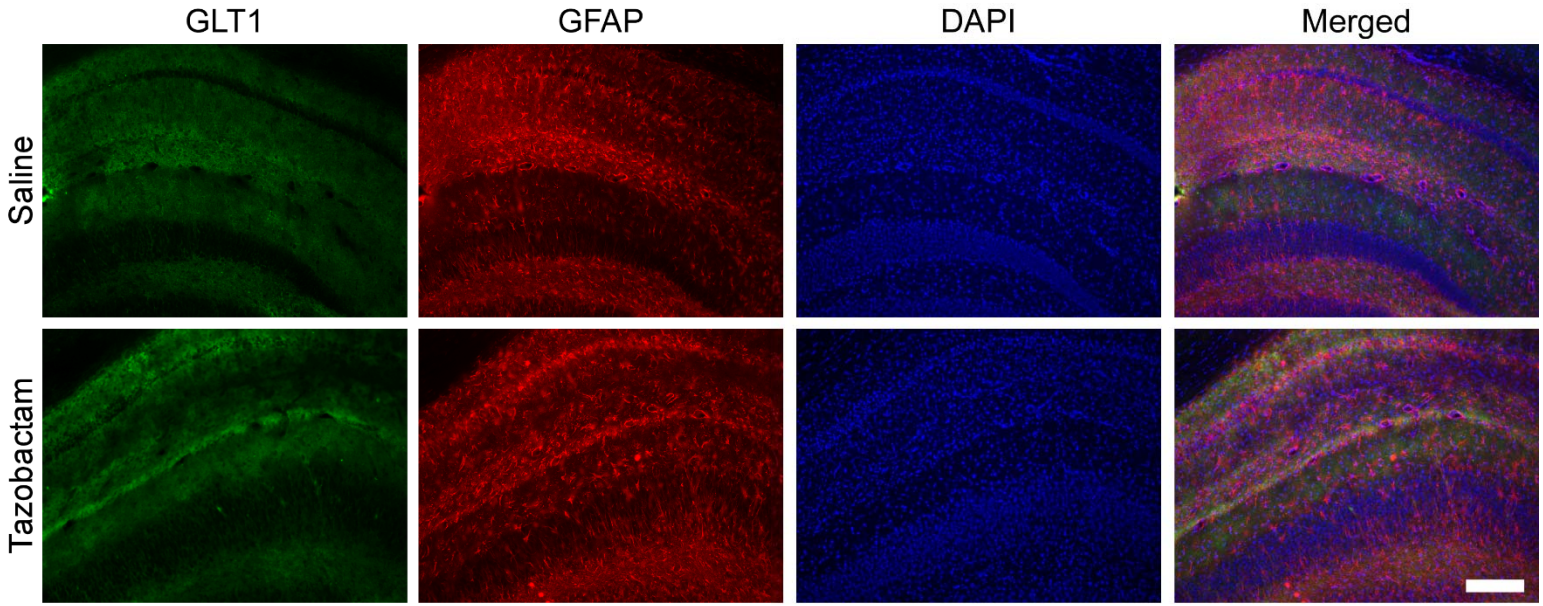


Figure 6.13. Two weeks of tazobactam treatment failed to ameliorate histological changes in the ipsilateral hippocampus in the intrahippocampal kainic acid (IHKA) model of epilepsy.

Glutamate transporter-1 (GLT1), glial fibrillary acidic protein (GFAP), 4,6-diamidino-2-phenylindole (DAPI), and merged immunoreactivity in the ipsilateral hippocampus after intrahippocampal kainic acid (74 nL of 20 mM solution) injections. All mice were sacrificed 14 days after IHKA injections. Upper panel: immunoreactivity after 14 days of daily i.p. saline injections. Lower panel: immunoreactivity after 14 days of daily i.p. tazobactam (20 mg/kg) injections. Scale bar = 200 µm.

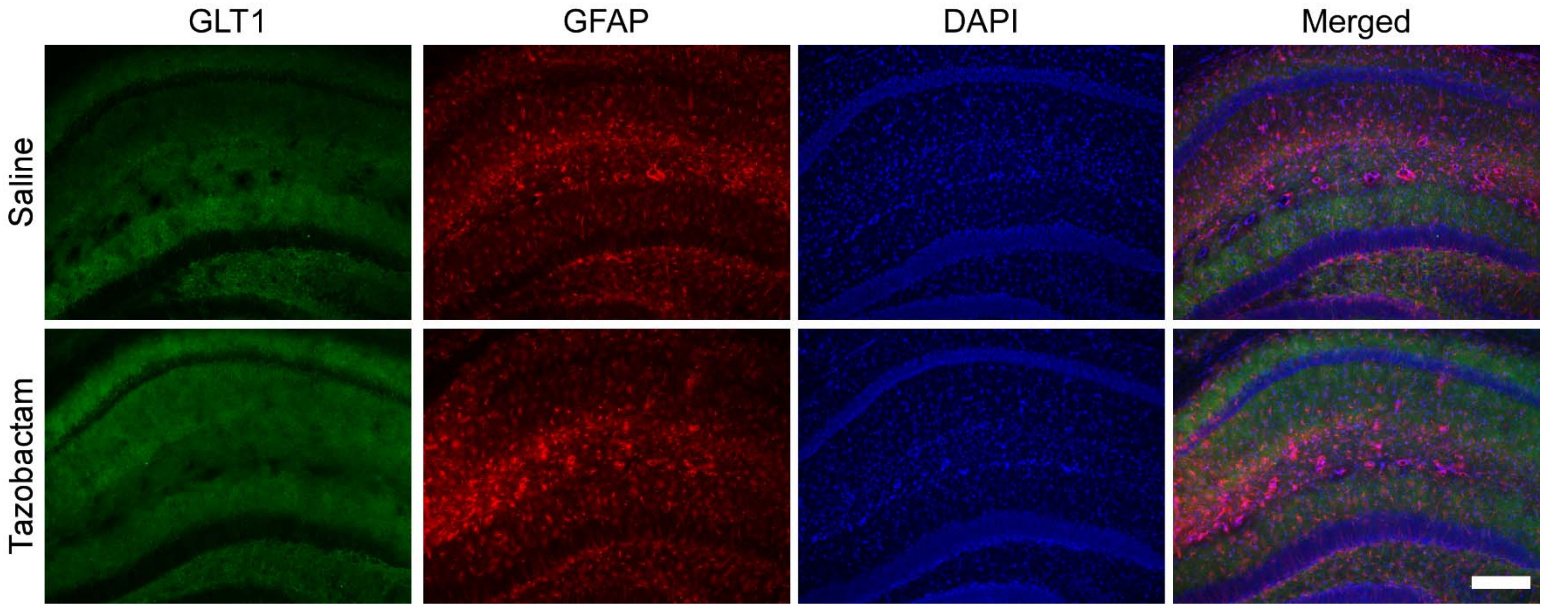


Figure 6.14. Two weeks of tazobactam treatment failed to ameliorate histological changes in the contralateral hippocampus in the intrahippocampal kainic acid (IHKA) model of epilepsy.

Glutamate transporter-1 (GLT1), glial fibrillary acidic protein (GFAP), 4,6-diamidino-2-phenylindole (DAPI), and merged immunoreactivity in the contralateral hippocampus after intrahippocampal kainic acid (74 nL of 20 mM solution) injections. All mice were sacrificed 7 days after IHKA injections. Upper panel: immunoreactivity after 14 days of daily i.p. saline injections. Lower panel: immunoreactivity after 14 days of daily i.p. tazobactam (20 mg/kg) injections. Scale bar = 200 μm.

6.4.4 Ceftriaxone fails to ameliorate histological changes in the IHKA model of epilepsy

Finally, I wanted to determine whether the well-established β-lactam drug, ceftriaxone, could prevent the downregulation of GLT1 and/or offer protection against histological changes in the IHKA model of epilepsy. All mice received intrahippocamapal kainic acid (74 nL of 20 mM solution) injections. Mice then received either 7 days of i.p. saline injections (control), 7 of pre-treatment with ceftriaxone, or 7 days of post-treatment with ceftriaxone (Table 6.2). One week after IHKA injections, all animals were sacrificed and tissue was processed. I again found no alterations in GLT1 and GFAP immunoreactivity between the saline- and ceftriaxone-treated groups in the ipsilateral hippocampus to IHKA injections (Figure 6.15). Similar structural changes (slight dispersion of cells in the granule cell layer) were noted in all 3 treatment paradigms. Likewise, no differences were seen in the contralateral hippocampus to injections in any group tested (Figure 6.16). Similar to what I have previously observed at this time point (Chapter 2), no structural changes were seen in the contralateral hippocampus 7 days after IHKA injections. Therefore, ceftriaxone failed to restore GLT1 immunoreactivity or reduce GFAP reactivity in the IHKA model of epilepsy.

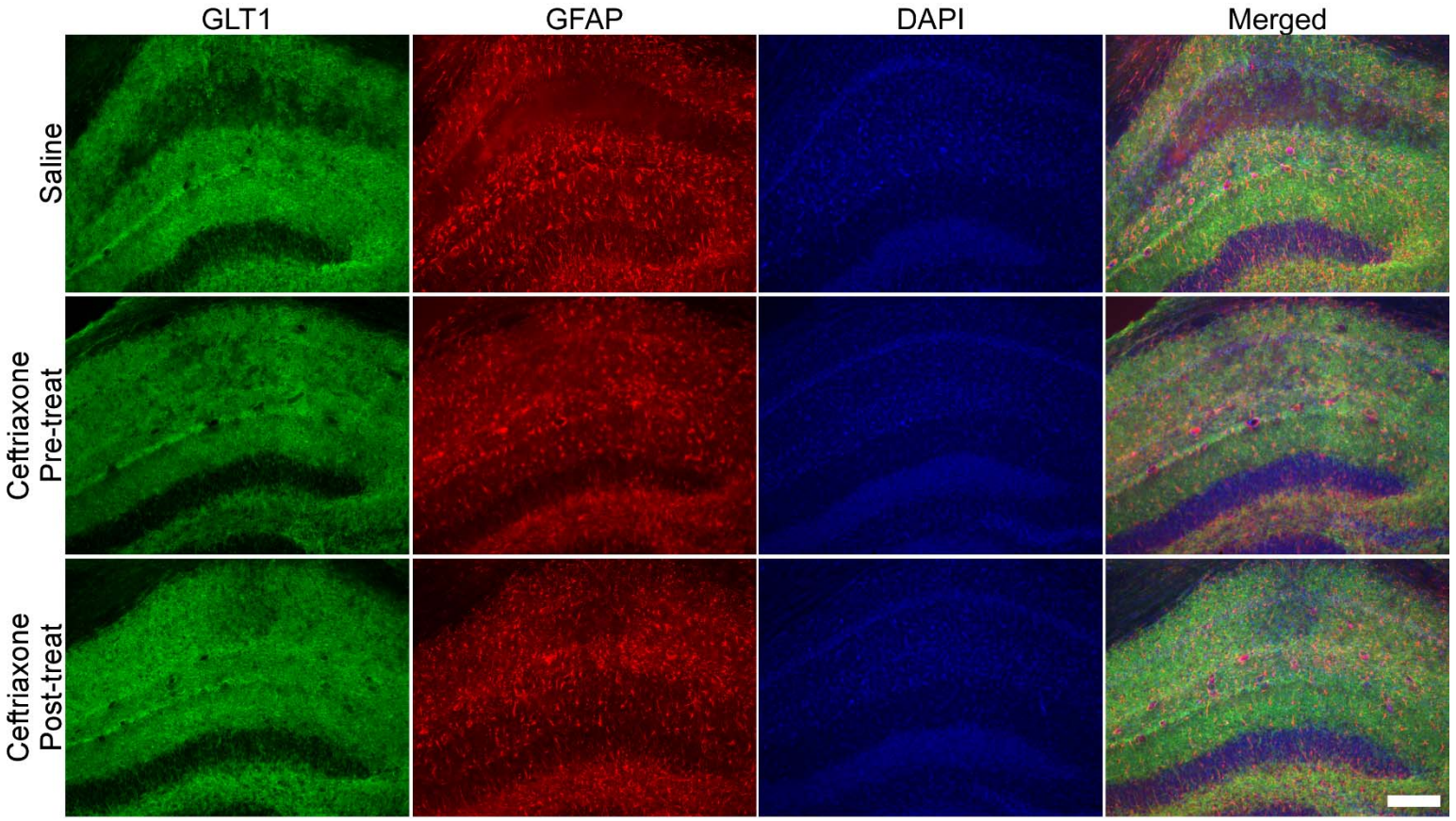


Figure 6.15. Ceftriaxone failed to ameliorate histological changes in the ipsilateral hippocampus in the intrahippocampal kainic acid (IHKA) model of epilepsy.

Glutamate transporter-1 (GLT1), glial fibrillary acidic protein (GFAP), 4,6-diamidino-2-phenylindole (DAPI), and merged immunoreactivity in the ipsilateral hippocampus after intrahippocampal kainic acid (74 nL of 20 mM solution) injections. All mice were sacrificed 7 days after IHKA injections. Upper panel: immunoreactivity after 7 days of daily i.p. saline injections. Middle panel: immunoreactivity after 7 days of daily i.p. ceftriaxone (200 mg/kg) injections before IHKA injections. Lower panel: immunoreactivity after 7 days of daily i.p. ceftriaxone (200 mg/kg) injections after IHKA injections. Scale bar = 200 μm.

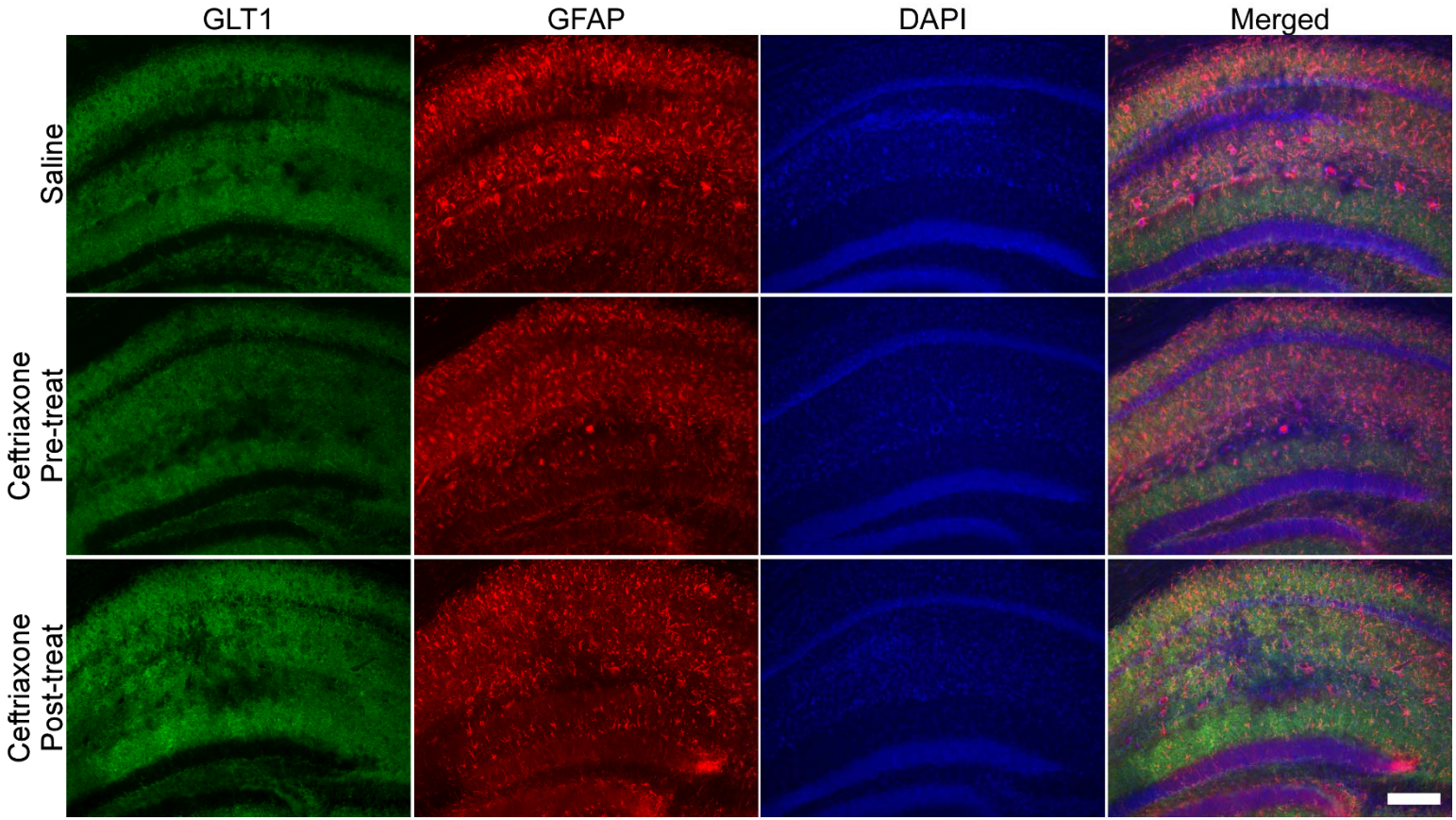


Figure 6.16. Ceftriaxone failed to ameliorate histological changes in the contralateral hippocampus in the intrahippocampal kainic acid (IHKA) model of epilepsy.
Glutamate transporter-1 (GLT1), glial fibrillary acidic protein (GFAP), 4,6-diamidino-2-phenylindole (DAPI), and merged immunoreactivity in the contralateral hippocampus after intrahippocampal kainic acid (74 nL of 20 mM solution) injections. All mice were sacrificed 7 days after IHKA injections. Upper panel: immunoreactivity after 7 days of daily i.p. saline injections. Middle panel: immunoreactivity after 7 days of daily i.p. ceftriaxone (200 mg/kg) injections before IHKA injections. Lower panel: immunoreactivity after 7 days of daily i.p. ceftriaxone (200 mg/kg) injections after IHKA injections. Scale bar = 200 μm.

6.5 Discussion

Here I have demonstrated a lack of effect of the β-lactam antibiotics ceftriaxone, clavulanic acid, and tazobactam on AQP4 and GLT1 expression in wild-type mice. GLT1 is a highly abundant protein that may represent about 1.3% of total tissue protein in the hippocampus (Lehre and Danbolt 1998). One previous study has demonstrated a lack of effect of ceftriaxone in wild-type mice but found a rescue of GLT1 protein when it was downregulated in AQP4 knockout mice (Yang, Li et al. 2013). Therefore, it is possible that the levels of GLT1 are at a "ceiling high" and β-lactam drugs are ineffective at increasing its expression unless expression levels are first reduced.

Thus far, only one study has reported that ceftriaxone can increase AQP4 expression (Lee, Ruby et al. 2013). Specifically, Lee *et al.* (2013) reported an increase in AQP4 mRNA in the caudate-putamen and nucleus accumbens in wild-type and equilibrative nucleoside transporter-1 (ENT1) knockout mice. They also reported an increase in AQP4 protein in the caudate-putamen, but no change in the nucleus accumbens (Lee, Ruby et al. 2013). The mechanism of AQP4 regulation, however, has not been addressed. I have demonstrated a lack of effect of ceftriaxone, clavulanic acid, or tazobactam on AQP4 expression in altering AQP4 expression in the cortex and hippocampus of wild-type mice. The discrepancy may lie in the genetic background of the mice (ENT1 knockout vs.

wild-type) and the area of the brain (cortex and hippocampus vs. caudate-putamen and nucleus accumbens) studied. Future studies should (1) determine the effect of ceftriaxone, if any, on AQP4 in disease models; and (2) investigate possible mechanisms of this effect.

Ceftriaxone has rescued GLT1 levels in models of ethanol withdrawal (Sari, Sakai et al. 2011; Lee, Ruby et al. 2013; Qrunfleh, Alazizi et al. 2013; Sari, Franklin et al. 2013; Sari, Sreemantula et al. 2013; Abulseoud, Camsari et al. 2014; Alhaddad, Das et al. 2014; Rao and Sari 2014; Sari, Toalston et al. 2016), substance abuse (Sari, Smith et al. 2009; Fischer, Houston et al. 2013; Dodman, Featherstone et al. 2015), ALS (Rothstein, Patel et al. 2005), visceral pain (Lin, Tian et al. 2009; Ackerman, Jellison et al. 2015), neuropathic pain (Inquimbert, Bartels et al. 2012), hypoxia (Jagadapillai, Mellen et al. 2014), ischemia (Chu, Lee et al. 2007), Huntington's disease (Miller, Dorner et al. 2008; Sari, Prieto et al. 2010), prepulse inhibition of the acoustic startle reflex (Bellesi, Melone et al. 2009), subarachnoid hemorrhage (Feng, Wang et al. 2014), spinal muscular atrophy (Nizzardo, Nardini et al. 2011), traumatic brain injury (Wei, Pan et al. 2012; Goodrich, Kabakov et al. 2013), thiamine deficiency (Jhala, Wang et al. 2011), and memory deficits in aquaporin-4 knockout mice (Li, Wang et al. 2012; Yang, Li et al. 2013). Others have demonstrated therapeutic effects of ceftriaxone, but did not investigate the levels of GLT1 in models of ischemic cortical lesions (Kim and Jones 2013), neuropathic pain (Amin, Hajhashemi et al.

2012; Hajhashemi, Hosseinzadeh et al. 2013), and seizures (Jelenkovic, Jovanovic et al. 2008; Rawls, Karaca et al. 2010). Region-specific ceftriaxone-induced increases in GLT1, with no effect in other areas of the brain, have also been reported. For example, in a model of thiamine deficiency, ceftriaxone increased GLT1 in the inferior colliculus but not the thalamus or frontal cortex (Jhala, Wang et al. 2011). The therapeutic benefit of ceftriaxone, however, has been debated. Several papers have shown that ceftriaxone does not increase levels of GLT1 (Melzer, Meuth et al. 2008; Thöne-Reineke, Neumann et al. 2008; Lai, Huang et al. 2011; Carbone, Duty et al. 2012; Cudkowicz, Titus et al. 2014), but may offer therapeutic benefits through other protective mechanisms. Clinical studies of ceftriaxone for the treatment of ALS revealed that although ceftriaxone was initially reported as tolerable and exhibiting linear pharmacokinetics (Berry, Shefner et al. 2013), ceftriaxone failed to show any clinical efficacy and resulted in adverse effects including gastrointestinal and hepatobiliary problems (Cudkowicz, Titus et al. 2014).

The therapeutic benefit of increasing GLT1 expression in an epilepsy model has been clearly demonstrated with transgenic mice (Kong, Takahashi et al. 2012). Ceftriaxone has offered anticonvulsant effects against pentylenetetrazole-evoked seizures (Jelenkovic, Jovanovic et al. 2008) and post-traumatic seizures (Goodrich, Kabakov et al. 2013), but has never been investigated in a chronic temporal lobe epilepsy model. All 3 β-lactam drugs tested in this chapter

(ceftriaxone, clavulanic acid, and tazobactam) displayed anti-seizure properties in an invertebrate seizure-like model (Rawls, Karaca et al. 2010). The effects of these β-lactam drugs on hippocampal GLT1 expression in an epilepsy model, however, have never been investigated. I have demonstrated for the first time that β-lactam drugs do not increase hippocampal GLT1 immunoreactivity in the IHKA model of TLE through the use of multiple treatment paradigms including pre-treatment, post-treatment, combined pre- and post-treatment, and varied treatment lengths using dosages that were previously reported to be effective in other models.

In this chapter, I determined that ceftriaxone may be an ineffective treatment for epileptogenesis. I have also demonstrated that GLT1 mRNA is largely unaffected in the IHKA model of epilepsy (Chapter 5; Hubbard, Szu et al. 2016), suggesting that GLT1 is downregulated at the post-transcriptional level. The proposed mechanism of action of ceftriaxone is increasing GLT1 mRNA through the nuclear factor-κB (NF-κB) pathway (Lee, Su et al. 2008). Therefore, it is possible that this treatment was ineffective due to the lack of mRNA regulation of GLT1 in the epilepsy model. Further understanding of GLT1 regulation (increased translation, post translational modifications, etc.) will be needed to find a suitable drug to ameliorate symptoms of epileptogenesis. It is interesting to note that ceftriaxone has been reported to have an anti-inflammatory effect in the brain (Melzer, Meuth et al. 2008; Wei, Pan et al. 2012). Therefore, it may be

effective at preventing the neuroinflammatory response seen in a number of epilepsy models (Hubbard and Binder 2016).

In conclusion, it is clear that modulating AQP4 and GLT1 expression could have a therapeutic effect in this model of epilepsy. The use of β-lactam drugs to do so, however, has proven to be ineffective. This is possibly due to the difference in the mechanism of action of these drugs and the mechanism of regulation of AQP4 and GLT1. Therefore, an increased understanding of the mechanism of regulation of both AQP4 and GLT1 in the IHKA model of epilepsy is needed. This would provide a more specific target for new antiepileptogenic treatment paradigms.

6.6 References

Abulseoud, O. A., U. M. Camsari, C. L. Ruby, A. Kasasbeh, S. Choi and D. S. Choi (2014). "Attenuation of ethanol withdrawal by ceftriaxone-induced upregulation of glutamate transporter EAAT2." Neuropsychopharmacology **39**(7): 1674-1684.

Ackerman, A. L., F. C. Jellison, U. J. Lee, S. Bradesi and L. V. Rodriguez (2015). "Glt1 glutamate receptor mediates the establishment and perpetuation of chronic visceral pain in an animal model of stress-induced bladder hyperalgesia." Am J Physiol Renal Physiol: ajprenal 00297 02015.

Al Awabdh, S., S. Gupta-Agarwal, D. F. Sheehan, J. Muir, R. Norkett, A. E. Twelvetrees, L. D. Griffin and J. T. Kittler (2016). "Neuronal activity mediated regulation of glutamate transporter GLT-1 surface diffusion in rat astrocytes in dissociated and slice cultures." Glia **64**(7): 1252-1264.

Alhaddad, H., S. C. Das and Y. Sari (2014). "Effects of ceftriaxone on ethanol intake: a possible role for xCT and GLT-1 isoforms modulation of glutamate levels in P rats." Psychopharmacology (Berl) **231**(20): 4049-4057.

Amin, B., V. Hajhashemi, H. Hosseinzadeh and K. Abnous (2012). "Antinociceptive evaluation of ceftriaxone and minocycline alone and in combination in a neuropathic pain model in rat." Neuroscience **224**: 15-25.

Arabadzisz, D., K. Antal, F. Parpan, Z. Emri and J. M. Fritschy (2005). "Epileptogenesis and chronic seizures in a mouse model of temporal lobe epilepsy are associated with distinct EEG patterns and selective neurochemical alterations in the contralateral hippocampus." Exp Neurol **194**(1): 76-90.

Bellesi, M., M. Melone, A. Gubbini, S. Battistacci and F. Conti (2009). "GLT-1 upregulation impairs prepulse inhibition of the startle reflex in adult rats." Glia **57**(7): 703-713.

Berry, J. D., J. M. Shefner, R. Conwit, D. Schoenfeld, M. Keroack, D. Felsenstein, L. Krivickas, W. S. David, F. Vriesendorp, A. Pestronk, J. B. Caress, J. Katz, E. Simpson, J. Rosenfeld, R. Pascuzzi, J. Glass, K. Rezania, J. D. Rothstein, D. J. Greenblatt and M. E. Cudkowicz (2013). "Design and initial results of a multi-phase randomized trial of ceftriaxone in amyotrophic lateral sclerosis." PLoS One **8**(4): e61177.

Binder, D. K., X. Yao, Z. Zador, T. J. Sick, A. S. Verkman and G. T. Manley (2006). "Increased seizure duration and slowed potassium kinetics in mice lacking aquaporin-4 water channels." Glia **53**(6): 631-636.

Bouilleret, V., V. Ridoux, A. Depaulis, C. Marescaux, A. Nehlig and G. Le Gal La Salle (1999). "Recurrent seizures and hippocampal sclerosis following intrahippocampal kainate injection in adult mice: electroencephalography, histopathology and synaptic reorganization similar to mesial temporal lobe epilepsy." Neuroscience **89**(3): 717-729.

Carbone, M., S. Duty and M. Rattray (2012). "Riluzole elevates GLT-1 activity and levels in striatal astrocytes." Neurochem Int **60**(1): 31-38.

Chen, M. L., F. Bao, Y. Q. Zhang and Z. Q. Zhao (2010). "Effects of aquaporin 4 deficiency on morphine analgesia and chronic tolerance: a study at spinal level." J Mol Neurosci **42**(2): 140-144.

Chu, K., S. T. Lee, D. I. Sinn, S. Y. Ko, E. H. Kim, J. M. Kim, S. J. Kim, D. K. Park, K. H. Jung, E. C. Song, S. K. Lee, M. Kim and J. K. Roh (2007). "Pharmacological Induction of Ischemic Tolerance by Glutamate Transporter-1 (EAAT2) Upregulation." Stroke **38**(1): 177-182.

Costa, C., R. Tortosa, A. Domenech, E. Vidal, M. Pumarola and A. Bassols (2007). "Mapping of aggrecan, hyaluronic acid, heparan sulphate proteoglycans and aquaporin 4 in the central nervous system of the mouse." J Chem Neuroanat **33**(3): 111-123.

Cudkowicz, M. E., S. Titus, M. Kearney, H. Yu, A. Sherman, D. Schoenfeld, D. Hayden, A. Shui, B. Brooks, R. Conwit, D. Felsenstein, D. J. Greenblatt, M. Keroack, J. T. Kissel, R. Miller, J. Rosenfeld, J. D. Rothstein, E. Simpson, N. Tolkoff-Rubin, L. Zinman and J. M. Shefner (2014). "Safety and efficacy of ceftriaxone for amyotrophic lateral sclerosis: a multi-stage, randomised, double-blind, placebo-controlled trial." Lancet Neurol **13**(11): 1083-1091.

Danbolt, N. C. (2001). "Glutamate uptake." Prog Neurobiol **65**(1): 1-105.

Ding, J. H., L. L. Sha, J. Chang, X. Q. Zhou, Y. Fan and G. Hu (2007). "Alterations of striatal neurotransmitter release in aquaporin-4 deficient mice: An in vivo microdialysis study." Neurosci Lett **422**(3): 175-180.

Dodman, K., R. E. Featherstone, J. Bang, Y. Liang and S. J. Siegel (2015). "Ceftriaxone reverses ketamine-induced lasting EEG and astrocyte alterations in juvenile mice." Drug Alcohol Depend **156**: 14-20.

Feng, D., W. Wang, Y. Dong, L. Wu, J. Huang, Y. Ma, Z. Zhang, S. Wu, G. Gao and H. Qin (2014). "Ceftriaxone alleviates early brain injury after subarachnoid hemorrhage by increasing excitatory amino acid transporter 2 expression via the PI3K/Akt/NF-kappaB signaling pathway." Neuroscience **268**: 21-32.

Fischer, K. D., A. C. Houston and G. V. Rebec (2013). "Role of the major glutamate transporter GLT1 in nucleus accumbens core versus shell in cue-induced cocaine-seeking behavior." J Neurosci **33**(22): 9319-9327.

Goodrich, G. S., A. Y. Kabakov, M. Q. Hameed, S. C. Dhamne, P. A. Rosenberg and A. Rotenberg (2013). "Ceftriaxone treatment after traumatic brain injury restores expression of the glutamate transporter, GLT-1, reduces regional gliosis, and reduces post-traumatic seizures in the rat." J Neurotrauma **30**(16): 1434-1441.

Hajhashemi, V., H. Hosseinzadeh and B. Amin (2013). "Antiallodynia and antihyperalgesia effects of ceftriaxone in treatment of chronic neuropathic pain in rats." Acta Neuropsychiatr **25**(1): 27-32.

Hubbard, J. A. and D. K. Binder (2016). Astrocytes and Epilepsy. Amsterdam, Netherlands, Elsevier, in press.

Hubbard, J. A., M. S. Hsu, M. M. Seldin and D. K. Binder (2015). "Expression of the Astrocyte Water Channel Aquaporin-4 in the Mouse Brain." ASN Neuro **7**(5).

Hubbard, J. A., J. I. Szu, J. M. Yonan and D. K. Binder (2016). "Regulation of astrocyte glutamate transporter-1 (GLT1) and aquaporin-4 (AQP4) expression in a model of epilepsy." Exp Neurol.

Inquimbert, P., K. Bartels, O. B. Babaniyi, L. B. Barrett, I. Tegeder and J. Scholz (2012). "Peripheral nerve injury produces a sustained shift in the balance between glutamate release and uptake in the dorsal horn of the spinal cord." Pain **153**(12): 2422-2431.

Jagadapillai, R., N. M. Mellen, L. R. Sachleben, Jr. and E. Gozal (2014). "Ceftriaxone preserves glutamate transporters and prevents intermittent hypoxia-induced vulnerability to brain excitotoxic injury." PLoS One **9**(7): e100230.

Jelenkovic, A. V., M. D. Jovanovic, D. D. Stanimirovic, D. D. Bokonjic, G. G. Ocic and B. S. Boskovic (2008). "Beneficial effects of ceftriaxone against

pentylenetetrazole-evoked convulsions." Exp Biol Med (Maywood) **233**(11): 1389-1394.

Jhala, S. S., D. Wang and A. S. Hazell (2011). "Loss of the glutamate transporter splice-variant GLT-1b in inferior colliculus and its prevention by ceftriaxone in thiamine deficiency." Neurochem Int **58**(5): 558-563.

Kim, K., S. G. Lee, T. P. Kegelman, Z. Z. Su, S. K. Das, R. Dash, S. Dasgupta, P. M. Barral, M. Hedvat, P. Diaz, J. C. Reed, J. L. Stebbins, M. Pellecchia, D. Sarkar and P. B. Fisher (2011). "Role of excitatory amino acid transporter-2 (EAAT2) and glutamate in neurodegeneration: opportunities for developing novel therapeutics." J Cell Physiol **226**(10): 2484-2493.

Kim, S. Y. and T. A. Jones (2013). "The effects of ceftriaxone on skill learning and motor functional outcome after ischemic cortical damage in rats." Restor Neurol Neurosci **31**(1): 87-97.

Kong, Q., K. Takahashi, D. Schulte, N. Stouffer, Y. Lin and C. L. Lin (2012). "Increased glial glutamate transporter EAAT2 expression reduces epileptogenic processes following pilocarpine-induced status epilepticus." Neurobiol Dis **47**(2): 145-154.

Lai, P. C., Y. T. Huang, C. C. Wu, C. J. Lai, P. J. Wang and T. H. Chiu (2011). "Ceftriaxone attenuates hypoxic-ischemic brain injury in neonatal rats." J Biomed Sci **18**: 69.

Lee, D. J., M. S. Hsu, M. M. Seldin, J. L. Arellano and D. K. Binder (2012). "Decreased expression of the glial water channel aquaporin-4 in the intrahippocampal kainic acid model of epileptogenesis." Exp Neurol **235**(1): 246-255.

Lee, M. R., C. L. Ruby, D. J. Hinton, S. Choi, C. A. Adams, N. Young Kang and D. S. Choi (2013). "Striatal adenosine signaling regulates EAAT2 and astrocytic AQP4 expression and alcohol drinking in mice." Neuropsychopharmacology **38**(3): 437-445.

Lee, S. G., Z. Z. Su, L. Emdad, P. Gupta, D. Sarkar, A. Borjabad, D. J. Volsky and P. B. Fisher (2008). "Mechanism of ceftriaxone induction of excitatory amino acid transporter-2 expression and glutamate uptake in primary human astrocytes." J Biol Chem **283**(19): 13116-13123.

Lehre, K. P. and N. C. Danbolt (1998). "The number of glutamate transporter subtype molecules at glutamatergic synapses: chemical and stereological quantification in young adult rat brain." J Neurosci **18**(21): 8751-8757.

Li, S., M. Mallory, M. Alford, S. Tanaka and E. Masliah (1997). "Glutamate transporter alterations in Alzheimer disease are possibly associated with abnormal APP expression." J Neuropathol Exp Neurol **56**(8): 901-911.

Li, Y. K., F. Wang, W. Wang, Y. Luo, P. F. Wu, J. L. Xiao, Z. L. Hu, Y. Jin, G. Hu and J. G. Chen (2012). "Aquaporin-4 deficiency impairs synaptic plasticity and associative fear memory in the lateral amygdala: involvement of downregulation of glutamate transporter-1 expression." Neuropsychopharmacology **37**(8): 1867-1878.

Lin, Y., G. Tian, K. Roman, C. Handy, J. B. Travers, C. L. Lin and R. L. Stephens, Jr. (2009). "Increased glial glutamate transporter EAAT2 expression reduces visceral nociceptive response in mice." Am J Physiol Gastrointest Liver Physiol **296**(1): G129-134.

Ma, T., B. Yang, A. Gillespie, E. J. Carlson, C. J. Epstein and A. S. Verkman (1997). "Generation and phenotype of a transgenic knockout mouse lacking the mercurial-insensitive water channel aquaporin-4." J Clin Invest **100**(5): 957-962.

Melzer, N., S. G. Meuth, D. Torres-Salazar, S. Bittner, A. L. Zozulya, C. Weidenfeller, A. Kotsiari, M. Stangel, C. Fahlke and H. Wiendl (2008). "A beta-lactam antibiotic dampens excitotoxic inflammatory CNS damage in a mouse model of multiple sclerosis." PLoS One **3**(9): e3149.

Miller, B. R., J. L. Dorner, M. Shou, Y. Sari, S. J. Barton, D. R. Sengelaub, R. T. Kennedy and G. V. Rebec (2008). "Up-regulation of GLT1 expression increases glutamate uptake and attenuates the Huntington's disease phenotype in the R6/2 mouse." Neuroscience **153**(1): 329-337.

Murphy-Royal, C., J. P. Dupuis, J. A. Varela, A. Panatier, B. Pinson, J. Baufreton, L. Groc and S. H. Oliet (2015). "Surface diffusion of astrocytic glutamate transporters shapes synaptic transmission." Nat Neurosci **18**(2): 219-226.

Nagelhus, E. A., T. M. Mathiisen and O. P. Ottersen (2004). "Aquaporin-4 in the central nervous system: cellular and subcellular distribution and coexpression with KIR4.1." Neuroscience **129**(4): 905-913.

Nielsen, S., E. A. Nagelhus, M. Amiry-Moghaddam, C. Bourque, P. Agre and O. P. Ottersen (1997). "Specialized membrane domains for water transport in glial cells: high-resolution immunogold cytochemistry of aquaporin-4 in rat brain." J Neurosci **17**(1): 171-180.

Nizzardo, M., M. Nardini, D. Ronchi, S. Salani, C. Donadoni, F. Fortunato, G. Colciago, M. Falcone, C. Simone, G. Riboldi, A. Govoni, N. Bresolin, G. P. Comi and S. Corti (2011). "Beta-lactam antibiotic offers neuroprotection in a spinal muscular atrophy model by multiple mechanisms." Exp Neurol **229**(2): 214-225.

Oshio, K., D. K. Binder, B. Yang, S. Schecter, A. S. Verkman and G. T. Manley (2004). "Expression of aquaporin water channels in mouse spinal cord." Neuroscience **127**(3): 685-693.

Paxinos, G. and K. B. J. Franklin (2001). The mouse brain in stereotaxic coordinates. San Diego, CA, Academic Press.

Qrunfleh, A. M., A. Alazizi and Y. Sari (2013). "Ceftriaxone, a beta-lactam antibiotic, attenuates relapse-like ethanol-drinking behavior in alcohol-preferring rats." J Psychopharmacol **27**(6): 541-549.

Racine, R. J. (1972). "Modification of seizure activity by electrical stimulation. II. Motor seizure." Electroencephalogr Clin Neurophysiol **32**(3): 281-294.

Rao, P. S. and Y. Sari (2014). "Effects of ceftriaxone on chronic ethanol consumption: a potential role for xCT and GLT1 modulation of glutamate levels in male P rats." J Mol Neurosci **54**(1): 71-77.

Rasmussen, B. A., D. A. Baron, J. K. Kim, E. M. Unterwald and S. M. Rawls (2011). "beta-Lactam antibiotic produces a sustained reduction in extracellular glutamate in the nucleus accumbens of rats." Amino Acids **40**(2): 761-764.

Rawls, S. M., F. Karaca, I. Madhani, V. Bhojani, R. L. Martinez, M. Abou-Gharbia and R. B. Raffa (2010). "beta-lactamase inhibitors display anti-seizure properties in an invertebrate assay." Neuroscience **169**(4): 1800-1804.

Riban, V., V. Bouilleret, B. T. Pham-Le, J. M. Fritschy, C. Marescaux and A. Depaulis (2002). "Evolution of hippocampal epileptic activity during the development of hippocampal sclerosis in a mouse model of temporal lobe epilepsy." Neuroscience **112**(1): 101-111.

Rothstein, J. D., S. Patel, M. R. Regan, C. Haenggeli, Y. H. Huang, D. E. Bergles, L. Jin, M. Dykes Hoberg, S. Vidensky, D. S. Chung, S. V. Toan, L. I. Bruijn, Z. Z. Su, P. Gupta and P. B. Fisher (2005). "Beta-lactam antibiotics offer neuroprotection by increasing glutamate transporter expression." Nature **433**(7021): 73-77.

Rothstein, J. D., M. Van Kammen, A. I. Levey, L. J. Martin and R. W. Kuncl (1995). "Selective loss of glial glutamate transporter GLT-1 in amyotrophic lateral sclerosis." Ann Neurol **38**(1): 73-84.

Sari, Y., K. M. Franklin, A. Alazizi, P. S. Rao and R. L. Bell (2013). "Effects of ceftriaxone on the acquisition and maintenance of ethanol drinking in peri-adolescent and adult female alcohol-preferring (P) rats." Neuroscience **241**: 229-238.

Sari, Y., A. L. Prieto, S. J. Barton, B. R. Miller and G. V. Rebec (2010). "Ceftriaxone-induced up-regulation of cortical and striatal GLT1 in the R6/2 model of Huntington's disease." J Biomed Sci **17**: 62.

Sari, Y., M. Sakai, J. M. Weedman, G. V. Rebec and R. L. Bell (2011). "Ceftriaxone, a beta-lactam antibiotic, reduces ethanol consumption in alcohol-preferring rats." Alcohol Alcohol **46**(3): 239-246.

Sari, Y., K. D. Smith, P. K. Ali and G. V. Rebec (2009). "Upregulation of GLT1 attenuates cue-induced reinstatement of cocaine-seeking behavior in rats." J Neurosci **29**(29): 9239-9243.

Sari, Y., S. N. Sreemantula, M. R. Lee and D. S. Choi (2013). "Ceftriaxone treatment affects the levels of GLT1 and ENT1 as well as ethanol intake in alcohol-preferring rats." J Mol Neurosci **51**(3): 779-787.

Sari, Y., J. E. Toalston, P. S. Rao and R. L. Bell (2016). "Effects of ceftriaxone on ethanol, nicotine or sucrose intake by alcohol-preferring (P) rats and its association with GLT-1 expression." Neuroscience **326**: 117-125.

Skucas, V. A., I. B. Mathews, J. Yang, Q. Cheng, A. Treister, A. M. Duffy, A. S. Verkman, B. L. Hempstead, M. A. Wood, D. K. Binder and H. E. Scharfman (2011). "Impairment of select forms of spatial memory and neurotrophin-dependent synaptic plasticity by deletion of glial aquaporin-4." J Neurosci **31**(17): 6392-6397.

Thöne-Reineke, C., C. Neumann, P. Namsolleck, K. Schmerbach, M. Krikov, J. H. Schefe, K. Lucht, H. Hörtnagl, M. Godes, S. Muller, K. Rumschüssel, H. Funke-Kaiser, A. Villringer, U. M. Steckelings and T. Unger (2008). "The beta-lactam antibiotic, ceftriaxone, dramatically improves survival, increases glutamate uptake and induces neurotrophins in stroke." J Hypertens **26**(12): 2426-2435.

Wei, J., X. Pan, Z. Pei, W. Wang, W. Qiu, Z. Shi and G. Xiao (2012). "The beta-lactam antibiotic, ceftriaxone, provides neuroprotective potential via anti-

excitotoxicity and anti-inflammation response in a rat model of traumatic brain injury." J Trauma Acute Care Surg **73**(3): 654-660.

Wu, N., X. Q. Lu, H. T. Yan, R. B. Su, J. F. Wang, Y. Liu, G. Hu and J. Li (2008). "Aquaporin 4 deficiency modulates morphine pharmacological actions." Neurosci Lett **448**(2): 221-225.

Yang, J., M. X. Li, Y. Luo, T. Chen, J. Liu, P. Fang, B. Jiang, Z. L. Hu, Y. Jin, J. G. Chen and F. Wang (2013). "Chronic ceftriaxone treatment rescues hippocampal memory deficit in AQP4 knockout mice via activation of GLT-1." Neuropharmacology **75**: 213-222.

Chapter 7: Lack of a physical interaction between glutamate transporter-1 (GLT1) and aquaporin-4 (AQP4)

7.1 Abstract

Maintenance of glutamate and water homeostasis in the brain is crucial to healthy brain activity. Astrocytic glutamate transporter-1 (GLT1) and aquaporin-4 (AQP4) are the main regulators of extracellular glutamate and osmolarity, respectively. Several studies have reported co-localization of GLT1 and AQP4, but the existence of a physical interaction between the two has not been well studied. Therefore, I used co-immunoprecipitation (co-IP) to determine whether a strong interaction exists between these two important molecules in mice on both a CD1 and C57BL/6 background. Furthermore, I used Western blot and immunohistochemistry to examine GLT1 levels in AQP4 knockout ($AQP4^{-/-}$) mice. I did not detect an AQP4-GLT1 precipitate, suggesting the lack of a strong physical interaction between AQP4 and GLT1. In addition, I determined that GLT1 protein levels remained unaltered in tissue from CD1 and C57BL/6 $AQP4^{-/-}$ mice. Finally, I used immunohistochemical analysis to determine that AQP4 and GLT1 do co-localize, but only in a region-specific manner. Taken together, my findings suggest that AQP4 and GLT1 do not have a strong physical interaction between them and are, instead, differentially regulated.

7.2 Introduction

The excitatory amino acid transporters are a family of five membrane proteins that are responsible for clearing glutamate from the extracellular space. Glutamate aspartate transporter (GLAST) and GLT1 are largely expressed by astrocytes; excitatory amino acid carrier-1 (EAAC1) and excitatory amino acid transporter (EAAT) 4 are predominantly found in neurons; and EAAT5 is exclusively found in rod photoreceptor and bipolar cells in the retina (Kim, Lee et al. 2011). GLT1 is responsible for the majority of glutamate clearance in the forebrain (Danbolt 2001). More recently, it was discovered that GLT1, although anchored to the membrane at synapses, can become untethered to perform rapid-activity-regulated surface diffusion to efficiently clear glutamate after synaptic activity (Murphy-Royal, Dupuis et al. 2015; Al Awabdh, Gupta-Agarwal et al. 2016). In this manner, GLT1 can shape excitatory postsynaptic currents.

A few studies have found that GLT1 co-localizes with another important brain protein, aquaporin-4 (AQP4) (Hinson, Roemer et al. 2008; Lee, Ruby et al. 2013; Yang, Li et al. 2013; Mogoanta, Ciurea et al. 2014). A member of the aquaporin family of water channels, AQP4 and is responsible for bi-directional fluid exchange in response to changes in the osmotic gradient. AQP4 is the main water channel in the CNS and, like GLT1, is found almost exclusively on astrocytes (Nielsen, Nagelhus et al. 1997; Nagelhus, Mathiisen et al. 2004; Hsu,

Seldin et al. 2011). AQP4 exhibits highly polarized expression with abundant levels found at sites of fluid transport, such as ventricular membranes, glia limitans, as well as pial and ependymal surfaces in contact with cerebrospinal fluid (Nielsen, Nagelhus et al. 1997; Rash, Yasumura et al. 1998; Nagelhus, Mathiisen et al. 2004; Oshio, Binder et al. 2004; Costa, Tortosa et al. 2007; Hubbard, Hsu et al. 2015).

Since the generation of AQP4 knockout ($AQP4^{-/-}$) mice (Ma, Yang et al. 1997), several different functions of AQP4 have been elucidated. It is now known that AQP4 plays a variety of roles in the brain, including (but not limited to) synaptic plasticity (Skucas, Mathews et al. 2011; Scharfman and Binder 2013), K^+ buffering (Binder, Yao et al. 2006), and macromolecular diffusion in the brain extracellular space (Binder, Papadopoulos et al. 2004). Therefore, $AQP4^{-/-}$ mice exhibit several deficits such as cognitive impairment (Skucas, Mathews et al. 2011; Fan, Liu et al. 2013; Scharfman and Binder 2013; Szu and Binder 2016), perturbed K^+ homeostasis (Strohschein, Hüttmann et al. 2011; Haj-Yasein, Bugge et al. 2015), and an enlarged extracellular space (Yao, Hrabetova et al. 2008; Haj-Yasein, Jensen et al. 2012).

Reduced levels of GLT1 protein have been reported in $AQP4^{-/-}$ mice (Zeng, Sun et al. 2007; Wu, Lu et al. 2008; Chen, Bao et al. 2010; Li, Wang et al. 2012; Yan, Wu et al. 2013; Yang, Li et al. 2013; Kong, Zeng et al. 2014). Therefore, this

expression and functional downregulation has been used to explain some of the impairments seen in AQP4$^{-/-}$ mice. For example, downregulation of GLT1 has been hypothesized to play a role in synaptic plasticity and memory formation deficits in the AQP4$^{-/-}$ mice (Li, Wang et al. 2012; Szu and Binder 2016). One study found an interaction between AQP4 and GLT1 in transfected HEK293 cells (Hinson, Roemer et al. 2008). A physical interaction between AQP4 and GLT1, however, has never been confirmed in tissue from healthy, wild-type mice. Therefore, I performed co-immunopreciptation on both C57BL/6 and CD1 mice. I found no AQP4-GLT1 precipitate. Furthermore, I used Western blotting and immunohistochemistry to demonstrate no altered GLT1 protein expression in AQP4$^{-/-}$ mice compared to wild-type mice. Therefore, a physical interaction between AQP4 and GLT1 is unlikely, although a weak interaction between the two proteins cannot be ruled out.

7.3 Methods

7.3.1 Animals

All experiments were conducted in accordance with National Institutes of Health guidelines and were approved by the University of California, Riverside Institutional Animal Care and Use Committee (IACUC). Animals were housed under a 12-hour light/dark cycle with food and water provided *ad libitum*. CD1

and C57BL/6 wild-type and AQP4 knockout mice were used. All animals were 8-10 weeks old.

7.3.2 Tissue collection

Mice were euthanized with fatal plus (Western Medical Supply) and perfused with phosphate buffered saline (PBS), pH 7.4, with protease inhibitors (Roche). Whole brains were quickly removed from C57BL/6 wild-type (n = 6), C57BL/6 AQP4$^{-/-}$ (n = 6), CD1 wild-type (n = 6), and CD1 AQP4$^{-/-}$ (n = 5) mice. A separate subset of mice were euthanized, perfused, and hippocampal and cortex tissue was microdissected out from C57BL/6 wild-type (n = 7), C57BL/6 AQP4$^{-/-}$ (n = 7), CD1 wild-type (n = 5), and CD1 AQP4$^{-/-}$ (n = 5) mice. Harvested tissue was homogenized using the Bullet Blender (Next Advance) and protein concentration was quantified via Bradford assay. Protein was frozen at -80°C until further processing.

For immunohistochemistry, C57BL/6 wild-type (n = 3), C57BL/6 AQP4 knockout (n = 3), CD1 wild-type (n = 3), and CD1 AQP4 knockout (n = 3) mice were transcardially perfused with ice-cold phosphate buffered saline (PBS), pH 7.4, followed by 4% paraformaldehyde, pH 7.4. Brains were quickly removed and postfixed in 4% paraformaldehyde overnight at 4°C followed by two days of

cryoprotection in 30% sucrose in PBS at 4°C. Brains were then frozen and stored at -80°C until further use.

7.3.3 Co-immunoprecipitation (co-IP)

Protein A agarose bead slurry (Roche) was equilibrated with 1% NP-40 substitute lysis buffer (50 mM Tris-HCl, pH 8; 150 mM NaCl; 1% NP-40 substitute). Protein samples (50 µg) were pre-cleared by incubation with the equilibrated beads and then added to a new tube. Rabbit anti-AQP4 (Millipore ABN411), mouse anti-GLT1 (C-terminal polyclonal antibody (Rothstein, Martin et al. 1994)), normal rabbit IgG (Invitrogen 10500C), or normal mouse IgG (Invitrogen 10400C) was added to the samples, which were then incubated overnight under rotation at 4°C. The next day, protein A agarose beads were added to each sample and incubated for 3 hours under rotation at 4°C. Samples were centrifuged and supernatant removed (but saved). Beads with bound sample were then washed with 1% NP-40 lysis buffer. Finally, an SDS loading buffer was added to each sample and samples were then boiled at 120°C for 10 minutes to both denature the protein and separate it from the beads. All tubes were centrifuged and the supernatant was saved for Western blot.

7.3.4 Western blot

Protein was resolved by SDS-PAGE using 10% polyacrylamide gels and then transferred to a nitrocellulose membrane. Membranes containing co-immunoprecipitated protein samples were probed with rabbit anti-AQP4 (1:1,000, Millipore ABN411) or mouse anti GLT1 (1:2,500 of a C-terminal polyclonal antibody (Rothstein, Martin et al. 1994)). Membranes containing whole brain, hippocampal, or cortical protein for quantification were probed with rabbit anti-GLT1 (1:5,000 of a C-terminal polyclonal antibody (Rothstein, Martin et al. 1994)) and mouse anti-β-actin (1:5,000, Sigma A1978) as an internal control. Bands were visualized using the Li-COR Odyssey Fc Western Imaging System. GLT1 lower bands were normalized to internal β-actin bands for quantification.

7.3.5 Immunohistochemistry

Brains were thawed and cut into 50 µm sagittal sections using a cryostat (Leica CM 1950, Leica Microsytems, Bannockburn, IL) and slices were stored in PBS at 4°C. Two slices from each animal (n = 3 for each group) were used. Endogenous peroxidase activity was quenched by incubating slices in 3% H_2O_2 for 1 hour at room temperature. This was followed by a 1 hour blocking step with 5% normal goat serum in 0.1 M PBS. Slices were then incubated with primary antibody to AQP4 (1:200, Millipore ABN411) and/or GLT1 (1:200, C-terminal

polyclonal antibody (Rothstein, Martin et al. 1994)) in 0.3% Triton X-100 overnight at 4°C. After washing slices with PBS, sections were incubated with species-specific secondary antibody conjugated with Alexa 488 or 594 and a tyramide signaling amplification (TSA) kit (Molecular Probes/Invitrogen) for visualization. Slices were mounted in Vectorshield with DAPI (Vector Laboratories) and confocal images were taken using the Leica SP5 inverted microscope.

7.4 Results

7.4.1 AQP4 and GLT1 do not co-immunoprecipitate

Co-immunoprecipitation was used to determine whether a physical interaction exists between AQP4 and GLT1. I found, however, no resulting precipitate in whole brain tissue from C57BL/6 (Figure 7.1) or CD1 (Figure 7.2) mice under the conditions of 1% NP-40 lysis buffer. Both proteins were only detectable in the supernatant, representing the unbound population of protein. As positive controls, I determined that both AQP4 and GLT1 can be successfully immunoblotted after immunoprecipitation. When no antibodies or only mouse or rabbit IgG were immunoprecipitated, neither AQP4 nor GLT1 were detected with immunoblotting. In addition, I immunoblotted AQP4 after immunoprecipitation of GLT1 in $AQP4^{-/-}$ tissue and saw no detectable AQP4 band in either the

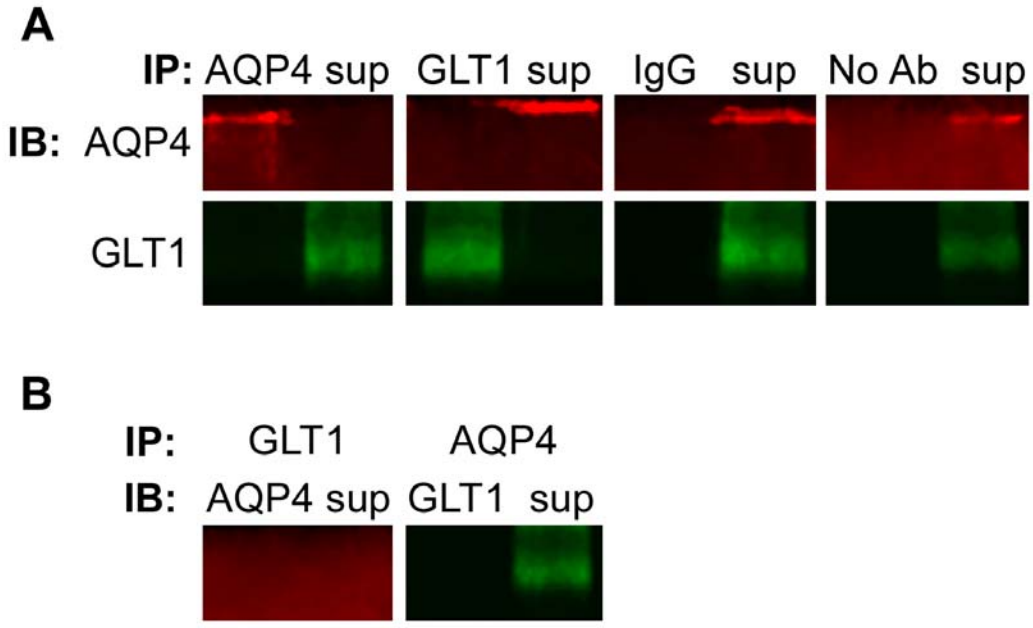


Figure 7.1. Lack of co-immunoprecipitation between glutamate transporter-1 (GLT1) and aquaporin-4 (AQP4) in C57BL/6 mice.
A. Co-immunoprecipitation of AQP4 and GLT1 in C57BL/6 wild-type mice. Representative images of AQP4, GLT1, normal IgG (mouse or rabbit), and no antibodies immunoprecipitated (IP) and either AQP4 or GLT1 immunoblotted (IB). In addition, the supernatant (sup) from each sample was also run to represent the unbound sample. **B.** Co-immunoprecipitation of GLT1 and AQP4 in C57BL/6 AQP4$^{-/-}$ tissue. After GLT1 was immunoprecipitated (IP), AQP4 was not detected in either the IP sample or the supernatant (sup). GLT1, however, was detected in the supernatant (but not the IP sample) after AQP4 was immunoprecipitated.

immunoprecipitated sample or the supernatant. When AQP4 was immunoprecipitated out from AQP4$^{-/-}$ tissue, GLT1 was only detectable in the supernatant (unbound) sample, as expected. Therefore, a strong physical interaction between AQP4 and GLT1 is unlikely.

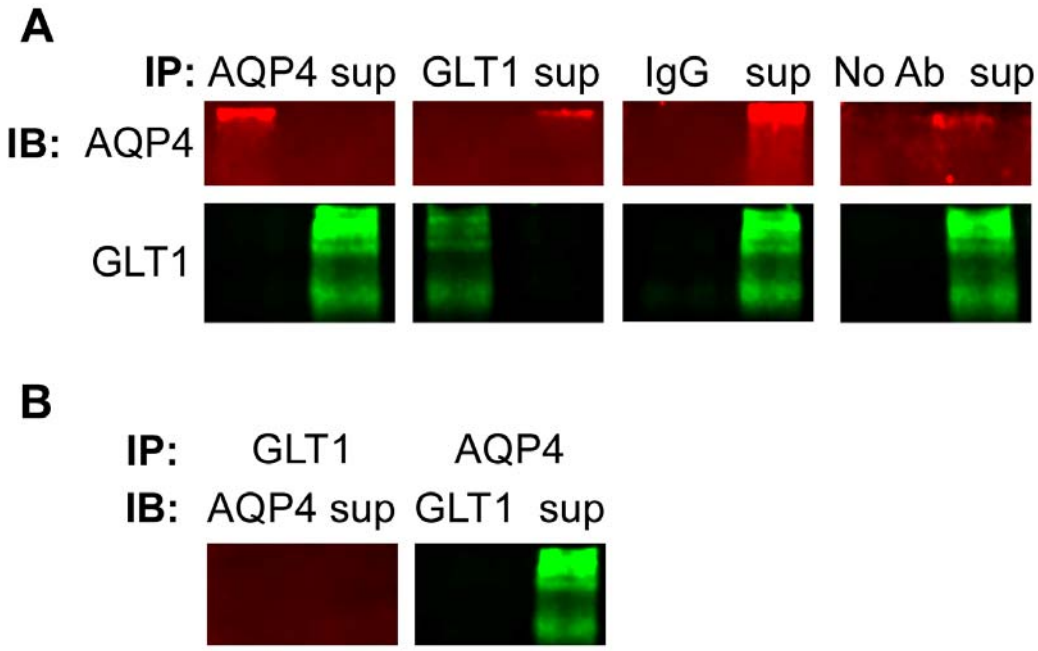


Figure 7.2. Lack of co-immunoprecipitation between glutamate transporter-1 (GLT1) and aquaporin-4 (AQP4) in CD1 mice.
A. Co-immunoprecipitation of AQP4 and GLT1 in CD1 wild-type mice. Representative images of AQP4, GLT1, normal IgG (mouse or rabbit), and no antibodies immunoprecipitated (IP) and either AQP4 or GLT1 immunoblotted (IB). In addition, the supernatant (sup) from each sample was also run to represent the unbound sample. **B.** Co-immunoprecipitation of GLT1 and AQP4 in CD1 AQP4$^{-/-}$ tissue. After GLT1 was immunoprecipitated (IP), AQP4 was not detected in either the IP sample or the supernatant (sup). GLT1, however, was detected in the supernatant (but not the IP sample) after AQP4 was immunoprecipitated.

7.4.2 GLT1 expression levels are not altered in AQP4 knockout mice

It is possible, however, for proteins to have a weak interaction that was not detected in our conditions. Therefore, I hypothesized that if GLT1 does interact with AQP4, then GLT1 levels may be downregulated in AQP4$^{-/-}$ mice. I

measured GLT1 protein levels in wild-type and AQP4$^{-/-}$ mice. I found no significant difference in GLT1 protein levels in whole brain tissue in either C57BL/6 or CD1 AQP4$^{-/-}$ mice compared to wild-type mice (Figure 7.3).

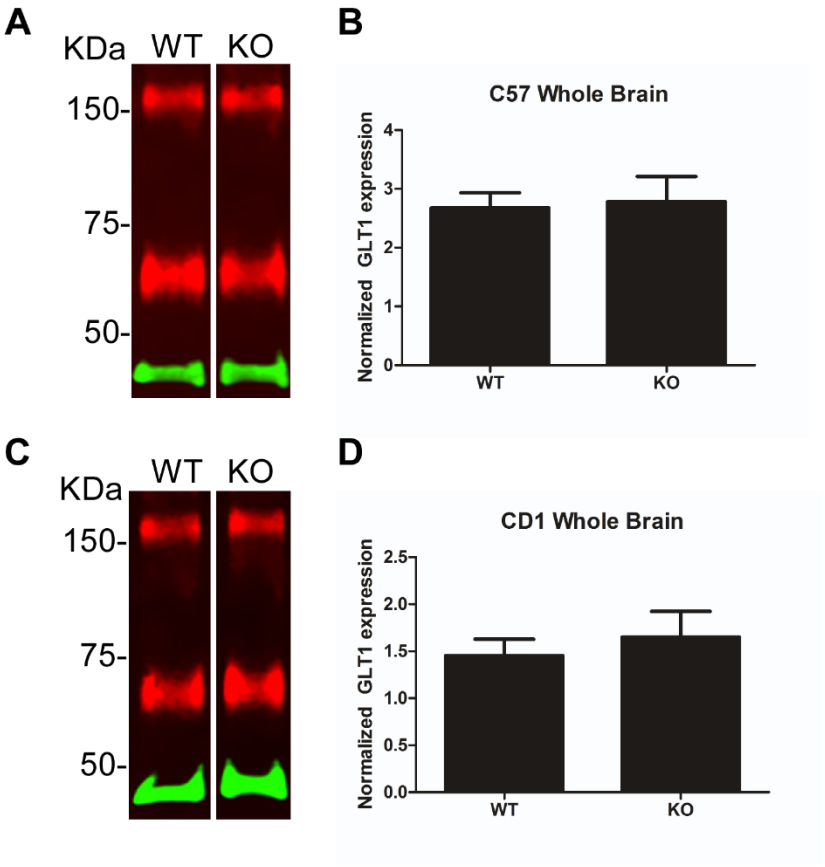


Figure 7.3. Glutamate transporter-1 (GLT1) protein expression in whole brain tissue from C57BL/6 and CD1 wild-type and aquaporin-4 (AQP4) knockout mice.
A. Representative Western blot of GLT1 (red) and β-actin (green) protein in whole brain tissue from C57BL/6 wild-type (WT) and AQP4 knockout (KO) mice. **B.** Quantification of whole brain tissue from C57BL/6 WT (n = 6) and KO (n = 6) mice. **C.** Representative Western blot of GLT1 (red) and β-actin (green) protein in whole brain tissue from CD1 wild-type (WT) and AQP4 knockout (KO) mice. **D.** Quantification of whole brain tissue from CD1 WT (n = 6) and KO (n = 5) mice. KDa = kilodaltons.

I next decided to look for region-specific downregulation of GLT1. Since GLT1 is the predominant glutamate transporter in the forebrain, I microdissected out hippocampal and cortex tissue and analyzed it for GLT1 levels. I found no

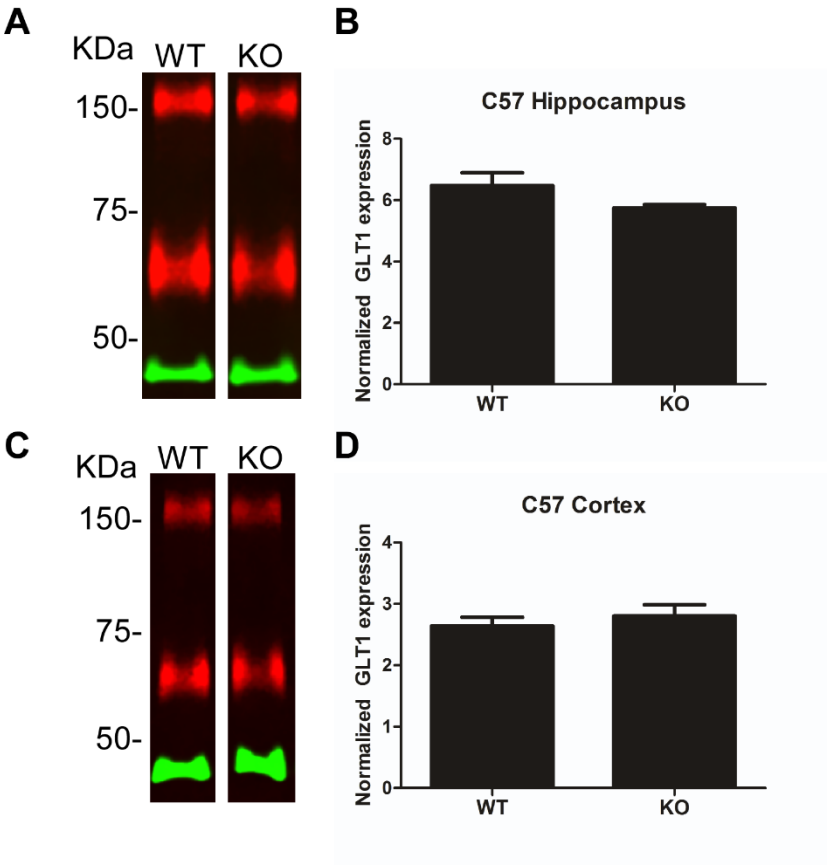


Figure 7.4. Glutamate transporter-1 (GLT1) protein expression in hippocampal and cortical tissue from C57BL/6 wild-type and aquaporin-4 knockout (AQP4) knockout mice.
A. Representative Western blot of GLT1 (red) and β-actin (green) protein in hippocampal tissue from C57BL/6 wild-type (WT) and AQP4 knockout (KO) mice. **B.** Quantification of hippocampal tissue from C57BL/6 WT (n = 7) and KO (n = 7) mice. **C.** Representative Western blot of GLT1 (red) and β-actin (green) protein in cortical tissue from C57BL/6 wild-type (WT) and AQP4 knockout (KO) mice. **D.** Quantification of cortical tissue from C57BL/6 WT (n = 7) and KO (n = 7) mice. KDa = kilodaltons.

changes in hippocampal or cortex levels of GLT1 in C57BL/6 AQP4$^{-/-}$ mice compared to C57BL/6 wild-type animals (Figure 7.4). This was confirmed with immunohistochemistry demonstrating no changes in GLT1 localization patterns

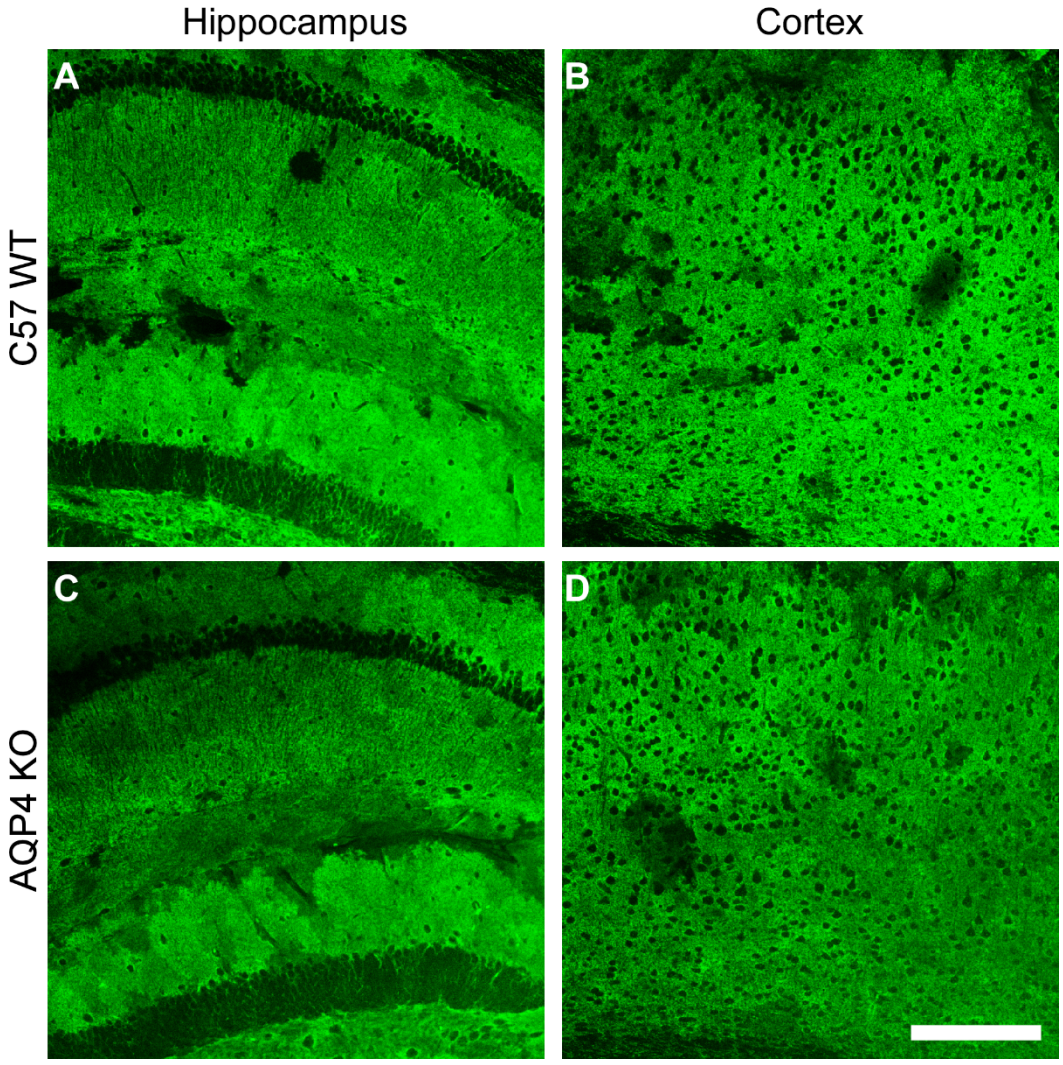


Figure 7.5. Glutamate transporter-1 (GLT1) immunoreactivity in C57BL/6 wild-type aquaporin-4 (AQP4) knockout mice.
20x images of GLT1 immunoreactivity in C57BL/6 wild-type **(A, B)** and AQP4 knockout **(C,D)** mice. Representative images of the hippocampus **(A, C)** and cortex **(B, D)** are shown. Scale bar = 200 µm. For each group, 2 slices from each animal (n = 3) were used.

in the hippocampus or cortex of C57BL/6 AQP4$^{-/-}$ mice (Figure 7.5). Similarly, no change in GLT1 protein (Figure 7.6) or immunoreactivity (Figure 7.7) levels were

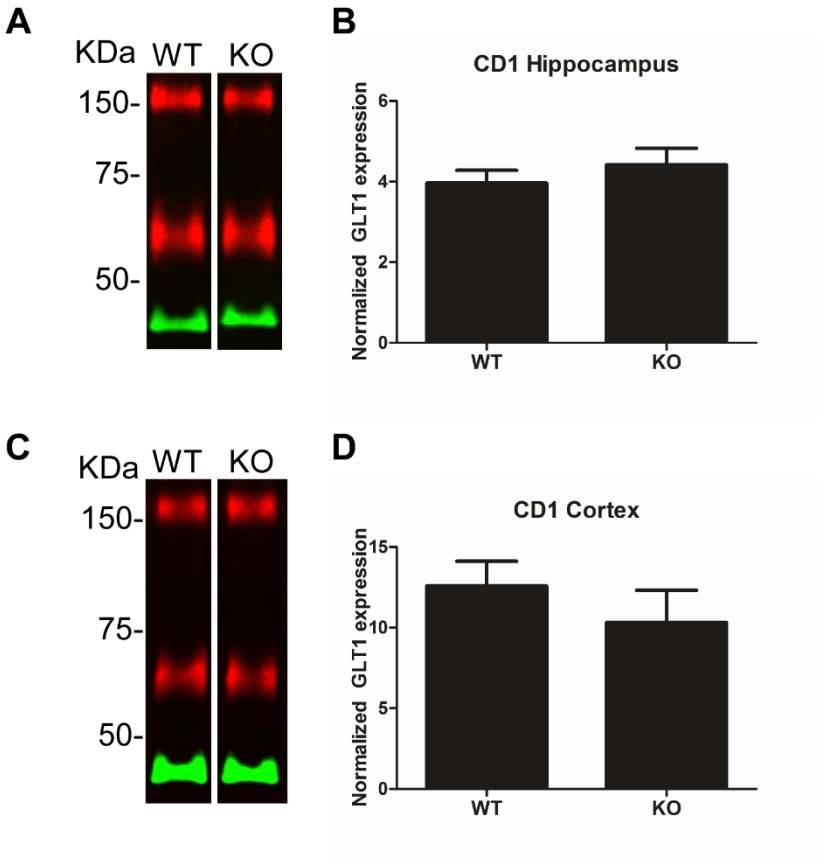


Figure 7.6. Glutamate transporter-1 (GLT1) protein expression in hippocampal and cortical tissue from CD1 wild-type and aquaporin-4 (AQP4) knockout mice.
A. Representative Western blot of GLT1 (red) and β-actin (green) protein in hippocampal tissue from CD1 wild-type (WT) and AQP4 knockout (KO) mice. **B.** Quantification of hippocampal tissue from CD1 WT (n = 5) and KO (n = 5) mice. **C.** Representative Western blot of GLT1 (red) and β-actin (green) protein in cortical tissue from CD1 wild-type (WT) and AQP4 knockout (KO) mice. **D.** Quantification of cortical tissue from CD1 WT (n = 5) and KO (n = 5) mice. KDa = kilodaltons.

observed in the hippocampus or cortex of CD1 AQP4$^{-/-}$ mice compared to wild-type mice.

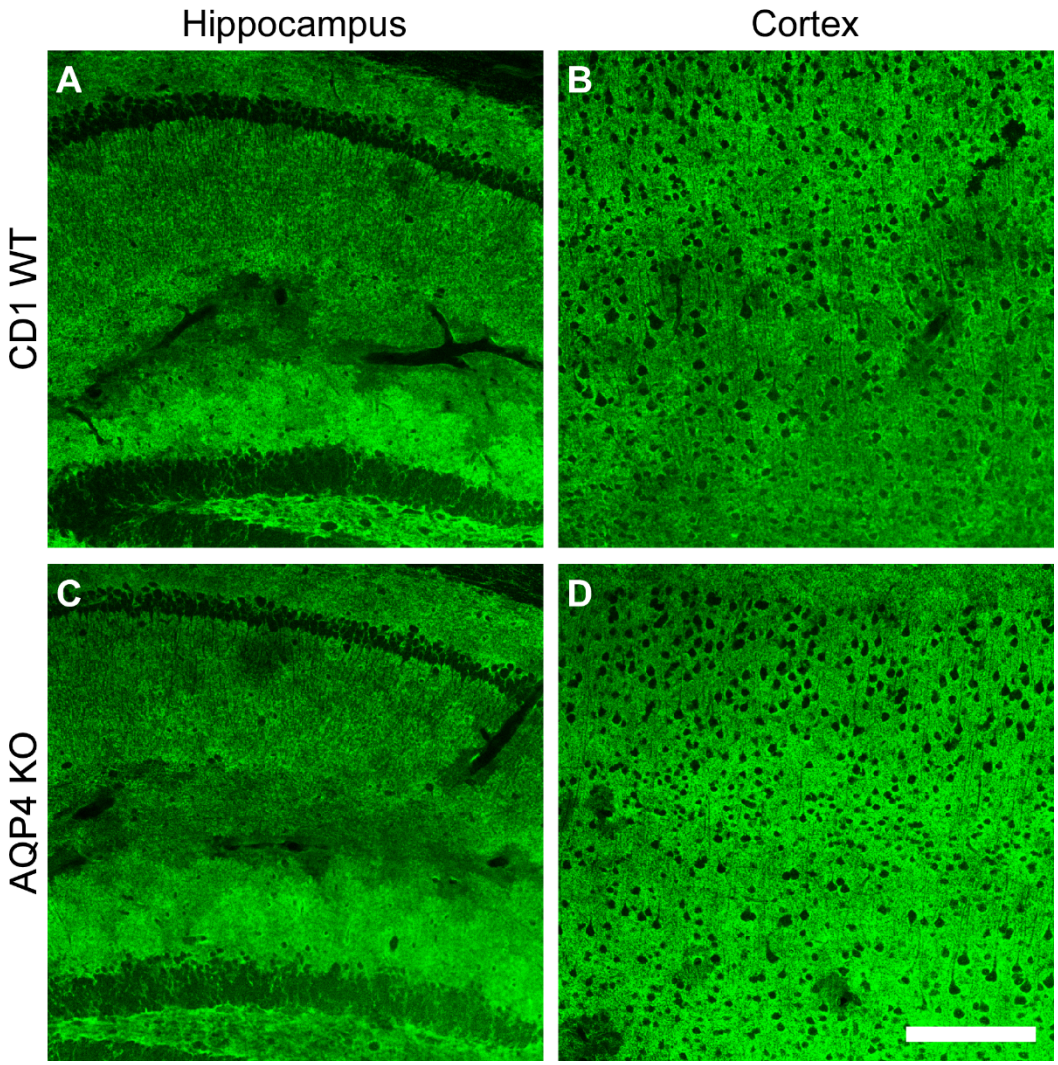


Figure 7.7. Glutamate transporter-1 (GLT1) immunoreactivity in CD1 wild-type and aquaporin-4 (AQP4) knockout mice.
20x images of GLT1 immunoreactivity in CD1 wild-type **(A, B)** and AQP4 knockout **(C,D)** mice. Representative images of the hippocampus **(A, C)** and cortex **(B, D)** are shown. Scale bar = 200 µm. For each group, 2 slices from each animal (n = 3) were used.

7.4.3 AQP4 and GLT1 co-localize in the brain

Finally, I examined both AQP4 and GLT1 immunoreactivity to determine whether any co-localization exists between these two proteins in the hippocampus of C57BL/6 and CD1 mice (Figure 7.8). GLT1 is highly expressed throughout the mouse hippocampus whereas AQP4 is largely found on astrocyte end-feet surrounding capillaries and in the stratum lacunosum moleculare (SLM) layer of

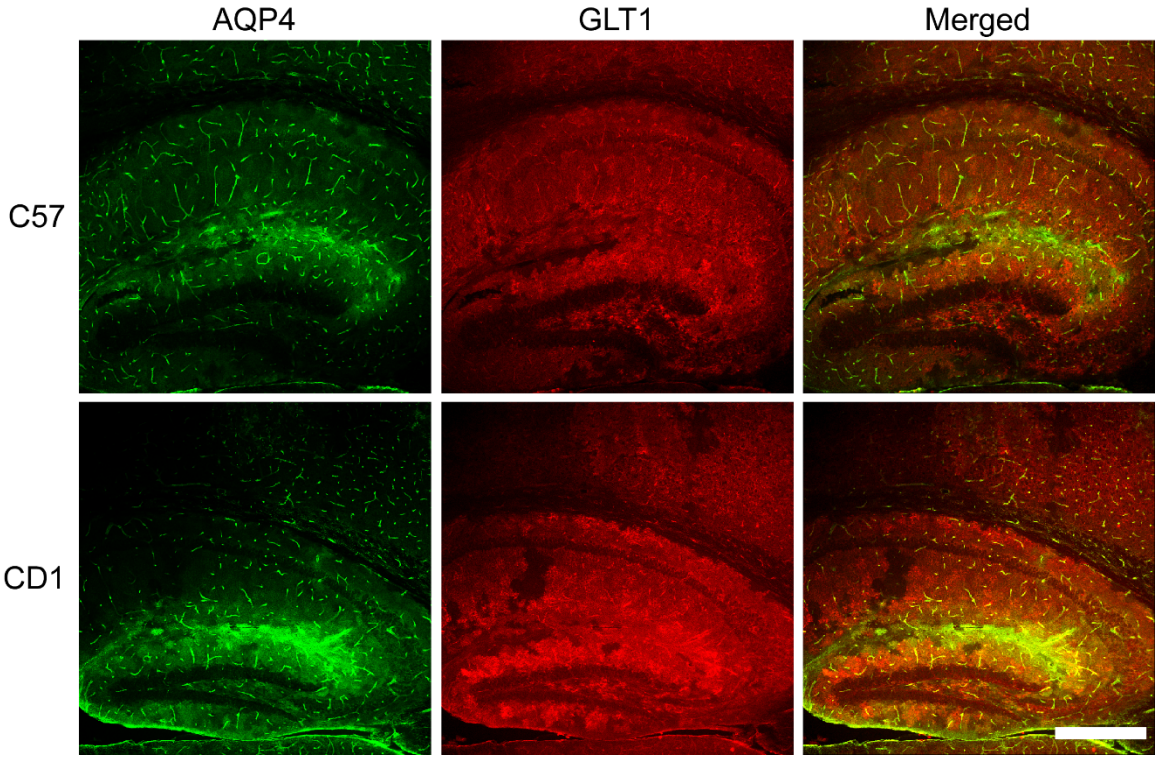


Figure 7.8. Aquaporin-4 (AQP4) and glutamate transporter-1 (GLT1) immunoreactivity in C57BL/6 and CD1 wild-type mice.
10x images of AQP4 (green), GLT1 (red), and merged immunoreactivity of the hippocampus of C57BL/6 (top panels) and CD1 (bottom panels) wild-type mice. Scale bar = 200 µm.

the hippocampus. AQP4 and GLT1 are highly co-localized in the SLM of both C57BL/6 and CD1 mice but lack co-localization in other layers of the hippocampus such as such as the stratum oriens and stratum radiatum. A small portion of the cortex can also be seen, demonstrating AQP4 and GLT1 co-expression again on astrocyte end-feet surrounding capillaries but only GLT1 cellular membrane expression throughout the cortex. Higher magnification

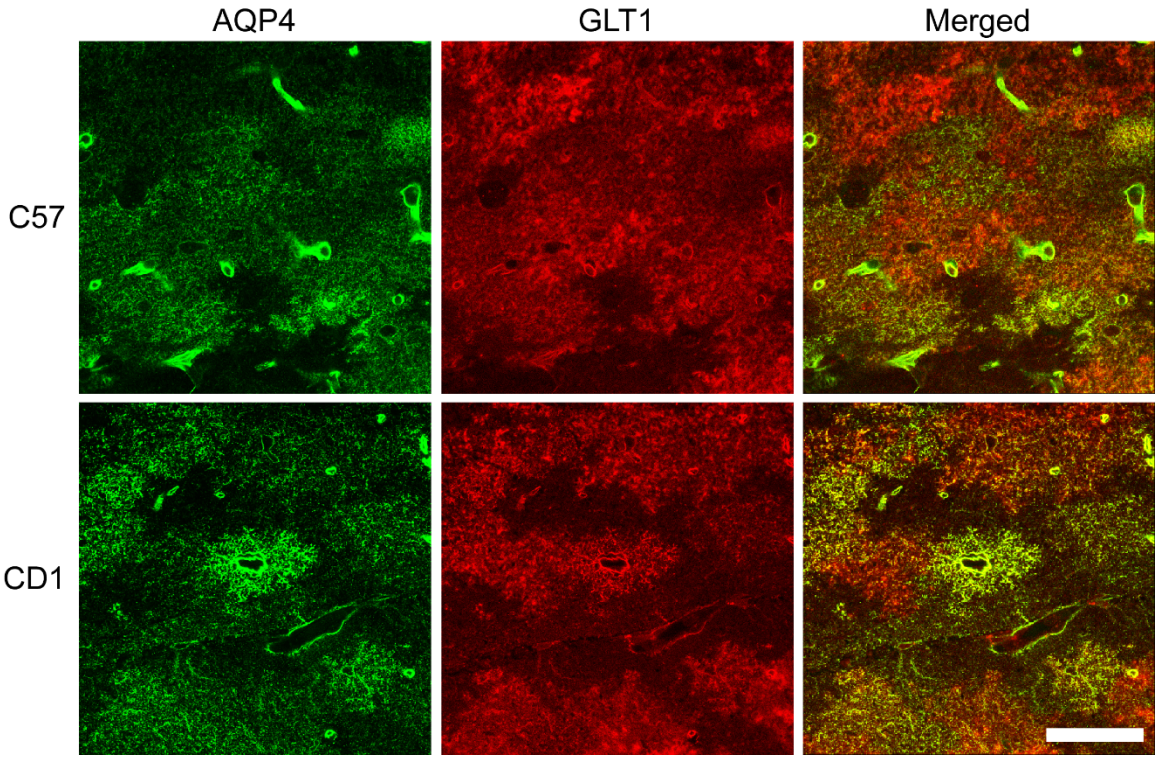


Figure 7.9. Aquaporin-4 (AQP4) and glutamate transporter-1 (GLT1) immunoreactivity in the hippocampus of C57BL/6 and CD1 wild-type mice. 63x images of AQP4 (green), GLT1 (red), and merged immunoreactivity of the hippocampus from C57BL/6 (top panels) and CD1 (bottom panels) wild-type mice. Although AQP4 and GLT1 are highly co-localized (seen as yellow in the Merged images), there are patches of GLT1 immunoreactivity that lack AQP4 immunoreactivity. Scale bar = 50 μm.

images confirmed abundant co-localization of AQP4 and GLT1 in the SLM layer of the hippocampus, although patches of GLT1-positive, AQP4-negative staining can be seen (Figure 7.9). In the cortex, AQP4 is almost exclusively found on astrocyte end-feet surrounding capillaries whereas GLT1 is expressed throughout (Figure 7.10). Therefore, AQP4 and GLT1 primarily lack co-localization in the cortex.

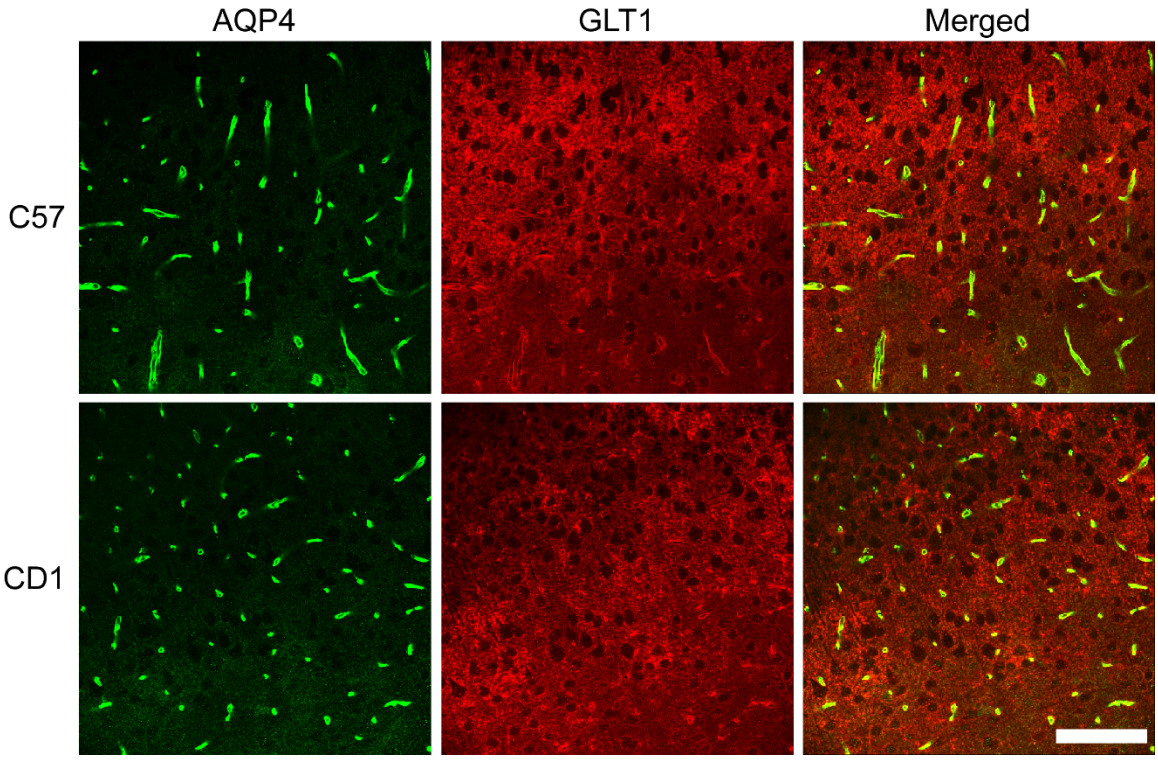


Figure 7.10. Aquaporin-4 (AQP4) and glutamate transporter-1 (GLT1) immunoreactivity in the cortex of C57BL/6 and CD1 wild-type mice.
40x images of AQP4 (green), GLT1 (red), and merged immunoreactivity in the cortex of C57BL/6 (top panels) and CD1 (bottom panels) wild-type mice. AQP4 is highly expressed on astrocyte end-feet surrounding capillaries and GLT1 is abundantly found on cell membranes. Scale bar = 100 μm.

7.5 Discussion

Here I used co-immunoprecipitation, Western blotting, and immunohistochemistry to determine (1) whether interaction between GLT1 and AQP4 exists; and (2) whether GLT1 levels are altered in mice lacking AQP4. I found that in conditions of 1% NP-40 lysis buffer, a mild detergent, GLT1 and AQP4 do not co-immunoprecipitate in either CD1 or C57BL/6 whole brain lysates, suggesting the lack of a strong physical interaction between the two proteins. A weak interaction, however, is still possible and cannot be ruled out. I also found no alterations in GLT1 expression in the whole brain, hippocampus, or cortex of wild-type and $AQP4^{-/-}$ mice. Furthermore, I observed region-specific co-localization of GLT1 and AQP4, rather than complete co-localization throughout the brain. Taken together, these data suggest the lack of any strong physical interaction between AQP4 and GLT1.

Several other studies have found co-localization between AQP4 and GLT1 in various regions of the brain and spinal cord (Hinson, Roemer et al. 2008; Lee, Ruby et al. 2013; Yang, Li et al. 2013; Mogoanta, Ciurea et al. 2014), but only one study has conducted a co-IP between AQP4 and GLT1. Hinson *et al.* (2008) solubilized GFP-labeled AQP4-transfected cells and probed the lysates with an antibody to GLT1; AQP4 was found to co-immunoprecipitate with GLT1 (Hinson, Roemer et al. 2008). This is in direct contrast to our results demonstrating a

complete lack of interaction between these two proteins. Our approaches, however, were very different. Although we both used a 1% NP-40 lysis buffer, I used tissue from both CD1 and C57BL/6 adult mice whereas Hinson *et al.* used *in vitro* techniques, specifically looking at HEK-293 cells transfected with a GFP-AQP4 construct. It is possible, however, that a weak interaction between AQP4 and GLT1 exists that was not detectable in my co-IP. Arguing against this interpretation is (1) the robust ability to immunoprecipitate both GLT1 and AQP4 with the antibodies used; and (2) the robust ability to detect supernatant GLT1 and AQP4 under the same conditions.

Although no other studies have reported on the physical interaction between AQP4 and GLT1, several other studies have examined GLT1 expression levels in $AQP4^{-/-}$ mice. Specifically, a reduction in GLT1 protein levels was reported in primary astrocyte cell cultures from cerebral cortices of wild-type and $AQP4^{-/-}$ mice (Zeng, Sun et al. 2007). GLT1 protein expression was reduced by less than 20% in spinal cord tissue (Chen, Bao et al. 2010) and by nearly 30% in the cerebellum (Yan, Wu et al. 2013) of $AQP4^{-/-}$ mice. A drastic reduction of GLT1 protein levels (~50%) was reported in the amygdala of $AQP4^{-/-}$ mice (Li, Wang et al. 2012). $AQP4^{-/-}$ mice clearly exhibited a region-specific reduction of GLT1 expression. In direct contrast to our findings, a 20-35% reduction in GLT1 hippocampal levels in $AQP4^{-/-}$ mice has been reported (Yan, Wu et al. 2013; Yang, Li et al. 2013; Kong, Zeng et al. 2014). Similarly, cortical regions of

AQP4$^{-/-}$ mice exhibited a 14-26% reduction of GLT1 expression (Wu, Lu et al. 2008; Yan, Wu et al. 2013). Further studies will be needed to clarify these discrepancies.

It has been hypothesized that a downregulation of GLT1 may be partially responsible for the impaired synaptic plasticity observed in AQP4$^{-/-}$ mice (Skucas, Mathews et al. 2011; Li, Wang et al. 2012; Szu and Binder 2016). Our findings, however, suggest that GLT1 levels are fully intact in AQP4$^{-/-}$ mice. Therefore, impairments such as difficulties in learning and memory formation in AQP4$^{-/-}$ mice cannot be accounted for by reduced GLT1-dependent glutamate clearance. As suggested by Skucas *et al.* (2011), synaptic plasticity deficits in AQP4$^{-/-}$ mice may be instead due to neurotrophin dysregulation (Skucas, Mathews et al. 2011). Specifically, AQP4 may be important to the regulation of the low-affinity neurotrophin receptor p75^{NTR}, which was downregulated in AQP4$^{-/-}$ mice (Skucas, Mathews et al. 2011).

Aquaporin-4 plays a role in regulating extracellular space (ECS) volume (Binder, Papadopoulos et al. 2004; Yao, Hrabetova et al. 2008). Specifically, AQP4$^{-/-}$ mice have an increase in ECS volume with no difference in tortuosity (Yao, Hrabetova et al. 2008). AQP4$^{-/-}$ mice also have delayed clearance of extracellular K^+ (Amiry-Moghaddam, Williamson et al. 2003; Binder, Yao et al. 2006; Haj-Yasein, Bugge et al. 2015). The uptake of K^+ into astrocytes after

neuronal activity produces a change in the osmotic driving force in favor of water uptake into astrocytes (Jin 2013). This uptake causes astrocytes to swell, thus reducing the ECS volume. With an increased ECS volume, such as in AQP4$^{-/-}$ mice, a reduced accumulation of K^+ may be observed after a mild stimuli and may not alter astrocyte swelling (Jin, Zhang et al. 2013; Anderova, Benesova et al. 2014). After neuroexcitation or more severe stimuli, such as hypoosmotic stress, oxygen glucose deprivation, or high K^+, reduced water permeability causes slowed ECS contraction (Anderova 2014, Jin 2013; Haj-Yasein 2012) and consequently may alter the electrochemical driving force for K^+ reuptake by astrocytes in AQP4$^{-/-}$ mice (Jin, Zhang et al. 2013).

Altered ECS dynamics may explain the different disease courses seen in AQP4$^{-/-}$ mice, such as in models of edema and epilepsy. AQP4 deficiency can be neuroprotective in cytotoxic edema but leads to a worsened prognosis (impaired water removal through glia limitans) in vasogenic edema (Papadopoulos, Manley et al. 2004). Similarly, AQP4$^{-/-}$ mice had a higher seizure threshold but prolonged seizure duration (Binder, Yao et al. 2006) and increased number of seizures (Lee, Hsu et al. 2012) in models of epilepsy. While the increased ECS volume may increase the threshold to seizure generation (Binder, Papadopoulos et al. 2004), slowed de-swelling of astrocytes could lead to prolonged and more severe seizures (Binder et al 2006). Therefore, perturbed extracellular space volume dynamics and consequently altered ion and neurotransmitter clearance, not

reduced GLT1 expression, may offer an alternative explanation to differences in disease progression seen in AQP4$^{-/-}$ mice.

7.6 References

Al Awabdh, S., S. Gupta-Agarwal, D. F. Sheehan, J. Muir, R. Norkett, A. E. Twelvetrees, L. D. Griffin and J. T. Kittler (2016). "Neuronal activity mediated regulation of glutamate transporter GLT-1 surface diffusion in rat astrocytes in dissociated and slice cultures." Glia **64**(7): 1252-1264.

Amiry-Moghaddam, M., A. Williamson, M. Palomba, T. Eid, N. C. de Lanerolle, E. A. Nagelhus, M. E. Adams, S. C. Froehner, P. Agre and O. P. Ottersen (2003). "Delayed K+ clearance associated with aquaporin-4 mislocalization: phenotypic defects in brains of alpha-syntrophin-null mice." Proc Natl Acad Sci U S A **100**(23): 13615-13620.

Anderova, M., J. Benesova, M. Mikesova, D. Dzamba, P. Honsa, J. Kriska, O. Butenko, V. Novosadova, L. Valihrach, M. Kubista, L. Dmytrenko, M. Cicanic and L. Vargova (2014). "Altered astrocytic swelling in the cortex of alpha-syntrophin-negative GFAP/EGFP mice." PLoS One **9**(11): e113444.

Binder, D. K., M. C. Papadopoulos, P. M. Haggie and A. S. Verkman (2004). "In vivo measurement of brain extracellular space diffusion by cortical surface photobleaching." J Neurosci **24**(37): 8049-8056.

Binder, D. K., X. Yao, Z. Zador, T. J. Sick, A. S. Verkman and G. T. Manley (2006). "Increased seizure duration and slowed potassium kinetics in mice lacking aquaporin-4 water channels." Glia **53**(6): 631-636.

Chen, M. L., F. Bao, Y. Q. Zhang and Z. Q. Zhao (2010). "Effects of aquaporin 4 deficiency on morphine analgesia and chronic tolerance: a study at spinal level." J Mol Neurosci **42**(2): 140-144.

Costa, C., R. Tortosa, A. Domenech, E. Vidal, M. Pumarola and A. Bassols (2007). "Mapping of aggrecan, hyaluronic acid, heparan sulphate proteoglycans and aquaporin 4 in the central nervous system of the mouse." J Chem Neuroanat **33**(3): 111-123.

Danbolt, N. C. (2001). "Glutamate uptake." Prog Neurobiol **65**(1): 1-105.

Fan, Y., M. Liu, X. Wu, F. Wang, J. Ding, J. Chen and G. Hu (2013). "Aquaporin-4 promotes memory consolidation in Morris water maze." Brain Struct Funct **218**(1): 39-50.

Haj-Yasein, N. N., C. E. Bugge, V. Jensen, I. Ostby, O. P. Ottersen, O. Hvalby and E. A. Nagelhus (2015). "Deletion of aquaporin-4 increases extracellular K(+) concentration during synaptic stimulation in mouse hippocampus." Brain Struct Funct **220**(4): 2469-2474.

Haj-Yasein, N. N., V. Jensen, I. Ostby, S. W. Omholt, J. Voipio, K. Kaila, O. P. Ottersen, O. Hvalby and E. A. Nagelhus (2012). "Aquaporin-4 regulates extracellular space volume dynamics during high-frequency synaptic stimulation: a gene deletion study in mouse hippocampus." Glia **60**(6): 867-874.

Hinson, S. R., S. F. Roemer, C. F. Lucchinetti, J. P. Fryer, T. J. Kryzer, J. L. Chamberlain, C. L. Howe, S. J. Pittock and V. A. Lennon (2008). "Aquaporin-4-binding autoantibodies in patients with neuromyelitis optica impair glutamate transport by down-regulating EAAT2." J Exp Med **205**(11): 2473-2481.

Hsu, M. S., M. Seldin, D. J. Lee, G. Seifert, C. Steinhauser and D. K. Binder (2011). "Laminar-specific and developmental expression of aquaporin-4 in the mouse hippocampus." Neuroscience **178**: 21-32.

Hubbard, J. A., M. S. Hsu, M. M. Seldin and D. K. Binder (2015). "Expression of the Astrocyte Water Channel Aquaporin-4 in the Mouse Brain." ASN Neuro **7**(5).

Jin, B. J., H. Zhang, D. K. Binder and A. S. Verkman (2013). "Aquaporin-4-dependent K(+) and water transport modeled in brain extracellular space following neuroexcitation." J Gen Physiol **141**(1): 119-132.

Kim, K., S. G. Lee, T. P. Kegelman, Z. Z. Su, S. K. Das, R. Dash, S. Dasgupta, P. M. Barral, M. Hedvat, P. Diaz, J. C. Reed, J. L. Stebbins, M. Pellecchia, D. Sarkar and P. B. Fisher (2011). "Role of excitatory amino acid transporter-2 (EAAT2) and glutamate in neurodegeneration: opportunities for developing novel therapeutics." J Cell Physiol **226**(10): 2484-2493.

Kong, H., X. N. Zeng, Y. Fan, S. T. Yuan, S. Ge, W. P. Xie, H. Wang and G. Hu (2014). "Aquaporin-4 knockout exacerbates corticosterone-induced depression by inhibiting astrocyte function and hippocampal neurogenesis." CNS Neurosci Ther **20**(5): 391-402.

Lee, D. J., M. S. Hsu, M. M. Seldin, J. L. Arellano and D. K. Binder (2012). "Decreased expression of the glial water channel aquaporin-4 in the intrahippocampal kainic acid model of epileptogenesis." Exp Neurol **235**(1): 246-255.

Lee, M. R., C. L. Ruby, D. J. Hinton, S. Choi, C. A. Adams, N. Young Kang and D. S. Choi (2013). "Striatal adenosine signaling regulates EAAT2 and astrocytic AQP4 expression and alcohol drinking in mice." Neuropsychopharmacology **38**(3): 437-445.

Li, Y. K., F. Wang, W. Wang, Y. Luo, P. F. Wu, J. L. Xiao, Z. L. Hu, Y. Jin, G. Hu and J. G. Chen (2012). "Aquaporin-4 deficiency impairs synaptic plasticity and associative fear memory in the lateral amygdala: involvement of downregulation of glutamate transporter-1 expression." Neuropsychopharmacology **37**(8): 1867-1878.

Ma, T., B. Yang, A. Gillespie, E. J. Carlson, C. J. Epstein and A. S. Verkman (1997). "Generation and phenotype of a transgenic knockout mouse lacking the mercurial-insensitive water channel aquaporin-4." J Clin Invest **100**(5): 957-962.

Mogoanta, L., M. Ciurea, I. Pirici, C. Margaritescu, C. Simionescu, D. A. Ion and D. Pirici (2014). "Different dynamics of aquaporin 4 and glutamate transporter-1 distribution in the perineuronal and perivascular compartments during ischemic stroke." Brain Pathol **24**(5): 475-493.

Murphy-Royal, C., J. P. Dupuis, J. A. Varela, A. Panatier, B. Pinson, J. Baufreton, L. Groc and S. H. Oliet (2015). "Surface diffusion of astrocytic glutamate transporters shapes synaptic transmission." Nat Neurosci **18**(2): 219-226.

Nagelhus, E. A., T. M. Mathiisen and O. P. Ottersen (2004). "Aquaporin-4 in the central nervous system: cellular and subcellular distribution and coexpression with KIR4.1." Neuroscience **129**(4): 905-913.

Nielsen, S., E. A. Nagelhus, M. Amiry-Moghaddam, C. Bourque, P. Agre and O. P. Ottersen (1997). "Specialized membrane domains for water transport in glial cells: high-resolution immunogold cytochemistry of aquaporin-4 in rat brain." J Neurosci **17**(1): 171-180.

Oshio, K., D. K. Binder, B. Yang, S. Schecter, A. S. Verkman and G. T. Manley (2004). "Expression of aquaporin water channels in mouse spinal cord." Neuroscience **127**(3): 685-693.

Papadopoulos, M. C., G. T. Manley, S. Krishna and A. S. Verkman (2004). "Aquaporin-4 facilitates reabsorption of excess fluid in vasogenic brain edema." FASEB J **18**(11): 1291-1293.

Rash, J. E., T. Yasumura, C. S. Hudson, P. Agre and S. Nielsen (1998). "Direct immunogold labeling of aquaporin-4 in square arrays of astrocyte and ependymocyte plasma membranes in rat brain and spinal cord." Proc Natl Acad Sci U S A **95**(20): 11981-11986.

Rothstein, J. D., L. Martin, A. I. Levey, M. Dykes-Hoberg, L. Jin, D. Wu, N. Nash and R. W. Kuncl (1994). "Localization of neuronal and glial glutamate transporters." Neuron **13**(3): 713-725.

Scharfman, H. E. and D. K. Binder (2013). "Aquaporin-4 water channels and synaptic plasticity in the hippocampus." Neurochem Int **63**(7): 702-711.

Skucas, V. A., I. B. Mathews, J. Yang, Q. Cheng, A. Treister, A. M. Duffy, A. S. Verkman, B. L. Hempstead, M. A. Wood, D. K. Binder and H. E. Scharfman (2011). "Impairment of select forms of spatial memory and neurotrophin-dependent synaptic plasticity by deletion of glial aquaporin-4." J Neurosci **31**(17): 6392-6397.

Strohschein, S., K. Hüttmann, S. Gabriel, D. K. Binder, U. Heinemann and C. Steinhäuser (2011). "Impact of aquaporin-4 channels on K+ buffering and gap junction coupling in the hippocampus." Glia **59**(6): 973-980.

Szu, J. I. and D. K. Binder (2016). "The Role of Astrocytic Aquaporin-4 in Synaptic Plasticity and Learning and Memory." Front Integr Neurosci **10**: 8.

Wu, N., X. Q. Lu, H. T. Yan, R. B. Su, J. F. Wang, Y. Liu, G. Hu and J. Li (2008). "Aquaporin 4 deficiency modulates morphine pharmacological actions." Neurosci Lett **448**(2): 221-225.

Yan, H. T., N. Wu, X. Q. Lu, R. B. Su, J. Q. Zheng and J. Li (2013). "Aquaporin-4 deficiency attenuates opioid dependence through suppressing glutamate transporter-1 down-regulation and maintaining glutamate homeostasis." CNS Neurosci Ther **19**(1): 12-19.

Yang, J., M. X. Li, Y. Luo, T. Chen, J. Liu, P. Fang, B. Jiang, Z. L. Hu, Y. Jin, J. G. Chen and F. Wang (2013). "Chronic ceftriaxone treatment rescues hippocampal memory deficit in AQP4 knockout mice via activation of GLT-1." Neuropharmacology **75**: 213-222.

Yao, X., S. Hrabetova, C. Nicholson and G. T. Manley (2008). "Aquaporin-4-deficient mice have increased extracellular space without tortuosity change." J Neurosci **28**(21): 5460-5464.

Zeng, X. N., X. L. Sun, L. Gao, Y. Fan, J. H. Ding and G. Hu (2007). "Aquaporin-4 deficiency down-regulates glutamate uptake and GLT-1 expression in astrocytes." Mol Cell Neurosci **34**(1): 34-39.

Chapter 8: Characterization of glutamate aspartate transporter (GLAST) expression in an epilepsy model

8.1 Abstract

Epilepsy is a chronic neurological condition that manifests as spontaneous seizures. The most common form is temporal lobe epilepsy (TLE). Traditionally, epilepsy was considered a neuronal disease but increasing evidence has suggested that astrocytes also play a major role in the disease. In particular, glutamate clearance through astrocytic glutamate transporter-1 (GLT1) and glutamate aspartate transporter (GLAST) is essential in maintaining glutamate homeostasis. If this system fails, then increased extracellular glutamate may lead to neuronal hyperexcitability and seizure generation. In a previous chapter, I discussed the regulation of GLT1 in the intrahippocampal kainic acid (IHKA) model of TLE. Here, I used the same model combined with immunohistochemistry, Western blotting, and real-time polymerase chain reaction to determine expression changes of GLAST during the development of epilepsy. I found an immediate increase in GLAST immunoreactivity in the ipsilateral hippocampus to kainic acid injections followed by a layer-specific downregulation at 7 days post IHKA injections. GLAST immunoreactivity returned to baseline levels by 30 days post IHKA injections. Both GLAST protein and mRNA levels remained unaltered with the exception of an increase in

GLAST mRNA in the contralateral hippocampus 7 days after IHKA injections. Therefore, only minor changes in GLAST expression were found in a mouse model of TLE. This is an important contradistinction to GLT1 which exhibited remarkable downregulation (Chapter 5).

8.2 Introduction

Epilepsy is a chronic seizure disorder resulting from abnormally synchronized activity among neurons. The most common form of epilepsy is TLE, characterized by seizures that originate in the temporal lobe. In TLE, seizures most commonly originate from the hippocampus (ILAE 1989). Sclerosis of the hippocampus, characterized by death of pyramidal neurons and dispersion of granule cell neurons, is the most prevalent histopathological abnormality in TLE (Blümcke, Thom et al. 2013). Other common features that present in hippocampal sclerosis include mossy fiber sprouting, microgliosis, astrogliosis, microvascular proliferation, and synaptic remodeling (Margerison and Corsellis 1966; Mathern, Pretorius et al. 1995; Blümcke, Beck et al. 1999; Clasadonte and Haydon 2012; de Lanerolle, Lee et al. 2012). Some of these features, such as astrogliosis, however, are not exclusive to the sclerotic hippocampus and therefore are not usually used to *define* hippocampal sclerosis (Chapter 2).

Astrogliosis is characterized by a profound change in astrocyte morphology. The cells become reactive (hypertrophic) and the expression of a number of genes and proteins become altered. This pathological feature occurs in several neurological disorders. Interestingly, astrogliosis is a highly heterogeneous and the expression changes that occur are disease- or injury-dependent (Zamanian, Xu et al. 2012). In TLE, astrogliosis occurs in both the sclerotic and non-sclerotic hippocampus (Lee, Hsu et al. 2012; Hubbard, Szu et al. 2016). It is possible that astrocytes in the sclerotic and non-sclerotic exhibit different expression profiles and therefore, it is important to examine both when studying TLE. For example, aquaporin-4 (AQP4) expression is upregulated in the sclerotic hippocampus but near control levels in the non-sclerotic hippocampus in a mouse model of TLE (Hubbard, Szu et al. 2016). Furthermore, glutamate transporter-1 (GLT1) exhibited different regulation patterns in the hippocampus that developed sclerosis compared to the one that did not in that same model (Hubbard, Szu et al. 2016).

It is well-established that high extracellular glutamate levels can lead to prolonged neuronal stimulation and consequently seizure activity and spread (During and Spencer 1993; Glass and Dragunow 1995; Tanaka, Watase et al. 1997; Campbell and Hablitz 2004; Hubbard, Hsu et al. 2013). Therefore, it is crucial to maintain low extracellular glutamate concentrations. Glutamate transporters are a family of 5 membrane proteins that clears glutamate after

neuronal activity. Glutamate transporter-1 (GLT1) and glutamate aspartate transporter (GLAST) are found primarily on astrocytes and together regulate extracellular glutamate levels in the forebrain (Kim, Lee et al. 2011). GLT1 is considered the primary regulator of extracellular glutamate in the brain and its expression is altered in a mouse model of TLE (Hubbard, Szu et al. 2016). Mice deficient in GLAST have prolonged electrical- and pentylenetetrazol-induced seizures (Watanabe, Morimoto et al. 1999). Although GLAST expression has been studied in models of TLE, the results have been equivocal (Simantov, Crispino et al. 1999; Ueda, Doi et al. 2001; Lopes, Soares et al. 2013). Therefore, a thorough time course study of GLAST expression could help elucidate the role, if any, that GLAST plays in the development of TLE.

In this chapter, I summarize experiments performed using the IHKA model of epilepsy to determine expression changes of GLAST. I collected tissue at 1, 4, 7 and 30 days post kainic acid-induced status epilepticus (SE) and examined mRNA, protein, and immunoreactivity using real-time polymerase chain reaction (RT-PCR), Western blotting, and immunohistochemistry, respectively. GLAST mRNA was largely unaltered, although a significant elevation was noted in the hippocampus contralateral to injections at 7 days post SE. Overall, no change in GLAST protein was observed. An increase in GLAST immunoreactivity was observed at 1 day post SE throughout the ipsilateral hippocampus. Furthermore, a transient layer-specific reduction in GLAST immunoreactivity was observed at 7

days post SE in the ipsilateral hippocampus. Overall, these results suggest that minor changes in GLAST expression occur in the IHKA model of epilepsy.

8.3 Methods

8.3.1 Animals

All experiments were conducted in accordance with the guidelines set forth by the National Institutes of Health and were approved by the University of California, Riverside Institutional Animal Care and Use Committee (IACUC). Animals were housed under controlled conditions with a 12 hour light and 12 hour dark cycle and had access to food and water *ad libitum*. CD1 male mice, 7-8 weeks old, from Charles River were used for all experiments.

8.3.2 Intrahippocampal injections

Mice were anesthetized with an intraperitoneal injection of 80mg/kg ketamine and 10 mg/kg xylazine and mounted in a stereotaxic frame. The skull was exposed and stereotaxic coordinates (Paxinos and Franklin 2001) were used to drill a small burr hole 1.8 mm posterior and 1.6 mm lateral from bregma with a high-speed drill (Drummond Scientific). Over a period of 4 minutes, mice were injected with either 74 nL of a 20 mM solution of kainic acid or an equal volume

of 0.9% saline using a microinjector (Nanoject, Drummond Scientific) at a depth of 1.9 mm. After kainic acid injections, all mice experienced status epilepticus (SE), defined by Racine scale stage 3-5 seizures (Table 2.1, Racine 1972) continuously for at least 3 hours, which spontaneously subsided. Animals that died due to SE were excluded from the study. Otherwise, at each time point n = 5 animals were euthanized with fatal plus (Western Medical Supply), perfused, and processed for each experiment, unless otherwise specified.

8.3.3 Immunohistochemistry

Mice were euthanized at 1, 4, 7, and 30 days post kainic acid-induced SE and 7 days post intrahippocampal saline injections (control). Transcardial perfusions were performed with ice-cold PBS, pH 7.4, followed by 4% paraformaldehyde, pH 7.4. Brains were quickly removed and postfixed in 4% paraformaldehyde overnight at 4°C followed by two days of cryoprotection in 30% sucrose in PBS at 4°C. Brains were frozen with ice-cold isopentane and stored at -80°C until they were cut into 50 µm coronal sections using a cryostat (Leica CM 1950, Leica Microsytems, Bannockburn, IL). Slices were stored in PBS at 4°C and all slices were processed simultaneously. Endogenous peroxidase activity was quenched by incubating slices in 3% H_2O_2 for 1 hour at room temperature. This was followed by a 1 hour blocking step with 5% normal goat serum in 0.1 M PBS. Slices were then incubated with primary antibody to GLAST (1:200, Abcam,

ab416) in 0.3% Triton X-100 overnight at 4°C. After washing slices with PBS, sections were incubated with species-specific secondary antibody conjugated with Alexa 488 and a tyramide signaling amplification (TSA) kit (Molecular Probes/Invitrogen) for visualization. Slices were mounted in Vectashield with DAPI (Vector Laboratories) and 10x images were taken using a fluorescence microscope (Leica DFC345 FX). For each group, 4 slices from each animal (n = 5 for all groups, except 4 days post SE, where n = 4) was used.

8.3.4 Western blot analysis

Whole hippocampal tissue was microdissected from the mouse brain at 1, 4, 7, and 30 days post IHKA or 7 days post saline injection (n = 5 for each group). Harvested tissue was homogenized using the Bullet Blender (Next Advance) in RIPA buffer (Sigma) containing complete protease inhibitors (Roche). Protein concentrations were assayed and protein was resolved by SDS-PAGE, 10% polyacrylamide, and transferred to a nitrocellulose membrane. The membranes were then probed for GLAST (1:500, Abcam, ab416) and β-actin (1:10,000, Sigma A1978) as an internal control. Bands were visualized and quantified using the Li-COR Odyssey Fc Western Imaging System and protein levels were normalized to internal β-actin levels. Both the upper and lower bands for GLAST are shown but only quantification of the lower band was included for simplicity.

8.3.5 Real-time polymerase chain reaction (RT-PCR) analysis

Whole hippocampus was microdissected from the mouse brain at 1, 4, 7, and 30 days post intrahippocampal kainic acid or 7 days post saline injections (for each group, n = 5). Harvested tissue was homogenized using the Bullet Blender (Next Advance). RNA was isolated using the Direct-Zol RNA mini prep kit (Zymo Research) and quantified using a nanodrop (Thermo Scientific NanoDrop 2000c Spectrophotometer). Both cDNA synthesis and RT-PCR were performed using the Bioline SensiFAST SYBR NO-ROX Kit and the CFX-96 detection system (Bio-Rad). Primers for GLAST and 18s RNA (Table 8.1) were purchased from Integrated DNA Technologies. The reaction conditions were as follows: 1 cycle for 10 min at 45°C, 1 cycle for 2 min at 95°C, 40 cycles for 5s at 95°C, and 1 cycle for 20s at 60°C. Results were quantified using the differential CT method representing the fold change in target gene expression. Both a no template control (NTC) and a no reverse transcriptase (NRT) control were included in each assay to detect any contamination or non-specific replication.

Target Gene	Forward Primer Sequence	Reverse Primer Sequence
GLAST	GGATGCGCGCTGTAGTCTAT	CGATCACGAAACCGAAGCAC
18s RNA	CTCAACACGGGAAACCTCAC	CGCTCCACCAACTAAGAACG

Table 8.1. Primers used for RT-PCR experiments.
All primers are listed in the 5' → 3' direction.

8.3.6 Statistical analysis

Statistical analysis was performed using a one-way ANOVA with *post-hoc* Bonferroni multiple comparisons test. All error bars are presented as the mean ± standard error of the mean (SEM). A statistically significant comparison to saline control was denoted with two asterisks (**) when $p < 0.01$. Any statistically significant differences between other time points were not indicated for the purpose of clarity.

8.4 Results

8.4.1 GLAST immunoreactivity in an epilepsy model

GLAST immunoreactivity in the ipsilateral hippocampus was imaged after saline injections and 1, 4, 7, and 30 days post kainic acid-induced SE (Figure 8.1). A marked increase in GLAST immunoreactivity was observed 1 day post SE throughout the hippocampus. By 4 days post-SE, however, GLAST immunoreactivity returned to control levels. Although marked morphological changes were observed at 7 days post SE, GLAST immunoreactivity remained similar to control levels with the exception of a significant reduction in the stratum radiatum. This reduction, however, was recovered by 30 days post SE. In the hippocampus contralateral to injections, GLAST exhibited similar

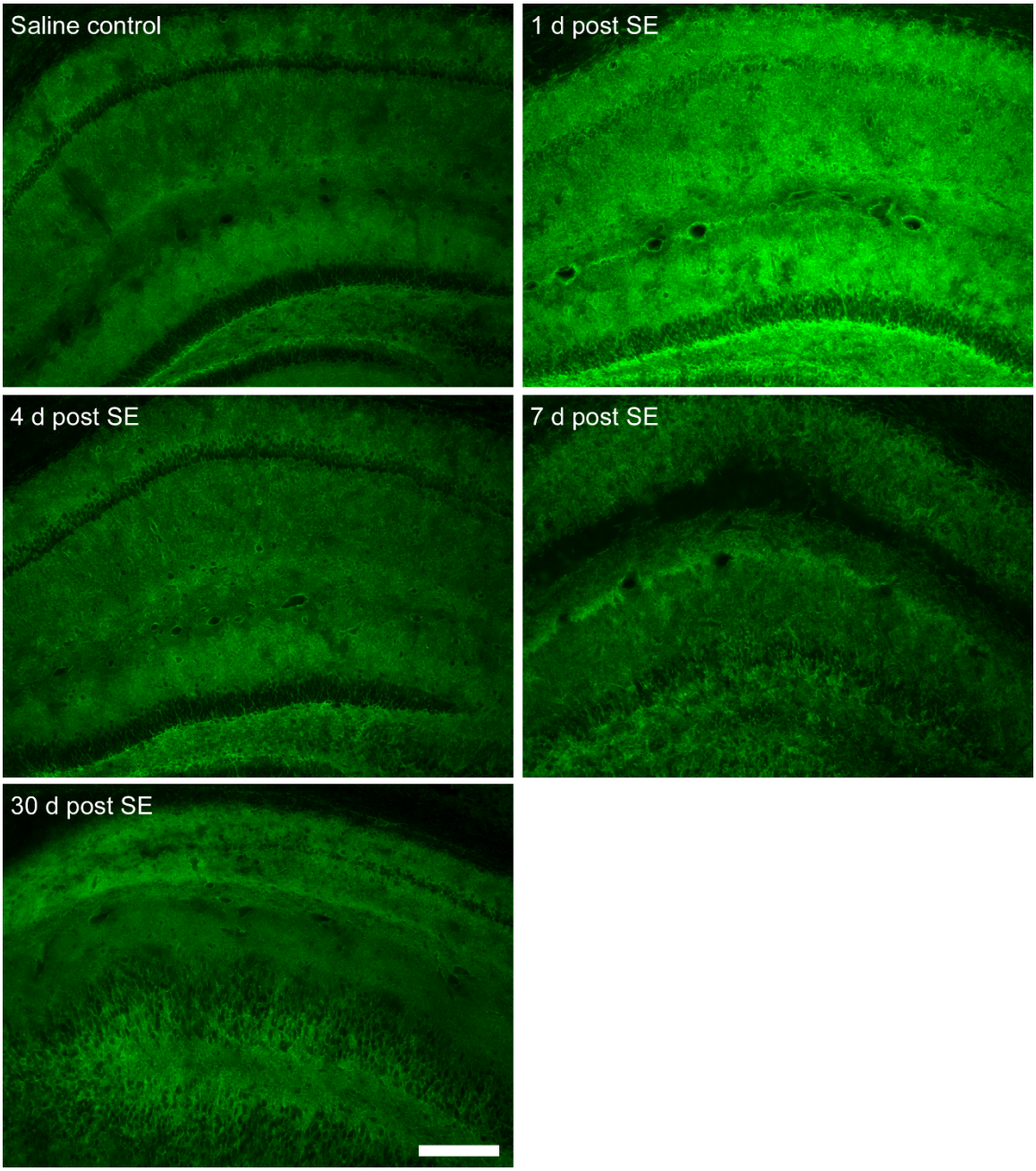


Figure 8.1. Glutamate aspartate transporter (GLAST) immunoreactivity in the ipsilateral hippocampus after kainic acid-induced status epilepticus (SE).
10x images of GLAST immunoreactivity in the ipsilateral hippocampus after saline injections (Saline control) and 1, 4, 7, and 30 days (d) post SE. Scale bar = 200 μm.

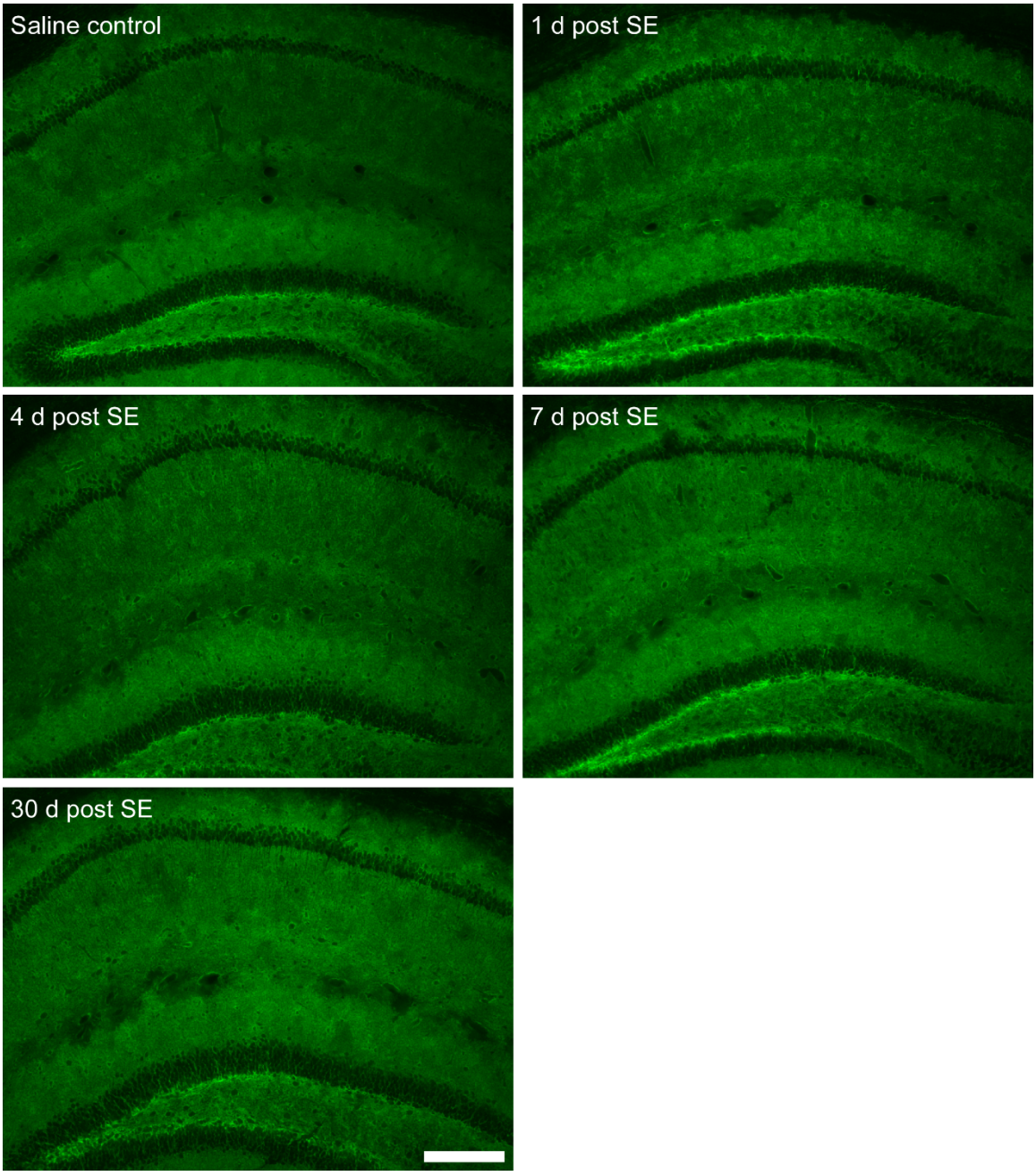


Figure 8.2. Glutamate aspartate transporter (GLAST) immunoreactivity in the contralateral hippocampus after kainic acid-induced status epilepticus (SE).
10x images of GLAST immunoreactivity in the contralateral hippocampus after saline injections (Saline control) and 1, 4, 7, and 30 days (d) post SE. Scale bar = 200 µm.

immunoreactivity to the controls at all time points post kainic acid-induced SE (Figure 8.2).

8.4.2 GLAST mRNA and protein in an epilepsy model

To determine any changes in GLAST protein and mRNA levels, Western blots and RT-PCR were performed on whole hippocampal tissue. In the ipsilateral hippocampus, no changes in either protein or mRNA levels were observed at any time point examined (Figure 8.3). In the contralateral hippocampus, however, a

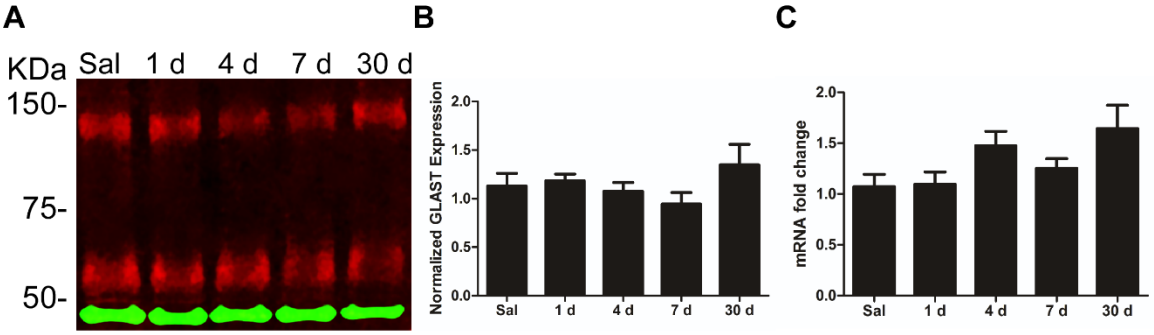


Figure 8.3. Glutamate aspartate transporter (GLAST) protein and mRNA levels in the ipsilateral hippocampus after kainic acid-induced status epilepticus (SE).
A. Representative Western blot of GLAST (red) and β-actin (green) protein from the ipsilateral hippocampus of a saline control (Sal) and 1, 4, 7, and 30 days (d) post kainic acid-induced SE. **B.** Quantification of GLAST lower band intensity normalized to β-actin at each time point in the ipsilateral hippocampus. **C.** Fold change in GLAST mRNA levels in the ipsilateral hippocampus of saline controls (Sal) and in tissue collected 1, 4, 7, and 30 days (d) post kainic acid-induced SE. For each time point, n = 5. KDa = kilodaltons.

hippocampus, no changes in either protein or mRNA levels were observed at any transient increase at 7 days post SE was observed (Figure 8.4). No changes in GLAST protein levels in the contralateral hippocampus were noted.

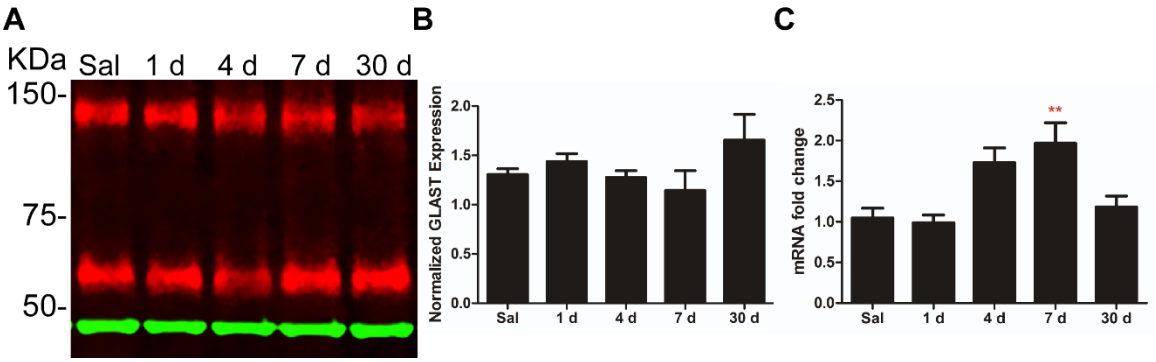


Figure 8.4. Glutamate aspartate transporter (GLAST) protein and mRNA levels after in the contralateral hippocampus after kainic acid-induced status epilepticus (SE).
A. Representative Western blot of GLAST (red) and β-actin (green) protein from the contralateral hippocampus of a saline control (Sal) and 1, 4, 7, and 30 days (d) post kainic acid-induced SE. **B.** Quantification of GLAST lower band intensity normalized to β-actin at each time point in the contralateral hippocampus. **C.** Fold change in GLAST mRNA levels in the contralateral hippocampus of saline controls (Sal) and in tissue collected 1, 4, 7, and 30 days (d) post kainic acid-induced SE. For each time point, n = 5. KDa = kilodaltons.

8.5 Discussion

Here I observed upregulated GLAST immunoreactivity at 1 day post kainic acid-induced SE, but did not observe any change in GLAST protein levels at that time point. In Chapter 5, I showed similar results with GLT1 where its immunoreactivity was upregulated at 1 day post SE, but whole hippocampal protein was unaltered (Hubbard, Szu et al. 2016). Upon further examination, it

was revealed that GLT1 protein was upregulated only in the dorsal hippocampus, thus matching the immunohistochemical studies. Therefore, it is possible that GLAST exhibits a similar behavior and GLAST regulation in the dorsal hippocampus is different from regulation in the ventral hippocampus.

Maintaining glutamate homeostasis is crucial to protect and sustain a healthy brain. Increased glutamate levels have been observed during and after seizure activity (During and Spencer 1993; Glass and Dragunow 1995; Tanaka, Watase et al. 1997; Campbell and Hablitz 2004). This may be due to decreased glutamate transporters in the brain. Here I have shown that reduced levels of GLAST immunoreactivity was observed in the stratum radiatum of the ipsilateral hippocampus 7 days post IHKA-induced SE. Otherwise, no change in GLAST protein levels or immunoreactivity were observed. Therefore, GLAST is likely not the key contributor to perturbed glutamate homeostasis and seizure activity. In Chapter 5, I demonstrated that GLT1 is downregulated as early as 4 days post IHKA-induced SE (Hubbard, Szu et al. 2016). The downregulation of these two crucial glutamate transporters at 7 days post SE together may contribute to the spontaneous seizures that occur in this model.

In studies of tissue from patients with TLE, GLAST mRNA was unaltered in both the sclerotic and non-sclerotic hippocampi (Proper, Hoogland et al. 2002). This is similar to what I observed at the 30 day time points in the ipsilateral (sclerotic)

and contralateral (non-sclerotic) hippocampi in the IHKA model. GLAST immunoreactivity, on the other hand, was increased or decreased in human TLE depending on the hippocampal region examined; for example, GLAST was increased in the CA2/3 stratum radiatum but decreased in the dentate gyrus in the sclerotic hippocampus (Mathern, Mendoza et al. 1999). In the IHKA model used in this study, GLAST expression was generally preserved in the sclerotic hippocampus. A detailed laminar-specific analysis, however, would be necessary to compare these results to this human tissue study.

Reduced levels of GLAST mRNA and protein were observed 60 days after intraamygdala kainic acid injections in both the ipsilateral and contralateral hippocampi (Ueda, Doi et al. 2001). GLAST hippocampal mRNA was elevated within 2 days after intraperitoneal injections of kainic acid but returned to baseline levels by 7 days post SE (Nonaka, Kohmura et al. 1998). Although I observed a transient increase in GLAST mRNA, it was at 7 days post SE. This difference could be due to the different modes of delivery (intraperitoneal vs. intrahippocampal). Despite the fact that histological changes are similar in these two models, the time course of cellular and molecular changes can differ drastically.

In conclusion, hippocampal GLAST expression may be slightly altered in models of temporal lobe epilepsy. These changes, however, were transient. Therefore,

it is likely that other perturbations, such as reduced GLT1 levels, are major contributors to seizure generation and spread. Future studies should focus on understanding the mechanisms behind astrocyte glutamate transporter regulation in epilepsy.

8.6 References

Blümcke, I., H. Beck, A. A. Lie and O. D. Wiestler (1999). "Molecular neuropathology of human mesial temporal lobe epilepsy." Epilepsy Res **36**(2-3): 205-223.

Blümcke, I., M. Thom, E. Aronica, D. D. Armstrong, F. Bartolomei, A. Bernasconi, N. Bernasconi, C. G. Bien, F. Cendes, R. Coras, J. H. Cross, T. S. Jacques, P. Kahane, G. W. Mathern, H. Miyata, S. L. Moshé, B. Oz, Ç. Özkara, E. Perucca, S. Sisodiya, S. Wiebe and R. Spreafico (2013). "International consensus classification of hippocampal sclerosis in temporal lobe epilepsy: a Task Force report from the ILAE Commission on Diagnostic Methods." Epilepsia **54**(7): 1315-1329.

Campbell, S. L. and J. J. Hablitz (2004). "Glutamate transporters regulate excitability in local networks in rat neocortex." Neuroscience **127**(3): 625-635.

Clasadonte, J. and P. G. Haydon (2012). Astrocytes and Epilepsy. Jasper's Basic Mechanisms of the Epilepsies. J. L. Noebels, M. Avoli, M. A. Rogawski, R. W. Olsen and A. V. Delgado-Escueta. Bethesda (MD).

de Lanerolle, N. C., T. S. Lee and D. D. Spencer (2012). Histopathology of Human Epilepsy. Jasper's Basic Mechanisms of the Epilepsies. J. L. Noebels, M. Avoli, M. A. Rogawski, R. W. Olsen and A. V. Delgado-Escueta. Bethesda (MD).

During, M. J. and D. D. Spencer (1993). "Extracellular hippocampal glutamate and spontaneous seizure in the conscious human brain." The Lancet **341**(8861): 1607-1610.

Glass, M. and M. Dragunow (1995). "Neurochemical and morphological changes associated with human epilepsy." Brain Research Reviews **21**: 29-41.

Hubbard, J. A., M. S. Hsu, T. A. Fiacco and D. K. Binder (2013). "Glial cell changes in epilepsy: overview of the clinical problem and therapeutic opportunities." Neurochem Int **63**(7): 638-651.

Hubbard, J. A., J. I. Szu, J. M. Yonan and D. K. Binder (2016). "Regulation of astrocyte glutamate transporter-1 (GLT1) and aquaporin-4 (AQP4) expression in a model of epilepsy." Exp Neurol.

ILAE (1989). "Proposal for revised classification of epilepsies and epileptic syndromes. Commission on Classification and Terminology of the International League Against Epilepsy." Epilepsia **30**(4): 389-399.

Kim, K., S. G. Lee, T. P. Kegelman, Z. Z. Su, S. K. Das, R. Dash, S. Dasgupta, P. M. Barral, M. Hedvat, P. Diaz, J. C. Reed, J. L. Stebbins, M. Pellecchia, D. Sarkar and P. B. Fisher (2011). "Role of excitatory amino acid transporter-2 (EAAT2) and glutamate in neurodegeneration: opportunities for developing novel therapeutics." J Cell Physiol **226**(10): 2484-2493.

Lee, D. J., M. S. Hsu, M. M. Seldin, J. L. Arellano and D. K. Binder (2012). "Decreased expression of the glial water channel aquaporin-4 in the intrahippocampal kainic acid model of epileptogenesis." Exp Neurol **235**(1): 246-255.

Lopes, M. W., F. M. Soares, N. de Mello, J. C. Nunes, A. G. Cajado, D. de Brito, F. M. de Cordova, R. M. da Cunha, R. Walz and R. B. Leal (2013). "Time-dependent modulation of AMPA receptor phosphorylation and mRNA expression of NMDA receptors and glial glutamate transporters in the rat hippocampus and cerebral cortex in a pilocarpine model of epilepsy." Exp Brain Res **226**(2): 153-163.

Margerison, J. H. and J. A. Corsellis (1966). "Epilepsy and the temporal lobes. A clinical, electroencephalographic and neuropathological study of the brain in epilepsy, with particular reference to the temporal lobes." Brain **89**(3): 499-530.

Mathern, G. W., D. Mendoza, A. Lozada, J. K. Pretorius, Y. Dehnes, N. C. Danbolt, N. Nelson, J. P. Leite, L. Chimelli, D. E. Born, A. C. Sakamoto, J. A. Assirati, I. Fried, W. J. Peacock, G. A. Ojemann and P. D. Adelson (1999). "Hippocampal GABA and glutamate transporter immunoreactivity in patients with temporal lobe epilepsy." Neurology **52**(3): 453-472.

Mathern, G. W., J. K. Pretorius and T. L. Babb (1995). "Quantified patterns of mossy fiber sprouting and neuron densities in hippocampal and lesional seizures." J Neurosurg **82**(2): 211-219.

Nonaka, M., E. Kohmura, T. Yamashita, S. Shimada, K. Tanaka, T. Yoshimine, M. Tohyama and T. Hayakawa (1998). "Increased transcription of glutamate-aspartate transporter (GLAST/GluT-1) mRNA following kainic acid-induced limbic seizure." Brain Res Mol Brain Res **55**(1): 54-60.

Paxinos, G. and K. B. J. Franklin (2001). The mouse brain in stereotaxic coordinates. San Diego, CA, Academic Press.

Proper, E. A., G. Hoogland, S. M. Kappen, G. H. Jansen, M. G. Rensen, L. H. Schrama, C. W. van Veelen, P. C. van Rijen, O. van Nieuwenhuizen, W. H. Gispen and P. N. de Graan (2002). "Distribution of glutamate transporters in the hippocampus of patients with pharmaco-resistant temporal lobe epilepsy." Brain **125**(Pt 1): 32-43.

Racine, R. J. (1972). "Modification of seizure activity by electrical stimulation. II. Motor seizure." Electroencephalogr Clin Neurophysiol **32**(3): 281-294.

Simantov, R., M. Crispino, W. Hoe, G. Broutman, G. Tocco, J. D. Rothstein and M. Baudry (1999). "Changes in expression of neuronal and glial glutamate transporters in rat hippocampus following kainate-induced seizure activity." Brain Res Mol Brain Res **65**(1): 112-123.

Tanaka, K., K. Watase, T. Manabe, K. Yamada, M. Watanabe, K. Takahashi, H. Iwama, T. Nishikawa, N. Ichihara, T. Kikuchi, S. Okuyama, N. Kawashima, S. Hori, M. Takimoto and K. Wada (1997). "Epilepsy and exacerbation of brain injury in mice lacking the glutamate transporter GLT-1." Science **276**: 1699-1702.

Ueda, Y., T. Doi, J. Tokumaru, H. Yokoyama, A. Nakajima, Y. Mitsuyama, H. Ohya-Nishiguchi, H. Kamada and L. J. Willmore (2001). "Collapse of extracellular glutamate regulation during epileptogenesis: down-regulation and functional failure of glutamate transporter function in rats with chronic seizures induced by kainic acid." J Neurochem **76**(3): 892-900.

Watanabe, T., K. Morimoto, T. Hirao, H. Suwaki, K. Watase and K. Tanaka (1999). "Amygdala-kindled and pentylenetetrazole-induced seizures in glutamate transporter GLAST-deficient mice." Brain Res **845**(1): 92-96.

Zamanian, J. L., L. Xu, L. C. Foo, N. Nouri, L. Zhou, R. G. Giffard and B. A. Barres (2012). "Genomic analysis of reactive astrogliosis." J Neurosci **32**(18): 6391-6410.

Chapter 9: Conclusions and future directions

9.1 Intrahippocampal kainic acid model of epilepsy

The intrahippocampal kainic acid (IHKA) model has proven to be a valuable tool in studying temporal lobe epilepsy. Not only is it a highly reproducible model, but it recapitulates histopathological aspects of the disease. In addition, this model provides a "latent" period which allows for the study of epileptogenesis. In Chapter 2, I showed changes in both neurons and glial cells including: (1) granule cell dispersion; (2) death of CA1 pyramidal neurons; (3) microgliosis; and (4) astrogliosis. In chapters 4, 5, and 8, I demonstrated that the expression of the astrocytic proteins aquaporin-4 (AQP4), glutamate transporter-1 (GLT), and, to a lesser extent, glutamate aspartate transporter-1 (GLAST) become altered in the IHKA model of epilepsy. Now that I have established that reproducible histopathological changes and altered membrane protein expression occur in this model of TLE, it would be valuable to study these important molecular and protein changes in other epilepsy models. For example, a direct comparison to the pilocarpine model of temporal lobe epilepsy could be made to determine the robustness of these changes. In addition, models of febrile seizures, post-traumatic epilepsy, or seizures due to blood-brain barrier (BBB) disruption could be assessed to determine the generality of AQP4, GLT1, and GLAST regulation as well as neuronal cell death/dispersion and gliosis in distinct epilepsy models.

9.2 Aquaporin-4 (AQP4) in epilepsy

In Chapter 3, I reviewed the expression pattern of AQP4 in the healthy brain. AQP4 protein levels were highest in the cerebellum and AQP4 exhibited laminar-specific expression patterns in the hippocampus. I then demonstrated AQP4 expression changes in the hippocampus after IHKA-induced epileptogenesis in Chapter 4. An immediate reduction of AQP4 protein with recovery over time was shown during epileptogenesis. At 30 days post IHKA-induced SE, increased AQP4 protein was found in the sclerotic, but not the non-sclerotic, hippocampus. A mechanistic explanation for this change, however, was not provided.

In 2001, Neely *et al.* demonstrated that AQP4 is tethered to the membrane through an interaction with α-syntrophin, a dystrophin-associated protein (Neely, Amiry-Moghaddam et al. 2001). Interestingly, initial examination of α-syntrophin (Neely, Amiry-Moghaddam et al. 2001) and dystrophin (Vajda, Pedersen et al. 2002) knockout mice suggested that total AQP4 expression was unaltered. Upon further investigation, it was discovered that although the overall AQP4 levels were unaltered, the polarized expression pattern of AQP4 was reversed. Immunogold or immunohistological analysis of AQP4 distribution in these knockout mice revealed that AQP4 expression was reduced in astrocytic end-feet membranes adjacent to blood vessels as well as perivascular and subpial membranes but was increased in areas facing neuropil (Frigeri, Nicchia et al.

2001; Neely, Amiry-Moghaddam et al. 2001; Vajda, Pedersen et al. 2002; Amiry-Moghaddam, Otsuka et al. 2003; Enger, Gundersen et al. 2012; Anderova, Benesova et al. 2014). This is in direct contrast to the normal expression pattern of AQP4 (Chapter 3). Furthermore, swollen perivascular and subpial anstroglial end-feet were found in α-syntrophin knockout mice (Frigeri, Nicchia et al. 2001; Amiry-Moghaddam, Otsuka et al. 2003). In response to ischemia or hyoosmotic stress, brain edema and astrocyte swelling were attenuated in α-syntrophin knockout mice (Amiry-Moghaddam, Otsuka et al. 2003; Anderova, Benesova et al. 2014). Together these data suggest that AQP4 localization is largely determined by α-syntrophin anchoring to the membrane.

Mislocalization of AQP4 following reduced α-syntrophin and dystrophin levels was observed in the i.p. kainic acid and pilocarpine models of TLE (Kim, Yeo et al. 2010; Alvestad, Hammer et al. 2013). In human TLE, an overall increase in AQP4 expression but a downregulation of α-syntrophin and dystrophin were noted (Lee, Eid et al. 2004; Eid, Lee et al. 2005; Das, Wallace et al. 2012). Immunogold electron microscopy again revealed that AQP4 density along perivascular membranes was reduced whereas neuropil AQP4 levels were unaltered (Eid, Lee et al. 2005). In focal cortical dysplasia (FCD) type IIB, AQP4 and dystrophin exhibited strong expression around the neuropil and dysplastic neurons with a reduction around vessels (Medici, Frassoni et al. 2011). Again, these data suggest that a perivascular loss of AQP4 is secondary to disruption of

the dystrophin complex. It is therefore likely that the increased AQP4 expression I observed in the sclerotic hippocampus (ipsilateral to injection, 30 days post SE; Chapter 4) may be accompanied by reduced α-syntrophin and dystrophin levels.

Whole hippocampal and dorsal hippocampal AQP4 levels were differently regulated during the early epileptogenic period (Chapter 4). Mislocalization could have occurred at these early time points. Future studies should use the IHKA and other models of epilepsy to (1) examine dystrophin complex expression changes during epileptogenesis; (2) determine whether the level of interaction between the dystrophin complex and AQP4 is altered over time; (3) and definitively confirm that α-syntrophin-induced AQP4 mislocalization is indeed the cause of AQP4 regulation in epilepsy. Evidence for dystrophin/α-syntrophin downregulation leading to AQP4 mislocalization has been either from knockout animal studies or expression studies in disease models. Direct evidence, such as antisense reduction of α-syntrophin in adult mice, would confirm this hypothesis. Furthermore, a detailed analysis comparing the sclerotic hippocampus to the non-sclerotic hippocampus would give insight into glial scarring and the formation of sclerosis.

Frigeri *et al.* (2001) determined that dystrophin knockout mice had a major reduction of AQP4 protein but not AQP4 mRNA (Frigeri, Nicchia et al. 2001). If α-syntrophin-induced mislocalization of AQP4 is the mechanism of dysregulation

in epilepsy, then targeting AQP4 mRNA may not exhibit any therapeutic benefit. The β-lactam drug ceftriaxone is thought to work though increasing transcription through the NF-κB pathway (Lee, Su et al. 2008). This could explain the lack of effect that ceftriaxone and other β-lactam drugs had on AQP4 expression (Chapter 8). Therefore, alternative approaches that target dystrophin-associated localization of AQP4 may be a better therapeutic option. A potential strategy may through agrin, a heparin sulfate proteoglycan of the extracellular matrix protein known to play a role in both the clustering of AQP4 into orthogonal arrays of particles and their insertion into astrocytic end-feet membranes (Noell, Fallier-Becker et al. 2007; Noell, Fallier-Becker et al. 2009; Wolburg, Noell et al. 2009; Fallier-Becker, Sperveslage et al. 2011).

9.3 Astrocytic glutamate transporters in epilepsy

Glutamate transporter-1 (GLT1) and glutamate aspartate transporter (GLAST) are astrocyte-specific regulators of extracellular glutamate concentrations. In Chapter 5, I demonstrated a unique regulation pattern of GLT1 in the IHKA model of epilepsy. An immediate upregulation of GLT1 was followed by a persistent downregulation of GLT1 protein as early as 4 days post SE. GLAST, on the other hand, only exhibited increased immunoreactivity in the ipsilateral hippocampus 1 day post IHKA injections (Chapter 8). Otherwise, very little regulation of GLAST was observed. Therefore, it is clear that GLT1

dysregulation plays a major role in epileptogenesis whereas GLAST regulation plays a more minor role. Furthermore, due to the lack of strong interaction between GLT1 and AQP4 (Chapter 7), it is likely that these two proteins are independently regulated.

In 2015, Murphy-Royal *et al.* (2015) transfected tagged GLT1 into astrocytes of mixed primary hippocampal cultures and monitored GLT1 mobility using nanoparticle tracking (Murphy-Royal, Dupuis et al. 2015). GLT1 gets untethered from the membrane and becomes highly mobile in response to neuronal activity and the uncaging of glutamate (Murphy-Royal, Dupuis et al. 2015). These results were expanded by Awabdh *et al.* (2016) who discovered that GLT1 can rapidly and reversibly cluster on membranes (Al Awabdh, Gupta-Agarwal et al. 2016). Glutamate and neuronal activity dispersed these clusters and regulated surface diffusion. Moreover, clustered GLT1 was more stable than diffuse GLT1 and diffuse GLT1 was more mobile than clustered GLT1 (Al Awabdh, Gupta-Agarwal et al. 2016). Both of these studies were done *in vitro* and confirmed that GLT1 diffusion was increased in the presence of neurons (Murphy-Royal, Dupuis et al. 2015; Al Awabdh, Gupta-Agarwal et al. 2016). A focal loss of GLT1 immunoreactivity and increased glutamate immunoreactivity near patches of neuronal death was reported in an i.p. kainic acid epilepsy model (Sakurai, Kurokawa et al. 2015). In the IHKA model, I found that GLT1 was differentially regulated in the dorsal hippocampus compared to the rest of the hippocampus

(Chapter 5). The dorsal and ventral hippocampi very exhibit different excitability properties (Akaike, Tanaka et al. 2001). Therefore, activity-dependent regulation of GLT1 mobility may account for the region-specific expression changes of GLT1.

In Chapter 5, I demonstrated that dorsal hippocampal GLT1 protein underwent significant changes during epileptogenesis, specifically at 1-7 days post IHKA-induced SE, but GLT1 mRNA underwent almost no change within that same time period. Therefore, GLT1 is not regulated solely at the transcriptional level and other mechanisms must be involved. I hypothesize that (1) GLT1 mRNA undergoes increased translation or (2) GLT1 protein is post-translationally modified. Previous studies have demonstrated that GLT1 can be regulated by sumoylation (Foran, Rosenblum et al. 2014) and S-nitrosylation (Raju, Doulias et al. 2015). Both post-translational modifications resulted in reduced glutamate uptake by GLT1 (Foran, Rosenblum et al. 2014; Raju, Doulias et al. 2015). Furthermore, when GLT1 was either sumoylated or nitrosylated, it became internalized, thus decreasing the membrane pool of GLT1. If GLT1 undergoes either post-translational modification in the IHKA model of epilepsy, then it would likely lead to the higher pools of cytoplasmic GLT1, decreased functional membrane GLT1, and consequently decreased glutamate uptake. Together, this could lead to accumulation of glutamate in the extracellular space, overexcitation of neurons, seizure generation and spread, and neuronal cell death. It would be

interesting to determine the levels of post-translational modification of GLT1 in the IHKA model of epilepsy.

It was previously believed that GLT1 protein was solely expressed on astrocytes and only GLT1 mRNA was found on neurons (Danbolt 2001). More recently, however GLT1 functional protein has been detected in axon terminals (Chen, Mahadomrongkul et al. 2004; Furness, Dehnes et al. 2008). To decipher the role of astrocytic versus neuronal GLT1, Petr *et al.* (2015) created conditional knockout mice. These studies revealed that the conditional deletion of GLT1 from astrocytes led to seizures, mortality, and decreased body weight (Petr, Sun et al. 2015), a similar phenotype to homozygous mice deficient in GLT1 (Tanaka, Watase et al. 1997). Furthermore, astrocytic GLT1 deletion significantly reduced glutamate uptake activity in reconstituted liposomes but only led to a small reduction in glutamate uptake in crude forebrain synaptosomes. The deletion of neuronal GLT1, on the other hand, had no effect on glutamate activity when reconstituted into liposomes, but did reduce synaptosomal glutamate uptake capacity by ~40% (Petr, Sun et al. 2015). Therefore, it is important to consider the contribution of neuronal GLT1 when interpreting the role of GLT1 in epileptogenesis, particularly at or near axon terminals. Future studies should examine the role of astrocytic versus neuronal GLT1 in the IHKA model of epilepsy.

The β-lactam drugs ceftriaxone, clavulanic acid, and tazobactam failed to regulate GLT1 protein expression in wild-type mice (Chapter 6). More importantly, neither ceftriaxone nor tazobactam alleviated immunohistological changes in GLT1 or GFAP expression in the IHKA model of epilepsy. This, however, is not too surprising if one considers the mechanism of action of ceftriaxone. As discussed previously, it is thought that this β-lactam antibiotic works to increase GLT1 expression by increasing transcription of GLT1 (Lee, Su et al. 2008). If GLT1 is not being transcribed or is constantly undergoing internalization during epileptogenesis, then increasing GLT1 mRNA may not be an effective treatment. Therefore, understanding the mechanism of GLT1 regulation during epileptogenesis is essential in determining how to best regulate this important protein. For example, if GLT1 is sumolyated, internalized, and degraded in epilepsy, then an appropriate antiepileptogenic drug would be an anti-sumolyation agent. Due to lack of interaction between AQP4 and GLT1 and the high probability that these molecules are differentially regulated, separate and distinct therapeutic mechanisms may be necessary to target the proteins individually. In either case, viral vectors, cellular transplants, or transcriptional activators may be promising options.

9.4 Summary

In conclusion, I have characterized glial cell changes in the IHKA model of epilepsy with a particular focus on AQP4 and GLT1 expression. I found that both proteins are significantly altered during early time points. More specifically, dorsal hippocampal AQP4 is immediately downregulated with a partial recovery over time. GLT1 protein exhibited an immediate increase before a persistent downregulation 4-7 days post IHKA-induced SE. Furthermore, AQP4 mRNA is significantly upregulated in the hippocampus whereas GLT1 mRNA remained largely unaltered. Taken together, my data suggest that both AQP4 and GLT1 play a role in the conversion of the healthy brain into an epileptic one. AQP4 and GLT1 are likely differentially regulated and future studies should focus on deciphering the mechanisms behind the changes during epileptogenesis. This information could then be used to create targeted interventions for the prevention of epilepsy.

9.5 References

Akaike, K., S. Tanaka, H. Tojo, S. Fukumoto, S. Imamura and M. Takigawa (2001). "Kainic acid-induced dorsal and ventral hippocampal seizures in rats." Brain Res **900**(1): 65-71.

Al Awabdh, S., S. Gupta-Agarwal, D. F. Sheehan, J. Muir, R. Norkett, A. E. Twelvetrees, L. D. Griffin and J. T. Kittler (2016). "Neuronal activity mediated regulation of glutamate transporter GLT-1 surface diffusion in rat astrocytes in dissociated and slice cultures." Glia **64**(7): 1252-1264.

Alvestad, S., J. Hammer, E. H. Hoddevik, O. Skare, U. Sonnewald, M. Amiry-Moghaddam and O. P. Ottersen (2013). "Mislocalization of AQP4 precedes chronic seizures in the kainate model of temporal lobe epilepsy." Epilepsy Res **105**(1-2): 30-41.

Amiry-Moghaddam, M., T. Otsuka, P. D. Hurn, R. J. Traystman, F. M. Haug, S. C. Froehner, M. E. Adams, J. D. Neely, P. Agre, O. P. Ottersen and A. Bhardwaj (2003). "An alpha-syntrophin-dependent pool of AQP4 in astroglial end-feet confers bidirectional water flow between blood and brain." Proc Natl Acad Sci U S A **100**(4): 2106-2111.

Anderova, M., J. Benesova, M. Mikesova, D. Dzamba, P. Honsa, J. Kriska, O. Butenko, V. Novosadova, L. Valihrach, M. Kubista, L. Dmytrenko, M. Cicanic and L. Vargova (2014). "Altered astrocytic swelling in the cortex of alpha-syntrophin-negative GFAP/EGFP mice." PLoS One **9**(11): e113444.

Chen, W., V. Mahadomrongkul, U. V. Berger, M. Bassan, T. DeSilva, K. Tanaka, N. Irwin, C. Aoki and P. A. Rosenberg (2004). "The glutamate transporter GLT1a is expressed in excitatory axon terminals of mature hippocampal neurons." J Neurosci **24**(5): 1136-1148.

Danbolt, N. C. (2001). "Glutamate uptake." Prog Neurobiol **65**(1): 1-105.

Das, A., G. C. t. Wallace, C. Holmes, M. L. McDowell, J. A. Smith, J. D. Marshall, L. Bonilha, J. C. Edwards, S. S. Glazier, S. K. Ray and N. L. Banik (2012). "Hippocampal tissue of patients with refractory temporal lobe epilepsy is associated with astrocyte activation, inflammation, and altered expression of channels and receptors." Neuroscience **220**: 237-246.

Eid, T., T. S. Lee, M. J. Thomas, M. Amiry-Moghaddam, L. P. Bjornsen, D. D. Spencer, P. Agre, O. P. Ottersen and N. C. de Lanerolle (2005). "Loss of perivascular aquaporin 4 may underlie deficient water and K+

homeostasis in the human epileptogenic hippocampus." Proc Natl Acad Sci U S A **102**(4): 1193-1198.

Enger, R., G. A. Gundersen, N. N. Haj-Yasein, M. Eilert-Olsen, A. E. Thoren, G. F. Vindedal, P. H. Petersen, O. Skare, M. Nedergaard, O. P. Ottersen and E. A. Nagelhus (2012). "Molecular scaffolds underpinning macroglial polarization: an analysis of retinal Muller cells and brain astrocytes in mouse." Glia **60**(12): 2018-2026.

Fallier-Becker, P., J. Sperveslage, H. Wolburg and S. Noell (2011). "The impact of agrin on the formation of orthogonal arrays of particles in cultured astrocytes from wild-type and agrin-null mice." Brain Res **1367**: 2-12.

Foran, E., L. Rosenblum, A. Bogush, P. Pasinelli and D. Trotti (2014). "Sumoylation of the astroglial glutamate transporter EAAT2 governs its intracellular compartmentalization." Glia **62**(8): 1241-1253.

Frigeri, A., G. P. Nicchia, B. Nico, F. Quondamatteo, R. Herken, L. Roncali and M. Svelto (2001). "Aquaporin-4 deficiency in skeletal muscle and brain of dystrophic mdx mice." FASEB J **15**(1): 90-98.

Furness, D. N., Y. Dehnes, A. Q. Akhtar, D. J. Rossi, M. Hamann, N. J. Grutle, V. Gundersen, S. Holmseth, K. P. Lehre, K. Ullensvang, M. Wojewodzic, Y. Zhou, D. Attwell and N. C. Danbolt (2008). "A quantitative assessment of glutamate uptake into hippocampal synaptic terminals and astrocytes: new insights into a neuronal role for excitatory amino acid transporter 2 (EAAT2)." Neuroscience **157**(1): 80-94.

Kim, J. E., S. I. Yeo, H. J. Ryu, M. J. Kim, D. S. Kim, S. M. Jo and T. C. Kang (2010). "Astroglial loss and edema formation in the rat piriform cortex and hippocampus following pilocarpine-induced status epilepticus." J Comp Neurol **518**(22): 4612-4628.

Lee, S. G., Z. Z. Su, L. Emdad, P. Gupta, D. Sarkar, A. Borjabad, D. J. Volsky and P. B. Fisher (2008). "Mechanism of ceftriaxone induction of excitatory amino acid transporter-2 expression and glutamate uptake in primary human astrocytes." J Biol Chem **283**(19): 13116-13123.

Lee, T. S., T. Eid, S. Mane, J. H. Kim, D. D. Spencer, O. P. Ottersen and N. C. de Lanerolle (2004). "Aquaporin-4 is increased in the sclerotic hippocampus in human temporal lobe epilepsy." Acta Neuropathol **108**(6): 493-502.

Medici, V., C. Frassoni, L. Tassi, R. Spreafico and R. Garbelli (2011). "Aquaporin 4 expression in control and epileptic human cerebral cortex." Brain Res **1367**: 330-339.

Murphy-Royal, C., J. P. Dupuis, J. A. Varela, A. Panatier, B. Pinson, J. Baufreton, L. Groc and S. H. Oliet (2015). "Surface diffusion of astrocytic glutamate transporters shapes synaptic transmission." Nat Neurosci **18**(2): 219-226.

Neely, J. D., M. Amiry-Moghaddam, O. P. Ottersen, S. C. Froehner, P. Agre and M. E. Adams (2001). "Syntrophin-dependent expression and localization of Aquaporin-4 water channel protein." Proc Natl Acad Sci U S A **98**(24): 14108-14113.

Noell, S., P. Fallier-Becker, C. Beyer, S. Kroger, A. F. Mack and H. Wolburg (2007). "Effects of agrin on the expression and distribution of the water channel protein aquaporin-4 and volume regulation in cultured astrocytes." Eur J Neurosci **26**(8): 2109-2118.

Noell, S., P. Fallier-Becker, U. Deutsch, A. F. Mack and H. Wolburg (2009). "Agrin defines polarized distribution of orthogonal arrays of particles in astrocytes." Cell Tissue Res **337**(2): 185-195.

Petr, G. T., Y. Sun, N. M. Frederick, Y. Zhou, S. C. Dhamne, M. Q. Hameed, C. Miranda, E. A. Bedoya, K. D. Fischer, W. Armsen, J. Wang, N. C. Danbolt, A. Rotenberg, C. J. Aoki and P. A. Rosenberg (2015). "Conditional deletion of the glutamate transporter GLT-1 reveals that astrocytic GLT-1 protects against fatal epilepsy while neuronal GLT-1 contributes significantly to glutamate uptake into synaptosomes." J Neurosci **35**(13): 5187-5201.

Raju, K., P. T. Doulias, P. Evans, E. N. Krizman, J. G. Jackson, O. Horyn, Y. Daikhin, I. Nissim, M. Yudkoff, K. A. Sharp, M. B. Robinson and H. Ischiropoulos (2015). "Regulation of brain glutamate metabolism by nitric oxide and S-nitrosylation." Sci Signal **8**(384): ra68.

Sakurai, M., H. Kurokawa, A. Shimada, K. Nakamura, H. Miyata and T. Morita (2015). "Excitatory amino acid transporter 2 downregulation correlates with thalamic neuronal death following kainic acid-induced status epilepticus in rat." Neuropathology **35**(1): 1-9.

Tanaka, K., K. Watase, T. Manabe, K. Yamada, M. Watanabe, K. Takahashi, H. Iwama, T. Nishikawa, N. Ichihara, T. Kikuchi, S. Okuyama, N. Kawashima, S. Hori, M. Takimoto and K. Wada (1997). "Epilepsy and exacerbation of

brain injury in mice lacking the glutamate transporter GLT-1." Science **276**(5319): 1699-1702.

Vajda, Z., M. Pedersen, E. M. Fuchtbauer, K. Wertz, H. Stodkilde-Jorgensen, E. Sulyok, T. Doczi, J. D. Neely, P. Agre, J. Frokiaer and S. Nielsen (2002). "Delayed onset of brain edema and mislocalization of aquaporin-4 in dystrophin-null transgenic mice." Proc Natl Acad Sci U S A **99**(20): 13131-13136.

Wolburg, H., S. Noell, K. Wolburg-Buchholz, A. Mack and P. Fallier-Becker (2009). "Agrin, aquaporin-4, and astrocyte polarity as an important feature of the blood-brain barrier." Neuroscientist **15**(2): 180-193.